# ABROGATING THE ONCOGENIC SIGNALING ASSOCIATED WITH TUMOR MUC1 IN PANCREATIC DUCTAL ADENOCARCINOMA

by

Mukulika Bose

A dissertation submitted to the faculty of
The University of North Carolina at Charlotte
in partial fulfillment of the requirements
for the degree of Doctor of Philosophy in
Biological Sciences

Charlotte

2022

Approved by:

_____
Dr. Pinku Mukherjee

_____
Dr. Shan Yan

_____
Dr. Didier Dreau

_____
Dr. Kausik Chakrabarti

_____
Dr. Cory Brouwer

©2022
Mukulika Bose
ALL RIGHTS RESERVED

# ABSTRACT

MUKULIKA BOSE. Abrogating the oncogenic signaling associated with tumor MUC1 in Pancreatic Ductal Adenocarcinoma. (Under the direction of DR. PINKU MUKHERJEE)

Pancreatic ductal adenocarcinoma (PDA) is one of the most lethal human cancers. The incidence rate of PDA nearly matches its mortality rate and the best treatment till date is surgical resection for which only 25% are eligible. Tumor recurrence and metastasis are the main causes of cancer-related mortality. MUC1 is a transmembrane glycoprotein expressed on most epithelial cells. It is overexpressed and aberrantly glycosylated in cancer and is known as tumor-associated MUC1 (tMUC1). More than 80% of PDAs express tMUC1. tMUC1 expression is found in the early stages of PDA development with subsequent increase in later stages. Transforming Growth Factor $\beta$ (TGF-$\beta$) is a cytokine that switches from a tumor-suppressor at early stages to a tumor promoter in the late stages of tumor development, by yet unknown mechanisms. Analysis of human PDA samples from TCGA database showed significant differences in gene expression and survival profiles between low and high MUC1 samples. Further, high MUC1 expression was found to positively correlate to TGF-$\beta$RII expression and negatively correlate to TGF-$\beta$RI expression in PDA cell lines. We hypothesized that MUC1 overexpression induces TGF-$\beta$ mediated non-canonical signaling pathway which is known to be associated with poor prognosis. In this study, we report that MUC1 overexpression in PDA cells directly activates the JNK pathway in response to TGF-$\beta$, and leads to increased cell viability via up-regulation and stabilization of c-Myc. Conversely, in low MUC1 expressing PDA cells, TGF-$\beta$ preserves its tumor-suppressive function and inhibits phosphorylation of JNK and stabilization of c-Myc. Knockdown of MUC1 in PDA cells also results in decreased phosphorylation of JNK and c-Myc in response to TGF-$\beta$ treatment. Taken together, the results indicate that overexpression of MUC1 plays a significant role in switching the function of TGF-$\beta$

from a tumor-suppressor to a tumor promoter by directly activating JNK. Lastly, we report that high-MUC1 PDA tumors respond to TGF-$\beta$ neutralizing antibody in vivo showing significantly reduced tumor growth while low-MUC1 tumors do not respond to TGF-$\beta$ neutralizing antibody further confirming our hypothesis. STAT3 is a transcription factor known to regulate proliferation, stemness, migration, invasion and apoptosis in cancer cells in a contextual manner. MUC1 and STAT3 have been reported to be involved in an auto-inductive loop and regulate each other's expressions in cancer cells. Phosphorylation of STAT3 at Y705 residue is associated with its activation and at S727 is related to its degradation, however, the role of differential phosphorylation of STAT3 in regulating cell fate and the factors regulating it have not been fully elucidated. Here we report, that MUC1 expression levels regulate the differential phosphorylation status of STAT3 in PDA cell lines. We report that STAT3-MUC1 pathway is constitively activated in high-MUC1 cancer cells, and therefore these cells are more sensitive to STAT3-inhibitor Napabucasin.

A monoclonal antibody called TAB004, has been developed specifically against human tMUC1 extracellular domain. We report that treatment with TAB004 significantly reduced the colony forming potential and survival of multiple PDA cell lines while sparing normal pancreatic epithelial cell line. Binding of TAB004 to tMUC1 induced cytoskeleton remodeling, ER stress and anoikis in PDA cells. The mechanisms underlying the anti-tumor effects of TAB004 were found to be reduced activation of the EGFR-PI3K signaling pathway, and degradation of tMUC1, thereby reducing its binding to the desmosomal proteins desmoplakin and junction plakoglobin ($\gamma$-catenin) and $\beta$-catenin and other oncogenic partners, thus compromising the ability of the cells to form colonies. Furthermore, TAB004 treatment reduced expression of the transcriptional targets of MUC1, for example, c-SRC and c-MYC. These reduction in oncogenic signaling triggered anoikis as measured by reduced expression of anti-apoptotic proteins, PTRH2 and BCL2. TAB004 treatment slowed the growth of

PDA xenograft compared to IgG control and enhanced survival of mice when combined with 5-FU. Since TAB004 significantly reduced colony forming potential and triggered anoikis in the PDA cells, we suggest that it could be used as a potential prophylactic agent to curb tumor relapse after surgery, prevent metastasis and help increase the efficacy of chemotherapeutic agents.

# DEDICATION

I would like to dedicate my dissertation to all my teachers (gurus) in life, starting with my parents Advocate Somenath Bose, Mrs. Kantasree Basu, grandparents Late Shri Benimadhab Bose and Smt. Bijoli Basu and my parents-in-law Mr. Sujoy Mitra and Mrs. Anjana Mitra. Especially, my mother, since I believe that I have gathered the courage to move out of my comfort zone and become the best version of myself looking only at her sacrifices in life. She had the grades and the brain to become a scientist and a physician, but had to sacrifice her career goals owing to unforeseen circumstances. However, I am thankful to the Almighty for having me fulfill my mother's dream through myself. I appreciate my father for being a rare combination of a strict but modern dad who always had my back through thick and thin. I have never felt the existence of a pressurizing society that would deter me from achieving my goals, thanks to him. My grandmother is a champion in her own way, from whom I have learnt how to be absolutely fearless and independent. I am grateful to my in-laws for their incredible support and for being my greatest cheerleaders. In addition to that, I would like to dedicate my dissertation to the wonderful mentors who I came across in my academic journey and who I draw inspiration from as eminent scientists as well as beautiful human beings. Professor Jayanta K. Pal, Dr. Shilpy Sharma, Dr. Bhaskar Gupta, Dr. Debanjan Mukhopadhyay and my Ph.D. advisor Professor Pinku Mukherjee. They have encouraged me to never settle for the less and have trusted in my potential. Prof. Mukherjee has a magnetic personality and is a gem of a person. Thanks to the Almighty for blessing me with such incredible mentors who have catalysed my psychological and intellectual evolution. Last but not the least, my husband, Dr. Bhaskar Mitra deserves a special mention for always trusting me and standing by my decisions.

# ACKNOWLEDGEMENTS

I would like to thoroughly express gratitude towards my Ph.D. advisor Professor Pinku Mukherjee for giving me this golden opportunity to realize my own worth and put my best foot forward. She has always provided the best guidance as an academic supervisor as well as a guardian. I would also like to whole-heartedly thank my Ph.D. dissertation committee members, Professor Shan Yan, Professor Didier Dreau, Professor Kausik Chakrabarti and Professor Cory Brouwer for their immense support and valuable advice. I am very thankful to Dr. Ru Zhou, Dr. Chandrav De, Ms. Sophia Shwartz, Ms. Priyanka Lala, Mr. Manuel Rodriguez Cardona and all the past members of the Mukherjee lab. Thanks a lot J. Alexa Sanders from the Department of Bioinformatics, UNCC, for collaborating with me on four papers. It is due to her support that we have been able to publish clinically relevant data in the journals. I am thankful to Professor Mukherjee's Irwin Belk Distinguished Professor Endowment funds and her Federal Grants from the National Institute of Health (NIH) and Department of Defense (DoD) for funding my research and stipend as a Research Assistant. I would like to acknowledge the Graduate School at UNC Charlotte for supporting me with the Graduate Assistant Support Plan and the Graduate Summer Scholarships. I would like to express my deepest gratitude to Dean Thomas L. Reynolds for supporting my work with the Thomas L. Reynolds Fellowship for two consecutive years and inducting me into the prestigious Phi Kappa Phi Honor Society UNC Charlotte Chapter. I would like to thank the Philanthropic Educational Organization (P.E.O.) for providing me with the P.E.O. International Peace Scholarship. I am extremely grateful to the Phi Kappa Phi Honor Society for selecting me as one of the ten students nationally to receive the Phi Kappa Phi Dissertation Fellowship, 2022.

TABLE OF CONTENTS

# LIST OF TABLES

# LIST OF FIGURES

# LIST OF ABBREVIATIONS

5-FU 5-Fluoro Uracil

ADCC Antibody Dependent Cellular Cytotoxity

ADCP Antibody Dependent Cellular Phagocytosis

AMH Anti-M*ü*llerian hormone

ANOVA Analysis of Variance

Apaf1 Apoptotic protease activating factor 1

ATCC American Tissue Culture Type

ATF4 Activating Transcription Factor 4

Bcl2 B-Cell Leukemia/Lymphoma 2

BIP Binding Immunoglobulin Protein

BIT-1 Bcl Inhibitor of Transcription-1

BM-MSC Bone Marrow-Derived Mesenchymal Stem Cell

BMP Bone Morphogenetic Protein

BsAbs Bispecific Antibodies

CanAg Cancer Antigen

CAR-T Chimeric Antigen Receptor-T

COX IV Cytochrome c oxidase subunit 4

CSC Cancer Stem Cell

Ctrl Control

DAVID Database for Annotation, Visualization and Integrated Discovery

DEG Differentially Expressed Genes

DGCA Differential Gene Correlation Analysis

DMEM Dulbecco's Modified Essential Medium

ECM Extracellular Matrix

EF2 Elongation Factor-2

EGF Epidermal Growth Factor

EGFR Epidermal Growth Factor Receptor

EMT Epithelial-to-Mesenchymal Transition

EMT-TF Epithelial-to-mesenchymal Transition-Transcription Factor

ER Endoplasmic Reticulum

FAK Focal Adhesion Kinase

FGF Fibroblast Growth Factor

FITC Fluorescein isothiocyanate

G418 Geneticin

GI Gastro Intestinal

GPCR G-Protein Coupled Receptor

HCC Hepatocellular Carcinoma

HIF-1 Hypoxia Inducible Factor-1

HMFG1 Human Milk Fat Globule1

HPDE Human Pancreatic Ductal Epithelial

HSP Heat Shock Protein

IACUC Institutional Animal Care and Use Committee

IC Inhibitory Concentration

IgG Immunoglobulin $\gamma$

IL Interleukin

JC-1 cationic carbocyanine dye

JNK Jun N-terminal Kinase

KD Knock Down

kDa kilo Dalton

KEGG Kyoto Encyclopedia of Genes and Genomes

KLH keyhole limpet hemocyanin

KO Knock Out

MAPK Mitogen Activated Protein Kinase

MET Mesenchymal-to-Epithelial Transition

MTT 3-(4, 5-dimethylthiazolyl-2)-2, 5-diphenyltetrazolium bromide

MUC1 Mucin1

MUC1-CT Mucin1-Cytoplasmic Tail

MUC1-CTF Mucin1-C-terminal fraction

MUC1-ECD Mucin1-Extracellular Domain

MUC1-N Mucin1-N terminal

MUC1-TMD Mucin1 Transmembrane Domain

Neo Neomycin

NK cells Natural Killer cells

NMR Nuclear Magnetic Resonance

NS non-significant

OS Overall Survival

PanIN Pancreatic Intraepithelial Neoplasia

PBS Phosphate Buffered Saline

PDA Pancreatuc Ductal Adenocarcinoma

PIK3R Phospho Inositide Kinase 3 Receptor

PPI Protein-Protein Interaction

PSM Peptide Spectrum Matches

pSTAT3 phosphorylated STAT3

PTRH2 Peptidyl-tRNA hydrolase 2

RASD1 Ras Related Dexamethasone Induced 1

RNA-seg RNA-sequencing

ROS Reactive Oxygen Species

RPMI Roswell Park Memorial Institute

SEA domain Sperm protein Enterokinase and Agrin domain

SEM Standard Error of Mean

siRNA small interfering RNA

SMAD Suppressor of Mothers against Decapentaplegic

SOX2 SRY-Box Transcription Factor 2

STAT3 Signal Transducer and Activator of Transcription3

TCGA The Cancer Genome Atlas

TGF-$\beta$ Transforming Growth Factor-$\beta$

TME Tumor Micro-Environment

tMUC1 tumor-Mucin1

TR Tandem Repeat

UBE2S Ubiquitin-conjugating Enzyme E2S

VEGF Vascular Endothelial Growth Factor

VHH antibodies Variable Domain Of Heavy-chain Antibodies

VNTR Variable Number Tandem Repeat

WWP1 WW Domain Containing E3 Ubiquitin Protein Ligase 1

# PREFACE

All of the work presented henceforth was conducted in the laboratory of Prof. Pinku Mukherjee in the Department of Biological Sciences at UNC Charlotte. All projects and associated methods were approved by the UNC Charlotte Research Ethics Board and IACUC. Some parts of Chapter 1 has been published as a review article in Trends in Molecular Medicine. A version of Chapter 2 has been published in Frontiers in Cell and Developmental Biology. A version of Chapter 3 will be submitted for publication in future. Chapter 4 has been published as a review article in Vaccines. A version of Chapter 5 has been published as a research article where the antibody has been developed by Prof. Mukherjee's group, and I was responsible for conceptualization, data collection, analysis and composition of the manuscript. Alexa Sanders was responsible for the TCGA data analysis and Dr. Chandrav De, Dr. Ru Zhou and Ms. Sophia Shwartz helped with the animal work.

I was the lead investigator for the projects mentioned in Chapters 2, 3 and 5 where I was responsible for all major areas of concept formation, data collection and analysis, as well as the majority of manuscript composition with revisions from Prof. Pinku Mukherjee.

# CHAPTER 1: INTRODUCTION

The pancreas is a 6 to 8 inches long organ located deeply and horizontally across the abdomen. One part of the pancreas is in between the stomach and the spine and the other part is located in the curved area of the duodenum. As shown in Figure 1.1, the pancreas can be divided into four parts. 1) Head - The head is the widest part of the pancreas found in the right side of abdomen, in the curve of the duodenum, 2) Neck - The neck is the thin section of the gland between the head and the body of the pancreas, 3) Body - This is the middle part between the neck and the tail. The superior mesenteric artery and vein run behind this part and 4) Tail - The tail is the thin tip of the pancreas in the left side of the abdomen, nearest to the spleen. The pancreatic duct runs along the length of the pancreas, and is joined by several small branches from the glandular tissue. The end of this duct is connected to the hepatobiliary duct, which delivers bile to the small intestine. (https://pathology.jhu.edu/pancreas/basics).

Around 95% of the pancreas is exocrine tissue that produces pancreatic enzymes to help in digestion. The other 5% consists of endocrine cells known as islets of Langerhans. The islets consist of $\gamma$, $\beta$, $\delta$ and P (F) cells that secrete glucagon, insulin, somatostatin, and pancreatic polypeptide respectively (https://www.medicalnewstoday.com/articles/10011#features).

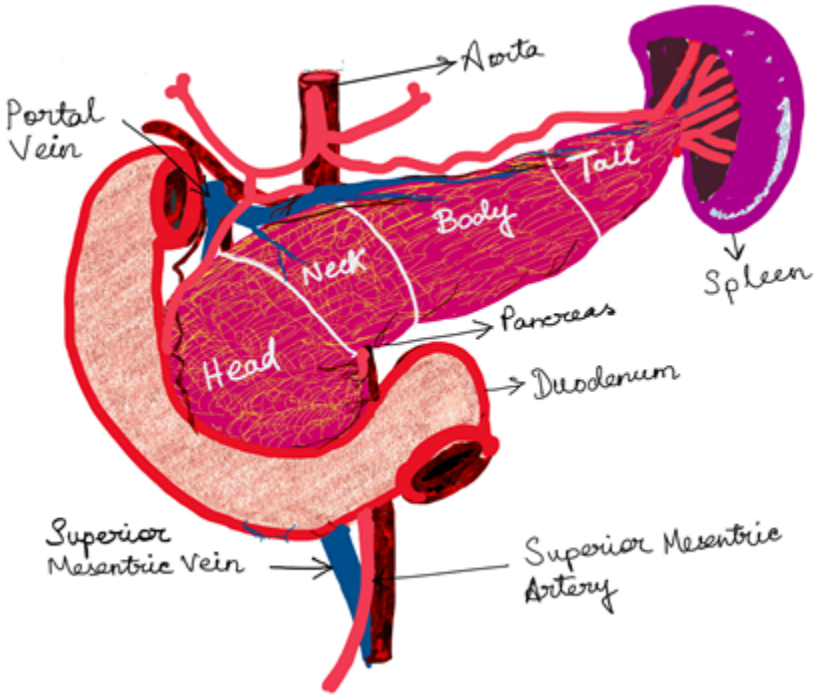


Figure 1.1: The anatomy of human pancreas

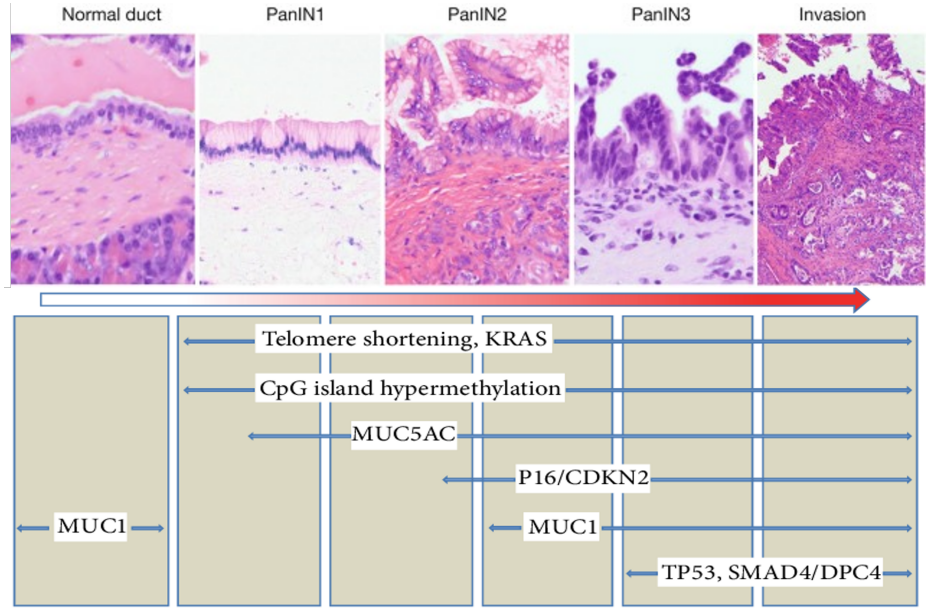


Figure 1.2: Stages of Pancreatic Intraepithelial Neoplasia (PanIN) lesions showing the timing of genetic aberrations associated with each stage of disease progression.

### 1.0.1 Pancreatic Cancer

Due to the deep location of the pancreas, most pancreatic tumors cannot be detected at early stages. There is a lack of symptoms of pancreatic cancer usually until the tumor begins to interfere with the normal function of the pancreas or other nearby organs. This leads to clinical detection at a very advanced stage leading to poor prognosis. Pancreatic tumors are mainly of two types. Pancreatic Ductal Adenocarcinoma (PDA), that arises in the exocrine cells of the duct or the acinar cells that secrete enzymes into the bile duct and Pancreatic Neuroendocrine Tumors or PanNETS that arise in the hormone-secreting endocrine cells. Neuroendocrine tumors make for only 5% of all pancreatic cancers (https://www.cancer.org/cancer/pancreatic-cancer/about/new-research.html). About 95% of all pancreatic tumors are Pancreatic Ductal Adenocarcinoma. It is the 13th most commonly diagnosed cancer worldwide. PDA is the 3rd leading cause of cancer-related deaths in the USA with a dismal 5-year survival rate of 11.5%, which is the lowest of all major cancers (https://seer.cancer.gov/statfacts/html/pancreas.html). In the past forty years, there has been no improvement in the therapy for PDA mainly due to late detection, highly fibrotic and resistant tumors and recurrence. The pancreas in located very close to the liver and touches the superior mesentric artery and vein, thus metastasis is common, making the prognosis worse. As shown in Figure 1.2, PanINs are microscopic (usually $<$ 5mm) flat or papillary lesions arising in the pancreatic ducts and are composed of columnar to cuboidal cells with varying amounts of mucin. They are classified into three grades: PanIN1A (flat) and PanIN-1B (papillary) are low-grade lesions with minimal cytological and architectural atypia. PanIN-2 lesions (intermediate-grade PanIN) show mild to moderate cytological and architectural atypia with frequent papillae. High-grade PanINs (PanIN3) are characterized by severe cytological and architectural atypia. PanIN-3 is also referred to as ‘carcinoma in situ‘. All PanINs are noninvasive lesions that do not invade the basement membrane. Pancreatic carcino-

genesis is thought to progress from low-grade to high-grade PanIN and then to invasive cancer; this histological progression is accompanied by the accumulation of genetic changes. The immunohistochemical characteristics of PanINs vary with the grade of dysplasia. MUC1, MUC2, and MUC5AC are frequently overexpressed in epithelial cancers of the gastrointestinal tract. MUC1 is typically expressed by the pancreatic ducts and acinar cells and is responsible for the surveillance of lumen formation. It is almost exclusively expressed in the higher-graded lesions (PanIN-2 PanIN-3) and often associated with an invasive PDA (https://pathology.jhu.edu/pancreas/medical-professionals/duct-lesions).

### 1.0.2 Treatment options

The best treatment option is surgical resection with chemotherapy and is beneficial in patients whose cancer cells have not spread to other abdominal vessels and adjacent organs. The most common option is the pancreatoduodenectomy (Whipple procedure) in which surgeons remove the head of the pancreas, the gallbladder, and the bile duct, and some portions of the stomach and small intestine. However, the proximity of the pancreas to major blood vessels, bile duct and intestine makes surgery very difficult. The American Society of Clinical Oncology estimates that only about 20% of patients are eligible for surgery.

The major challenges in treating PDA are both at the genetic and cellular levels. There are innumerable mutational changes that generate genetic instability and heterogeneity, thus giving rise to tumor growth and resistance to treatments. The heterogeneity is found not only among patients but also within a single primary tumor. There is a variety of mutations that leads to PDA, and each mutation is present in a small percentage of patients, making it difficult to find molecular subtypes [1, 2]. Multiple signaling pathway alterations could explain the presence of multiple resistance mechanisms to a certain extent. Some of the key mutations identified are KRAS, CDKN2A/p16, TP53 and SMAD4 with the concomitant activation of downstream

signaling pathways [3]. Moreover, the cancer stem cells (CSCs) contribute to the acquisition of a more dormant, plastic and resistant tumor state. Pancreatic CSCs account for 0.5%-1.0% of all pancreatic cancer cells; they have an increased capacity for self-renewal and have unique metabolic and chemoresistance properties that put them at an advantage to escape therapeutic interventions, leading to disease progression and relapse. One of the reasons for the failure of current therapies in clinic is that they are not adequately designed to target CSCs. In addition, PDA metastasizes microscopically very early in the disease course, thus limiting the effectiveness of surgery, chemotherapy and radiation [4]. Several studies have reported that components within the PDA microenvironment are responsible for poor prognosis and the difficulty in targeting the tumor cells. The PDA tumor micro-environment (TME) is characterized by dense desmoplasia and immunosuppression. Extensive desmoplasia results in decreased stromal vascularization, reduced immune cell infiltration and hypoxia, inducing aggressive tumor growth and blocking drugs from entering the cells.

The PDA cells have hyperactivated EGFR, MAPK, PI3K, TGF-$\beta$, STAT3, c-SRC, c-MYC and other signaling pathways that provide increased capacity for self-renewal, drug-resistance, migration, invasion and resistance to apoptosis and anoikis.

Anoikis is a form of apoptosis that occurs in epithelial cells when they detach from the extracellular matrix or other surrounding cells. Anoikis resistance is a hallmark of cancer metastasis as it confers the ability to evade cell death in disseminated cells, so that they can remain in a dormant stage while migrating to different locations and then colonize after finding a favorable niche. This leads to a secondary tumor and metastasis, the main cause of cancer mortality. The plasticity of the cancer cells allows them to adopt a quasi-mesenchymal phenotype that they use to disseminate from the primary tumor. This adaptation is called Epithelial-to-Mesenchymal Transition (EMT), where the cells down-regulate expression of epithelial markers and concomitantly up-regulate mesenchymal markers on the surface. This phenotype facilitates

in migration of cells from one location to another. However, for successful secondary tumor to form, the quasi-mesenchymal cells need to revert back to an epithelial stage to form colonies at the new anatomic site. This reversion is called Mesenchymal-to-Epithelial Transition (MET). EMT is a known hallmark of metastasis, however, only EMT is not sufficient to cause recurrence or metastasis. Unless the cells can undergo MET to colonize the secondary site, there is no tumor formed. Many oncogenic factors help the cancer cells maintain this plasticity and help them adapt according to the situation [5]. These factors include but are not limited to hyperactivated EGFR, TGF-$\beta$, c-SRC, c-MYC and STAT3.

### 1.0.3 Mucin1

Mucin1 or MUC1 is a heterodimeric transmembrane glycoprotein that is normally expressed on the surface of most glandular or luminal epithelial cells of the mammary gland, esophagus, stomach, duodenum, pancreas, uterus, prostate, and lungs, and is also found in hematopoietic cells. In normal cells, MUC1 is only expressed on the apical surface and is heavily glycosylated with the core peptide sequestered by the carbohydrate residues (Figure 1.3). During the malignant transformation of cells, there is a manifold increase in the expression of MUC1, and due to the loss of apico-basal polarity of the cancer cell, MUC1 is found all around the cell surface and in the cytoplasm. Moreover, there is aberrant and hypo-glycosylation of the extracellular domain (ECD), thus exposing the core peptide. This form of MUC1 is called the tumor-associated MUC1 or tMUC1. Due to its presence in most epithelial tumors and the distinction between the normal and the tumor forms, MUC1 was ranked as the second most targetable antigen out of 75 to develop cancer vaccines by the National Cancer Institute in 2009 [6].

MUC1 was the first mucin to be structurally characterized and plays a dynamic role as a host mucosal barrier to infection [7, 8]. In epithelial cells it has an anti-inflammatory role, however, after interaction with a pathogen for a long time, it can

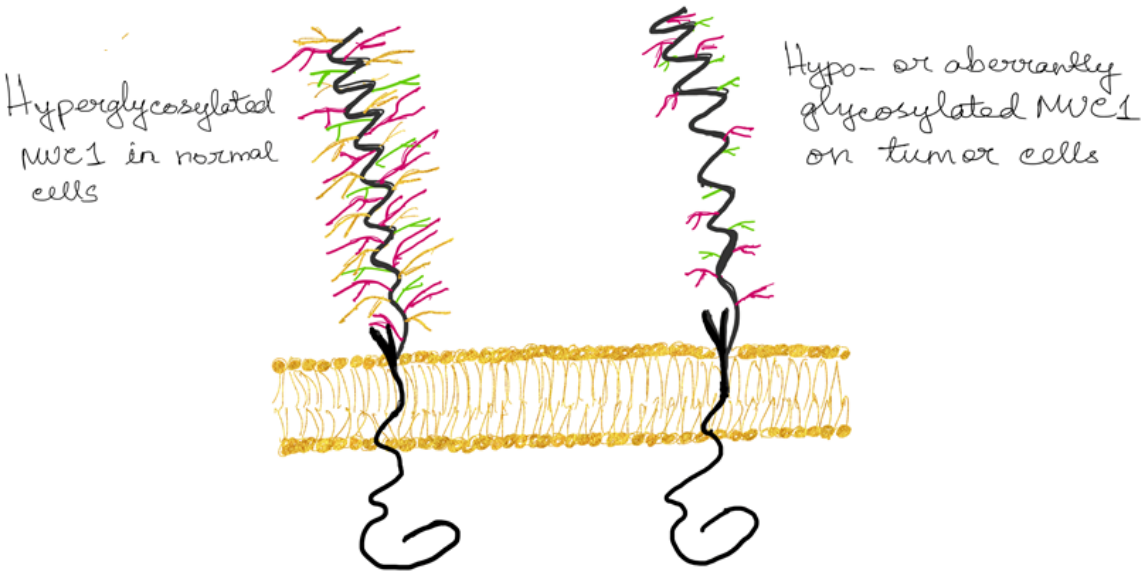


Figure 1.3: The extracellular N-terminal domain of MUC1 on a normal cell (left) is hyperglycosylated and that of MUC1 on a tumor cell (right) is aberrantly glycosylated.

have a pro-inflammatory role as well. These dynamic changes potentiate initiation of infection-induced cancers and the susceptibility of an individual to developing a certain type of infection-induced cancer is regulated, at least in part, by the individual's glycome signature. The crosstalk of MUC1 with microbes and the role it plays in development of diseases in terms of the glyco-evasion hypothesis has been well documented [9].

### 1.0.4 Structure

MUC1 is a single-pass type I transmembrane glycoprotein with a hyperglycosylated extracellular domain (ECD). This ECD extends up to 200-500 nm from the cell surface [10, 8]. In healthy tissues, MUC1 provides protection to the underlying epithelia. The extended sugar residues have a negative charge and form a physical barrier, conferring an anti-adhesive property on MUC1, which in turn prevents entry of pathogens. The chains of glycosyl residues form oligomers and give rise to a mucinous gel that has lubricating properties. This lubrication protects the underlying epithelia against

desiccation, alterations in pH, and microbial infections [6]. Phosphorylation of the intracellular cytoplasmic tail (MUC1-CT) leads to activation of downstream signaling pathways. The turnover rate of MUC1 is probably maintained by a phenomenon known as 'shedding', in which the CT is separated from the ECD by proteolysis [7, 11]. The mechanism of MUC1 shedding is well documented [12]. MUC1-ECD can bind to bacteria and be shed from the epithelial surface. This shedding could lead to phosphorylation of MUC1-CT, thus regulating inflammatory responses, epithelial cell adhesion, differentiation, and apoptosis. The direct link between MUC1-ECD shedding and activation of the MUC1-CT is not well established. However, it is known that MUC1 acts as a signaling receptor that senses external environmental cues and activates intracellular signaling pathways [6, 12].

Based on the N-glycosylation state of the ECD, the molecular weight of MUC1-C can vary from 17 to 25 kDa. Under normal conditions, MUC1 exists on the plasma membrane as a heterodimeric complex. However, the complex dissociates following stimulation with the proinflammatory cytokines interferon-$\gamma$ (IFN-$\gamma$) and tumor necrosis factor-$\alpha$ (TNF-$\alpha$), and this is catalyzed by the sheddase activities of the enzymes TNF-$\alpha$ converting enzyme (TACE), also called disintegrin and metalloprotease domain containing protein-17(ADAM17) and matrix metalloproteases (MMPs). These enzymes cause release of MUC1-N from MUC1-C, and also catalyze the cleavage of the ECD of MUC1-C, thereby generating smaller peptide fragments MUC1* and MUC1-CTF15 [13, 14, 15]. These cleavage products of sheddases contain a shorter ECD. MUC1* consists of a 45 amino acid ECD and promotes tumor growth [16]. MUC1* has also been detected in human embryonic stem cells (hESCs), where it functions as a growth factor receptor for a metastasis-associated protein (NM23-H1) [17]. MUC1 CTF15 contains a shorter ECD chain of 27 amino acids that is recognized by nicartrin, a substrate receptor for $\gamma$-secretase. $\gamma$-Secretase further cleaves MUC1-C into shorter peptide fragments with a molecular mass of 8-10 kDa, which

are rapidly degraded. In most normal and tumor cells, MUC1 CTF15 is undetectable as it is rapidly degraded [18].

MUC1-C is short, comprising a 58 amino acid ECD, a 28 amino acid transmembrane domain (TMD), and a 72 amino acid cytoplasmic tail (CT). The MUC1-CT has seven tyrosine residues that are highly conserved across all mammalian species. These are phosphorylated and the CT acts as a binding site for various kinases and protooncogenes. Following phosphorylation of these tyrosine residues, and cleavage of MUC1-CT from the MUC1-ECD, the CT binds to transcription factors and is translocated into the nucleus where it drives transcription of oncogenes. MUC1-CT itself does not have a DNA-binding domain, but it acts as a transcriptional coactivator that aids in binding of other transcription factors to target gene promoters [6].

Figure 1.4 shows that the cytoplasmic tail of MUC1 is a busy docking site for many kinases that phosphorylate and activate MUC1-downstream oncogenic signaling. As a result of this activation, there is increased proliferation, survival, migration in cancer cells.

Figure 1.6 shows that the functions of the extracellular domain of tMUC1 include but are not limited to cell-cell adhesion and anti-adhesion, invasion, migration and metastasis. The intracellular cytoplasmic tail binds to several protooncogenes and acts as a cotranscription factor to drive tumorigenesis.

MUC1 is regulated at the transcriptional level by multiple factors, including the hypoxia inducible factor 1 $\alpha$ (HIF1-$\alpha$) and STATs in response to interferon $\gamma$ (IFN$\gamma$) and interleukin-6 (IL6) signaling [19, 20]. In addition, EGFR can also activate STAT3 in breast cancer tissues [21] and EGFR activation promotes MUC1 expression [22]. Intriguingly, MUC1 binds to the proximal promoter of EGFR and enhances its expression [23] and regulates its localization as well [24].

In Figure 1.6, the cytoplasmic domain of MUC1 is phosphorylated by EGFR and

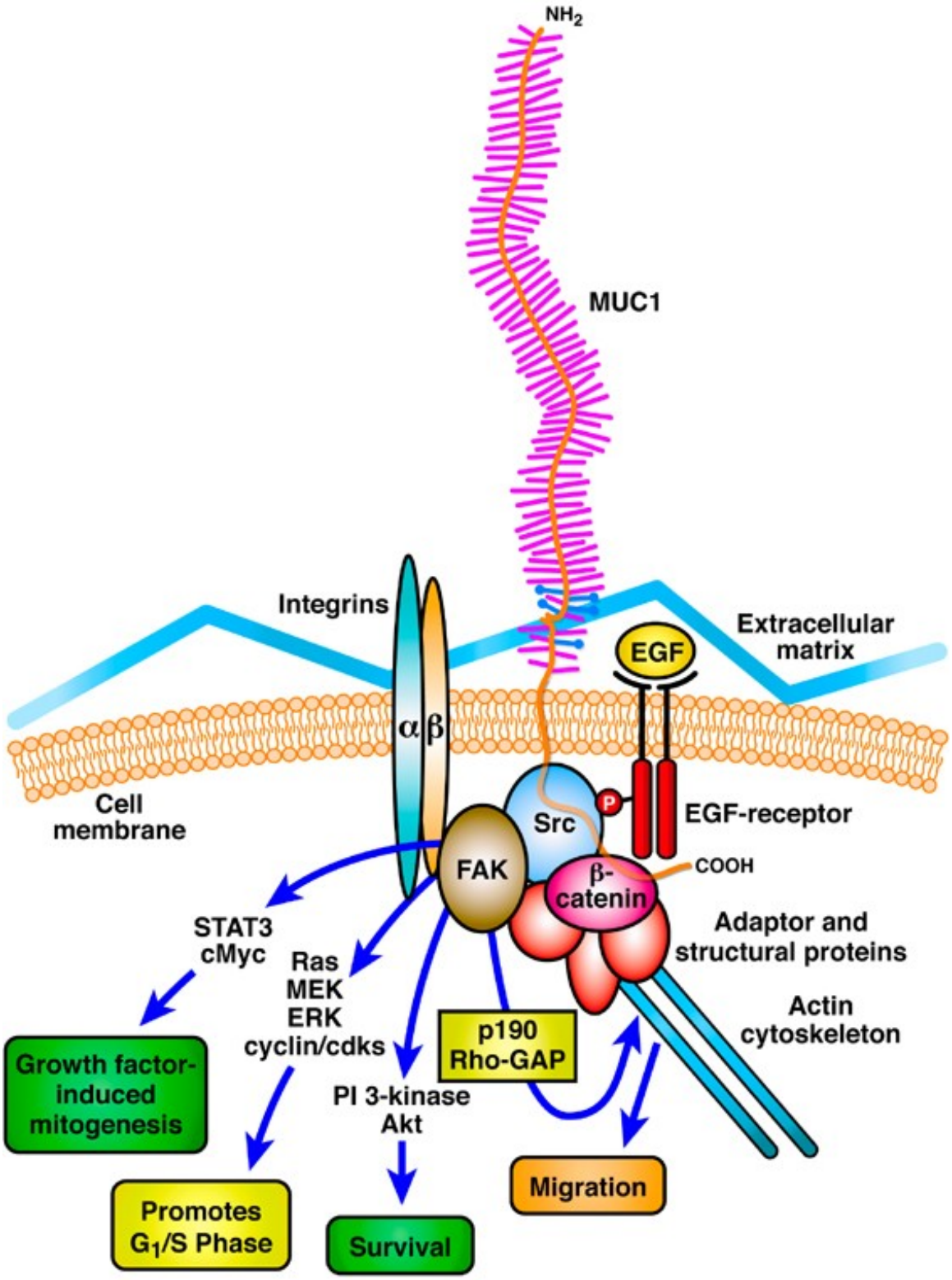


Figure 1.4: The cytoplasmic tail of MUC1.

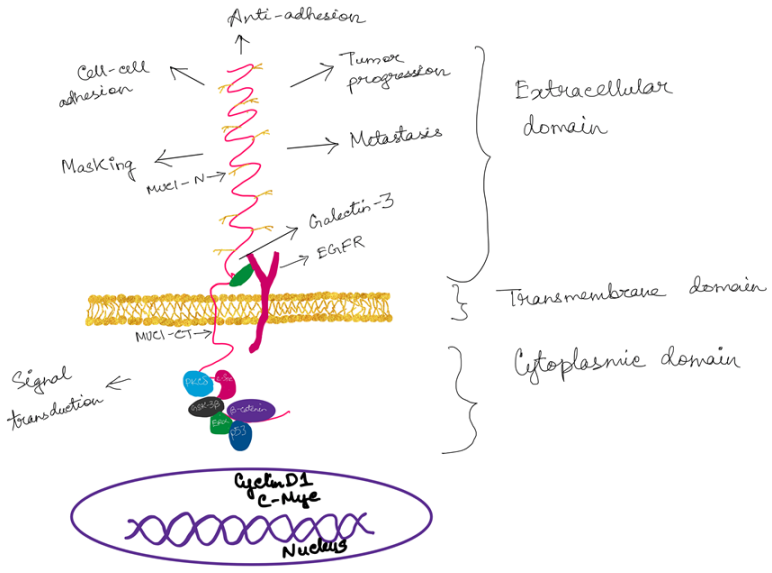


Figure 1.5: The functions of the extracellular domain of tumor-MUC1.

Src, among other proteins, and Src phosphorylation can induce rac activity and cytoskeletal change leading to an increase in cell motility. Phosphorylation by EGFR promotes cell motility, and interaction with HiF1-$\alpha$ drives PDGF-A transcription, positively affecting $\beta$-catenin transcriptional activity [25]. The cytoplasmic domain of MUC1 interacts with cofactors, such as $\beta$-catenin, p120-catenin, and estrogen receptor $\beta$ among other transcription factors, promoting nuclear translocation of these proteins and driving expression of Epithelial-to-Mesenchymal Transition (EMT) genes [25]. MUC1 expression is upregulated by STAT1/STAT3 binding to the MUC1 promoter, and MUC1 mRNA is downregulated by binding of mir-125b/mir-145. Picture has been adapted from [25].

MUC1 overexpression is sufficient to induce transformation [26]. MUC1 is translated from a single transcript into a polypeptide that undergoes autocleavage into two subunits, which in turn form a heterodimer. MUC1 thus consists of an extracellular N-terminal mucin subunit (MUC1-N) that forms a complex with the transmembrane C-terminal subunit (MUC1-C) [27]. MUC1-C contains a 58 amino acid extracellu-

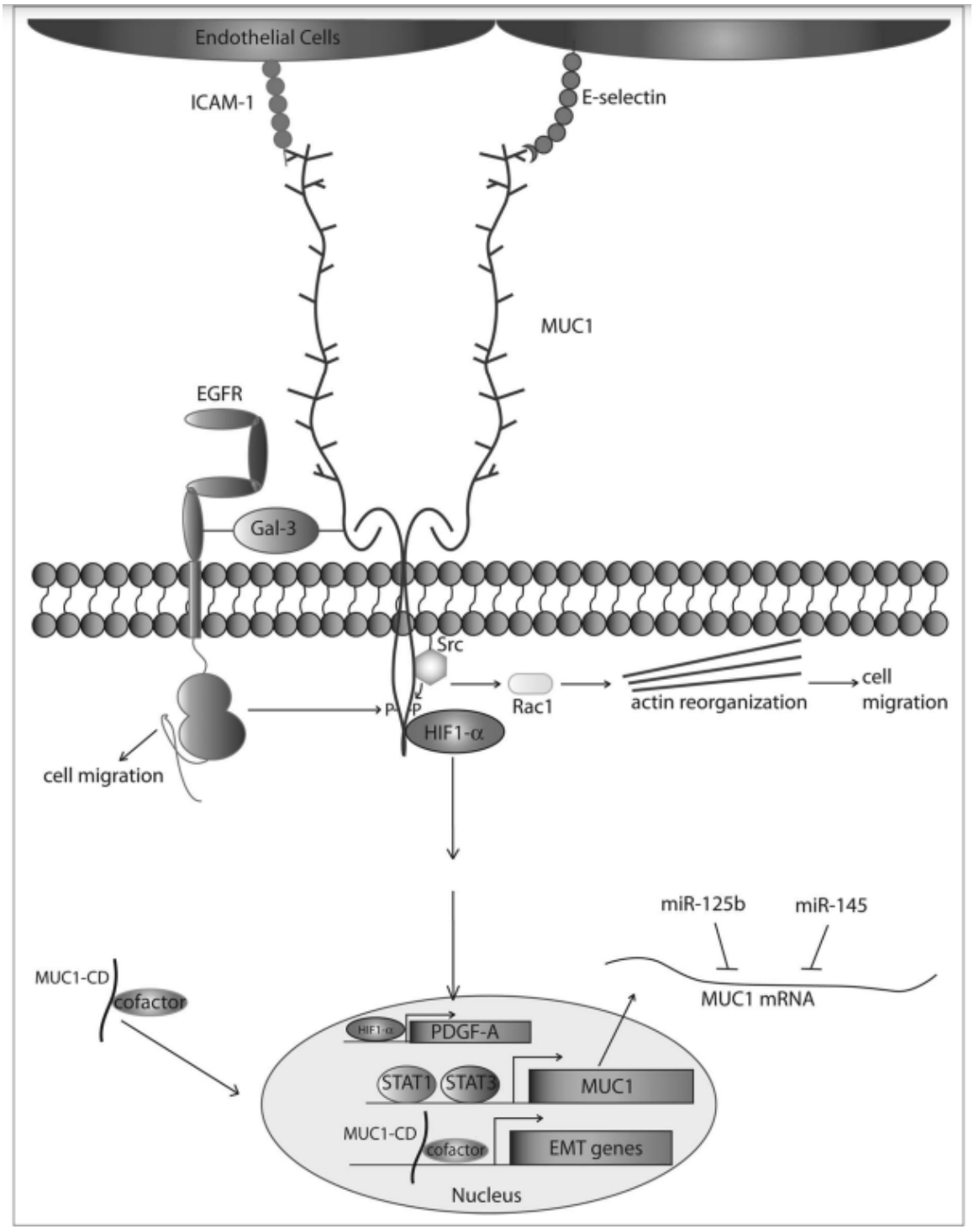


Figure 1.6: MUC1 drives metastatic progression. The protein core of underglycosylated MUC1 interacts with iCAM-1, e-selectin, and Galectin-3 using the extracellular domain.

lar domain that interacts with galectin-3 and thereby forms complexes with EGFR [28] and a cytoplasmic domain consisting of 72 amino acids including a Cys-Glu-Cys (CQC) motif necessary for MUC1-C oligomerization and function [29]. The MUC1 cytoplasmic domain (MUC1-CD) also contains sites that function as substrates for phosphorylation by EGFR, c-Met, c-Src, c-Abl, glycogen synthase kinase $3\beta$, and protein kinase C [30]. MUC1-CD binds directly to the Wnt effector $\beta$-catenin and contributes to activation of the Wnt pathway [30]. c-Src phosphorylation of MUC1-CD increases the binding of MUC1-CD to $\beta$-catenin [30]. MUC1-CD also interacts with the inhibitor of $\kappa$B kinase (IKK) complex and RelA, and contributes to activation of the NF-$\kappa$B pathway [31, 32]. MUC1-C thus has the potential for multiple functions in cell signaling and gene regulation as an adaptor or scaffold for interactions with client proteins that, in certain settings, are regulated by MUC1-CD phosphorylation [30].

MUC1 mediates production of growth factors such as connective tissue growth factor (CTGF), platelet-derived growth factor A (PDGF-A), and PDGF-B that promote activation of the MAPK and PI3K/Akt pathways, potentiating proliferation and survival of tumor cells [33, 34, 35, 36]. Upon epidermal growth factor (EGF) stimulation, MUC1-C directly associates with epidermal growth factor receptor (EGFR) and translocates to the nucleus. It subsequently binds to cyclin D1 (CCND1) and v-myb myeloblastosis viral oncogene homolog-like 2 (MYBL2) promoters enabling G1/S phase gene expression [24].

It is postulated that altered glycosylation enables tMUC1 to function as a ligand for cell adhesion molecules such as selectins and intercellular adhesion molecule-1 (I-CAMs), aiding adherence of MUC1-expressing circulating tumor cells (CTCs) to endothelial cells and seeding at distant sites that establishes secondary tumors [37]. Selectins are known to bind the carbohydrate epitope sLeX [38]. In colon cancer cells, increases in sLeX expression on MUC1 are associated with high metastasis [39], as

this antigen interacts with E and P selectins. In melanoma, MUC1 overexpression interferes with integrin-mediated cell adhesion to the extracellular matrix, increasing cancer cell invasiveness [40]. MUC1 is known to bind to several cytoskeletal and desmosomal proteins, for example, Desmoplakin, Junction Plakoglobin ($\gamma$-catenin), Keratins, Galectins etc. and helps in establishment of colonies during secondary tumor formation. MUC1 enhances CIN85-dependent breast cancer cell migration and invasion in vitro [41]. However, ectopic expression of MUC1 enhances the motility induced by CIN85. When tested in vivo in a tumor metastasis mouse model of B16 melanoma, CIN85-depleted melanoma cells exhibited few or no lung metastasis and, overexpression of MUC1 recovered the shCIN85-reduced metastatic process. CIN85/MUC1 complex was reported to be associated with invadopodia-related molecules in promoting the invasive and metastatic potential of breast cancer [41].

Most anticancer treatments work by inducing apoptosis in cancer cells. However, many cancer cells acquire apoptotic pathway defects and, therefore, do not respond to these treatments. MUC1 assists cancer cells in evading cell death by preventing the activation of the extrinsic as well as intrinsic apoptotic pathway. MUC1-CT is known to bind to the p18 subunit of Caspase 8 and competitively inhibit its binding to FADD, thus blocking activation of the extrinsic apoptosis. In 3Y1 rat fibroblasts, MUC1 overexpression selectively upregulates expression of the antiapoptotic protein, B cell lymphoma extra-large (Bcl-xL), and inactivates the proapoptotic protein, Bcl2-associated agonist of cell death (Bad) [34]. In hypoxic cells, elevated reactive oxygen species (ROS) levels can activate apoptotic pathways. However, MUC1 overexpression decreases intracellular ROS levels by upregulating the expression of superoxide dismutase, catalase, and glutathione peroxidase [42]. It has been reported that MUC1 blocks hypoxia-induced cell death in colon cancer cells by mediating decreases in intracellular ROS concentration and reducing prolyl hydrolase-3 (PHD-3) activity that suppresses HIF-1$\alpha$ stability [43]. MUC1 is known to bind HSP-70 and translocate

into the mitochondria and block release of cytochrome-C into the cytoplasm. This blocks the mitochondrial or intrinsic apoptotic pathway.

Another common mechanism by which cancer cells evade drug-induced cell death is via upregulation of adenosine triphosphate (ATP)-dependent membrane efflux pumps or ATP-binding cassette (ABC) transporters. It has been shown that MUC1 increases resistance to chemotherapeutic drugs by upregulating multidrug resistance genes and protein expression, in particular, multidrug resistance protein 1 (MRP1) [44] and upregulation of the PI3K-Akt pathway[45].

### 1.0.5 MUC1-CT signaling

MUC1-CT translocates to the nucleus in association with $\beta$-catenin, represses E-CADHERIN expression, and upregulates expression of the EMT inducers Snail, Slug, Vimentin, and Twist [46]. As a consequence, the adherens junctions are destabilized and profound cytoskeleton rearrangement occurs, reducing contacts between cancer cells and facilitating basement membrane invasion. MUC1 also induces EMT at the post-transcriptional level by modulating the expression of miRNAs that control EMT-related gene expression. In addition, PDGF-B stimulation promotes nuclear localization of the MUC1 CT/$\beta$ catenin transcriptional complex, increasing the invasive potential of PDA cells [47]. Furthermore, MUC1 associates with Cbl-interacting protein of 85 kDa (CIN85) and colocalizes to the invadopodia-like structures aiding breast cancer cell invasion [41]. Such mechanisms could account for clinical findings that MUC1 overexpression leads to metastasis and poor prognosis in pancreas, gall bladder, and colon cancer patients [48, 49, 50]. The tMUC1 undergoes interactions with many transmembrane receptors and components of the extracellular matrix, such as ICAM-1, an adhesion receptor on the surface of endothelial and peritumoral stromal cells, E-selectin, a receptor present on the endothelial cell surface. In addition, interactions between MUC1 and E-selectin may promote MUC1 binding to ICAM-1 on the endothelial cell surface. The MUC1-ICAM-1 interaction promotes

the migratory capacity of tumor cells through the microenvironment, by facilitating interaction between epithelial and endothelial cells, enabling adhesion of circulating cancer cells to the inner lining of the blood vessel, slowing cell velocity and allowing escape from the blood vessel. Furthermore, upon interacting with ICAM-1, Src interacts with the MUC1-CD, an interaction that promotes Src-mediated cytoskeletal rearrangements. The Src family of nonreceptor tyrosine kinases, through their ability to regulate integrin activation and cytoskeletal function, has long been regarded as key mediators of metastatic progression. Plakoglobin (also known as $\gamma$-catenin) is an adaptor protein found in both desmosomes and adherens junctions, and it also localizes to nuclei in various cells [51, 52]. Proteins that interact with plakoglobin include classic and desmosomal cadherins, $\alpha$-catenin, plakophilins, and desmoplakin [53, 54]. Plakoglobin is critical for the early stages of desmosomal assembly and is also an important regulator of cell adhesion and motility. The adhesive strength of desmosomes was shown to be downregulated by phosphorylation of plakoglobin following activation of EGFR. This resulted in the dissociation of desmoplakin, which is an important prerequisite for cell movement during wound healing [55]. Plakoglobin also plays an important role in several signaling cascades during the processes of cell motility, cell proliferation, and apoptosis [56, 57]. Plakogobin was also found to regulate cell motility through Rho and fibronectin dependent Src signaling [58]. Studies also show that MUC1 interaction with ErbB2, another member of the EGFR family of receptor tyrosine kinases, promotes the nuclear localization of a MUC1-$\gamma$-catenin complex [59]. $\gamma$-catenin or Plakoglobin, like $\beta$-catenin, is a transcription factor in the Wnt pathway, and can affect genes involved in motility and metastasis. $\gamma$-catenin suppresses cell motility and metastasis by downregulating fibronectin [58], by organizing the actin cytoskeleton through modulation of Rho-family GTPases, and by upregulating Nm23-H1, a known metastasis suppressor [60]. It has been speculated by the authors of this study that MUC1 could be sequestering $\gamma$-catenin to promote

cell motility [59].

### 1.0.6 Clinical applications of MUC1 as a cancer biomarker

Shed MUC1-N found in the sera of cancer patients is used as a biomarker for cancer staging and monitoring relapse following therapy. For example, carbohydrate antigen 15.3 (CA 15.3, MUC1) and carbohydrate antigen 19.9 (CA 19.9, sLea antigen, found on several glycoproteins including MUC1) are commonly used for the detection of breast and pancreatic cancers, respectively [61, 62]. Because MUC1-N is also released from stressed cells, the clinical utility of MUC1 measurement is confined to monitoring treatment efficacy in cancer patients. A clinical study in PDA patients demonstrated that, out of 13 putative biomarkers tested, a significant correlation was observed between elevated MUC1 protein expression and poor patient survival[63]. A new human tumor-MUC1 specific antibody, TAB004 has been developed for diagnostic and therapeutic purposes and it shows high specificity for tMUC1-N. It was developed by immunizing Balb/c mice with KCM tumor lysates. These lysates were prepared from spontaneous pancreatic lesions that develop in the KrasG12D mouse that also has a transgenic human MUC1, it is called the PDA.MUC1 or KCM mouse. TAB004 specifically detects MUC1-N in the carcinoma tissue, cancer stem cells (CSCs), and in the serum of pancreatic cancer patients in a stage-dependent manner [64]. TAB004 is also being developed for use as a diagnostic marker and therapeutic agent for other epithelial cancers, including breast, ovarian, and prostate.

In Figure 1.7, MUC1 cDNA vaccine, M-FP vaccine and imMucin vaccine induce immune response to MUC1 tumor antigen. 90Y-muHMGF1 antibody binds glycosylated extracellular MUC1 and increases survival in human patients. HMFG2 and C595 antibodies bind the protein core of underglycosylated MUC1 and reduce tumor burden in mouse models of cancer. GP1.4 binds to MUC1 protein and decreases proliferation and invasion. GO-203 peptide binds to the juxtamembrane domain of MUC1 and blocks MUC1 homodimerization, preventing MUC1 activity and causing

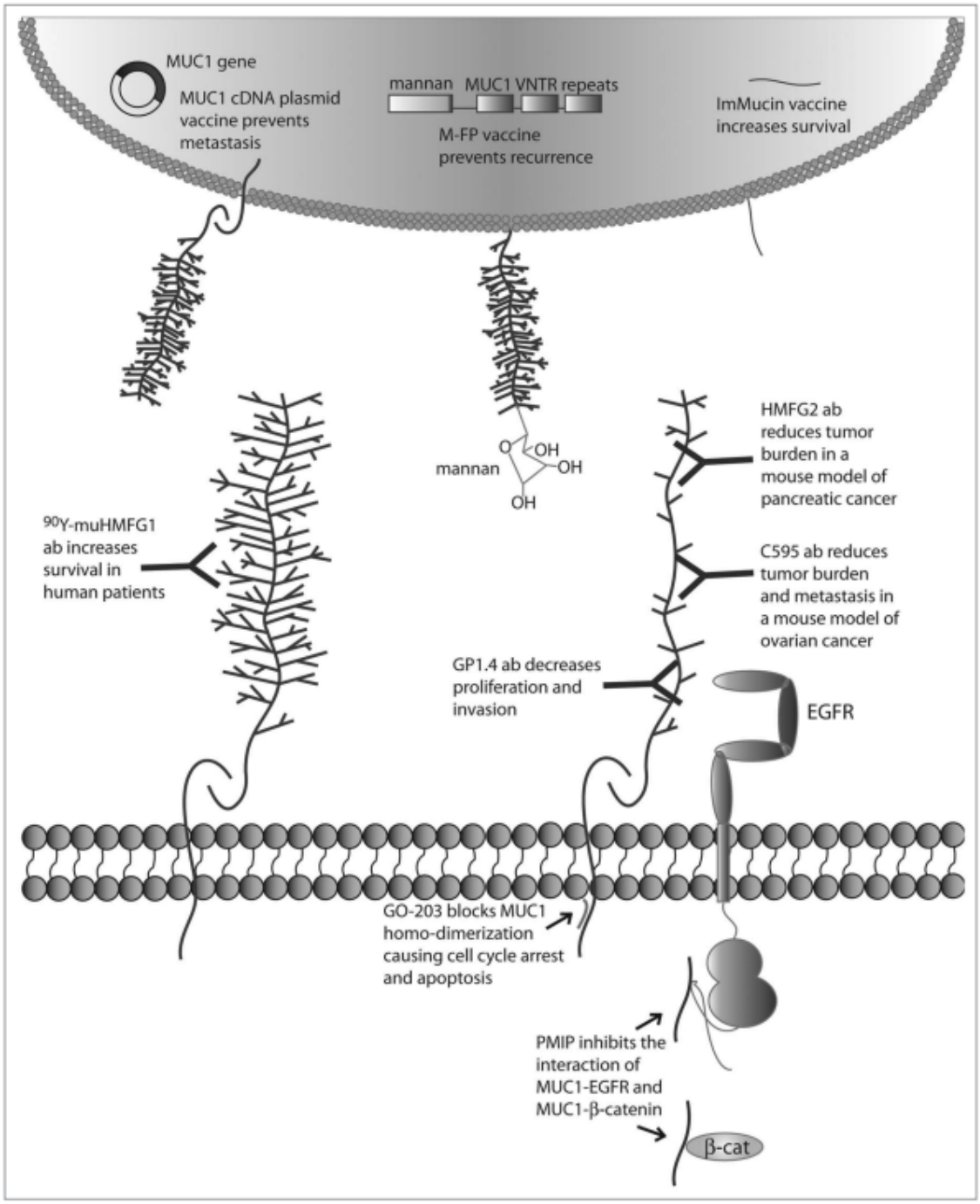


Figure 1.7: Targeted therapies directed against MUC1.

cell cycle arrest and apoptosis. PMiP decoy peptide inhibits MUC1-eGFr interaction and MUC1-$\beta$-catenin interaction, decreasing eGFr activity and inhibiting proliferation and invasion and inhibiting tumor growth and metastasis in mouse models of cancer. Picture has been adapted from [25].

Previously, the development of MUC1-based immune therapies was focused on MUC1-N. Recently the oncogenic properties and accessibility of MUC1-CT have been unveiled, making it an attractive druggable target. A cell penetrating peptide-based inhibitor of MUC1-CT, GO-203, is in Phase I clinical trials for the treatment of breast cancer (http://clinicaltrials.gov/show/NCT01279603). This inhibitor peptide binds to the CQC motif of MUC1-CT to block MUC1-C dimerization, nuclear translocation, and oncogenic signaling [65].

This dissertation aims to address the following: In Chapter 2, the role of MUC1 expression in regulating TGF-$\beta$ signaling and function in PDA has been elucidated. In a previous publication from our lab, it was shown that MUC1 regulates SMAD4 independent functioning of TGF-$\beta$ in PDA. We have reported for the first time that MUC1 expression levels correlate to significantly differentially expressed genes in the TGF-$\beta$, MAPK and BMPK pathways, using RNA sequencing data from TCGA. We also show that over-expression of MUC1 plays a significant role in switching the TGF-$\beta$ function from a tumor-suppressor to a tumor promoter by directly activating the non-canonical TGF-$\beta$ pathway protein JNK. Also, we report that high-MUC1 PDA tumors better respond to TGF-$\beta$ neutralizing antibody in vivo showing significantly reduced tumor growth compared to low-MUC1 tumors. In Chapter 3, it has been elucidated for the first time that MUC1 expression levels regulate the differential phosphorylation status of STAT3 in PDA. In previous studies, STAT3 and MUC1 were reported to regulate each other's expression in an auto-inductive loop. Napabucasin is a STAT3 inhibitor, which was in clinical trials for GI cancers including pancreatic cancer, however, the trial was discontinued due to futility. Since STAT3 and MUC1

are involved in an auto-inductive loop regulating each other's expressions, we hypothesized that Napabucasin should be able to attenuate tumorigenic properties of PDA cells by disrupting the STAT3-MUC1 axis. Also, since the STAT3-MUC1 pathway is the constitutively active survival pathway in high MUC1 cancer cells, these cells were more sensitive to Napabucasin treatment compared to low MUC1 cells. Napabucasin was found to reduce overall MUC1 levels in PDA and anti-MUC1 antibody TAB004 enhanced the efficacy of Napabucasin against the resistant PDA cell line HPAFII. In Chapter 4, the potential of anti-MUC1 therapies in GI cancers has been reviewed. In Chapter 5, the mechanism of action of an anti-tMUC1 antibody called TAB004 has been reported. Targeting tMUC1 with TAB004 was found to degrade MUC1 by the autophagy-lysosomal pathway, thus leading to successful reduction of anoikis-resistance markers in PDA cell lines. Finally, in Chapter 6, the dissertation concludes with its major findings and its future implications.

# CHAPTER 2: OVEREXPRESSION OF MUC1 INDUCES NON-CANONICAL TGF-$\beta$ SIGNALLING IN PANCREATIC DUCTAL ADENOCARCINOMA

## 2.1 Introduction

Pancreatic Cancer is currently the third leading cause of cancer related deaths in the United States (http://pancreatic.org/). It has been projected to become the second leading cause of cancer related deaths in the US, surpassing colorectal cancer by the year 2030 (http://pancreatic.org/). About 95% of pancreatic cancers are pancreatic ductal adenocarcinomas (PDA) with patients demonstrating a median survival rate of less than 6 months and a 5-year survival rate of 9% in the US [66]. In the US, the rate of new pancreatic cancer cases is 13.1 per 100,000 people per year and the mortality rate is 11.0 per 100,000 people per year [67]. Therefore, it has a mortality rate that nearly matches its incidence rate.

The transforming growth factor $\beta$ (TGF-$\beta$) signaling pathway belongs to a large superfamily that primarily consists of TGF-$\beta$ (including isoforms of TGF-$\beta$1, 2, and 3), bone morphogenetic proteins, activins, and inhibins [68]. This family of growth factors activates many biological signals, such as cell growth, apoptosis, differentiation, immune response, angiogenesis, and inflammation [69, 70, 71]. Deregulation of the TGF-$\beta$ pathway can lead to cancer, among other ailments [72]. In normal environments and early cancers, TGF-$\beta$ regulates epithelial cells as a tumor suppressor by controlling cell cycle and inducing apoptosis. However, in certain cases, once the cancer is established, a switch occurs and TGF-$\beta$ becomes a tumor promoter. TGF-$\beta$ induces invasion and migration and eventually leads to epithelial-to-mesenchymal transition (EMT) [73]. This process helps facilitate the migration and invasion of cancer cells to distant locations leading to metastasis, the major cause of cancer-related

deaths [74].

The canonical TGF-$\beta$ signaling is initiated by the binding of a TGF-$\beta$ cytokine to a pair of specific transmembrane receptors, TGF-$\beta$RI and TGF-$\beta$RII [75]. This activates the cytoplasmic serine/threonine kinase domains of the TGF-$\beta$ receptors [76], which leads to further activation downstream. In normal environments, TGF- $\beta$ binds to its specific receptors TGF-$\beta$RII and TGF-$\beta$RI, in sequence. This leads to the phosphorylation of SMAD2/3 via the cytoplasmic Serine/Threonine kinase domain of TGF-$\beta$RI [77]. SMAD2 has been identified as a tumor suppressor and mediator of the antiproliferative TGF-$\beta$ and activin responses [78]. SMAD2/3 trilocalizes with SMAD4 [79]. This leads the heterotrimer complex to the nucleus to induce transcriptional changes that influence cell regulation [79, 80]. However, frequent alterations and changes in the TGF-$\beta$ pathway occur in cancer, especially in PDA. Dysregulated TGF-$\beta$ signaling activates ERK1/2 and JNK [81] leading to an increase in aggressive cancer characteristics, such as growth, invasion, migration, and metastasis [82].

Mucin-1 (MUC1) is a Type I transmembrane glycoprotein that influences tumor progression and metastasis in PDA [6]. Tumor-associated MUC1 is overexpressed and aberrantly glycosylated in more than 80% of PDA cases [83, 30, 46, 6, 84]. In normal environments, MUC1 is expressed on the apical surface of ductal cells to provide a protective barrier [85]. However, upon tumorigenesis MUC1 expression is no longer restricted to the apical surface. At this point, MUC1 glycosylation decreases and the protein becomes overexpressed across the cell surface, placing it into the close vicinity of many growth factor receptors [30]. MUC1 oncogenic signaling, which plays an important role in increased metastasis and invasion, is promoted through the cytoplasmic tail (MUC1-CT). The MUC1-CT is a highly conserved 72-amino acid long domain containing seven tyrosine residues that are phosphorylated by non-receptor tyrosine kinases, such as c-SRC [86, 87]. Importantly, MUC1 modulates TGF-$\beta$ signaling in PDA cell lines that were engineered to overexpress MUC1. We

established that TGF-$\beta$ signaling required tyrosine phosphorylation of the MUC1-CT via tyrosine kinase c-SRC [88]. Here we deepen our understanding of MUC1 regulation of TGF-$\beta$ signaling in PDA cells that are genetically varied and that express varying levels of endogenous MUC1. We establish that the level of MUC1 expression plays a definitive role in inducing the TGF-$\beta$ -induced non-canonical pathway. In the presence of high levels of MUC1, TGF-$\beta$ activates the JNK pathway, and enhances cell viability by activating and stabilizing c-Myc. In PDA cells with low levels of MUC1, TGF-$\beta$ induces growth inhibition. Taken together, our study suggests a novel role of MUC1 in TGF-$\beta$ signaling in PDA. The in vivo data demonstrates that high-MUC1 PDA responds well to the TGF-$\beta$ neutralizing antibody while low MUC1 PDA does not.

## 2.2 Results

### 2.2.1 Differential Gene Expression Profiles in TGF-$\beta$, MAPK and BMP Pathways in High Versus Low MUC1 PDA Samples

Since the role of MUC1 in oncogenesis is well known, we utilized the TCGA database to look for differences in the gene expression profiles between samples with low MUC1 and moderate/high-MUC1 expression (Figure 2.1A). Out of >4,000 genes that were differentially expressed (data not shown), the top 30 genes that are involved in the TGF-$\beta$, MAPK and BMP pathways were selected to create the heatmap since these pathways are known to be regulated by TGF-$\beta$. Several known transcription factors like CREB3L3, FOXH1, PLA2G3, BMP4 as well as immune related genes such as the IL1R1 and IL1R2 were upregulated in high MUC1 samples which are all associated with increased epithelial to mesenchymal transition (EMT) and poor survival [89, 90, 91]. It is highly interesting to note that GREM 1, a key pro-fibrogenic factor in PDA [92] is upregulated in MUC1-high PDA and downregulated in MUC1-low PDA. Furthermore, INHBA, a ligand for TGF-$\beta$ and associated with tumorigenesis [93] is upregulated in high-MUC1 and downregulated in low-MUC1 PDA. In contrast, we found downregulation of MAPK10, MAPK12, RASD1 and AMH in MUC1-high and

upregulation of the same genes in MUC1-low PDA. Downregulation of these genes correlate with poor survival (human protein atlas). These data indicate the differential TGF-$\beta$ signaling in high versus low MUC1 PDAs where TGF-$\beta$ predominantly promotes oncogenic signaling in high-MUC1 PDA. The protein-protein interaction networks of these 30 genes in low vs high MUC1 samples are shown in Supplementary Figure 2.7, further confirming the functional role of MUC1 in TGF-$\beta$ associated oncogenic signaling. Thus, it was not surprising that MUC1 expression had a significant correlation with poor overall survival (OS) in PDA patients (Figure 2.1B).

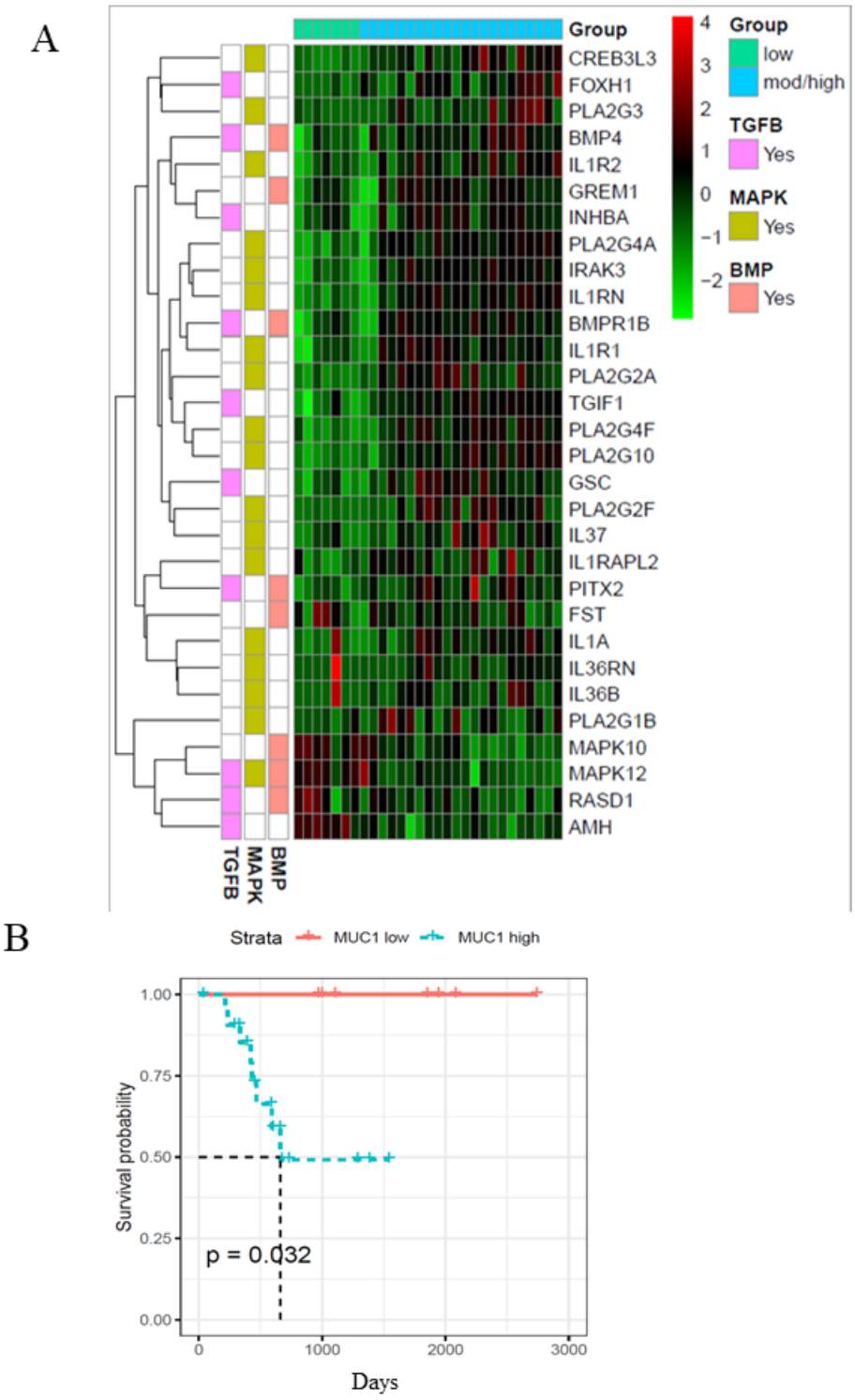


Figure 2.1: Heatmap showing top 30 differentially expressed genes in high/moderate vs low MUC1 PDA samples from TCGA.

In Figure 2.1, A. Top panel shows the color key for MUC1 expression in the 29 PDA samples. Right hand side shows the color key histogram for expression levels of each gene named on the right.Left hand side color key shows the genes associated with each of the three pathways in pink (TGF-$\beta$), green (MAPK) and peach (BMP). Genes with a false discovery rate adjusted $p<0.05$ are shown. B. Kaplan-Meier curve for overall survival (OS) in the 29 PDA patients from TCGA in low (blue) vs high/moderate (red) groups are shown.

### 2.2.2 High -MUC1 Expression in PDA Cells Positively Correlates to TGF-$\beta$RII and Negatively Correlates to TGF-$\beta$RI Levels

Several studies have shown that MUC1 overexpression in PDA is linked to enhanced growth and metastasis [33, 94, 46]. Since TGF-$\beta$ signaling starts with binding of TGF-$\beta$ to its receptors followed by activation of the same, we investigated the correlation between MUC1 and TGF-$\beta$ receptor expression levels in select PDA cell lines. We selected a panel of human PDA cell lines with varying levels of MUC1 expression (Figure 2.2A), and assessed the expression of MUC1, TGF-$\beta$RI and TGF-$\beta$RII by Western Blotting (Figure 2.2B). Results were profound. All high-MUC1 PDA cells (CFPAC, HPAC, HPAFII, and BxPC3. MUC1) expressed lower levels of TGF-$\beta$RI and significantly higher levels of TGF-$\beta$RII as compared to the low-MUC1 PDA cells (Panc01, MiaPaca2, Su86.86, and BxPC3. Neo). By statistical analysis, these results show a negative correlation (-0.2381) between MUC1 and TGF-$\beta$ RI expression (Figure 2.2B) and a significantly high overall positive correlation (0.8810 with a p value of $<0.01$) between MUC1 and TGF-$\beta$ RII expression (Figure 2.2C).

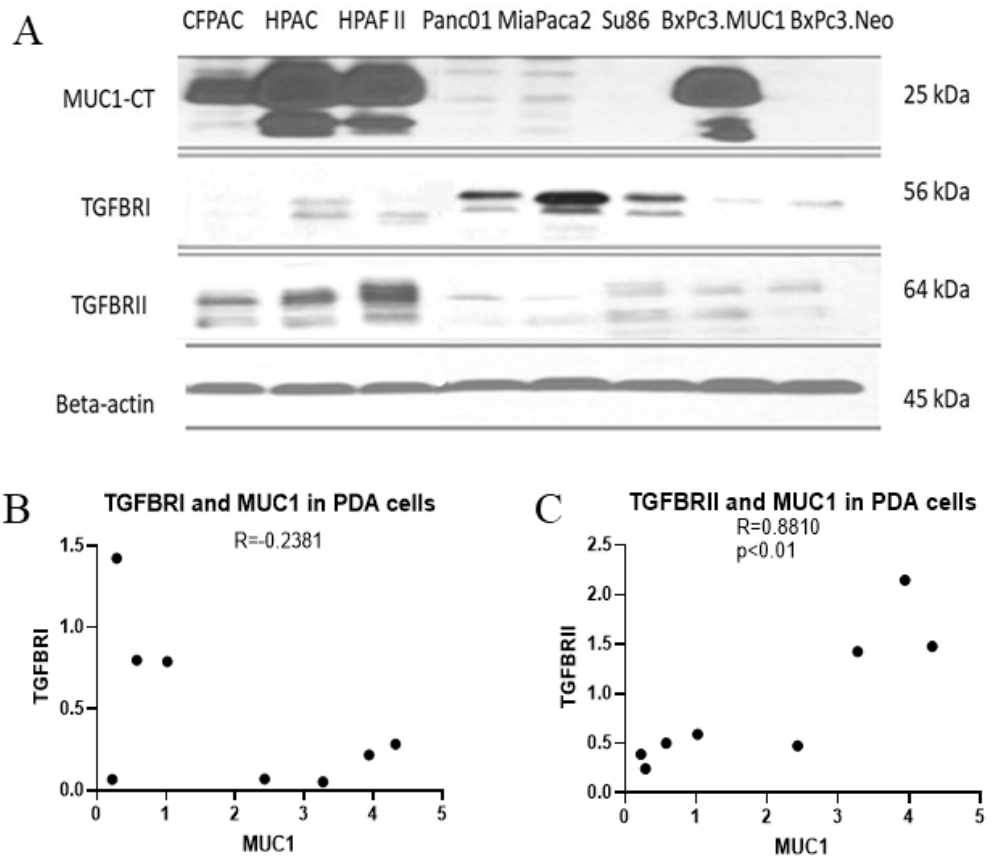


Figure 2.2: High MUC1 expression in PDA cells positively correlates to TGF-$\beta$RII and negatively correlates to TGF-$\beta$RI levels.

In Figure 2.2, A. The expression of MUC1-CT, TGF-$\beta$RI, TGF-$\beta$RII, and endogenous loading control $\beta$-actin in a panel of PDA cell lines, determined by Western blot. B. Densitometric analysis of MUC1 expression versus TGF-$\beta$RI expression shows a negative correlation (Spearmans correlation coefficient r=-0.2381, NS). C. Densitometric analysis of MUC1 expression versus TGF-$\beta$RII expression shows a significantly positive correlation (Spearmans correlation coefficient r=0.8810, p=0.0072).

### 2.2.3 TGF-$\beta$ Induces Activation of the Non-Canonical Signaling in High MUC1 PDA Cells

Since the receptor levels are associated with the canonical and non-canonical TGF-$\beta$ signaling pathways, we examined changes in phosphorylation of JNK and c-Myc in response to TGF-$\beta$ in high versus low-MUC1 PDA cell lines (HPAFII and Mia-

Paca2 respectively). We overexpressed MUC1 in MiaPaca2 cells and downregulated MUC1 in HPAFII cells. We observed profound changes in JNK and c-Myc activation. MiaPaca2. MUC1 cells (MiaPaca2 transfected with full-length MUC1) showed significant increase in pJNK and p-c-Myc in response to TGF-$\beta$. Interestingly, there was no activation of pJNK and reduced activation of p-c-Myc in the MiaPaca2. Neo cells (MiaPaca2 transfected with empty vector) in response to TGF-$\beta$ as compared to MiaPaca2. MUC1 cells (Figure 2.3A,C). In MiaPaca2. Neo, there was no phosphorylation of JNK even at 20 min (Supplementary Figure 2.8) post TGF-$\beta$ treatment, however, in MiaPaca2. MUC1, there was phosphorylation of JNK starting at 10 min post TGF-$\beta$ treatment (Figures 2.3A,C). Phosphorylation of c-Myc at Ser62 is a marker of stability of c-Myc [95]. In response to TGF-$\beta$, there was a decrease in both phosphorylated Ser62 and total c-Myc in MiaPaca2. Neo cells but increased p-c-Myc and c-Myc in MiaPaca2. MUC1 cells. These results corroborate the hypothesis that TGF-$\beta$ slows proliferation in low MUC1 PDA cells but promotes the same in MUC1 high cells (Figures 2.3A,C). In contrast, HPAFII showed high levels of pJNK and JNK as well as p-c-Myc in response to TGF-$\beta$, both of which were significantly reduced when MUC1 was knocked down using specific siRNA (Figures 2.3B,D). There is some background phosphorylation of c-Myc in HPAFII. MUC1 siRNA because the MUC1 KO is not 100%, however, it is clear that c-Myc phosphorylation has reduced significantly even at 70% KD (Figures 2.3D,E). Taken together, this confirms that MUC1 is associated with activation of the JNK pathway, as found in previous studies [96]. In this study we correlate this activation with response to TGF-$\beta$.

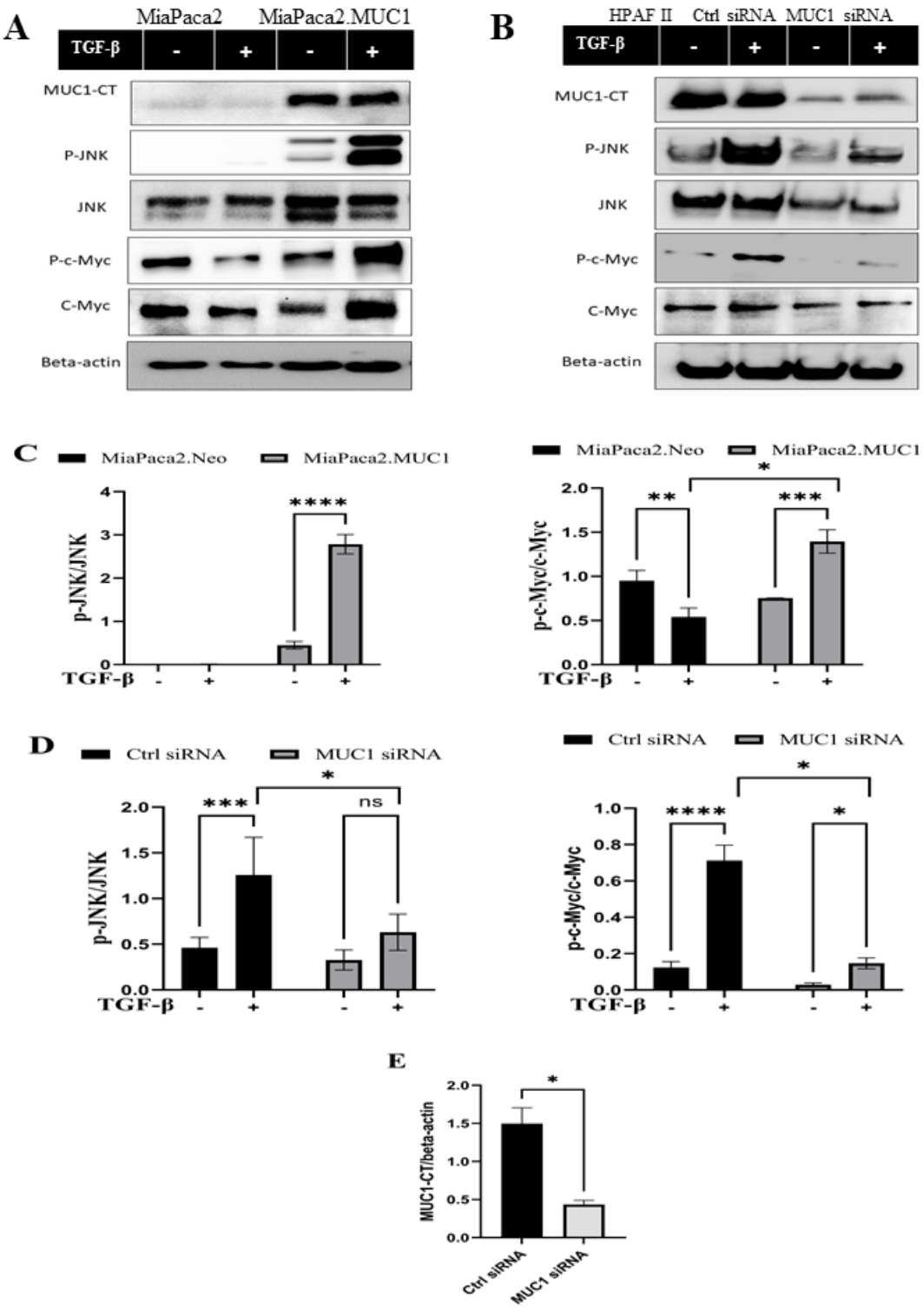


Figure 2.3: Over expression of MUC1 leads to increased phosphorylation of JNK and c-Myc and knockdown of MUC1 reduces phosphorylation of JNK and c-Myc.

In Figure 2.3, A. Western blot expression of phosphorylation of JNK and c-Myc compared to total JNK and total c-Myc in MiaPaca2 vs MiaPaca2.MUC1 cells in response to 10ng/ml of TGF-$\beta$ at 10 minutes. B. Western blot expression of phosphorylation of JNK and c-Myc compared to total JNK and total c-Myc in HPAFII cells treated with control siRNA vs MUC1 siRNA in response to 10ng/ml of TGF-$\beta$ at 10 minutes. C. Densitometric analysis of fold change of expressions of pJNK/Total JNK and p-c-Myc/Total c-Myc normalized to endogenous $\beta$-actin is presented in MiaPaca2 cells. D. Densitometric analysis of fold change of expressions of pJNK/Total JNK and p-c-Myc/Total c-Myc normalized to endogenous $\beta$-actin is presented in HPAFII cells. E. Knockdown efficiency of MUC1 in HPAFII after 72 hrs of siRNA treatment. Data are presented as means ± SEM of n=3; Unpaired Students t-test and one-way ANOVA were used to analyze the differences between treatment groups. *p $<$ 0.05, ** p $<$ 0.01, ***p$<$0.001, **** p$<$0.0001.

### 2.2.4 Differential Viability of High and Low MUC1 PDA Cells in Response to TGF-$\beta$

Since JNK signaling promotes cell growth [97], we next assessed cell viability in vitro in high-MUC1(HPAFII) and low-MUC1 (MiaPaca2) cells in response to TGF-$\beta$. TGF-$\beta$ treatment significantly reduced the viability of MiaPaca2 in 48 hr and HPAFII. MUC1siRNA in 24 hr, and increased the viability of HPAFII and MiaPaca2. MUC1 cells after 72 hr (Figure 2.4A-D). Furthermore, this effect was enhanced with 96 hr of incubation (Supplementary Figure 2.3A, B). This is also in line with our previously published work where we showed that treatment with TGF-$\beta$ led to increased apoptosis in MUC1-low PDA cells.

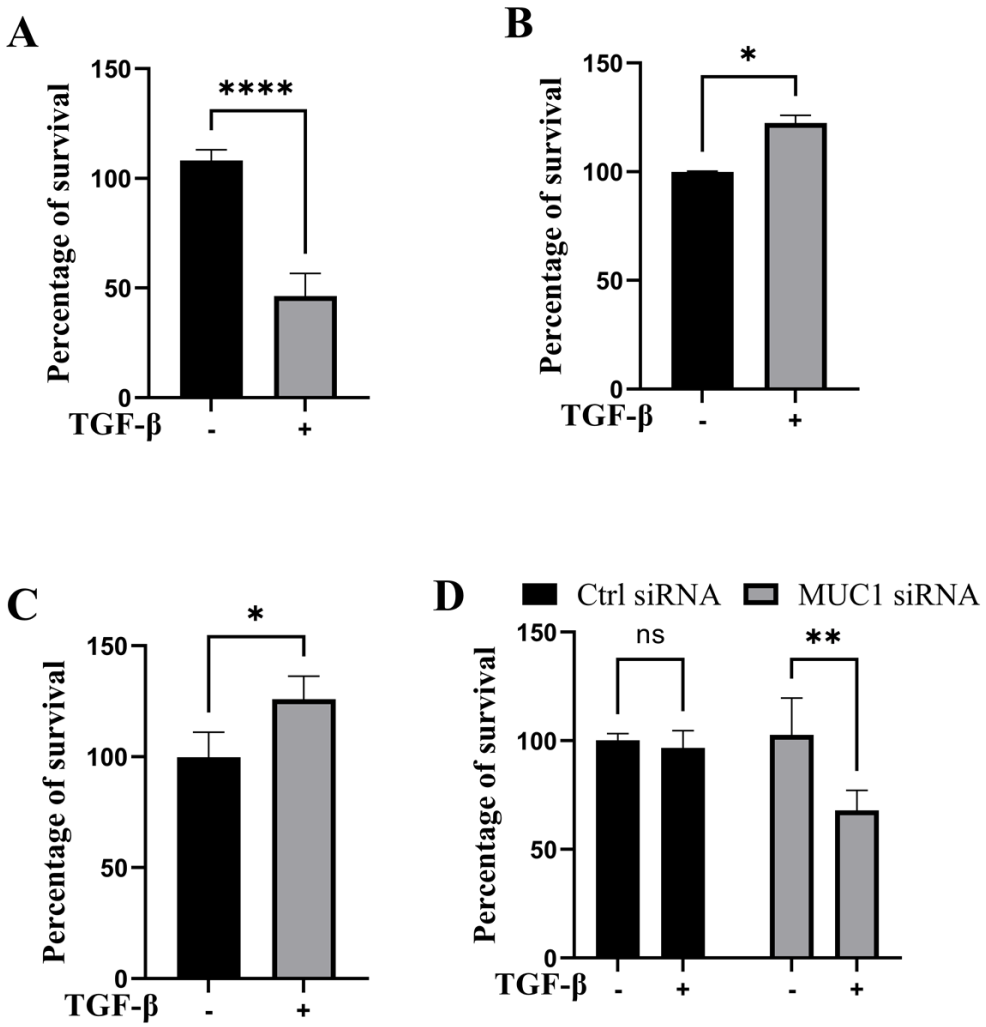


Figure 2.4: TGF-$\beta$ neutralizing antibody treatment significantly reduced high-MUC1 (HPAFII) but not low MUC1 (MiaPaca2) tumor growth in vivo.

In Figure 2.4, A. A schematic of the xenograft study showing the treatment with control IgG and TGF-$\beta$ (20$\mu$g/100$\mu$l per mouse). B. On the left: Tumor growth of HPAFII (n=5 for TGF-$\beta$ neutralizing Ab and n=4 for IgG isotype) is shown. On the right: Tumor growth of MiaPaca2 (n=6 for both groups) is shown. Tumor growth was determined biweekly by caliper measurements and tumor size in mm3 193 is plotted. C. Wet weight of HPAFII tumors (left) and MiaPaca2 tumors (right) respectively

are shown. Two-way ANOVA was used to compare between the different treatment groups. *$p<0.05$, NS: non-significant. D. Immunohistochemistry showing expression of MUC1 in MiaPaca2 (left) and HPAFII (right) tumors.

### 2.2.5 TGF-$\beta$ Neutralizing Antibody Treatment Significantly Dampens High-MUC1 Tumor Growth but has No Significant Effect on Low MUC1 Tumors *in vivo*

Given that our data showed that high level of MUC1 promotes non-canonical signaling pathway in response to TGF-$\beta$, we hypothesized that treatment with anti-TGF-$\beta$ neutralizing antibody would hamper growth of high-MUC1 but not of low MUC1 tumors in vivo. Athymic Nude-Foxn1nu mice were inoculated with HPAFII or MiaPaca2 cells subcutaneously. Once tumors were established, mice were injected intra-tumorally with either control IgG or TGF-$\beta$ neutralizing antibody three times a week for 2 weeks (Figure 2.5A). We observed significant reduction in tumor growth (Figure 2.5B) and tumor wet weight (Figure 2.5C) when HPAFII tumor bearing mice were treated with TGF-$\beta$ antibody as compared to those in the control IgG group. In contrast, MiaPaca2 tumors did not respond to TGF-$\beta$ neutralizing antibody treatment (Figure 2.5B). Even though it is not statistically significant, there was a trend of increased tumor burden in TGF-$\beta$ antibody treated MiaPaca2 tumors than the IgG treated group (Figure 2.5C). Since TGF-$\beta$ acts as a tumor promoter in high-MUC1 PDA cell lines and as a tumor suppressor in low-MUC1 PDA cell lines, it makes sense that neutralizing TGF-$\beta$ in high-MUC1 cells (HPAFII), reduced tumor growth as the tumor promoting effect of TGF-$\beta$ was inhibited by the antibody. On the other hand, in low-MUC1 cells (MiaPaca2), TGF-$\beta$ serves as a tumor suppressor and therefore when the tumor suppressing effect of TGF-$\beta$ was neutralized, tumor growth was increased, albeit not significantly. The MUC1 expression in MiaPaca2 and HPAFII tumors are shown in Figure 2.5D The TGF-$\beta$ expression levels in MiaPaca2 and HPAFII tumors at endpoint are shown in Supplementary Figure 2.10A. The treat-

ment did not have any adverse effect on the body weight of the mice (Supplementary Figure 2.10B).

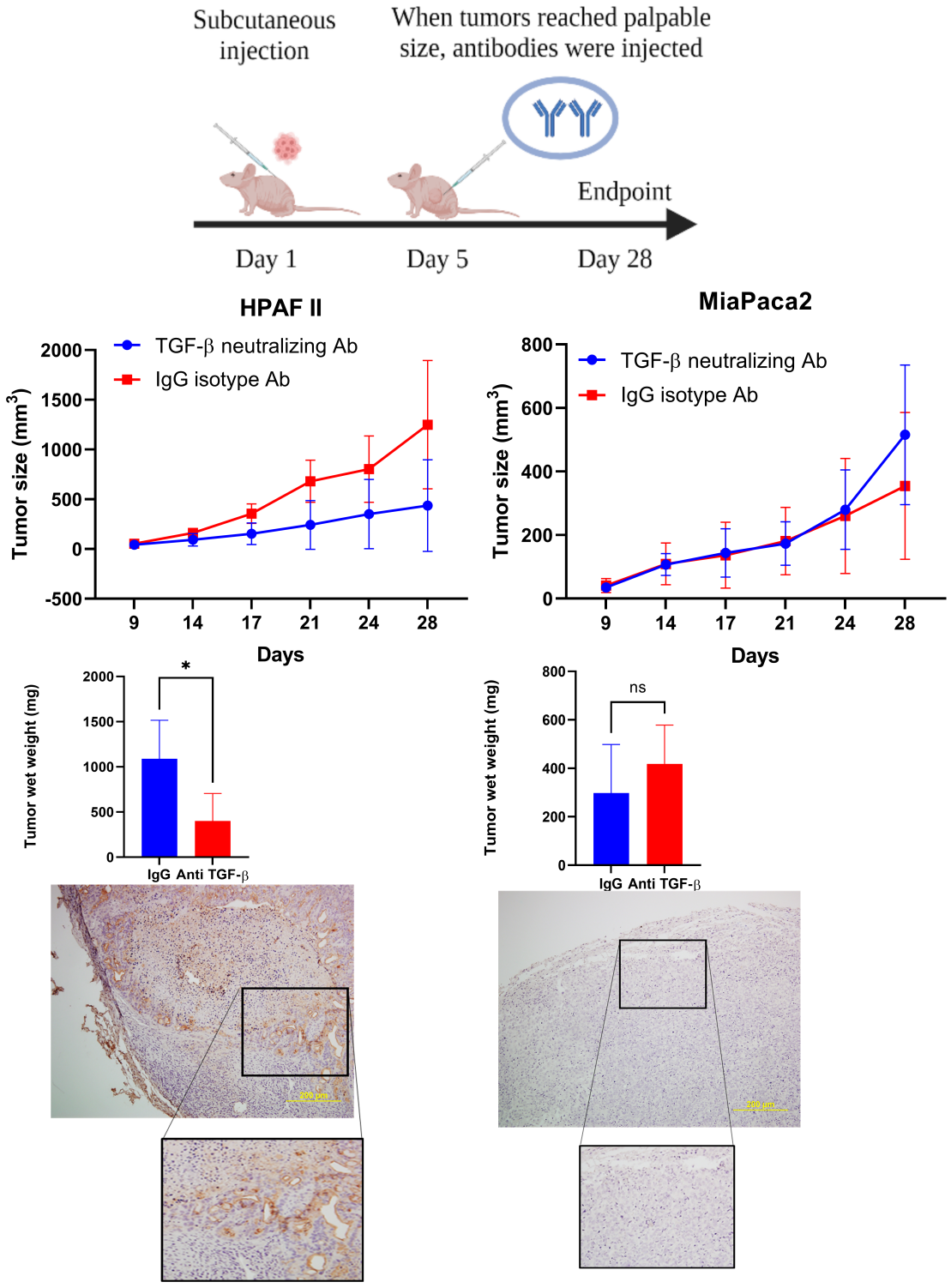


Figure 2.5: TGF-$\beta$ neutralizing antibody treatment significantly reduced high-MUC1 (HPAFII) but not low MUC1 (MiaPaca2) tumor growth in vivo.

In Figure 2.5, A. A schematic of the xenograft study showing the treatment with control IgG and TGF-$\beta$ (20$\mu$g/100$\mu$l per mouse). B. On the left: Tumor growth of HPAFII (n=5 for TGF-$\beta$ neutralizing Ab and n=4 for IgG isotype) is shown. On the right: Tumor growth of MiaPaca2 (n=6 for both groups) is shown. Tumor growth was determined biweekly by caliper measurements and tumor size in mm3 is plotted. C. Wet weight of HPAFII tumors (left) and MiaPaca2 tumors (right) respectively are shown. Two-way ANOVA was used to compare between the different treatment groups. *$p<0.05$, NS: non-significant. D. Immunohistochemistry showing expression of MUC1 in MiaPaca2 (left) and HPAFII (right) tumors.

## 2.3 Discussion

MUC1 is a very interesting molecule. In normal cells, it provides protection against infection and inflammation, however, in cancer cells, MUC1 is aberrantly glycosylated and overexpressed and increases inflammation and aids oncogenesis [98, 27, 99]. In 2009, the National Cancer Institute had ranked MUC1 as the second most targetable antigen out of 75 to develop cancer vaccines [100]. MUC1 is overexpressed in more than 80% of PDA cases [6] and TGF-$\beta$ signaling plays an important oncogenic role in majority of cancers especially in PDA [101]. The data presented here demonstrates that MUC1 regulates TGF-$\beta$ signaling and function in PDA cells. In our previous study, we reported that overexpression of MUC1 in BxPC3 cells (BxPC3. MUC1) enhanced the induction of epithelial to mesenchymal transition, and invasive potential in response to TGF-$\beta$ while resisted TGF-$\beta$ induced apoptosis by downregulating levels of cleaved caspases. We also showed that mutating the seven tyrosines in MUC1-CT to phenylalanine reverses the TGF-$\beta$ induced invasiveness [88].

To further assess the clinical significance of MUC1 and TGF-$\beta$ signaling crosstalk, we first analyzed the gene expression profiles in high and low MUC1 PDA patient samples registered in the TCGA dataset. We analyzed 29 RNA-seq samples which were from all stages, reducing the stage bias in the analysis (Supplementary Table

2.1). We found >4,000 genes differentially expressed (data not shown), however, we selected to further study the genes that were a part of the MAPK/JNK, BMP and TGF-$\beta$ pathways, because these pathways are known to be highly regulated by TGF-$\beta$. The top 30 genes that were found to be differentially expressed in low vs high MUC1 tumors have significant roles in inflammation, cancer progression and OS (Figure 2.1A,B). Most of the genes upregulated in high/moderate MUC1 samples (Figure 2.1A) are known to be involved in increased proliferation and induction of epithelial to mesenchymal transition (EMT) or worse OS in the human pancreatic cancer, for example, CREB3L3 (CAMP Responsive Element Binding Protein three Like 3) (https://www.genecards. org/cgi-bin/carddisp.pl?gene=CREB3L3), FOXH1(Forkhead box protein H1) [102], BMP4 (Bone morphogenetic protein 4) [103], IL1R2, receptor to IL-1, a cytokine known to be secreted by pancreatic cancer cells [104, 105, 106], GREM1 (Gremlin 1), a key pro-fibrogenic factor known to increase pancreatic inflammation and progression [92], INHBA (Inhibin $\beta$A), a ligand of the TGF-$\beta$ superfamily known to be overexpressed in pancreatic cancer [93, 107], BMPR1B, the bone morphogenetic protein (BMP) receptor family of transmembrane serine/threonine kinases (https://www.cancer-genetics.org/BMPR1B.html), TGIF1 (TGF-B Induced Factor Homeobox 1) [108], GSC (Goosecoid Homeobox) [109, 110] and PITX2 (paired-like homeodomain transcription factor 2, also known as pituitary homeobox 2), [111, 112, 113].

Genes that were upregulated in low-MUC1 PDA samples (MAPK12, RASD1, and AMH) were found to be favorable for OS in pancreatic cancer (Human protein atlas) (Figures 2.1A,B). Specifically, RASD1 (Ras Related Dexamethasone Induced 1) encodes a member of the Ras superfamily of small GTPases and is induced by dexamethasone (https://www.genecards.org/cgi-bin/carddisp.pl?gene=RASD1) and is considered to be a tumor suppressor [114, 115]. The PPI network analysis in high vs low MUC1 shows MAPK12 and MAPK10 interacting with each other and both

downregulated in high MUC1 samples. AMH is downregulated in high MUC1 samples and is shown clustering with the BMP4 network. RASD1 is downregulated and clusters with CREB3L3 (Supplementary Figure 2.7).

It is very important to mention here that we only had 29 PDA samples from the TCGA to distinguish based on MUC1 expression levels, out of which only seven were low MUC1. Although all the 30 genes were differentially expressed in low vs high/moderate MUC1 samples with statistical significance, due to the low sample size being a limitation in this particular study, it is difficult to conclude any correlations with certainty. The findings need to be validated with a larger cohort in the future. However, despite the low sample size, we found that MUC1 expression had a significant correlation with poor OS in PDA patients (Figure 2.1B) confirming its clinical significance as a biomarker yet again. For our downstream analysis, we selected JNK (a component of the MAPK pathway) since MAPK was commonly altered in all the three differentially regulated pathways (MAPK, TGF-$\beta$ and BMP-4) from the heatmap.

Using a panel of human PDA cell lines, we demonstrated that high-MUC1 expression is positively correlated to TGF-$\beta$RII expression (Figure 2.2B) with a high statistical significance, a receptor that activates the non-canonical pathway. Furthermore, there was a trend of negative correlation between high-MUC1 expression and TGF-$\beta$RI expression, albeit not significant, a receptor that activates the canonical SMAD pathway, known to drive cells towards cell death and apoptosis [116].

If TGF-$\beta$ mainly activates TGF-$\beta$ receptor II in high-MUC1 PDA cells, it should lead to increased activation of the noncanonical pathway genes. Accordingly, we found that overexpression of MUC1 in MiaPaca2 cells induced increased phosphorylation of JNK and c-Myc (Figure 2.3A,B), which signify activation of the non-canonical pathway associated with cellular proliferation and invasion [96]. TGF-$\beta$ significantly increased phosphorylation of c-Myc at Ser62, which is a marker of stability of c-

Myc [95]. On the other hand, HPAFII treated with control siRNA had high levels of phosphorylated JNK and c-Myc with TGF-$\beta$ exposure, but when MUC1 was downregulated using a specific siRNA, the phosphorylation of JNK and c-Myc were significantly reduced (Figure 2.3B), thus, TGF-$\beta$ destabilized c-Myc when MUC1 expression is low in PDA cells (Figure 2.3C). Overall, the data show the important contribution of MUC1 in driving the TGF-$\beta$ mediated non-canonical pathway.

As was expected, TGF-$\beta$ treatment reduced cell viability in low MUC1 PDA cell line MiaPaca2 but increased cell viability in high MUC1 PDA cell line HPAFII (Figure 2.4A). However, when MUC1 was overexpressed in MiaPaca2, TGF-$\beta$ increased the viability of these cells significantly (Figure 2.4B), and when MUC1 was knocked down in HPAFII cells, TGF-$\beta$ reduced cell viability (Figure 2.4C), thus clearly showing MUC1-dependent gain-offunction and loss-of function in TGF-$\beta$ signaling switch towards a tumor promotor.

If indeed TGF-$\beta$ signaling is critical for the aggressive growth of high-MUC1 PDA tumors, then neutralizing TGF-$\beta$ with an antibody in vivo would dampen tumor growth. Confirming our hypothesis, neutralizing TGF-$\beta$ treatment in high-MUC1 HPAFII tumors significantly reduced tumor progression andreduced tumor burden (Figure 2.5B), whereas the same treatment almost hastened tumor growth in low MUC1 MiaPaca2 tumors (Figure 2.5B). These data conform with our hypothesis that blocking TGF-$\beta$ will be beneficial in PDA with high-MUC1 but may aid in tumor growth in low-MUC1 PDA. A schematic diagram illustrates our current understanding of MUC1s role in switching TGF-$\beta$ signaling from a canonical tumor suppressive to a non-canonical tumor promoting pathway (Figure 2.6).

The data has uncovered a major role of MUC1 in regulating the paradoxical function of TGF-$\beta$ in PDA. To the best of our knowledge, this is the first report that shows significant changes in gene expression profiles in the TGF-$\beta$, MAPK and BMP signaling pathways in patient-derived RNA-seq samples from PDA, based solely on

MUC1 expression levels. These data indicate the clinical relevance of MUC1 in modulating the TGF-$\beta$ signaling in PDA. In addition to the bioinformatics data, we report significant correlation of MUC1 to TGF-$\beta$RII protein expression levels in a panel of human PDA cell lines which informs the downstream signaling in response to TGF-$\beta$. Thus, TGF-$\beta$ activates the non-canonical JNK pathway in the high-MUC1 PDA cells (which also express higher TGF-$\beta$RII). While, in the low MUC1 cells (that express higher levels of TGF-$\beta$RI), TGF-$\beta$ reduces viability and inhibits growth possibly leading to apoptosis.

Finally, our study also shows that PDAs with high-MUC1 are more likely to respond to anti-TGF-$\beta$ therapy but PDAs with low- MUC1 will probably have poorer prognosis with the same treatment. Therefore, MUC1 expression may be used as a surrogate biomarker to determine the efficacy of future TGF-$\beta$-targeted treatments for PDA and possibly other gastrointestinal cancers. Thus, we suggest that MUC1 expression may be used as a biomarker to personalize the treatment with TGF-$\beta$ targeted treatment modalities. We recognize that further studies need to be performed to elucidate the causal relationships between MUC1 and the other differentially expressed genes in the TGF-$\beta$ pathway, however, using genetically identical PDA cells that had MUC1 knocked down or MUC1 overexpressed, we have addressed the causal relationship between MUC1 and TGF-$\beta$ signaling.

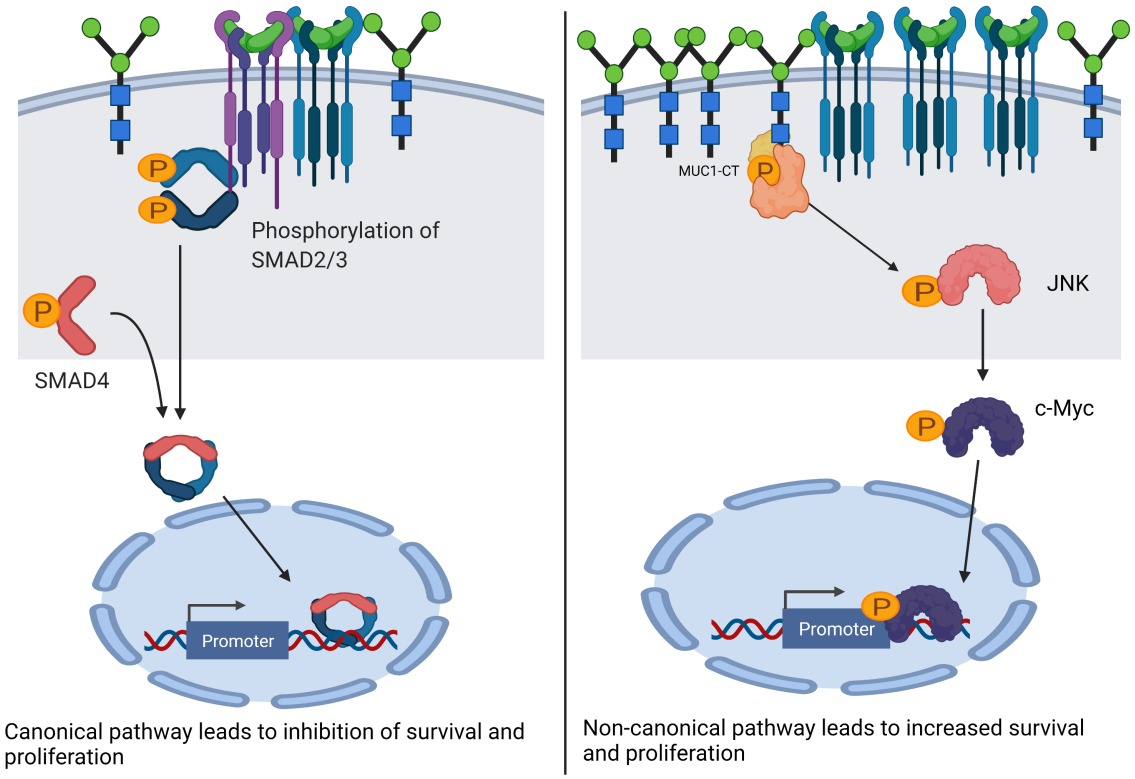


Figure 2.6: Schematic diagram of the proposed mechanism of TGF-$\beta$ signaling and functions in high versus low MUC1 PDA.

In Figure 2.6, Left panel shows activation of SMAD-dependent canonical pathway in low-MUC1 PDA cells. TGF-$\beta$ ligands bind to the membranous TGF-$\beta$ receptor (TGF-$\beta$RII) homodimers with high affinity. TGF-$\beta$RII binding allows dimerization with TGF-$\beta$ type I receptor (TGF-$\beta$RI) homodimers, activation of the TGF-$\beta$RI kinase domain and signal transduction via phosphorylation of the C-terminus of receptor-regulated SMADs (R-SMAD), SMAD2 and SMAD3. The SMAD2/3 dimer then forms a heterotrimeric complex with SMAD4 which translocates in the nucleus [80, 117]. This leads to growth inhibition, cell cycle arrest and apoptosis of PDA cells, thus TGF-$\beta$ acts as a tumor suppressor. Right panel shows activation of SMAD-independent non-canonical pathway in high-MUC1 PDA cells. In this pathway, binding of TGF-$\beta$ mainly to TGF-$\beta$-RII most likely increases phosphorylation of c-SRC which in turn phosphorylates MAPK, followed by JNK and c-Myc [118]. This

phosphorylation cascade activates the MAPK/JNK pathway and stabilizes c-Myc which translocates into the nucleus to increase transcription of oncogenic proteins and leads to increased growth, invasion and EMT of PDA cells [119]. MUC1-CT also aids in the process by its oncogenic signaling. Thus, in high-MUC1 PDA cells TGF-$\beta$ acts as a pro-tumorigenic cytokine. The schematic was created with BioRender.com.

## 2.4 Materials and Methods

### 2.4.1 TCGA Gene Expression Analysis

Twenty-nine pancreatic adenocarcinoma tumor RNA-Seq data were downloaded from the Genomic Data Commons data portal [120]. All tumor samples were from the PAAD project data generated by The Cancer Genome Atlas (TCGA) Research Network: http://cancergenome.nih.gov/. The tumor samples were separated in two groups based on their MUC1 expression: MUC1 low expression group and MUC1 moderate/ high expression group. Seven tumor samples had extremely low MUC1 expression values. HTSeq-counts data was input into DESeq2 (version 1.32.0) to identify differentially expressed genes in MUC1 moderate/high vs MUC1 low expression samples [121]. Genes with an adjusted p-value $<0.05$ and $\log_2$ fold change difference greater than two were considered differentially expressed. Gene set enrichment analysis was performed with all the DEGs. The enrichR package in R was used to identify enriched gene sets from Gene Ontology (GO) Biological Process, Molecular Function, and Cellular Component (2021) and the KEGG database (2021) [122]. The top 10 sets were collected from each database. There are a few pathways of specific interest in this study: the MAPK, BMP, and TGF-beta signaling pathway. DEGs were filtered to only include those that are involved in at least one of these pathways. Thirty genes in these three pathways were differentially expressed and used for further analysis. A heatmap was created with these pathway DEGs, using pheatmap (version 1.0.12) package in R. To further visualize the effects of MUC1 expression, only low and high MUC1 expressed samples were included (samples with moderate MUC1

expression were excluded). DESeq2 analysis was conducted with only these samples and a protein-protein interaction (PPI) network was created from the DEGs, using the STRING database (1.7.0). The list of DEGs were input into the STRING protein query to create a PPI network for the significant genes. The STRING database is a collection of known and predicted protein-protein interactions identified from multiple types of sources [123]. The identified PPI network was visualized in Cytoscape (version 3.9.0) [124] with the color of the nodes representing the gene log fold change value. The Kaplan-Meier plot was generated by calculating the survival curve using the survival package (3.1-8) in R and visualized using the survminer (0.4.9) package in R.

### 2.4.2 Cell Lines and Culture

Human PDA cell lines (CFPAC, HPAC, HPAF-II, Panc1, MiaPaca2, Su86.86 and BxPc3) were obtained from American Type Culture Collection and cultured as instructed. Cell lines were maintained in Dulbecco's Modified Eagle Medium (DMEM; Gibco), Minimal Essential Media (MEM; Gibco), or Roswell Park Memorial Institute 1,640 medium (RPMI; with, L-glutamine; ThermoFisher). All media was supplemented with 10% fetal bovine serum (FBS; Gibco or Hyclone), 3.4mM L-glutamine, 90 units (U) per ml penicillin, 90 $\mu$g/ml streptomycin, and 1% Non-essential amino acids (Cellgro). Cells were kept in a 5% $CO_2$ atmosphere at 37°C. MUC1 WT sequence was cloned into the pLNCX. 1 vector consisting of the neomycin resistance gene (neo) and confirmed by DNA sequencing. MiaPaca2. MUC1 and MiaPaca2. Neo were generated by transfection with Lipofectamine 3,000 (Thermo Fisher) according to the manufacturers protocol and maintained in medium containing Geneticin (G418; Invitrogen, Carlsbad, CA, USA) [46]. Neo cells had the empty vector with the G418 resistance gene (neo) and MUC1 cells had the full length MUC1 gene and G418 resistance gene (neo). Every passage of MiaPaca2 transfected cells were maintained in a final concentration of 150 $\mu$g/ml of the antibiotic G418 (50 mg/ml) (Thermo Fisher) to

ensure positive selection. HPAFII cells were serum-starved for 24 hr and then treated with control siRNA from Life Technologies or MUC1 siRNA from Perkin Horizon according to the respective manufacturers protocol using Lipofectamine RNAiMAX Transfection Reagent (Thermo Fisher Scientific) for 72 hr, followed by treatment with TGF-$\beta$. For all experiments, cell lines were passaged no more than 10 times.

### 2.4.3 Treatment With TGF-$\beta$ and Western Blotting

The cell lines used were MiaPaca2. Neo, MiaPaca2. MUC1, HFAFII. control-siRNA, and HPAFII. MUC1siRNA. Cells were serum starved for 48 hr and treated with either 10 ng/ml of human TGF-$\beta$ (Peprotech, Rocky Hill, NJ, USA) or the vehicle (citrate buffer) for 10min. HPAFIICell lysates were prepared and western blotting performed as previously described [46]. Membranes were blocked with commercial blocking buffer (Thermo Fisher) for 30 min at room temperature and incubated with primary antibodies overnight at 4°C. The antibodies used were: Armenian hamster monoclonal anti-human MUC1 cytoplasmic tail (CT2) antibody (1:500). MUC1 CT antibody CT2 was originally generated at Mayo Clinic and purchased from Neomarkers, Inc. (Portsmouth, NH) [125]. CT2 antibody recognizes the last 17 amino acids (SSLSYNTPAVAATSANL) of the cytoplasmic tail (CT) of human MUC1. Membranes were also probed with the following antibodies from Cell Signaling Technology (1:1,000), p-JNK, total JNK, $\beta$-Actin (Mouse, 3,700), p-c-Myc (Ser62) (Invitrogen), total c-Myc (Invitrogen). Other antibodies used include TGF-$\beta$RI (Abcam, 1:200, Rabbit, ab31013) and TGF-$\beta$RII (Abcam, 1:1,000, Rabbit, ab61213). Densitometric analysis was conducted using the ImageJ software and percent change was calculated accordingly. First, each density unit for the particular protein was normalized to their respective $\beta$-actin density and then represented as phospho/total.

### 2.4.4 MTT Assay

5,000 cells were plated in 96 well plates and allowed to grow overnight. After serum starvation for 24 hr, the cells were treated either with control buffer or 10 ng/ml of TGF-$\beta$ in triplicates for 24-96 hr. Then 20$\mu$l of MTT solution (5 mg/ml) was added to each well and incubated for 3-4 hr at 37°C. Following that, the media with MTT was removed and 200$\mu$l of DMSO was added to each well to dissolve the formazan crystals for 10 min and the O.D. was measured with a plate reader (Multiskan, Thermo Fisher) at 560 nm.

### 2.4.5 Xenograft Studies

Athymic Nude-Foxn1nu mice were purchased from Harlan Laboratories and housed at UNC Charlotte's vivarium. These mice were injected subcutaneously with tumor cells. 3 x 106 HPAFII cells (50$\mu$l) (n = 9) or 5 x 106 MiaPaca2 cells (50$\mu$l) (n= 12) were injected with Matrigel (50$\mu$l) (total = 100$\mu$l) subcutaneously into the flank of male or female Athymic Nude-Foxn1nu mice [126]. Once the tumors reached a palpable size (~3 x 3mm, ~5 days post tumor inoculation), mice were separated into four different groups. Groups 1 and 2 had HPAF-II tumors and groups 3 and 4 had MiaPaca2 tumors. Groups 1 and 3 were treated with the isotype control IgG antibody (20$\mu$g/100ul per mouse) three times a week for 2 weeks. Groups 2 and 4 were treated with the monoclonal TGF-$\beta$ neutralizing antibody (LifeTech) (20$\mu$g/100$\mu$l per mouse) three times a week for 2 weeks. Mice were monitored daily for general health and tumors were palpated. Caliper measurements were taken three times a week over 28 days until endpoint and once euthanized, tumor wet weight was taken (tumor size: 15 x 15mm) (Figure 2.5A). This study and all procedures were performed after approval from the Institutional Animal Care and Use Committee of UNC Charlotte.

### 2.4.6 Immunohistochemistry

For nonenzymatic antigen retrieval, sections were heated to 85°C in Dako antigen retrieval solution for 90 min and cooled for 20 min; all subsequent steps occurred at room temperature. To quench endogenous peroxidase, slides were rinsed and incubated in methanol/2% $H_2O_2$ for 10 min. Sections were then washed, blocked in 50% fetal bovine serum (FBS) in PBS for 45 min, and incubated overnight with primary antibodies. Sections were incubated for 1 hr with secondary antibody, developed with a diaminobenzidine (DAB) substrate (Vector Inc., Burlingame, CA, USA), counterstained with hematoxylin, and mounted with Permount. Primary antibodies used were Armenian hamster anti-MUC1 cytoplasmic tail (CT), CT2 (1:50) and anti-TGF-$\beta$ antibody (Novus Biologicals) (1:10). Secondary antibodies used were rat anti-hamster HRP conjugated antibody (1:100, Jackson Labs) and anti-mouse HRP conjugated antibody (Cell Signaling Technology) (1:50). IgG conjugated to horseradish peroxidase was used as negative control. Immunopositivity was assessed using light microscopy and images taken at 100x magnification.

### 2.4.7 Statistical Analysis

The data are expressed as the mean ± SEM of n = 3. Differences between groups were examined using unpaired two-tailed t-tests, one-way and two-way ANOVAs. Statistical comparisons were made using the GraphPad Prism 9.0. p-values of $<0.05$ were considered statistically significant ($^*p < 0.05$; $^{**}p < 0.01$; $^{***}p < 0.001$; $^{****}p < 0.0001$).

## 2.5 Supplementary Materials

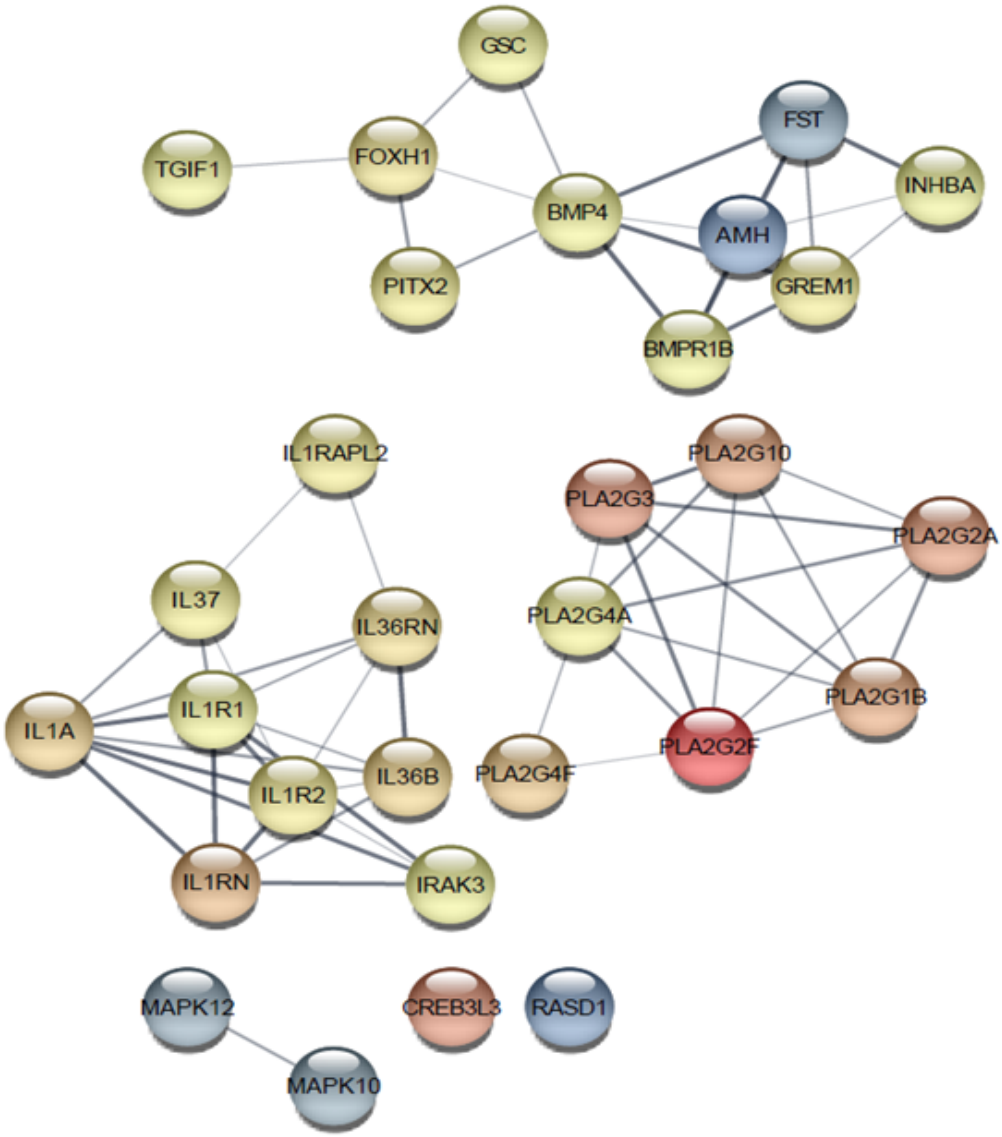


Figure 2.7: The Protein-protein-interaction network as determined by STRING and visualized in Cytoscape for the 30 genes in the TGF-$\beta$, MAPK and BMP4 pathways.

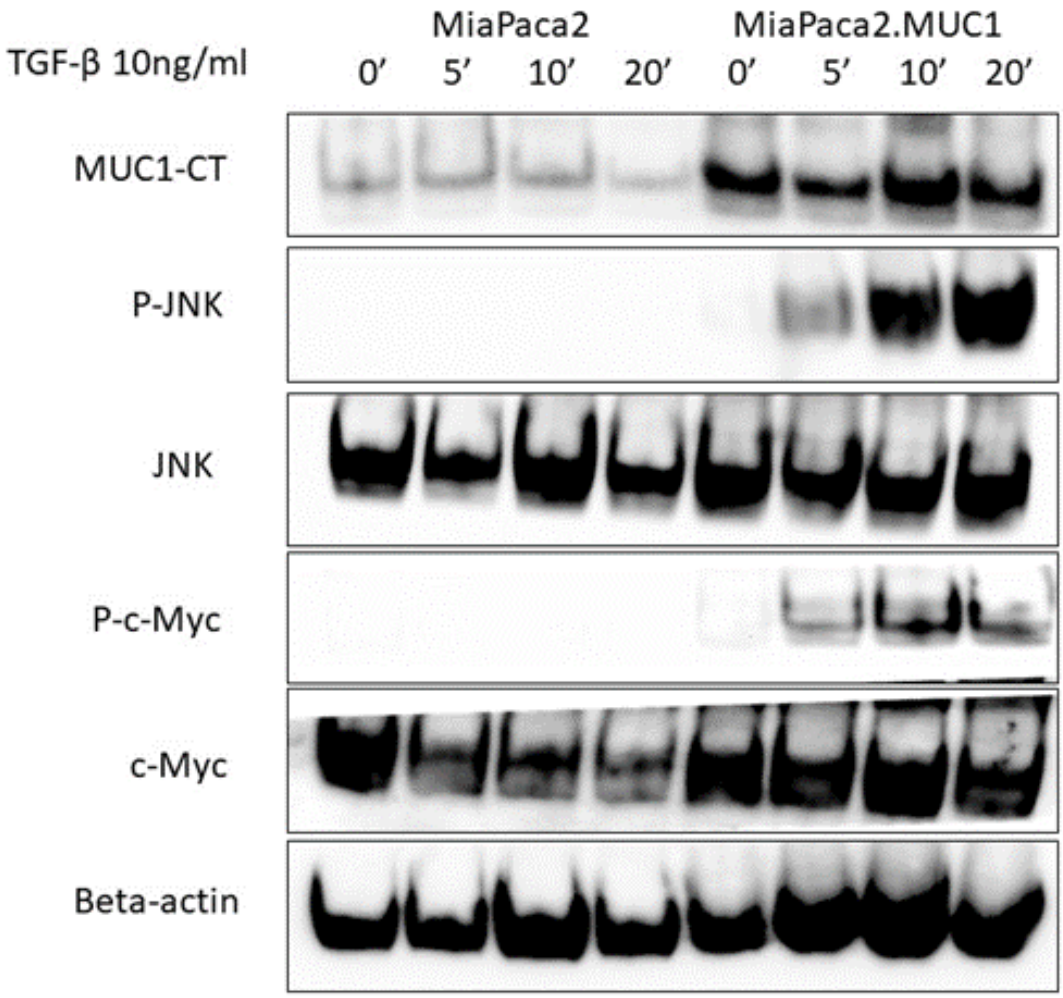


Figure 2.8: Overexpression of MUC1 leads to increased phosphorylation of MAPK, JNK and c-Myc.

In Supplementary Figure 2.8, Western blot expression of phosphorylation of JNK and c-Myc compared to total MAPK, total JNK and total c-Myc in MiaPaca2 vs MiaPaca2.MUC1 cells in response to 10ng/ml of TGF-$\beta$ at 0, 5, 10 and 20 minutes. $\beta$-actin was used as endogenous loading control.

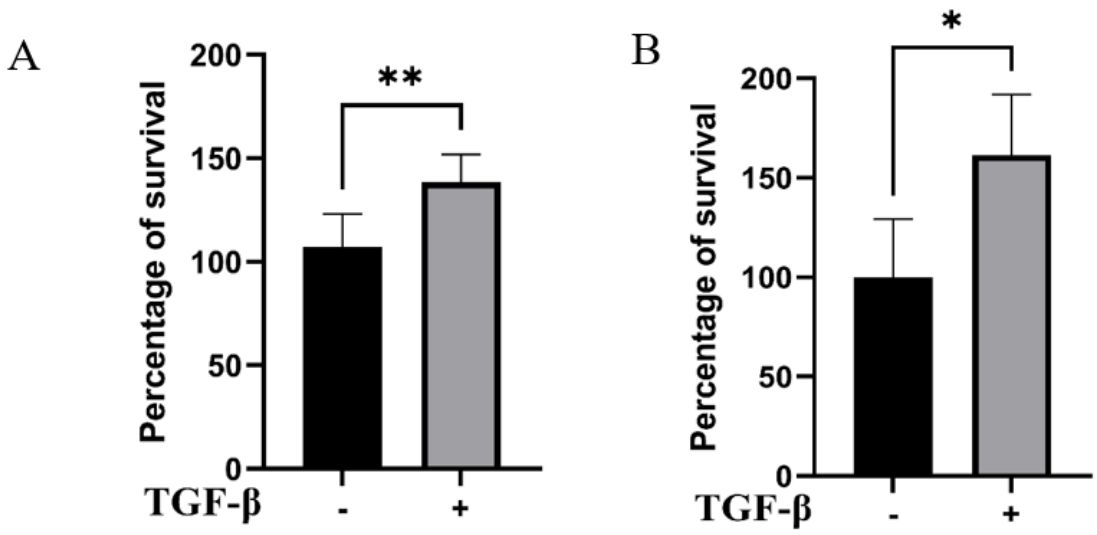


Figure 2.9: TGF-$\beta$ exposure increases viability in cells with high MUC1.

In Supplementary Figure 2.9, MTT cell viability assay on A. HPAFII and B Mia-Paca2.MUC1 cells with 10ng/ml of TGF-$\beta$ for 96 hrs. All data are shown as means $\pm$ SEM of n=3. Unpaired t-test was performed to compare between treated and untreated cells for all experiments. * $p < 0.05$, ** $p < 0.01$, *** $p<0.001$, **** $p<0.0001$.

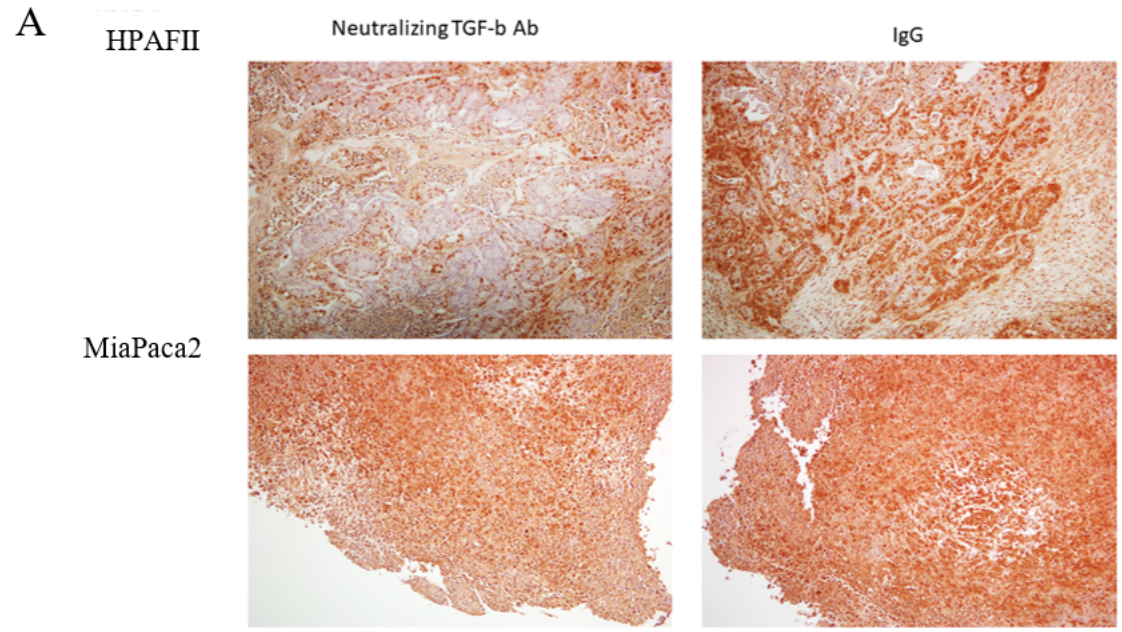


(a) Immunohistochemistry for TGF-$\beta$. Top. HPAFII tumor tissues and Bottom. MiaPaca2 tumor tissues showing TGF-$\beta$ expression in mice treated with neutralizing TGF-$\beta$ antibody (left) and isotype control IgG (right).

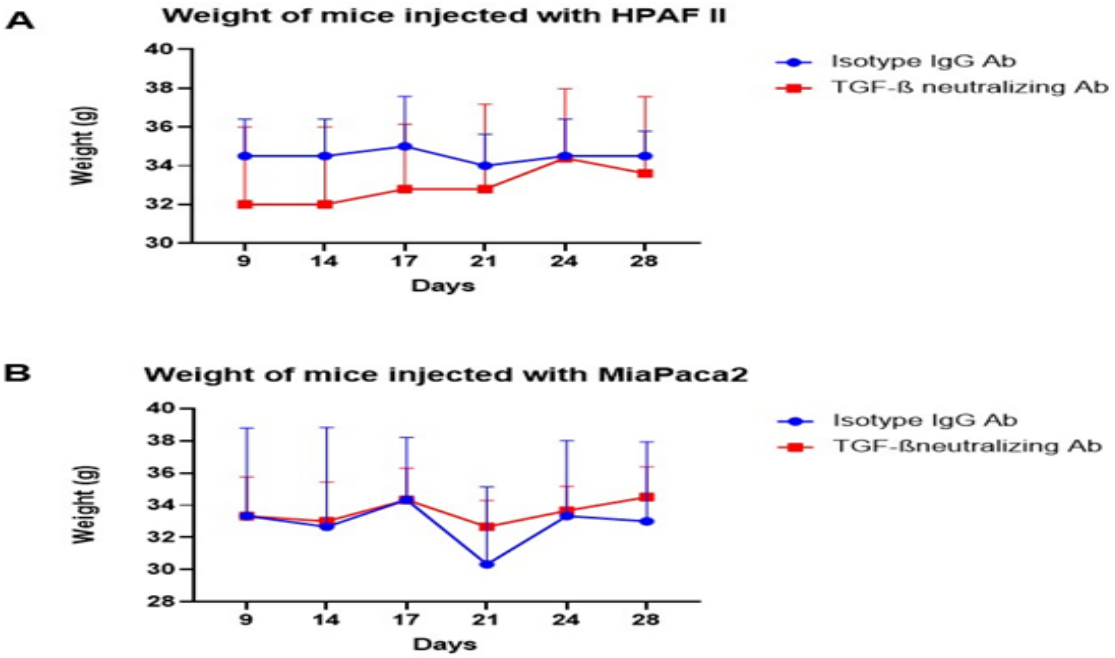


(b) Body weights of all mice remained consistent over the period of the in vivo study. Body weights of all nude mice injected with Top. HPAFII cells and Bottom. MiaPaca2 cells and treated with IgG isotype antibody (blue) and TGF-$\beta$ neutralizing antibody (red) over the period of 28 days starting from the day of treatment are shown.

Figure 2.10: Supplementary data on xenograft studies

Table 2.1: Table showing the characteristics of the 29 PDA samples from TCGA.

| | **Total** | | **OS, days** | **p-value** |
|---|---|---|---|---|
| | **N** | **%** | **Mean** | |
| **Gender** | | | | 0.9 |
| Male | 18 | 62 | 942.91 | |
| Female | 11 | 38 | 778.67 | |
| **Age** | | | | 0.2 |
| <65 | 15 | 52 | 1067.87 | |
| >65 | 14 | 48 | 597.86 | |
| **Tumor Stage** | | | | 0.01 |
| i | 1 | 3 | 2741 | |
| ia | 1 | 3 | 454 | |
| ib | 5 | 17 | 1516 | |
| iia | 4 | 14 | 878.25 | |
| iib | 15 | 52 | 477.73 | |
| iv | 1 | 3 | 603 | |
| Not Reported | 2 | 7 | 1165 | |
| **Primary Diagnosis** | | | | 0.01 |
| Adenocarcinoma, NOS | 20 | 69 | 513.75 | |
| Neuroendocrine carcinoma, NOS | 8 | 28 | 1705.88 | |
| Adenocarcinoma with mixed subtypes | 1 | 3 | 466 | |
| **Tissue Origin** | | | | 0.1 |
| Head of Pancreas | 16 | 55 | 546.69 | |
| Tail of Pancreas | 4 | 14 | 917.25 | |
| Body of Pancreas | 5 | 17 | 1810.40 | |
| Pancreas, NOS | 3 | 10 | 730.33 | |
| Overlapping lesion of NOS | 1 | 3 | 729 | |

# CHAPTER 3: MOLECULAR CROSSTALK BETWEEN MUC1 AND STAT3 INFLUENCES OUTCOME TO NAPABUCASIN THERAPY

## 3.1 Introduction

Signal transducer and activator of transcription 3 (STAT3) belongs to a family of transcription factors comprising STAT1, STAT2, STAT3, STAT4, STAT5A, STAT5B, and STAT6. In humans, this is encoded by the STAT3 gene. STAT3 is activated by several cytokines and growth factors such as IL-6, IL-9, IL-10, IL-27, tumor necrosis factor $\alpha$, monocyte chemotactic protein-1, epidermal growth factor, platelet-derived growth factor, granulocyte colony-stimulating factor,and granulocyte-macrophage colony-stimulating factor. Activated STAT3 plays an important role in cancer development by regulating transcription of genes associated with cell development, differentiation, proliferation, survival, and angiogenesis [127].

STAT3 activation has been detected in several malignancies, and its inhibition led to reversal of the malignant phenotype. STAT3 can be constitutively activated by upstream signaling components, including increased cytokine (IL-6 and IL-10) production, activated receptor (cytokine receptors, epidermal growth factor receptor) and nonreceptor tyrosine kinases (including Janus kinases [JAKs] and Src). Recently, mutated hyperactive forms of STAT3 have been detected in tumors, with the majority of mutations found in the SH2 domain of STAT3.

STAT3 activation has been described in nearly 70% of solid and hematological tumors [128]. STAT3 is constitutively activated by phosphorylation of Tyr705, in human tumor specimens, PDA cell lines in vitro and in PDA xenografts [129, 130, 131, 132]. Studies in conditional knockout mice demonstrate that the STAT3 pathway is inactive in normal pancreas, and it is not required for pancreatic development and

homeostasis [133]. However, STAT3 was found to be necessary for the development of the acinar-to-ductal metaplasia process, an early event in PDA pathogenesis, which is mediated by ectopic expression of the Pdx1 transcription factor, a key regulator in early pancreatic cancer development [130]. STAT3 is shown to be activated and overexpressed in ductal carcinoma cells as compared to the ducts from chronic pancreatitis [129]. Functional inactivation of STAT3 in a subset of PDA cell lines led to significant inhibition in cell proliferation in vitro and reduced tumor growth in vivo. Inhibition of activated STAT3 resulted in the delay in G1/S-phase progression due to inhibition of cyclin-dependent kinase 2 activity because of increased expression of p21/WAF1. Overall, the study clearly showed that with malignant transformation, activated STAT3 promotes proliferation of cells by modulating G1/S-phase progression and supports the malignant phenotype of human pancreatic cancer.

Cytoplasmic STAT3 monomers dimerize when phosphorylated at the Tyrosine 705 (Y705) by Janus kinases (JAKs) associated with cytokine-stimulated receptors, and then translocate to the nucleus, where the homodimers activate target gene transcription [134]. STAT3 can also be phosphorylated at Serine 727 (S727) by members of the mitogen-activated protein kinases (MAPK) and c-Jun N-terminal kinase families [134]. While phosphorylated Y705 (pY705) is generally believed to be essential for STAT3 transcriptional activity; the function of phosphorylated S727 (pS727) remains controversial, as this modification has been reported to have both down- and upregulatory effects on STAT3 transcriptional activity [135, 136, 137, 138].

In summary, STAT3 activation is associated with proliferation, inhibition of apoptosis and cellular transformation [139, 140]. However, activation of STAT3 also suppresses tumor growth [141] and induces differentiation and apoptosis in some contexts [142, 143, 144]. The mechanisms underlying STAT3's diverse and sometimes opposing roles are still largely unknown. It is assumed that STAT3 recruits specific co-activators and activates distinct gene expression programs based on the genetic

background, type and developmental stage of the cell [145]. This hypothesis raises an interesting issue of whether STAT3 pY705 and pS727 play a role in this process, considering their significance in STAT3-mediated control of gene transcription. Phosphorylation of Y705 is believed to be the key event in the transcriptional activation of STAT3 [146].

One potential transcriptional target of STAT3, that is important in oncogenesis is MUC1 [147]. The promoter of the MUC1 gene contains a STAT-responsive element, and STAT3 constitutively binds to the promoter of the MUC1 gene [148, 149]. Inhibition of STAT3 expression reduced expression of MUC1 genes and inhibited cellular motility in breast cancer cells [149]. There is convincing evidence that the aberrantly overexpressed MUC1 is associated with transformation, tumorigenicity, invasion, and metastasis of carcinomas and thus could be an important downstream target of STAT3. [150, 26, 151, 152, 153]. Furthermore, MUC1-C binds directly to JAK1 and STAT3 and promotes JAK1-mediated phosphorylation of STAT3. In turn, activated STAT3 induces expression of the MUC1 gene, in an autoinductive loop. Therefore, it has been proposed that targeting STAT3 and MUC1 together may be a strategy for enhanced anti-tumor efficacy [154].

Since the STAT3-MUC1 signaling is constitutively activated in high-MUC1 cancer cells, we hypothesized that MUC1 regulates the activity of STAT3 and that high-MUC1 cells will be more sensitive to STAT3-inhibition. In this study we aimed to understand the role of MUC1 in regulating differential phosphorylation of STAT3 and whether inhibiting STAT3 by Napabucasin interrupts MUC1-STAT3 interaction and downstream oncogenesis.

STAT3 has been a target for developing cancer therapy for a while, without successful transition into the clinic. For example, the STAT3 inhibitor Napabucasin or BBI608 was under phase III clinical trials for GI cancers, including pancreatic cancer, however, the trial was discontinued due to futility [155]. To better understand the

causes of treatment failure, the complex STAT3 signaling needs to be elucidated.

## 3.2 Results

### 3.2.1 Napabucasin inhibits survival, invasion, clonogenic and spheroid forming potential of PDA cells

PDA cell lines CFPAC, MiaPaca2 and HPAFII were treated with increasing concentrations of Napabucasin for 48 hrs. Napabucasin significantly reduced the spheroid (Figure 3.1 A) and colony (Figure 3.1 B) forming potentials of CFPAC and MiaPaca2 cells. It also significantly reduced the viability of PDA cells (Figure 3.1 C). HPAFII cells, however, were resistant to Napabucasin and responded only at very high doses. The invasion potential of all three PDA cells were reduced significantly after 72 hrs of treatment (Figure 3.1 D). Overexpression of MUC1 in cancer cells increased their sensitivity to Napabucasin, however, on blocking the homodimerization of MUC1, the sensitivity was reversed (Figure 3.1 E).

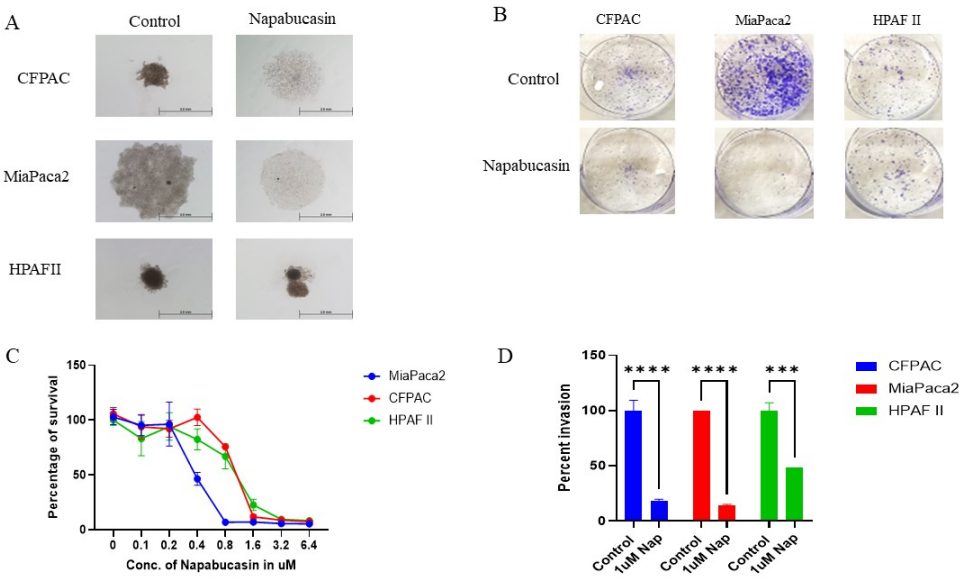


Figure 3.1: Anti-tumorigenic effect of Napabucasin on PDA cells

In Figure 3.1, A. the spheroid forming and B. colony forming potential, C. survival

and D. invasion potential of PDA cells CFPAC, MiaPaca2 and HPAF II have been shown.

### 3.2.2 Napabucasin is more potent in high MUC1 cancer cells

We aimed to study the pharmacodynamics of Napabucasin in low vs high MUC1 cancer cells. We treated a panel of human and murine cancer cells with increasing concentrations of Napabucasin. Human and murine cancer cell lines were stably transfected with either an empty vector or full length MUC1, and designated with the suffices "Neo" and "MUC1", respectively. These cells included human pancreatic cancer cells MiaPaca2.Neo and MiaPaca2.MUC1 and BxPc3.Neo and BxPc3.MUC1 and murine colon cancer cell lines MC38.Neo and MC38.MUC1, breast cancer cell lines C57MG.Neo and C57MG.MUC1, ovarian cancer cell lines MOVCAR.Neo and MOVCAR.MUC1 and pancreatic cancer cell lines KCM and KCKO.

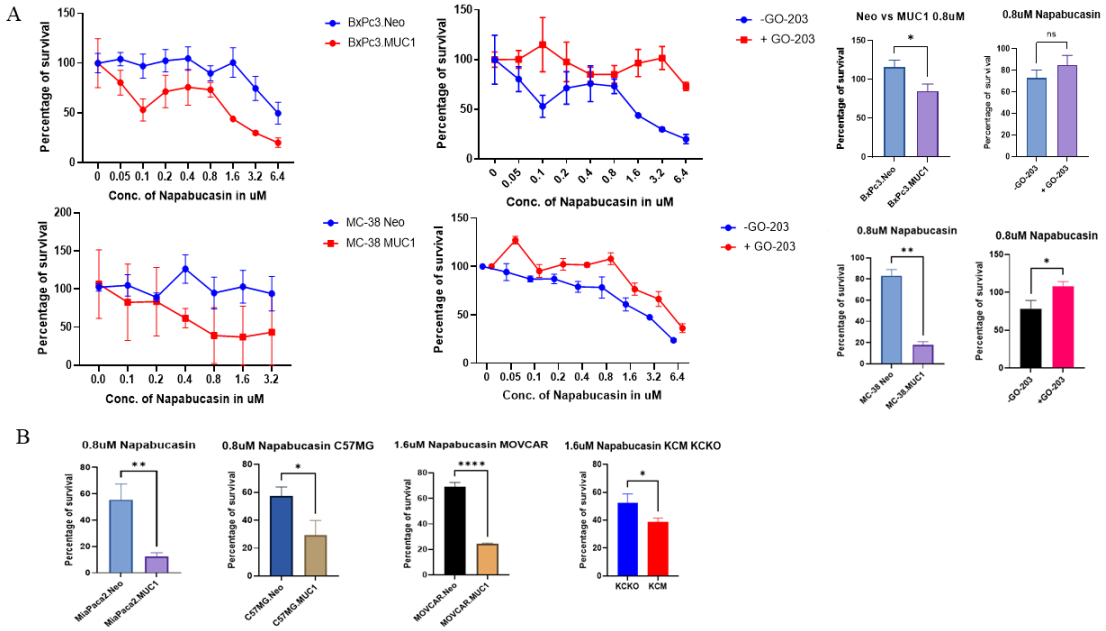


Figure 3.2: Napabucasin is more potent in high MUC1 cancer cells

A. Survival assays on cells transfected with either empty vector (Neo) or full-length MUC1 with or without 1-2 hours of pre-treatment with 10$\mu$M of MUC1-homodimerization blocking peptide GO-203 followed by the indicated concentrations

of Napabucasin treatment have been shown. (Left) BxPc3.Neo and BxPc3.MUC1 (top left), BxPc3.MUC1 before and after treatment with GO-203 (top right), MC38.Neo and MC38.MUC1 (bottom left) and MC38.MUC1 before and after GO-203 treatment (bottom right) to increasing concentrations of Napabucasin. (Right) Survival assay showing the sensitivity of A. (top) BxPc3.Neo and BxPc3.MUC1 and (bottom) MC38.Neo and MC38.MUC1 to 0.8$\mu$M Napabucasin and that of BxPc3.MUC1 and MC38.MUC1 before and after treatment with 10$\mu$M of GO-203. B. Survival assay showing the sensitivity of MiaPaca2.Neo and MiaPaca2.MUC1, C57MG.Neo and C57MG.MUC1, MOVCAR.Neo and MOVCAR.MUC1 and KCKO and KCM cells to 0.8$\mu$M Napabucasin.

Human PDA cell lines MiaPaca2.Neo and MUC1, BxPc3.Neo and MUC1, murine PDA cell lines KCM and KCKO (MUC1 KO), murine ovarian cancer cell lines MOVCAR.Neo and MUC1, murine breast cancer cell lines C57MG.Neo and MUC1, and murine colon carcinoma cell lines MC38.Neo and MUC1 were used to determine the $IC_{50}$ doses of Napabucasin. We found that the $IC_{50}$ of Napabucsin in cancer cells expressing high exogenous MUC1 were significantly lower than that in all low or no-MUC1 cancer cell lines (Figure 3.2). In order to rescue the differential potency of Napabucasin, we treated BxPc3.Neo and MUC1 and MC38.Neo and MUC1 cells with a MUC1-CT homodimerization- inhibitor peptide GO-203 for 1-2 hrs, followed by treatment with increasing concentrations of Napabucasin. After blocking MUC1-CT homodimerization for 1-2 hrs, the $IC_{50}$ values of Napabucasin in the high-MUC1 cancer cells increased and became similar to their low-MUC1 expressing counterparts. This data supports the idea that MUC1-CT homodimerization leads to constitutive activation of the STAT3-MUC1 pathway in high-MUC1 cancer cells, thus making them more sensitive to Napabucasin. In addition to that, 0.8 -1.6 $\mu$M was the concentration at which the difference in potency between low and high MUC1 cancer cells was at its peak.

### 3.2.3 MUC1 levels determine the phosphorylation status of STAT3

In a couple of studies, it has been shown that phospho-S727 regulates STAT3 activity by enhancing dephosphorylation of phospho-Y705 and triggers a multistep inactivation of STAT3 by rapid dissociation of pY705-SH2 through C-terminal tail modulation [156, 157]. To assess if MUC1 expression levels have any effect on differential phosphorylation of STAT3, we overexpressed full-length MUC1 in MiaPaca2 cells and knocked MUC1 down in HPAF II cells with a specific siRNA. We found that overexpression of MUC1 in MiaPaca2 cells, increased phosphorylation at Y705 and KD of MUC1 in HPAFII cells decreased phosphorylation at Y705 (Figure 3.3). In addition, STAT3 in MiaPaca2.MUC1 cells had decreased phosphorylation at Ser727 but increased phosphorylation in MUC1 KD HPAF II cells (Figure 3.3). Hence, MUC1 expression is crucial for the phosphorylation status of STAT3 and its activity.

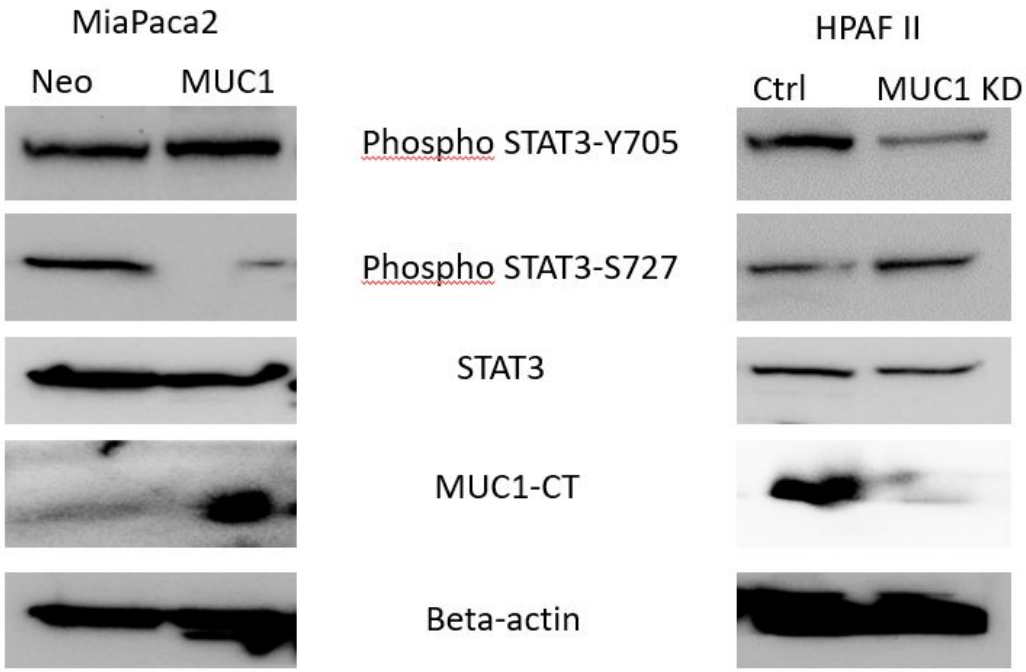


Figure 3.3: Western blot showing differential phosphorylation of STAT3 regulated by MUC1.

Figure 3.3, shows the expression of P-STAT3 Tyrosine 705 and Serine 727, total STAT3, MUC1-CT and $\beta$-actin on (left) MiaPaca2.Neo and MiaPaca2.MUC1 cells and (right) HPAFII with control siRNA and HPAFII with MUC1 knockdown.

### 3.2.4 Napabucasin reduces phosphorylation of STAT3 at Y705 and disrupts STAT3-MUC1 interaction

To assess the mechanism of action of Napabucasin in high vs low MUC1 PDA cells, we treated the cells expressing high, moderate and low levels of MUC1 with Napabucasin for 48 hours and checked the phosphorylation of STAT3 at Y705, expression levels of MUC1, and the effect on STAT3-MUC1 interaction. After treatment with Napabucasin, high-MUC1 CFPAC cells had significantly lower levels of pSTAT3 at Y705, decreased MUC1 expression (Figure 3.4A) and the binding of STAT3 to MUC1 was reduced in CFPAC cells but not in resistant HPAF II cells (Figure 3.4B). In contrast, we did not observe these effects in phosphorylation in the low MUC1 MiaPaca2 post Napabucasin treatment. This corroborates with our hypothesis that in high-MUC1 PDA cells, the STAT3-MUC1 signaling is constitutively activated as a survival pathway. HPAFII was found to be resistant to Napabucasin, and we found no difference in STAT3 phosphorylation or MUC1 levels in this cell line.

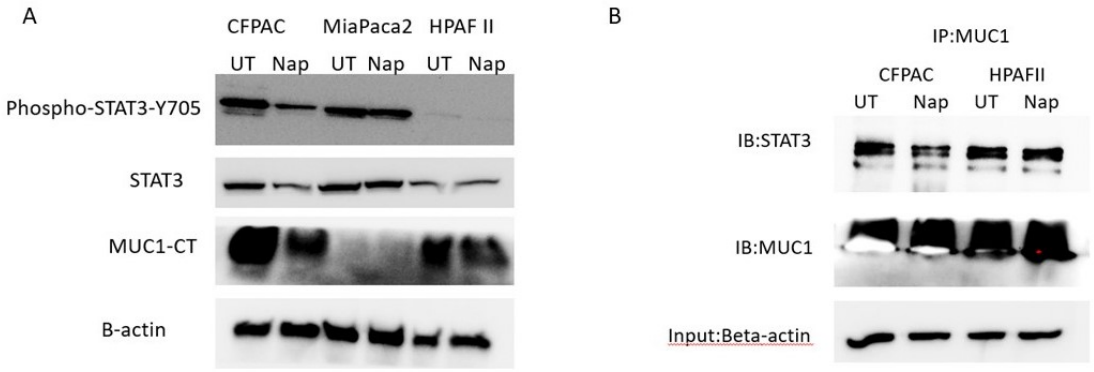


Figure 3.4: Mechanism of action of Napabucasin in high vs low MUC1 PDA cells.

In Figure 3.4, A. Western blot showing expression of P-STAT3 Tyrosine 705,

STAT3, MUC1-CT in CFPAC, MiaPaca2 and HPAFII cells before and after treatment with 2 $\mu$M of Napabucasin for 48 hours. $\beta$-actin was used as endogenous control. B Western blot showing expression of STAT3 and MUC1 in CoIP samples from CFPAC and HPAFII lysates before and treatment with 2 $\mu$M of Napabucaisn for 48 hours. 20 $\mu$g was used as input.

### 3.2.5 Combined targeting of STAT3 and MUC1 overcomes Napabucasin resistance partially

Since the HPAFII cell line was resistant to Napabucasin but is also a high-MUC1 expressing cell line, we hypothesized that targeting MUC1 in these cells in combination with Napabucasin might help overcome the resistance by breaking the autoinductive loop in which STAT3 and MUC1 co-operate. We treated HPAFII with Napabucasin in combination with an anti-MUC1 antibody TAB004, and found that to some extent TAB004 enhanced the anti-tumor efficacy of Napabucasin against the HPAFII cell line (Figure 3.5).

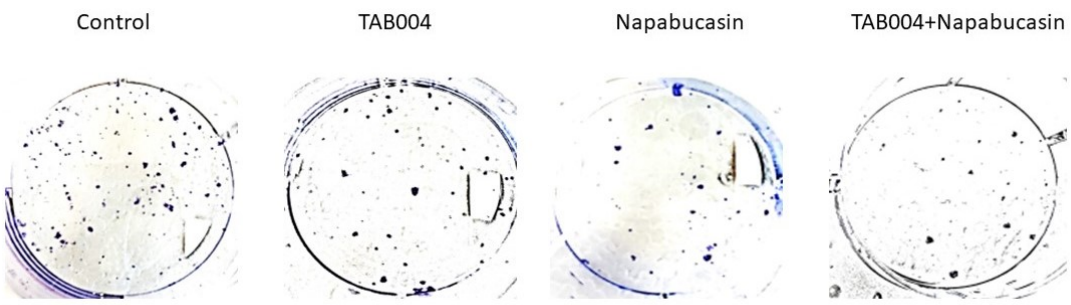


Figure 3.5: (Left to right) Colony forming assay on HPAFII cells with 10$\mu$g/ml of TAB004, 0.4$\mu$M of Napabucasin and both combined.

### 3.2.6 STAT3 expression correlates with poor overall survival in all epithelial cancers and MUC1 and STAT3 co-expression correlate with poor overall survival in gastrointestinal cancers

To assess the translational significance of STAT3-MUC1 partnership in epithelial cancers, mostly GI cancers, we analysed tumor data from TCGA and found that STAT3 was significantly overexpressed in majority of epithelial cancers vs normal (Figure 3.6a)and correlated with overall poorer survival (Figure 3.6b). We divided the tumor samples into low and high MUC1 groups and performed gene correlation analysis of STAT3 pathway genes and MUC1 gene expression. Differential gene correlation analysis showed over 170 significantly differentially expressed genes in the STAT3 pathway (Figure 3.6c). Also, STAT3 and MUC1 co-expression significantly correlated with overall poorer survival in GI cancers, thus showing the amplifying effect MUC1 has on STAT3 activity (Figure 3.6d) [158].

## 3.3 Discussion

STAT3 has been a target for developing cancer therapy for long, including GI cancers. Although current standard treatments for GI cancers are somewhat efficient, recurrence is still inevitable especially in PDA [159]. Many studies have indicated that presence of pancreatic cancer stem cells (PSCs), may be a major cause of disease relapse [160]. Therefore, targeting PSCs is a promising strategy to eradicate PDA. Given the well-documented role of overactive STAT3 signaling in PDA, the therapeutic potential of targeting this pathway should be emphasized. Multiple attempts to develop inhibitors against STAT3 pathway have been reported, and a variety of STAT3 inhibitors, including chemicals, STAT3-binding peptides, and siRNA reagents, have been developed with various degrees of success [161, 162].

Napabucasin (BBI608), a novel STAT3-specific inhibitor, was identified by [163]. They revealed that Napabucasin efficiently suppressed metastasis and relapse of a

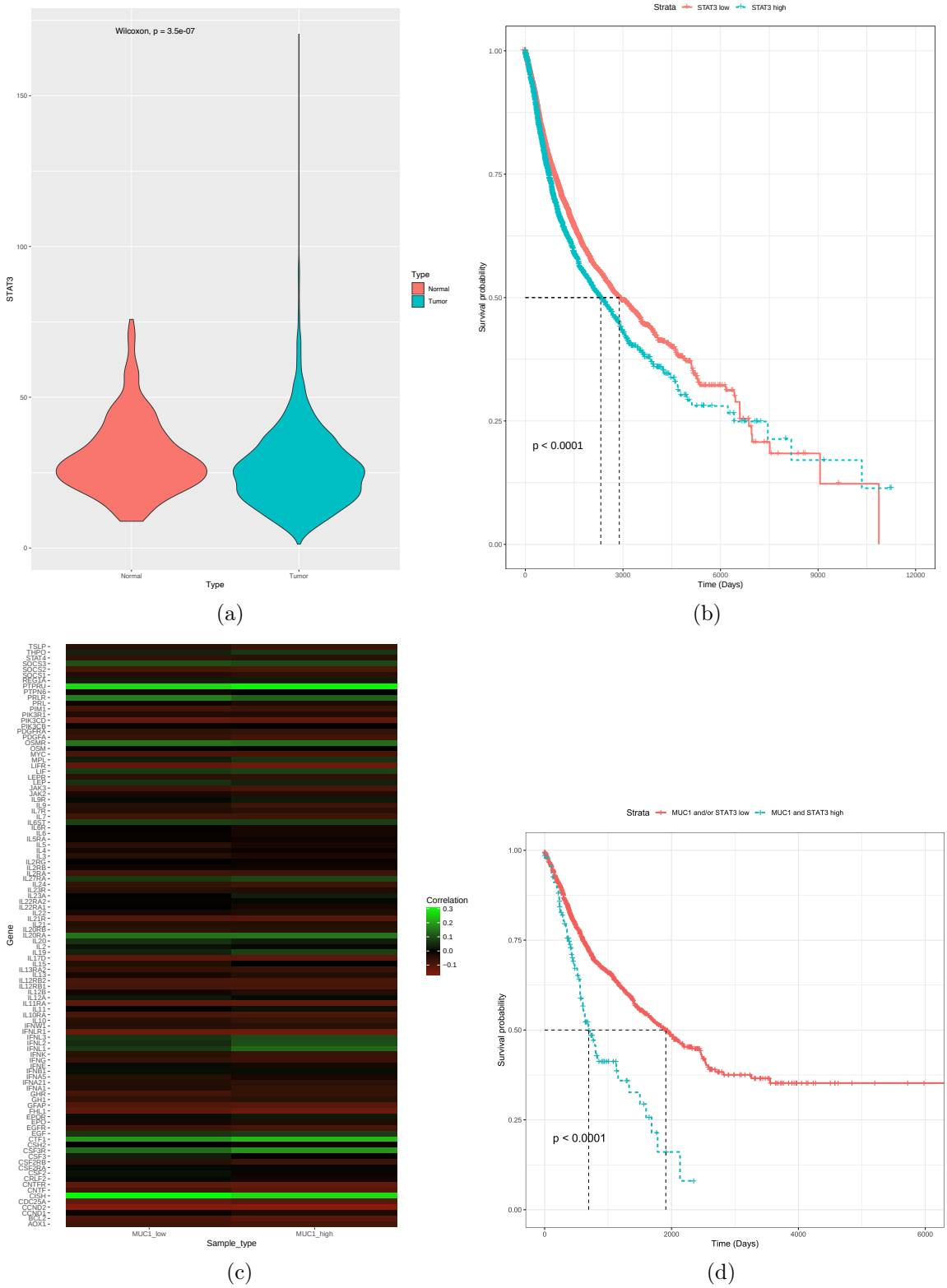


Figure 3.6: a. Graph showing increased expression of STAT3 in epithelial tumors. b. Kaplan-Meier survival plot showing correlation of STAT3 with overall poor prognosis in epithelial cancers. c. Heatmap showing differentially expressed genes in the STAT3 pathway in high vs low MUC1 tumors. d. Kaplan-Meier survival curve showing correlation of MUC1 and STAT3 co-expression in gastrointestinal cancers.

variety of cancers by inhibition of STAT3-driven gene transcription. Importantly, Napabucasin treatment impairs spheroid formation of liver cancer stem cells and downregulates the expression of stemness genes such as SOX2, BMI-1, Nanog, and c-Myc. Considering the promising preclinical data of Napabucasin as both a monotherapy and in combination with conventional chemotherapeutic methods, several clinical trials have been performed [164]. Furthermore, a phase III trial of Napabucasin for refractory colorectal cancer highlighted STAT3 as an essential target for the treatment of patients with elevated pSTAT3 expression [165]. However, to improve outcomes in the clinic, it is cruicial to find subpopulations of tumors that will be more sensitive to Napabucasin.

To our knowledge, this is the first study to evaluate the role of MUC1 in differential phosphorylation and regulation of STAT3 in the context of Napabucasin's efficacy. We confirmed that Napabucasin significantly inhibited cell proliferation, invasion, colony and spheroid formation in PDA cells (Figure 3.1). Following treatment with Napabucasin, the phosphorylation of STAT3 at Y705 was decreased in high-MUC1 CFPAC and HPAF II cells but not in low-MUC1 MiaPaca2 cells (Figure 3.3A). Napabucasin treatment also significantly reduced the expression of MUC1 in PDA cells and reduced binding of MUC1 to STAT3 in high-MUC1 CFPAC cells (Figure 3.3B). However, the Napabucasin did not reduce the interaction of STAT3 with MUC1 in the resistant cell line HPAFII. This could be due to a couple of reasons. First, the dose of 2$\mu$M was not enough to reduce the binding, or, there are other factors stabilizing the two proteins in HPAF II cells.

Since we found that the MUC1-STAT3 pathway was constitutively activated in high-MUC1 cells as the principal survival pathway, we hypothesized that high-MUC1 cells will be more sensitive to Napabucasin. Accordingly, we found that overexpression of MUC1 in different types of cancer cells conferred sensitivity to Napabucasin (Figure **??**).

We wanted to further explore the mechanism of regulation of STAT3 by MUC1. Therefore, we overexpressed MUC1 in a low MUC1 cell line MiaPaca2 and knocked MUC1 down in the high-MUC1 cell line HPAFII. We found that when MUC1 is overexpressed, there is increased phosphorylation of STAT3 at its activation site Y705 with a concomitant decrease in phosphorylation at its degradation site S727, in addition, when MUC1 is knocked down, the reverse is observed (Figure 3.7). In a study by [166] the underlying mechanism of the downregulated STAT3 protein level was mediated by protein synthesis inhibition induced by Napabucasin. We found that Napabucasin significantly impairs the binding of STAT3 and MUC1 which is a novel pharmacological mechanism of Napabucasin (Figure 3.8).

To assess the clinical relevance of our findings, we analysed RNA sequencing data across all gastrointestinal cancers available in TCGA and found that STAT3 is overexpressed in GI cancers, correlates to overall poorer survival (Figure 3.6A-B). We also identified more than 170 differentially expressed genes in the STAT3 pathway in high vs low MUC1 tumors (Figure 3.6C). In addition to that we found that co-expression of MUC1 and STAT3 correlated to further poorer overall survival in GI cancers, proving that MUC1 enhances the oncogenic activation of STAT3 (Figure 3.6D).

In our study, we reveal that Napabucasin treatment reduced STAT3 expression along with MUC1 expression levels and is more potent against high-MUC1 cells. Overall, our results support the potential use of Napabucasin as an efficacious anti-tumor therapeutic agent with a probability of better outcome in high-MUC1 tumor sub-populations, especially in combination with anti-MUC1 therapeutic agents.

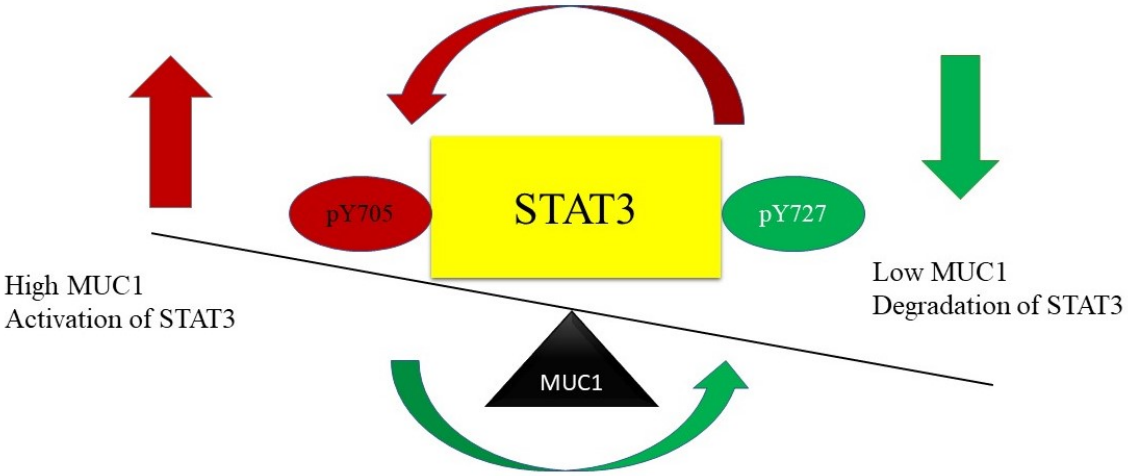


Figure 3.7: Proposed mechanism of regulation of STAT3 activity by MUC1

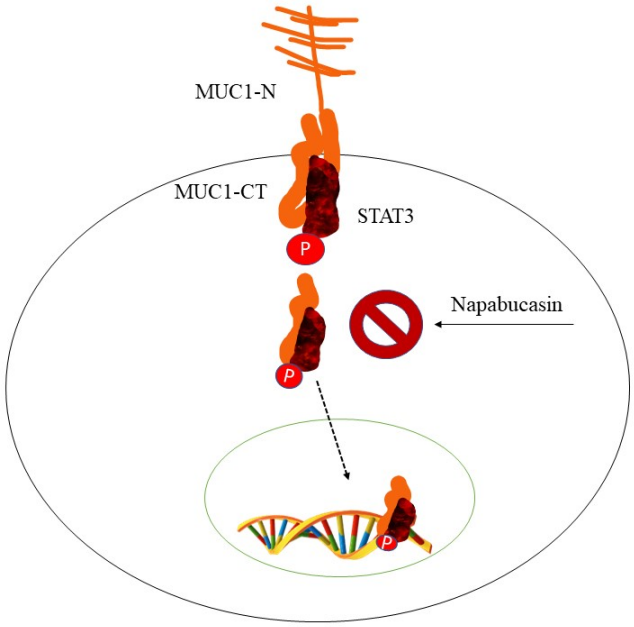


Figure 3.8: Mechanism of action of Napabucasin in high-MUC1 cancer cells

## 3.4 Materials and Methods

### 3.4.1 TCGA Data Analysis

1. TCGA Gene Expression Analysis

   RNA-sequencing data from 7,572 epithelial cancer samples available from TCGA

was analysed and STAT3 expression values in normal and tumor samples were plotted. The types of cancers include breast, lung, endometrium, kidney, head-neck, thyroid, prostate, colon, stomach, bladder, liver, cervix, pancreas, esophagus, adrenal, and gallbladder cancer. Plot was created using ggplot2 (version 3.3.5) package in R (version 3.6.3).

2. Gene Correlation Analysis

   Tumor samples from TCGA cancer projects were split into MUC1 low/high group based on the MUC1 gene expression relative to the average MUC1 gene expression in normal samples. Datasets was filtered to remove lowest expressed genes by the dispersion measure. Differential gene correlation analysis was performed on these two groups using DGCA (Differential Gene Correlation Analysis) in R (version 3.6.3). Gene correlation analysis was run, using the Benjamini-Hochberg p-adjustment measure. STAT3 pathway genes were selected and their correlation values with MUC1 were visualized in a heatmap, using ggplot2 (version 3.3.5) package in R.

3. Survival Analysis

   Survival analysis for STAT3 and overall survival in 13,509 cancer samples were computed using the Kaplan-Meier estimate and plots were made using ggplot2 (3.3.5) package in R (3.6.3). The average expression for STAT3 in normal samples was used to determine if tumor samples were low or high in STAT3 expression.

   Survival analyses for MUC1/STAT3 expression and overall survival in 2,055 gastric cancer type samples were computed using the Kaplan-Meier estimate and plots were made using ggplot2 (3.3.5) package in R (3.6.3). The average expression for MUC1/STAT3 in normal samples was used to determine if tumor samples were low or high in MUC1/STAT3 expression.

4. Cell lines and culture

Human PDA cell lines (CFPAC, HPAF-II and MiaPaca2) and murine cancer cell lines MC38 (colon), C57MG (breast), MOVCAR (ovarian) and KCM and KCKO (pancreatic) were obtained from American Type Culture Collection and cultured as instructed. Cell lines were maintained in Dulbeccoâs Modified Eagle Medium (DMEM; Gibco). All media was supplemented with 10% fetal bovine serum (FBS; Gibco or Hyclone), 3.4 mM l-glutamine, 90 units (U) per ml penicillin, 90 $\mu$g/ml streptomycin, and 1% Non-essential amino acids (Cellgro). Cells were kept in a 5% $CO_2$ atmosphere at 37°C. MUC1 WT sequence was cloned into the pLNCX.1 vector consisting of the neomycin resistance gene (neo) and confirmed by DNA sequencing. Neo cells had the empty vector with the G418 resistance gene (neo) and MUC1 cells had the full length MUC1 gene and G418 resistance gene (neo). All cells with Neo and MUC1 were generated by transfection with Lipofectamine 3000 (Thermo Fisher) according to the manufacturer's protocol and maintained in medium containing Geneticin (G418; Invitrogen, Carlsbad, CA, USA) [46]. Every passage of Neo or MUC1 transfected cells were maintained in a final concentration of 150 $\mu$g/ml of the antibiotic G418 (50 mg/ml) (Thermo Fisher) to ensure positive selection. HPAFII cells were serum-starved for 24 hrs and then treated with control siRNA from Life Technologies or MUC1 siRNA from Perkin Horizon according to the respective manufacturers protocol using Lipofectamine RNAiMAX Transfection Reagent (Thermo Fisher Scientific) for 72 hrs. For all experiments, cell lines were passaged no more than 10 times.

Treatment With Napabucasin and Western Blotting

The cell lines used were MiaPaca2. Neo, MiaPaca2. MUC1, HPAFII. controlsiRNA, and HPAFII. MUC1siRNA. Cells were treated with either 2 $\mu$M Napabucasin (Selleckchem, USA) or the vehicle (phosphate buffer saline) for

48 hrs. Cell lysates were prepared and western blotting performed as previously described [46]. Membranes were blocked with commercial blocking buffer (Thermo Fisher) for 30 min at room temperature and incubated with primary antibodies overnight at 4°C. The antibodies used were: Armenian hamster monoclonal anti-human MUC1 cytoplasmic tail (CT2) antibody (1:500). MUC1 CT antibody CT2 was originally generated at Mayo Clinic and purchased from Neomarkers, Inc. (Portsmouth, NH) [125]. CT2 antibody recognizes the last 17 amino acids (SSLSYNTPAVAATSANL) of the cytoplasmic tail (CT) of human MUC1. Membranes were also probed with the following antibodies from Cell Signaling Technology (1:1,000), p-STAT3 (Y705), total STAT3, $\beta$-Actin, and from ABclonal (1:1000) p-STAT3 (S727) and $\beta$-actin. Densitometric analysis was conducted using the ImageJ software. First, each density unit for the particular protein was normalized to their respective $\beta$-actin density and then represented as phospho/total. MTT Assay and addition of MUC1 blocking peptide 5,000 cells were plated in 96 well plates and allowed to grow overnight. Next day, the cells were treated either with PBS or increasing concentrations of Napabucasin in triplicates for 24-96 hr. Then 20$\mu$l of MTT solution (5 mg/ml) was added to each well and incubated for 3-4 hr at 37°C. Following that, the media with MTT was removed and 200$\mu$l of DMSO was added to each well to dissolve the formazan crystals for 10 min and the O.D. was measured with a plate reader (Multiskan, Thermo Fisher) at 560 nm. For blocking MUC1 signaling, the peptide GO-203 was added to the cells 2 hrs before treatment with Napabucasin.

5. Colony Forming Assay

   500-1000 cancer cells were plated in a 6-well tissue culture plate and allowed to adhere overnight. Next day, the cells were treated with increasing concentrations of Napabucasin (0.1, 0.2, 0.4, 0.8 and 1.6$\mu$M) for 7-14 days (depending on

the doubling time of each cell line). PBS was used as the control. After 7-14 days, the media was removed, colonies were washed with PBS and fixed with 3:1 solution of Methanol: Acetic acid for 5 minutes, followed by staining with 0.5% (w/v) of Crystal Violet in Methanol for 15 minutes. Then the colonies were washed under running tap water, images were taken, and colonies were counted manually. Colonies consisting of >25 cells were considered. The number of colonies in Napabucasin treated wells were calculated as a percentage of colonies in the PBS treated wells and plotted as a kill curve in GraphPad Prism. A p value of $<0.05$ was considered significant.

6. Invasion Assay

   Cells were serum starved for 18 hrs before plating for the invasion assay. 50,000 CFPAC, MiaPaca2 and HPAFII cells were plated over transwell inserts (Sarstedt) precoated with diluted Matrigel (1:1) in serum free media, with 1 $\mu$M of Napabucasin. The cells were allowed to invade through the Matrigel coating for 72 hrs towards the serum-containing medium in the bottom chamber. After 72 hrs, only the control wells were swabbed with a cotton swab, followed by staining of all inserts with 5% crystal violet. The excess stain was washed off and the inserts were allowed to dry. The membrane was cut and dipped in 10% acetic acid for 10 minutes to elute the dye, which was read by a Spectrophotometer at 560 nm. Percent invasion was calculated as (O.D. of Napabucasin treated sample / O.D. of PBS treated sample) X 100.

7. Spheroid Formation Assay

   Non-adherent U-bottom 96-well plates (Nunc, Thermo Fisher) were seeded with 5000 cells and centrifuged at 1000xg for 10 minutes. These cells were treated with 1$\mu$M of Napabucasin and the health of cells and size and integrity of the spheroids were monitored and pictures were taken with an inverted microscope

at 4X after 72 hrs.

8. Statistical Analysis

The data are expressed as the mean±SEM of n = 3. Differences between groups were examined using unpaired two-tailed t-tests, one-way and two-way ANOVAs. Statistical comparisons were made using the GraphPad Prism 9.0. p-values of <0.05 were considered statistically significant (*p $<$ 0.05; **p â< 0.01; ***p $<$ 0.001; ****p $<$ 0.0001).

# CHAPTER 4: POTENTIAL OF ANTI-MUC1 ANTIBODIES AS A TARGETED THERAPY FOR GASTROINTESTINAL CANCERS

## 4.1 Global Burden of GI Cancers

Gastrointestinal (GI) cancers collectively refer to cancers of the esophagus and stomach (gastroesophageal cancers), the colon and rectum (colorectal cancers), pancreas, liver, gallbladder, small intestine, appendix, and anus. Following lung cancer (18.4%), colorectal cancer (9.2%), stomach cancer (8.2%), and liver cancer (8.2%) form the leading causes of cancer-related deaths worldwide [167].

According to the American Cancer Society (ACS) (www.cancer.org), gastrointestinal (GI) cancers have the highest incidence and are the second leading cause of cancer-related deaths in the United States. Esophageal cancer is the seventh most commonly diagnosed cancer and the $6^{th}$ leading cause of cancer-related deaths worldwide [167]. It is often detected late and there are usually no early symptoms. The overall five-year survival rate for advanced esophageal cancer in the United States is about 15% [168]. Stomach cancer, or gastric cancer, is the fifth most common cancer in the world and the second highest cause of cancer-related deaths globally [169].

Pancreatic Cancer is the twelfth most common cancer globally and the seventh leading cause of cancer-related deaths [170]. However, in the US it is the third leading cause of cancer-related deaths and is projected to become the second by the end of the year 2020. Most of the pancreatic tumors are detected at a very advanced stage thus making it a lethal disease. It has a dismal 5% 5-year survival rate globally, a mean life expectancy of $<$6 months, and a high degree of resistance to standard therapy. In the US the five-year survival rate is 9%, which is the lowest of all major cancers. Liver cancer is the sixth most commonly diagnosed cancer and the fourth

leading cause of cancer-related deaths worldwide [168]. Colorectal cancer is the third most common cancer worldwide and the second leading cause of cancer mortality.

Chemotherapy and radiation therapy alone or in combination with surgery remain the main modes of treatment so far. However, various immunotherapies are undergoing trials with monoclonal antibodies, combination therapies, CAR-T cell, dendritic cell therapies etc. In the last 40 years, the incidence and mortality of GI cancers have only increased without improvement in therapy. The main challenge is to target specific antigens that are not expressed in normal tissues. Mucins have always been shown to be key immunological players in various chronic and infectious diseases including cancer. In this review, we will provide a detailed overview of various immunotherapies developed against the mucin protein MUC1 in GI cancers including monoclonal antibodies, CAR-T cells and bi-specific antibodies that have successfully been through preclinical and clinical trials. We will also provide perspectives on how some of these antibodies target specific hallmarks of cancer so that they can be combined with other drugs for better outcomes in the clinic.

## 4.2 MUC1 as a Target Antigen in GI Cancers

### 4.2.1 Structure of MUC1

Mucins are high molecular weight glycoproteins and their main function is to lubricate epithelial cell surfaces and protect them against invading pathogens [170]. Mucins are broadly divided into secretory gel-forming mucins (MUC2, MUC5AC, MUC5B, MUC6, MUC7 and MUC19, as protective barriers for underlying mucosal cells) and membrane-bound mucins (MUC1, MUC3A, MUC3B, MUC4, MUC12, MUC13, MUC15, MUC16, MUC17, and MUC20) that have a transmembrane, N-terminal extracellular domain (ECD), and a C-terminal cytoplasmic tail. Secretory gel-forming mucins work as protective barriers for underlying mucosal cells, while membrane-bound mucins also play a key role in cell signaling pathways and cellular interactions [170, 171, 172].

Mucin 1 or MUC1 (also known as episialin, PEM, EMA, H23Ag, MCA, and CA15-3) was the first transmembrane mucin to be identified and structurally characterized [8, 173, 174, 175]. MUC1 is a single pass type I transmembrane glycoprotein with a hyperglycosylated extracellular N-terminal domain that extends up to 200-500 nm from the cell surface [7, 176]. Normally, MUC1 is expressed on the apical surface of glandular or luminal epithelial cells of almost all tissues including the mammary gland, stomach, lungs, esophagus, duodenum, pancreas, uterus, prostate, and the hematopoietic cells [177, 178]. In healthy tissues, the extended hyperglycosylated branches of MUC1 create a physical barrier and prevent pathogenic access, thus protecting the underlying epithelia [179, 180]. The extended sugar branches form a mucinous gel by oligomerization and protect the underlying epithelia from desiccation, pH changes, and invading microbes [30]. During translation, MUC1 is cleaved [181, 182], and the extracellular domain with tandem repeats (25-100) is bound to the membrane by noncovalent interaction with the C-terminal domain of MUC1 (MUC1-CD) that consists of a short extracellular domain (ED), the transmembrane domain (TM) and the cytoplasmic domain (MUC1-CT). The MUC1 gene encodes a single polypeptide chain which is cleaved by auto-proteolysis process at a sea -urchin sperm protein enterokinase and agrin (SEA) domain to generate two peptide fragments and heterodimeric MUC1 [7, 11]. The subunit or MUC1-C contains a C-terminal cytoplasmic domain (MUC1-CT) with 69 amino acids, a hydrophobic transmembrane domain (TMD) with 28 amino acids and a short extracellular domain (ECD) with 58-amino acids that is noncovalently attached to the N-terminal extracellular domain (MUC1-N) or subunit [183]. The cytoplasmic tail of MUC1 (MUC1-CT) aids in signal transduction [30, 184].

Among different types of glycosylation, O- and N-glycosylations dominate in MUC1 [185]. The MUC1-N subunit in normal cells, consists of a heavily O-glycosylated-VNTR (variable number of tandem repeat) sequence of 20-21 amino acids (PDTR-

PAPGSTAPPAHGVTSA), which masks the peptide core and protects it from cleavage by proteolytic enzymes, and also prevents it from undergoing clathrin-mediated endocytosis [186]. The molecular weight of MUC1 can vary between 250-500 kDa based on the percentage of glycosylation (in the range of 50-90% of its molecular mass) and the number of tandem repeats [187]. N-glycosylation of MUC1 occurs at five potential sites, one in the ECD of MUC1-CD, and four in the degenerate repeat of MUC1-N [173]. N-glycosylation patterns are important for MUC1 folding, sorting, apical expression and secretion, whereas O-glycosylation is crucial for its biological properties [188, 189].

MUC1 glycosylation depends on the tissue of origin and is regulated by a large number of glycosyltransferases. O-glycosylation is initiated by adding N-acetylgalactosamine (GalNAc) to the VNTR region highly rich in threonine (Thr) and serine (Ser) residues. Following that, a large family of up to 20 distinct polypeptide GalNAc transferases (ppGalNAc-Ts) form the initial O-linked GalNAc -Ser/Thr structure (Tn antigen) in the endoplasmic reticulum (ER) and ER-Golgi compartments. This forms the initial O-linked GalNAc -Ser/Thr structure (Tn antigen) [190]. Following the formation of Tn antigen, GalNAc residue can be further modified by various distinct glycosyltransferases and construct di erent glycan structures of core 1 also known as T or TF (Thompson-Friedenreich) antigen (by addition of Gal residue) and core 3 (by adding GlcNAc 1-3GalNAc ) and Sialyl-Tn antigen (STn, by addition of sialic acid residue). Glycosylation continues by extension and chain termination by the addition of carbohydrates such as sialic acid [190, 191, 192].

However, in cancer cells, MUC1 mostly displays hypoglycosylation of the core glycans, like sialyation of Tn and T antigens via sialyltransferase enzymes that lead to premature chain termination [193, 194, 195, 196]. MUC1 expression has been shown to be up to 10 times higher in many human carcinomas than in normal tissues, which provides resistance to chemotherapy [196, 25, 197]. Therefore, antibodies against tu-

mor associated MUC1 are more likely to bind to the antigen on the surface of tumor cells and not MUC1 on the surface of normal cells. This makes tMUC1 a top molecular target to both detect cancers as well as design antibodies against the altered glycopeptide epitopes in the TR domain. These antibodies are also used to design human T cells to target tMUC1, called Chimeric Antigen Receptor T-cells (CAR T cells) [198, 199, 200].

### 4.2.2 Role in GI Tumors

MUC1 is overexpressed and aberrantly glycosylated in most human epithelial cancers [201]. The aberrantly glycosylated MUC1 expressed on malignant cells, called the tumor associated MUC1 or tMUC1 renders usually inaccessible MUC1 epitopes open to detection. MUC1 has been a molecule of interest for immunotherapy for a long time. It is a highly overexpressed cell surface antigen and has altered glycosylation in tumors [6]. However, MUC1 has been shown to play a paradoxical role following infections, acting as an anti-inflammatory molecule in healthy cells and as a pro-inflammatory molecule in cancer cells [98]. In 2009, the National Cancer Institute (NCI) had ranked tMUC1 as the second most targetable antigen out of 75 for developing cancer vaccines [100]. MUC1 has been reported to play a role in tumorigenesis by inhibition of cell death and promotion of metastasis [202, 203, 204]. MUC1 induces signaling through its cytoplasmic domain (MUC1-CT) and binds to the EGFR family of growth factor tyrosine kinases and enhances signaling through ERK activation and cell proliferation [205]. MUC1-CT interacts with $\beta$-catenin, stabilizes it and co-activates Wnt signaling [206]. MUC1 overexpression and its interactions with p53 and FOXO3a transcription factor dampen drug-induced apoptosis and resist oxidative cell damage [207, 208]. MUC1 also reduces pro-apoptotic signaling via the heat shock protein (HSP) 90, PI3K/Akt and Caspase-8 pathways [203, 209, 34]. An increase in depolarized MUC1 leads to the disruption of the normal cell-cell and cell-matrix adhesion and increase in cell-endothelial adhesion, allowing increased metastasis in

preclinical models [210]. The hypoglycosylated tMUC1 has increased interaction with cell adhesion molecules ICAM-1 and E-selectin, both of which can improve cellular migration and vascular invasion [211]. MUC1 confers drug resistance in pancreatic ductal adenocarcinoma cells by upregulating multidrug resistance genes [45]. MUC1 has also been reported to increase metastasis through the induction of platelet-derived growth factor (PDGF-A) expression by hypoxia inducible factor (HIF)1-$\alpha$ [212] and leads to epithelial-to-mesenchymal transition in pancreatic cancer [46, 94]. MUC1 has also been shown to regulate function of transforming growth factor-$\beta$ (TGF-$\beta$) and switch it from a tumor suppressor to a tumor promoter in PDA cells [88, 213]. MUC1 is a prognostic factor that marks poor outcome in gastric cancer patients [214]. Expression of MUC1 has also been reported to be significantly correlated to metastasis in colorectal cancer [202].

Overexpression in multiple epithelial tumors, expression all over the surface of a tumor cell due to loss of apicobasal polarity in cancer cells, thus making it accessible to antibodies and tumor-specific aberrant glycosylation with truncated carbohydrate antigens Tn and TF in the VNTR region are features that make MUC1 an attractive target for immunotherapy [198]. Various preclinical and clinical trials have been performed in GI cancers with antibodies against different MUC1 domains (MUC1-N, SEA and MUC1-C), some of them targeting specific hallmarks of cancer (Figure 4.1).

The objective of this review is to highlight the recent advances made in the treatment of gastrointestinal cancers utilizing antibodies, immunoconjugates and antibody-derived molecular therapies against tMUC1. We have also provided perspectives on how different anti-MUC1 antibodies target different hallmarks of cancer and thus can be utilized as a combination therapy to have better clinical outcomes.

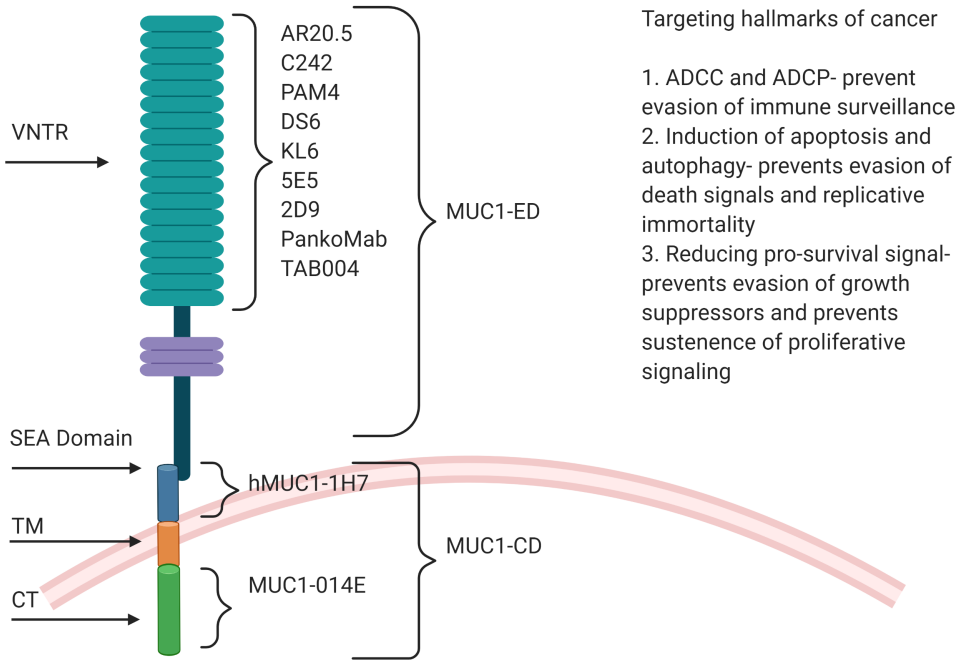


Figure 4.1: A schematic diagram showing the different antibodies recognizing different domains of MUC1 and also the hallmarks of cancer that they target.

In Figure 4.1, the various domains of MUC1 are denoted with different colors, ED and VNTR in sea green, SEA domain in blue, transmembrane domain in orange, and CT in light green.

## 4.3 Anti-MUC1 Antibodies in Preclinical and Clinical Trials

Antibody-based immunotherapy has been used for cancer treatment for the past two decades and is one of the most effective ways to treat hematological malignancies and solid tumors [215, 216]. Monoclonal antibodies (mAbs) can be generated by immunizing immunocompetent mice with tumor antigens or tumor cell lysates, or synthetically engineered to bind to specific proteins on cancer cells [217, 218]. The fundamental mechanism of therapeutic mAbs are to tag cancer cells for phagocytosis by macrophages or killing by NK or effector T-cells, block the downstream signaling of the target molecule, induce programmed cell death (or autophagy) in the antigen

expressing cancer cell, and aid in targeted delivery of therapeutic agents to specifically destroy cancer cells [217, 218, 219]. Many anti-MUC1 antibodies are in clinical trials or under pre-clinical or experimental studies. The anti-MUC1 antibody-based therapeutics developed against GI cancers that are in pre-clinical and clinical trials have been summarized in Tables 4.1 and 4.2 respectively.

Table 4.1: MUC1 antibodies under preclinical trials for GI cancers.

| **Antibody** | **Epitope** | **Original Antigen** | **Treatment under Trial** | **GI Cancer Type** | **Year** | **Reference** |
|---|---|---|---|---|---|---|
| KL-6 | a sialylated sugar of Krebs von den Lugen-6 (KL-6) PDTRPAP sequence | a sialylated sugar of Krebs von den Lugen-6 (KL-6) PDTRPAP sequence | 99mTc labeled anti-KL-6/MUC1 | Pancreatic Cancer | 2008 | [220, 221], [222] |
| MY.1E12 | sialyla2-3galactosylh1-3 Nacetylgalactosaminide linked to a distinct threonine in the MUC1 tandem repeat | HMFG | 3-ICG-acyl-1,3-thiazolidine-2-thione | Gastric Cancer | 2008 | [223, 224], [225, 226] |
| 5E5, 2D9 | Tn or STn in the tandem repeat domain | GalNAc-glycosylated MUC1glycopeptide (VTSAPDTRPAPGS TAPPAHG) conjugated to KLH | 5E5 MUC1-CAR-T cells | Pancreatic Cancer | 2016 2019 | [227] |
| hMUC1-1H7 | extracellular domain of MUC1 C-terminal subunit (MUC1-C) | recombinant human (rh) protein including extracellular region of MUCI-c (rhMUC1-EC192) obtainedfrom MCF7 cells | hMUC1-1H7 | Pancreatic Cancer | 2004 | [228, 229] |

MUC1 antibodies under preclinical trials for GI cancers (contd.)

| **Antibody** | **Epitope** | **Original Antigen** | **Treatment under Trial** | **GI Cancer Type** | **Year** | **Reference** |
|---|---|---|---|---|---|---|
| TAB004 | STAPPVHNV within the TR sequence | Protein lysate from MUC1-expressing tumors that developed in a MUC1 transgenic mice (PDA mice) that expressed human MUC1 | (1) TAB 004<br>(2) CAR-T cell therapy<br>(3) Bispecific antibody | Pancreatic Cancer | 2008-2019 | [83, 230], [231, 232], [233, 234] |

Table 4.2: MUC1 antibodies under clinical trials for GI cancers.

| **Antibody** | **Epitope** | **Original antigen** | **Treatment under trial** | **GI cancer type** | **Clinical trial status** | **Year** | **Reference** |
|---|---|---|---|---|---|---|---|
| huC242 | Sialyl-Lewis a epitope CanAg glycoprotein which is similar to MUC1 | Human colorectal adenocarcinoma cell line COLO205 | huC242-DM4 | Non-colorectal Cancer, Pancreatic Cancer; Locally Advanced and metastatic Stomach, Gastric and other GI cancers | Phase I completed; Phase II withdrawn | 2006 2008 | [221], [222], [223], [224] [225], [226] |
| huPAM4 | Domain located between the amino terminus and start of the repeat domain of a MUC1 antigen (non-VNTR) and react with MUC5AC | Mucin purified from the xenografted RIP I human pancreatic carcinoma | 111In-huPAM4 | Pancreatic Cancer | Phase I terminated | 2006 | [227], [228], [229] |
| hPAM4 (Clivatuzumab) | Domain located between the amino terminus and start of the repeat domain of a MUC1 antigen (non-VNTR) and react with MUC5AC | Mucin purified from the xenografted RIP I human pancreatic carcinoma | 90Y-hpAM4 (Clivatuzumab); 90Y-hpPAM4-Tetraxetan & Gemcitabine vs Placebo & Gemcitabine | Pancreatic Cancer; Metastatic Pancreatic Cancer | Phase I and II complete; Phase III terminated | 2008 2013 | [83], [230] |

MUC1 antibodies under clinical trials for GI cancers (contd.)

| **Antibody** | **Epitope** | **Original antigen** | **Treatment under trial** | **GI cancer type** | **Clinical trial status** | **Year** | **Reference** |
|---|---|---|---|---|---|---|---|
| SAR566658 huDS6-DM4 | O-linked glycans with $\alpha$2,3-sialylated and $\beta$1,4-galactosylated termini in VNTR | Human serous ovarian carcinoma | SAR566658 huDS6-DM4 | Pancreas | Phase II completed | 2010 | |
| PankoMab-GEM™ (Gatipotuzumab) | Epitope... PDT*RP..., where T* is O-glycosylated with GalNAca1- or a similar short, non-sialylated glycan such as Galb1-3GalNAca1- (core-1) | Tumor MUC1 from a desialylated human breast cancer source | PankoMab-GEM™ (Gatipotuzumab); Combination of Gatipotuzumab and anti-EGFR Tomuzotuximab | Pancreatic; Colorectal | Phase I ongoing; Recruiting for Phase I | 2010 2017 | [231], [232], [235], [234] |
| PD-1 inhibitor armed with an anti-MUC1 and anti-CD-3 bispecific anti-body | Information Unavailable | Information Unavailable | PD-1 inhibitor armed with an anti-MUC 1 and anti-CD3 bispecific antibody | Advanced Gastric, Colorectal, Pancreatic and Liver cancers | Recruiting for Phase II | 2018 | [236] |

MUC1 antibodies under clinical trials for GI cancers (contd.)

| **Antibody** | **Epitope** | **Original antigen** | **Treatment under trial** | **GI cancer type** | **Clinical trial status** | **Year** | **Reference** |
|---|---|---|---|---|---|---|---|
| AR20.5 | DTRPAP and DTnRPAP | MUC1 from an ovarian cancer patient, derived from human fluids and breast cancer cell MCF-7 culture medium | (1) AR20.5<br>(2) Combination of mAb-AR20.5, anti-PD-L1 and Poly ICLC | (1) Advanced adenocarcinoma<br>(2) Pancreatic Cancer | (1) Phase I completed<br>(2) Phase I/II ongoing | 2004<br>2018 | [186]<br>[237], [238] |

### 4.3.1 Monoclonal Antibodies

### 4.3.2 Antibodies Recognizing Non-Glycopeptide Epitope

Human milk fat globule 1 (HMFG1) is an IgG1 murine antibody with kappa light chain, recognizing PDTR epitope within the VNTR region of MUC1-ED. The humanized HMFG1 (AS1402, huHMFG1, Therex, BTH-1704, R-1550) was generated by transferring the complementarity determining regioDe murine HMFG1 onto selected human framework with the same affinity to MUC1 [239, 240]. To directly target MUC1 positive advanced pancreatic tumors and trigger neutrophil-mediated immune response, the binding capacity of this mAb in combination with a polysaccharide $\beta$ 1,3/1,6 glucan (derived from S.cerevisiae) as an immune stimulator with two drugs Gemcitabine and Imprime PGG was evaluated [241]. The secondary objectives were to characterize the adverse effects, time to progression, clinical response, progression-free and overall survival. However, this phase Ib trial (NCT02132403) was terminated due to drug recall. PAM4 is another IgG1 murine mAb, generated by immunizing mice with mucin purified from the xenografted RIP I human pancreatic carcinoma [242]. This mAb can recognize 85% of the pancreatic carcinomas and 50% of the colon carcinomas. However, it does not detect breast, ovarian, renal, prostate and liver cancers [243]. It has been reported that PAM4 is not related to the core epitopes of VNTR and that it also binds to other mucin proteins like MUC5AC [242, 244]. In the preclinical studies, 131I- and 90Y-labeled PAM4, was shown to control pancreatic cancer with enhanced survival and clinical responses in pancreatic cancer patients [245, 243]. In the phase I clinical trial, 131I-PAM4 IgG and 99mTc-PAM4 Fab0 showed the specific tumor localization in four out of five patients, therefore ensuring these are ideal candidates for further trials [243, 246]. Humanized PAM4 (hPAM4, IMMU-107) also known as clivatuzumab was constructed and radiolabeled with Yttrium (90Y) and used for patients with stage III and IV of pancreatic cancer. In a phase I trial, it was shown that 90Y-Clivatuzumab tetraxetan was well

tolerated with toxicity restricted to the bone marrow and manageable hematologic toxicity was seen at the maximal tolerated dose of 90Y. Tumor targeting was observed in most patients by using $^{111}$In-labeled antibody, and even with mucin antigen present in the serum, there were apparently no issues with the biodistribution or clearance of the antibody. All patients demonstrated disease progression at or after week eight, and some of them had stable target lesions at four weeks after treatment [247]. Hence, combination of chemotherapy and radioimmunotherapy agents was considered for future trials. Phase I/II trials with 80 participants are ongoing (NCT00603863) to test whether different doses of 90Y-hPAM4 in combination with gemcitabine are safe to give in patients with previously untreated pancreatic cancer. Clinical efficacy of Y-clivatuzumab tetraxetan (DOTA) with or without low-dose gemcitabine (PANCRIT$^{TM}$-1) was assessed in a phase I/II/III trial with metastatic pancreatic cancer patients which appeared to be an active first-line therapy for pancreatic cancer [248], but eventually, it was discontinued due to insufficient improvement in overall survival in comparison to placebo [NCT01956812]. GP1.4 is an anti-MUC1 antibody that caused internalization of EGFR in pancreatic cancer cells. This inhibited ERK phosphorylation by EGF stimulation in a MUC1 dependent manner. Inhibition of ERK phosphorylation by GP1.4 resulted in the suppression of proliferation and migration of pancreatic cancer cells [249]. TAB004 is a murine IgG1 mAb that was initially developed by immunizing Balb/c mice with lysates from MUC1-expressing tumors that developed in a human tMUC1 bearing transgenic mouse [83]. TAB004 targets the epitope area with sequence STAPPVHNV present within the TR sequence (AA950-958) of hypoglycosylated tMUC1 [177, 30, 230, 250]. TAB004 distinguishes between normal and tumor-associated forms of MUC1 solely based on the expression of hypo-glycosylated or aberrantly glycosylated MUC1. TAB004 alone or in conjugation with dye-doped mesoporous silica nanoparticles was used to detect breast cancer in vivo [232, 251]. TAB004 was also shown to be a diagnostic marker for cancer stem

cells and circulating MUC1 in mice and patients with pancreatic cancer [64]. TAB004 in combination with IL2 was shown to improve survival in PDA models by the following mechanisms: (1) reduction in tumor-induced immune regulation and (2) increasing recruitment of CD45+CD11b+ cells, thus increasing antibody-dependent-cellular-cytotoxicity or antibody-dependent-cellular-phagocytosis (ADCC/ADCP) [231]. It has also been reported that, the TAB004 antibody induces complement-independent growth inhibitory effect on PDA cells and significantly increases the anti-tumor efficacy of chemotherapy drugs like 5-FU, Gemcitabine and Paclitaxel [232]. In another study, humanized TAB004 was conjugated to 111In and 225Ac-DOTA and this immunoconjugate not only could target the tumor specifically but also showed complete preclinical response in triple negative breast cancer [252]. MUC1-014E is another anti-MUC1 antibody raised against an intracellular nonrepeating 19-amino-acid sequence (RYVPPSSTDRSPYEKVSAG) of the MUC1-CT, using a synthetic peptide with the 7-amino-acid epitope (STDRSPY). MUC1-014E showed sharp and specific staining of carcinoma cells, but no staining in fibroblasts, endothelial cells, and inflammatory cells. High rates of positive immunohistochemical staining (97-100%) was found in 107 gastrectomy specimens compared with the other MUC1-related antibodies (MUC1-DF3, MUC1-Ab-5 and PAb anti-MUC1*1110-ecd). MUC1-014E also recognized isolated cancer cells of signet-ring cell carcinoma (sig) and non-solid type poorly differentiated stomach adenocarcinoma (por2). Therefore, this mAb could be used to detect cells in scirrhous gastric cancer [253]. hMUC1-1H7 is an anti-hMUC1 murine mAb developed against a recombinant MUC1 obtained from the breast cancer cell MCF7. It significantly reduced proliferation of breast cancer cells in which it is internalized and specifically localized in MUC1-expressing tumors in the xenograft mouse models. hMUC1-1H7 is specific for the extracellular domain of MUC1-CD and can bind to shed MUC1 as well [229]. It has also been reported that, G3 can inhibit EGF-mediated ERK phosphorylation and cyclin D1 expression, thus, inhibiting

EGFR signaling pathways in pancreatic cancer models [228].

### 4.3.3 Antibodies Recognizing Glycopeptide Epitopes

PankoMab is a murine IgG1, kappa light chain mAb recognizing tMUC1 glycopeptide. It has shown a reduced rate of binding to circulating tMUC1 and mononucleated cells in the serum of colon and pancreatic cancer patients [254]. There are various chimeric and humanized formats of PankoMab under clinical trials as suitable candidates for therapeutic and diagnostic applications [255]. PankoMab-GEM™(PMG) also known as Gatipotuzumab (previously known as PankoMab-GEM™), is a glycooptimised mAb with many advantages. For example, it has higher tumor specificity and affinity with an increased number of binding sites, reduced binding to shed MUC1 from colon and pancreatic carcinoma, no binding to peripheral blood mononucleated cells, stronger ADCC, and rapid internalization compared to other antibodies [255]. Its mechanisms of action include ADCC and ADCP. A phase I study in patients with tMUC1 positive advanced solid tumor showed that PMG was safe, well tolerated and showed promising anti-tumor activity [256]. The phase 2 study evaluated the efficacy and safety of PMGs maintenance therapy compared to placebo in patients with recurrent ovarian, fallopian tube or primary serous peritoneal cancer [257]. This randomized double blinded study reported that PMG failed to improve the time without disease recurrence when given as a single entity [257]. However, it showed a good safety profile, hence, targeting tMUC1 by this antibody in combination with other standard chemotherapy or developing a bi-specific antibody to modulate the immune system holds promise to improve its anti-tumor efficacy [257]. AR20.5 (BrevaRex) is a murine monoclonal antibody (IgG1) developed by immunizing mice with three different sources including MUC1 derived from an ovarian cancer patient, human fluids and MCF-7 cell culture medium. It reacts with six amino acids within the VNTR region (DTRPAP). However, addition of a single GalNAc enhanced the binding affinity of AR20.5 to the MUC1 epitope [186]. AR20.5 forms a complex with

circulating MUC1 and/or transmembrane MUC1 on tumor cells. This complex can be internalized by dendritic cells which facilitates effective antigen-processing and cross-presentation of MUC1 to T cells, and leads to the activation of cytotoxic T cells to kill the tumor [258]. In the phase I trial of AR20.5 patients with advanced adenocarcinoma were treated, it induced MUC1-specific immune responses, did not have dose-limiting toxicity, and induced no hypersensitivity reactions. The 2-mg dose showed the strongest biological activity, and was evaluated in future trials [259]. The combination of AR20.5, anti-PD-L1 antibody and PolyICLC rejected human MUC1 expressing tumors and provided a long-lasting, MUC1-specific cellular immune response, which when adoptively transferred to human MUC1 transgenic (MUC.Tg) mice, provided protection against tumor formation. CD8+ cells were found to be the effectors for the MUC1-specific immune response generated by this combination. In the US, a phase I/II clinical trial is ongoing for pancreatic cancer by OncoVent Co., Ltd., with this combination [260]. The DS6 antibody is an IgG1 murine antibody recognizing the CA6 sialoglycotope of tMUC1 that is overexpressed in a variety of solid tumors, including ovarian, breast, cervical, pancreatic and lung cancers. DS6 detects a CA6 antigen that is different from well-characterized tumor-associated antigens, such as MUC1, CA125 and the histo-blood group-related antigens sLea, sLex and sTn [261]. DS6 specifically binds to the tandem repeat domain of CA6-positive MUC1 based on the presence of mucin type O-linked glycans with $\alpha$2,3-sialylated and $\beta$1,4-galactosylated termini [262]. Humanized DS6 (huDS6) antibody was conjugated to the cytotoxic maytansinoid derivative drug DM4 through a cleavable linker. The ADC was called SAR566658 and it showed antitumor efficacy against CA6-positive human pancreas, cervix, bladder, and ovary in vivo tumor xenograft models, with a minimal effective dose correlating with CA6 expression as well as better efficacy than standard-of-care nontargeted tubulin binders. SAR566658 was used in a phase I clinical trial with 114 patients with refractory solid tumors. It showed a satisfac-

tory safety profile and antitumor activity. Tumor improvement was shown in 35-60% of patients at different dosages of SAR566658 [263]. The monoclonal IgG1-kappa antibody C242 was developed by immunizing a mouse with human colorectal adenocarcinoma cell line COLO205. Humanized C242 (HuC242 or Cantuzumab) has the CA242 epitope and reacts with a novel glycoform of MUC1 also known as CanAg glycoprotein (cancer antigen) [236]. CanAg is very highly glycosylated, rich in fucose and sialic acid and Hx-CanAg (heavy subunit) is very similar to MUC1 in amino acid composition, but L-CanAg (light subunit) is different. Deglycosylated H-CanAg can be recognized by the monoclonal antibodies SM-3 and HMFG-2 [237]. Also, due to its high expression in most pancreatic, biliary and colorectal cancers, CanAg is a potential candidate for mAb-based therapies. In a phase I trial, Cantuzumab was conjugated to an anti-microtubule agent mertansine (DM1) and different doses were used to treat colon and rectum carcinomas or other malignancies with positive CanAg antigen as a single intravenous infusion. Results showed that HuC242-DM1 is safe and well tolerated with effective antitumor activity [238, 264]. In another phase I trial, cantuzumab conjugated to potent cytotoxic maytansinoid drug ravtansine (DM4), called IMGN242, was found to be well tolerated in colorectal and pancreatic cancer patients at 168 mg/m2 dose. This provided a basis to perform phase II clinical studies [265]. The phase II trial was started in CanAg-expressing gastric cancer patients at a dose of 168 mg/m2.

The data has been amended to differentiate the administered dose of IMGN242 based on the patientâs plasma CanAg levels [266]. KL-6 is a mouse IgG1 mAb that specifically recognizes a sialylated sugar of Krebs von den Lugen-6 (KL-6), which is considered a MUC1-derived glycoprotein antigen. The minimal antigenic epitope for binding of this antibody is PDTRPAP. It has been reported that anti-KL-6/MUC1 mAb increased aggregation of MUC1 glycoproteins at one pole of the cell, called capping of MUC1 on the surface and facilitated E-cadherin-mediated cell-cell interaction

in breast cancer cell lines YMB-S and ZR-75-1S. Anti-KL-6 also enhanced the cytotoxic activity of lymphokine-activated killer (LAK) cells. The mechanism of action of this antibody is capping of MUC1 and restoring cell-cell adhesion by E-cadherin, which induces cell cycle arrest by upregulation of the cyclin-dependent kinase, p27 [267]. This also leads to increased accessibility for effector cells to kill tumor cells [220, 221, 222]. 99mTc labeled anti-KL-6/MUC1 antibody was shown to be a tumor-specific radiotracer that detects pancreatic cancer in vivo, but no further information is available [268].

MY.1E12 is another murine anti-humanMUC1 mAb that binds toMUC1 bearing sialylated O-linked oligosaccharides. MY.1E12 was generated by immunizing mice with HMFG. It can identify colon carcinoma tissue [223, 224]. MY.1E12 specifically reacts to T structure (ST) attached to Thr8. The sialylation of the T structure (ST) enhances its reactivity with MUC1 [225]. ICG-N-hydroxysulfosuccinimide ester (ICG-sulfo-OSu) and 3-ICG-acyl-1,3-thiazolidine-2-thione (ICG-ATT) were developed as infrared fluorescent-labeling reagents, and anti-human CEA antibody and FMY.1E12 were labelled with 3-ICG-acyl-1,3-thiazolidine-2-thione. This was shown to recognize the gastric cancer tissue specimens with a strong fluorescent signal [226]. 5E5 and 2D9 are mouse IgG1k mAbs that were generated by immunization of wild-type Balb/c mice with GalNAc-glycosylated MUC1 glycopeptide (VTSAPDTRPAPGSTAPPAHG) conjugated to KLH. These antibodies exhibited high selectivity for MUC1 tandem repeat glycopeptides with Tn and STn O-glycans and showed preference for Tn-MUC1 glycoforms that had the highest O-glycan occupancy. They can bind to MUC1 with Tn or STn in the GSTA sequence of tandem repeats but do not bind to the GSTA epitope carrying T [227].

### 4.3.4 Bispecific Antibodies for MUC1

Bispecific antibodies (bsAbs) can recognize two distinct epitopes or antigens simultaneously and therefore enhance the ability of immune cells to engage to tumor cells.

Recently, MUC1 has been considered for designing bsAbs. MUC1-CD16-Bi antibody is a novel bispecific antibody generated via a Serine-Glycine linkage between single domain antibodies (VHH segments) against tMUC1, and CD16 presented on natural killer (NK) cells. The bsAb against MUC1 named MUC1-Bi-1 was humanized by grafting the CDRs of both segments to DP-47 V-segment. Both MUC1-Bi-1 and its humanized version specifically detected tMUC1 on several cancer cell lines (SKOV3, HT29, and LS174) and potentially introduced them to NK cells. These bsAbs had no binding affinity and cytotoxicity to MUC1 negative CHO and HepG2 cells even in the presence of NK cells [269, 270]. Different types of bsAbs were constructed with binding affinity to both tMUC1 and CD3 on T-cells. Fab'-S-NB fragments of OKT-3 mAb (anti-CD3) and Fab-SH fragments of MUSE11 mAb (anti-tMUC1) were used to generate the first bsAb which increased the antitumor activity of CD3+ T-LAK cells. MUSE11 is a mouse IgG1 mAb developed against the ascites fluid of gastric cancer patients. The epitope of this antibody could be within the amino acid sequence PDTRPAPG of tMUC1 [271]. MUC1 x CD3 BsAb was constructed with MUSE11 (anti tMUC1) and OKT-3 (anti-CD3), and MUC1 x CD2S BsAb was constructed with MUSE11 and 15E8 (anti-CD28) antibodies. The Fab-SH from MUSE11 and Fab-S-NB of mouse IgG1 15E8 (anti-CD28) antibodies were used. These BsAbs showed growth inhibition of TFK-1 cancer cells and bile duct carcinoma in SCID mice [272]. The BsAbs (MUC1 x CD3 BsAb and MUC1 x CD28 BsAb) together exhibited 60% cytotoxicity in vitro, similar to that shown by BsAb (MUC1 x CD3) alone. Although reduction in tumor growth was limited, simultaneous administration of a combination of three bsAbs (M x 3, M x 28 and M x 2 bsAb) with peripheral blood mononuclear cells (PBMCs) or T-LAK cells in vitro showed higher cytotoxicity against MUC1-expressing bile duct carcinoma cells [272]. Mx3 diabody is a recombinant BsAb generated using the variable domains of two mAbs directed at effector cells, one against CD3 (OKT-3, mouse IgG2a) and the other against CD28

(l5E8, mouse IgGl), and MUSE11 (mouse IgGl), directed at tMUC1 [273]. One chain consists of a variable heavy chain specific for MUC1 linked to a variable light chain specific for CD3 with a short polypeptide linker GlyGlyGlyGlySer (GGGGS). The second chain has a variable light chain specific for MUC1 linked to a variable heavy chain specific for CD3. Therefore, Mx3 diabody can specifically bind to both MUC1 and CD3 positive LAK cells with a T cell phenotype (T-LAK). Mx3 diabody with T-LAK showed growth inhibition in about 98% of TFK-1 cells with an effector:target ratio of 10 [273]. Mx3 was fused genetically to the mutated superantigen staphylococcal enterotoxin A (SEA) D227A to specifically target bile duct carcinoma (BDC). This super-antigen fused diabody also showed the potential to inhibit the BDC cell line TFK-1 and reduce tumor size when compared to the Mx3 diabody alone [274]. A bsAb containing F(ab0)2/F(ab0) fragments with a functional chemical linker is the anti-MUC1/anti-Ga chelate. A mouse IgG1 12H12 mAb raised against a mouse glycosylated form of MUC1 called TAG-12 was combined to another mouse IgG3 anti-Ga chelate mAb. Prior to 3A10 F(ab0)coupling, the 12H12 F(ab0)2 fragment was labeled with 125I. This bispecific-mAb showed improved immunoscintigraphic tumor localization in breastcarcinoma bearing mice [275]. Another bsAb has been constructed with a novel PD-1 inhibitor-induced cytokine- induced killer cells (CIKs) armed with an anti-tMUC1 and anti-CD3 antibodies. This bsAb is currently under several phase II randomized clinical trials for advanced gastric, kidney, lung, breast, colorectal, pancreatic and liver cancers, but there is no further information available ([NCT03554395], [NCT03540199], [NCT03501056], [NCT03524261], [NCT03524274], [NCT03509298], and [NCT03484962]) [276].

## 4.4 CAR-T Cells Targeting MUC1

TAB004 has been used to make a CAR-T cell construct, which has exhibited significant cytotoxic activity against pancreatic cancer cells and reduced growth of orthotopic pancreatic tumors in a NOD-SCID mouse model [234]. Some PDA cells, for

example CFPAC and HPAF II, were found to be resistant to the therapy and several genes were overexpressed in them such as indoleamine 2, 3-dioxygenases-1 (IDO1), cyclooxygenase 1 and 2 (CO x 1/2), and galectin-9 (Gal-9) [234]. This study showed that combining biological inhibitors of IDO1, CO x 1/2, and Gal-9 with the CAR-T cells resulted in significant enhancement of CAR-T cell cytotoxicity against PDA cells.

5E5 mAb showed high specificity to breast cancer cells and tissue [198, 274] and was used to develop MUC1 CAR-T cells. These CAR-T cells showed cytotoxicity against leukemia and pancreatic cancer cells and also enhanced survival of mice by eliminating the barriers for engagement of the endogenous immune system [199, 277].

## 4.5 Molecular Interactions between MUC1 and Its Antibodies

X-ray crystallography of antibody crystal structures [278] and NMR analysis of glycopeptides [279] are used to understand the biochemical interactions or molecular recognition between the antigen and antibody. The Tn antigen is one of the most important structural motifs of tMUC1 found widely in many different aggressive carcinomas [280, 281]. It has been shown by years of extensive effort to develop antibodies targeting tMUC1 having the Tn antigen, that most anti-MUC1 antibodies do not directly bind to carbohydrates. However, the binding affinities with the immunodominant MUC1 are shown to be significantly increased by O-glycosylation in this area [282, 283, 284]. AR20.5 bound to the glycopeptide with stronger affinity than the naked peptide. These observations led to the hypothesis that the antibody must specifically bind the carbohydrate as well as the peptide. X-ray crystallography of the structures of AR20.5 [186] and SM3 [285] in complex with both peptide and glycopeptide revealed that the carbohydrate did not have any specific polar contacts with the antibody. The high affinity for the glycopeptide and the lack of specific binding contacts of AR20.5 suggest that glycosylation of MUC1 stabilizes an extended bioactive conformation of the peptide that is recognized by the antibody. Evidence

suggests that glycosylation of the peptide alters the conformational equilibrium of the antigen, and this allows the antibody to select the correct conformation. Therefore, glycosylation of MUC1 is important for the generation of high affinity therapeutic antibodies [186]. The anti-MUC1 KL-6 antibody distinguishes between the ST, Tn, and T antigens at the same O-glycosylation site independent of the modifications at other potential sites [221, 283, 284]. The NMR study suggests that KL6 mAb strictly recognizes the epitope from the extended trans conformation of a glycopeptide, which has been modified with the ST antigen. Detailed molecular recognition studies on MUC1 and anti-MUC1 antibodies and the use of synthetic glycopeptide library to develop a new class of antibodies targeting "dynamic glycopeptidic neoepitopes" with disease-relevant O-glycosylation in immunodominant mucin domains have been described recently [286].

The lack of carbohydrate-binding specificities in most anti-MUC1 mAbs is a huge challenge for the development of MUC1-based therapeutic antibodies. Antibodies binding to cancer-relevant glycopeptidic neoepitopes with higher specificities in carbohydrate recognition will be beneficial in the development of anti-MUC1 mAbs as therapeutic and diagnostic agents in the clinical settings.

## 4.6 Concluding Remarks and Future Perspectives

In spite of MUC1 being a top target, multiple trials with MUC1 antibodies and antibody-derived immunotherapies have failed to translate to the clinic. Most of the trials have been discontinued for not being sufficiently effective. There may be various reasons for the inefficiency of the antibodies. As of now, many anti-MUC1 antibodies have been developed against the highly immunogenic VNTR region of MUC1 $\alpha$ chain (MUC1-ED) [287]. After cleavage at the SEA domain, the MUC1-N is often shed from the surface of cells and released into the peripheral blood. The shed $\alpha$ subunits (MUC1-N) sequester anti-MUC1 antibodies against the VNTR region, preventing them from binding to the surface MUC1 [255]. To overcome this problem, antibodies

against MUC1-CD could be used as a more effective strategy. Shedding of MUC1-N increases its levels in the serum of patients with various cancers [288, 289, 290], thus, reducing the specificity and effective binding of the antibodies to MUC1 on the tumor cells [288, 291]. Therefore, serum levels of MUC1 in different cancer patients need to be evaluated to find an effective dose of the antibodies [292]. In addition, bsAbs can be made by combining immune checkpoint inhibitors such as anti-PD1 and anti-PD-L1 antibodies with anti-MUC1 antibodies. This will increase engagement of the immune cells with the tumor. In recent years, antibodies are being designed against the other domains of MUC1 including SEA, extracellular, and intracellular MUC1-CT. Therefore, rational designing of antibodies and combination therapy strategies are important to achieve a good safety and efficacy profile against MUC1 expressing cancers. Antibodies to the non-glycopeptide part of the VNTR region have not been able to generate an effective cellular or humoral immune response to tMUC1 [293]. Antibodies to MUC1 peptide also do not effectively recognize MUC1-expressing tumor cells. However, antibodies raised against shortened glycopeptide structures with a simple T antigen (T, Gal$\beta$1-3GalNAc), sialyl Tn (NeuAc$\alpha$2-6GalNAc) and Tn (GalNAc) elicit the strongest immune response against MUC1-expressing tumor cells [294]. This happens due to the specific presence of Tn and STn glycans on MUC1 expressing cancer cells, but not on normal epithelial cells and the blocked regions of the VNTR domain get exposed to recognition by antibodies, thereby, producing tumor-specific recognition sites. As evident, studying the glycosylation changes have led to the development of potentially effective MUC1-based immunotherapy [295, 212]. Some anti-MUC1 antibodies can recognize the MUC1 epitopes on both normal epithelial and tumor cells thus compromising the specificity [296]. Also, heterogeneity of MUC1 expression levels, the glycosylation pattern and subcellular distribution contribute to reduced binding efficiency. The different glycoforms may confer an evolutionary advantage on the tumor cells to be resistant against antibody-based therapies [296, 297].

Therefore, a combination of antibodies that can detect many glycoforms of MUC1 can be considered for clinical trials. Anti-MUC1 antibodies directed against the SEA domain target the junction of MUC1 $\alpha$ and $\beta$ subunits, which is composed of intact epitopes from both [298, 299]. These anti-SEA domain antibodies have shown high affinity and effectivity compared to antibodies targeting the VNTR region [299]. The mechanism of action anti-MUC1 mAbs target one or more hallmarks of cancer. For example, some antibodies have been reported to show ADCC and ADCP, some others block anti-apoptotic mechanisms thus inducing cell death, also some antibodies reduce expression of pro-survival genes. Gatipotuzumab is a glycooptimized antibody developed by Glycotopes GlycoExpress™platform that significantly improved treatment outcome with mechanisms such ADCC, tumor cell phagocytosis and induction of apoptosis compared to non-glycooptimized biotherapeutics [257]. Other antibodies against MUC1 glycopeptide, such as 5E5 and 1B2, have been shown to be effective as immunotherapy strategies because of their high specificity to tMUC1 and ability to induce ADCC [300]. Therefore, by utilizing the mechanism of action of an antibody, strategies could be developed to eliminate the tumor.

However, a decrease in concentration of anti-MUC1 antibodies targeting the tumor and their poor internalization due to the extracellular MUC1-N barrier remain major hurdles. To overcome this, development of antibody fragments can be considered [295, 301]. Also, a whole or fragmented antibody could be conjugated to potent drugs to target specific types of tumor cells. For example, Napabucasin, which is a STAT-3 inhibitor was under Phase III clinical trials for PDA but was discontinued due to futility [302]. However, it has been shown that high-MUC1 PDA cells are more sensitive toward the STAT-3 inhibitor Napabucasin [303]. Therefore, anti-MUC1 antibodies armed with Napabucasin may be a promising strategy to eliminate high-MUC1 tumors. Bispecific and trispecific antibodies armed with anti-PD-1, anti-MUC1 and anti-CD3 are new products under clinical trials [276].

# CHAPTER 5: TARGETING TUMOR-ASSOCIATED MUC1 OVERCOMES ANOIKIS-RESISTANCE IN PANCREATIC CANCER

## 5.1 Introduction

Currently, cancer is the second leading cause of death worldwide and the main cause is not the primary tumor, but metastasis and recurrence. Cancer cells metastasize after successful detachment from surrounding cells or the extracellular matrix (ECM), migrating to distal locations, followed by reattachment, and proliferation in the new site [304]. Cancer cells employ different mechanisms to avoid anoikis, thus enhancing their invasiveness and potential for metastasis. These include ligand-dependent or independent oncogenic signals that induce pro-survival signaling pathways, leading to stemness, proliferation, and invasion [305]. Anoikis is an apoptotic event, which is activated to clear detached cells [306] via induction of both the intrinsic and extrinsic apoptotic pathways. Pro-apoptotic events are activated in the mitochondria to trigger the activity of effector caspases for elimination of detached cells and restoration of tissue homeostasis. For detached cells that have undergone epithelial-to-mesenchymal transition (EMT), it is crucial to resist anoikis to colonize a new organ. Anoikis resistance, is an emerging hallmark of metastatic malignancies since it provides cells with an advantage of anchorage-independent survival during tumor dissemination [307, 308, 309, 310]. Different factors have been reported to aid in anoikis-resistance in cancer cells including but not limited to changes in cell adhesion molecules, enhanced production of reactive oxygen species (ROS) and growth factors like EGF, FGF and VEGF, activation of oncogenic signaling pathways, upregulation of stemness factors, hypoxia and autophagy. Especially in PDA, the anoikis resistance mechanisms are mostly driven by changes in glucose metabolism, STAT3

upregulation, BCL2 activation, activation of c-SRC in a FAK independent manner. The PI3K-Akt pathway has been reported to drive anoikis resistance in anchorage-independent cells [305]. Mucin 1 or MUC1 is a heterodimeric transmembrane glycoprotein with a hyperglycosylated extracellular N- terminal domain that extends out of the cell surface. MUC1 is expressed on the apical surface of glandular or luminal epithelial cells of almost all normal tissues. The MUC1 single polypeptide chain is cleaved by auto-proteolysis at a sea -urchin sperm protein enterokinase and agrin (SEA) domain to generate two peptide fragments and heterodimeric MUC1. The $\beta$ subunit or MUC1-C contains a C-terminal cytoplasmic domain (MUC1-CT), a hydrophobic transmembrane domain (TMD) and a short extracellular domain (ECD) with 58-amino acids that is noncovalently attached to the N-terminal extracellular domain (MUC1-N) or $\alpha$ subunit [6],[27]. MUC1-ECD engages in extracellular signaling through sensing of external stimuli, followed by reprogramming of downstream gene expression profiles of cells [308, 309]. In tumor tissues, MUC1 is overexpressed, hypo- and aberrantly glycosylated, which exposes its core peptide and makes it accessible to immunotherapy [311]. Hypo-glycosylated MUC1 shows increased intracellular uptake by clathrin-mediated endocytosis and decrease in degradation. Thus, hypoglycosylation may foster MUC1 oncogenic signaling by decreasing its cell surface levels and increasing intracellular accumulation [6]. The receptor-like functions of MUC1 provide adhesive/anti-adhesive functions to the cells. The transmembrane MUC1-CT subunit is 72 amino acid residues-long and acts as a highly busy docking site for numerous signaling molecules [312]. It directly interacts with several transcription factors, and physically occupies multiple promoter regions [27]. Although, MUC1 lacks a DNA binding domain, it acts as a transcriptional co-activator or adaptor protein and its presence in transcriptional complexes significantly enhances recruitment of other co-factors and promoters of oncogenic transcription factors [6]. Transcriptional regulation and other oncogenic functions are significantly modulated by post-translational

modifications of MUC1-CT. For example, the MUC1-CT has seven tyrosine residues that are highly conserved across all mammalian species. Phosphorylation of these tyrosine residues increase the binding affinity of multiple kinases to MUC1-CT, thus enabling activation of downstream oncogenic signaling [312].

TAB004 is a mouse monoclonal IgG1 antibody that was developed by immunizing Balb/c mice with lysates from MUC1-expressing tumors that spontaneously developed in a transgenic tMUC1 bearing mouse [202]. The epitope of TAB004 is present within the TR sequence (AA950-958) of hypo-glycosylated tMUC1 [313, 83, 177]. TAB004 can differentiate between the normal and tumor-associated forms of MUC1 based on the hypo-glycosylation or aberrant glycosylation of MUC1. Several studies showing TAB004s tumor specificity, and its diagnostic and therapeutic potential have been published [30, 230, 64, 232, 251, 231, 252, 314, 234]. However, the mechanism of action of TAB004 in intracellular signaling has not yet been elucidated.

Thus far, TAB004 has primarily been used as a vehicle for targeted therapy and imaging. The rationale of this study is to understand the intracellular oncogenic signaling changes post binding of TAB004 to surface tMUC1 in epithelial tumor cells, with a focus on PDA. Our long-term goal is to optimize therapeutic strategies to prevent metastasis and recurrence. There is significant lack of understanding of the mechanism(s) of action of tumor-specific antibodies with regards to how it may alter intracellular oncogenic signaling within a cell. Thorough analysis of the intracellular signaling of an antibody after binding to its target may clarify some of the causes of resistance development and its clinical potential. Overexpression of MUC1 has long been associated with high metastatic potential and poor prognosis in cancer patients [202]. MUC1 O-glycosylation has been reported to promote resistance to anoikis, and removing the glycosyl residues opened up interaction of cell death receptors to their ligands, leading to apoptosis. Both MUC1-ECD and MUC1-CT were found to contribute to anoikis-resistance in epithelial cancer cells [313]. In this study, we

show how targeting MUC1-ECD with TAB004 antibody can slow tumor growth by overcoming anoikis-resistance through inhibition of altered oncogenic signaling via MUC1-CT.

## 5.2 Results

### 5.2.1 MUC1 is overexpressed in majority of epithelial cancers, correlates with poor overall survival and anoikis-resistance genes

We confirmed MUC1 overexpression in majority of epithelial cancers as analyzed from the TCGA database (Figure 5.1A). Compared to normal samples (n=1,603), the expression of MUC1 was significantly higher in tumor samples across multiple tumor types (n=13,509) (Figure 5.1A). Overexpression of MUC1 was found to be significantly correlated (p=0.017) with poorer overall survival in epithelial tumors (n=12,042) across 48 different tumor types (Figure 5.1B). The TCGA dataset was analysed for significantly differentially expressed genes (DEGs) in normal vs tumor samples in human PDA (data not shown). The list of DEGs was curated for finding a subset of nine genes that are associated with anoikis resistance, as determined from the literature, and from those that were significantly upregulated in PDA (Figure 5.1C). These nine genes belong to the family of growth factor and its receptors (EGF, EGFR), GPCRs (PI3K and PI3KR), non-receptor tyrosine kinases (c-SRC), transcription factors (c-MYC) or regulators of apoptosis (PTRH2 and BCL2). These genes were found to be significantly associated with stemness, drug resistance, regulation of actin cytoskeleton, focal adhesion, autophagy, and apoptosis by KEGG pathway analysis (Figure 5.1D). Survival data showed that overexpression of these nine genes significantly correlated with overall poorer prognosis in epithelial cancers (Figure 5.1E). The list from Figure 5.1C was further filtered to find correlation with MUC1 expression in normal vs tumor samples. Seven out of nine genes showed a trend of positive correlation with MUC1 expression levels in normal vs tumor samples in PDA (Figure 5.1F). PTRH2 and SRC were filtered out due to high variability.

The types of epithelial cancers analysed and patient characteristic table are in the Supplementary Tables 5.1 and 5.2.

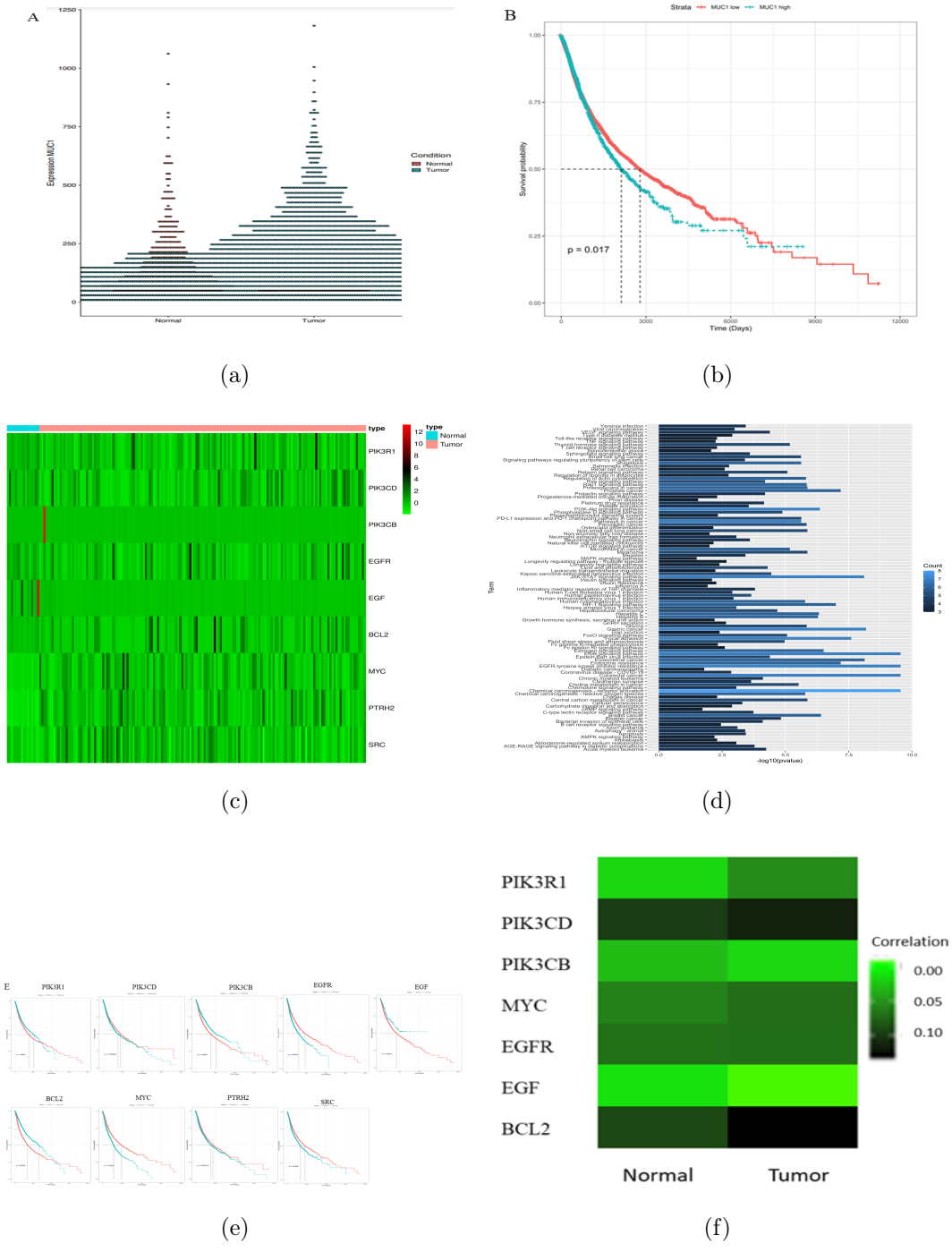


Figure 5.1: MUC1 is overexpressed and correlates with anoikis-resistance and poor overall survival.

In the Figure 5.1, (a) MUC1 gene expression values in normal and tumor samples from the pan-cancer analysis. A total of 15,112 samples were included, 13,509 tumor and 1,603 normal samples. Plot was generated from the Differential Gene Correlation Analysis (DGCA) (1.0.2) package in R (3.6.3). (b) Kaplan-Meier survival analysis with MUC1 gene expression from pan-cancer analysis. (c) Heatmap showing scaled expression values for genes PIK3R1, PIK3CD, PIK3CB, EGFR, EGF, BCL2, MYC, PTRH2, and SRC in samples obtained from the TCGA pancreatic cancer (PAAD) project. (d) Pathway analysis was performed for the following genes: BCL2, EGF, EGFR, MYC, PIK3CB, PIK3CD, PIK3R1, PTRH2, and SRC, and the list of KEGG pathways that these genes were significantly associated with are shown as a bar plot. (e) Kaplan-Meier survival analyses with expression of the nine genes from pan-cancer analysis. (f) Heatmap showing gene correlation values with MUC1 expression, calculated from DGCA, in PIK3R1, PIK3CD, PIK3CB, EGFR, EGF, MYC, and BCL2 genes for normal vs. tumor samples (PAAD project) (The SRC and PTRH2 genes were filtered out during pre-processing filtering steps).

### 5.2.2 Treatment with TAB004 reduces survival, colony forming potential and invasion in PDA cells

A panel of PDA cell lines were analyzed for their MUC1 expression using TAB004-FITC, that binds to tumor-associated MUC1 (tMUC1) (Figure 5.2A). CFPAC and Capan 2 cells expressed high levels of tMUC1 on their surface, HPAF II expressed medium levels and MiaPaca2 expressed low levels of tMUC1. TAB004 treatment significantly reduced the colony forming ability (Figure 5.2B) in a dose dependent manner. The $IC_{50}$ values for each cell line are shown in the table and representative images of the colony forming plates for Capan 2 and CFPAC are also shown in Figure 5.2B. In general, PDA cells expressing higher tMUC1 showed higher $IC_{50}$. To confirm that cell survival was impacted, we used the MTT assay on CFPAC, MiaPaca2, and normal HPDE cells and show that post TAB004 treatment, the PDA cells have 50%

survival while normal cell line remains unaffected (Figure 5.2C). HPDE normal cells did not form colonies and therefore was not included in the colony forming assay. Further, TAB004 treatment significantly reduced the percent of CFPAC cells that invaded the matrix in a trans-well invasion assay (Figure 5.2D). When tested in combination with other chemotherapy drugs, TAB004 enhanced the anti-tumor efficacy of 5-FU and Gemcitabine but not paclitaxel as measured by significant reduction in survival of CFPAC cells in the combination group of TAB004 and drugs (Supplementary Figure 5.9).

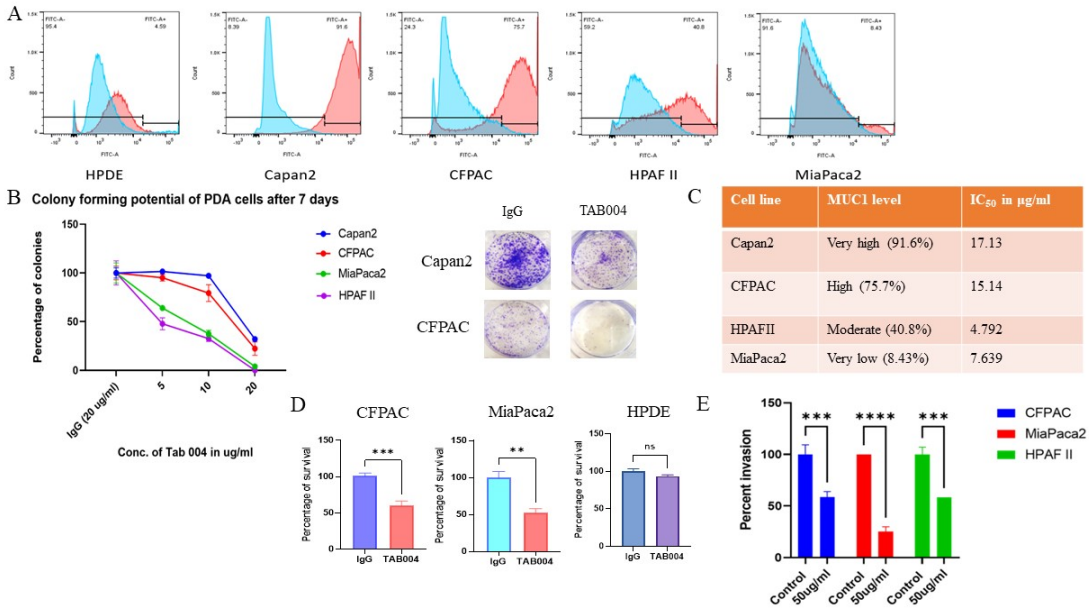


Figure 5.2: TAB004 reduces tumorigenic properties of PDA cells.

In Figure 5.2, A. Expression of MUC1 in PDA cells HPDE, Capan2, CFPAC, HPAFII and MiaPaca2 (left to right). B. (Left) Graph showing percent of colonies formed by the four PDA cell lines with increasing concentrations of TAB004 (5, 10 and 20$\mu$g/ml) after 7 days. Percentage of colonies were calculated as ((Number of colonies in TAB004 treated wells / Number of colonies in IgG treated wells) X 100) (Right) Representative image showing the number of colonies in 20$\mu$g/ml IgG and TAB004 treated Capan2 (top) and CFPAC cells (bottom). C. Table showing the

MUC1 expression levels of the PDA cells and the respective IC50 values of TAB004. D. Graphs showing the percentage of survival in CFPAC, MiaPaca2 and HPDE (left to right) cells after 48 hrs of treatment with 80$\mu$g/ml of TAB004 by MTT assay. E. Invasion was determined by standard transwell assay and results are presented as percentage of cells invading the Matrigel after treatment with 10$\mu$g/ml and 20$\mu$g/ml of IgG and TAB004 for 48 hrs. Percent invasion was calculated as ((O.D. of TAB004 treated sample with conc. x/ O.D of IgG treated sample with conc. x) X 100). All the experiments were performed in three independent replicates and the data are represented as ± SEM.

### 5.2.3 Treatment with TAB004 reduces activation of EGFR-PI3K pathway as measured by phosphorylation of EGFR and PI3K

To evaluate the effect of TAB004 treatment on downstream oncogenic signaling, we assessed the EGFR-PI3K pathway post treatment with TAB004. CFPAC cells were serum-starved overnight and treated with EGF with or without pre-treatment with TAB004. EGF induced phosphorylation of EGFR and PI3K in CFPAC cells within 10 minutes (Figure 5.3A-B). When the cells were pre-treated with TAB004 for 20 minutes, EGFR and PI3K phosphorylation was significantly reduced (Figure 5.3A-B).

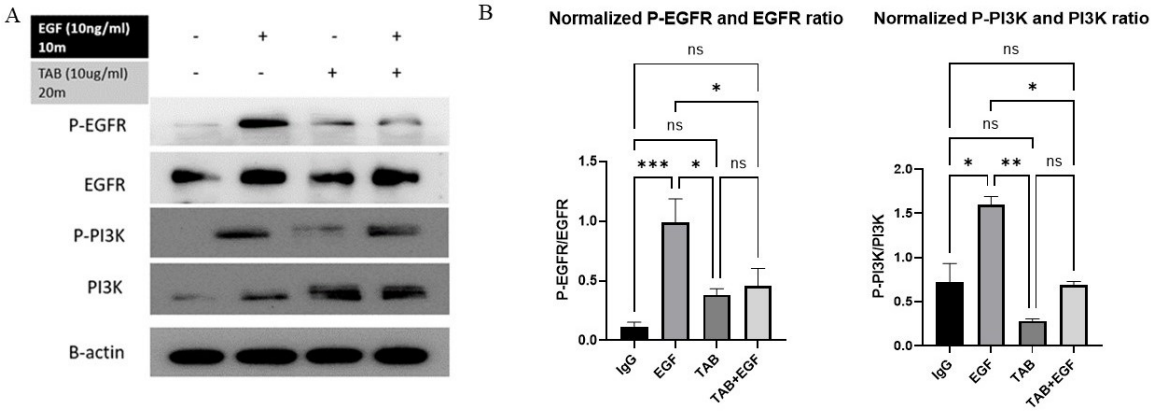


Figure 5.3: TAB004 blocks EGFR-PI3K pathway.

In Figure 5.3, A. Western blot showing levels of P-EGFR, EGFR, P-PI3K and PI3K before and after treatment with 10ng/ml of EGF for 10 minutes and 10$\mu$g/ml of IgG or TAB004 for 20 minutes. $\beta$-actin was used as endogenous loading control. B. Densitometric analyses of expression levels of the proteins after normalization with $\beta$-actin levels. All the experiments were performed in three independent replicates and data are presented as ±SEM of n=3.

### 5.2.4 Gene expression changes induced by treatment with TAB004 in PDAC cells

To further understand the underlying mechanism of TAB004âs anti-tumor effects, we performed transcriptomics on two PDA cell lines CFPAC (tMUC1-high) and MiaPaca2 (tMUC1-low) post 24h treatment with either IgG or TAB004. The DEGs in CFPAC primarily belonged to the metabolic pathway genes or to the cell-cycle and apoptosis regulating genes (Figure 5.4A). The DEGs involved in cell cycle regulation and apoptosis include E2F1, WRAP73, ZC3H4, CIAPIN1, TMEM127, TRIB2, protein degradation (ASB16-AS1 and UBE2S), cell-cell adhesion and extracellular matrix remodeling and migration (CDH23, CNTN2, CCBE1), endoplasmic reticulum stress and hypoxia (SCAMP5, EGLN3) (Figure 5.4B). We confirmed the induction of autophagy by LC3B staining in TAB004 treated CFPAC cells after 24 hrs and there was a significantly higher number of cells undergoing autophagy after TAB004 treatment vs IgG treatment (Figure 5.4C).

In MiaPaca2, most changes were observed in the amino acid transport and metabolism (SLC6A9, PSAT1, MTHFD2, PHGDH,), ER stress (ATF4) and autophagy (ATF4 and SLC7A5) (Figure 5.4B). It is important to mention that ATF4 promotes transcription of genes linked to amino acid sufficiency and protection of cells against metabolic consequences of ER stress [315]. It activates the transcription of asparagine synthetase (ASNS) in response to amino acid deprivation or ER stress [316]. In both the cell lines, autophagy was confirmed by increased lysosomal activity on TAB004 treatment, which could not be rescued after pre-treating the cells with autophagy

inhibitor Chloroquine phosphate (Figure 5.4B).

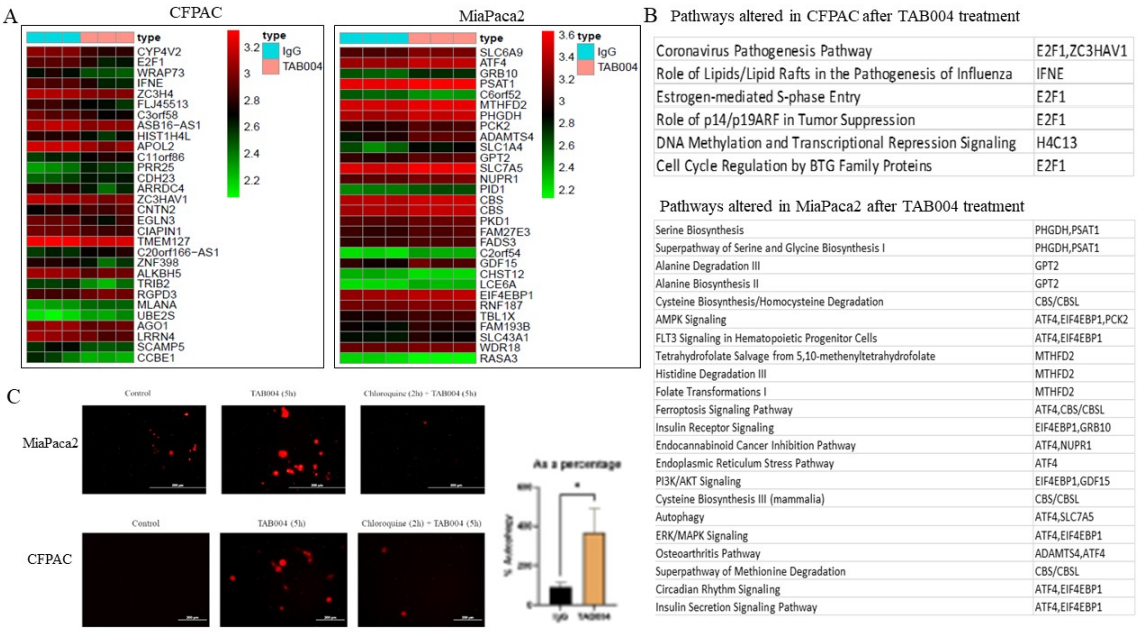


Figure 5.4: TAB004 induces nutrient starvation, ER stress and autophagy in PDA cells.

In Figure 5.4, A. Heatmap showing top 30 differentially expressed genes in (left) CFPAC and (right) MiaPaca2 cells after 24 hrs of treatment with TAB004. Fold change of DEGs in TAB004 samples were calculated as a ratio of the IgG treated samples and the genes with a p value of $<0.05$ between treatment groups were considered significant. B. Significantly altered pathways in CFPAC (top) and MiaPaca2 (bottom) cells were plotted from Ingenuity pathway analysis. C. (Left) Fluorescence microscopy images of MiaPaca2 (top) and CFPAC (bottom) cells stained with Lysotracker Deep Red before and after treatment with 20 $\mu$g/ml of IgG and TAB004 for 5 hours with or without 2 hours of pre-treatment with 100 $\mu$M Chloroquine phosphate. (Right) Flow cytometry analysis of CFPAC cells treated with 20$\mu$g/ml of TAB004 for 24 hrs and stained with LC3B antibody. Percent autophagy was calculated as a fold change of LC3B+ cells in TAB004 treated samples vs IgG treated samples. All experiments were performed in three independent replicates and data are shown as

±SEM.

### 5.2.5 TAB004 leads to degradation of MUC1, disrupts MUC1-CT signaling and induces apoptosis

Assuming that TAB004 treatment induces nutrient deprivation and autophagy (based on Figure 5.4), we evaluated if the treatment with TAB004 led to increased degradation of MUC1 protein itself in CFPAC cells. After 48 hrs of TAB004 treatment, there was significant reduction in cytoplasmic MUC1 levels, although no significant change in nuclear MUC1 was observed (Figure 5.5A). We hypothesized that due to degradation of MUC1, the binding site for many cytoskeleton maintaining proteins and intracellular kinases and protooncogenes may be reduced, thus leading to "anoikis". TAB004 treatment significantly reduced protein levels of EGFR, c-SRC, STAT3, c-MYC, and MUC1 (using both the MUC1-N and MUC1-CT antibodies) (Figure 5.5B). These binding partners also happen to be transcriptional targets of MUC1-CT [317, 154, 318, 22]. Thus, the essential drivers of survival, stemness and anoikis resistance may have decreased binding to MUC1-CT, therefore, reducing further downstream signaling.

Since the EGFR-PI3K activation was reduced post treatment with TAB004 (Figure 5.3) and because this pathway is known to confer anoikis resistance in cancer cells [319], we determined the levels of PTRH2 and BCL2 after 48 hrs of TAB004 treatment (Figure 5.5C). Treatment with TAB004 showed reduction in expression levels of PTRH2 and BCL2 (Figure 5.5C) as well as showed increased expression of Apaf1 and cleavage of Caspases 9 and 3 (Figure 5.5D). We isolated mitochondria in TAB004 treated CFPAC cells by subcellular fractionation and found that cytochrome C subunit 4 (COX IV) was released only in the cytosolic fraction of the TAB004 treated cells (Figure 5.5E). Release of cytochrome C is a hallmark of intrinsic or mitochondrial apoptosis activation. To check if there is mitochondrial membrane damage, we stained treated cells with JC-1 dye and found that TAB004 induces mitochondrial

membrane damage in PDA cells (Figure 5.5F). The quantification of the number of apoptotic cells is shown in Figure 5.5F insert.

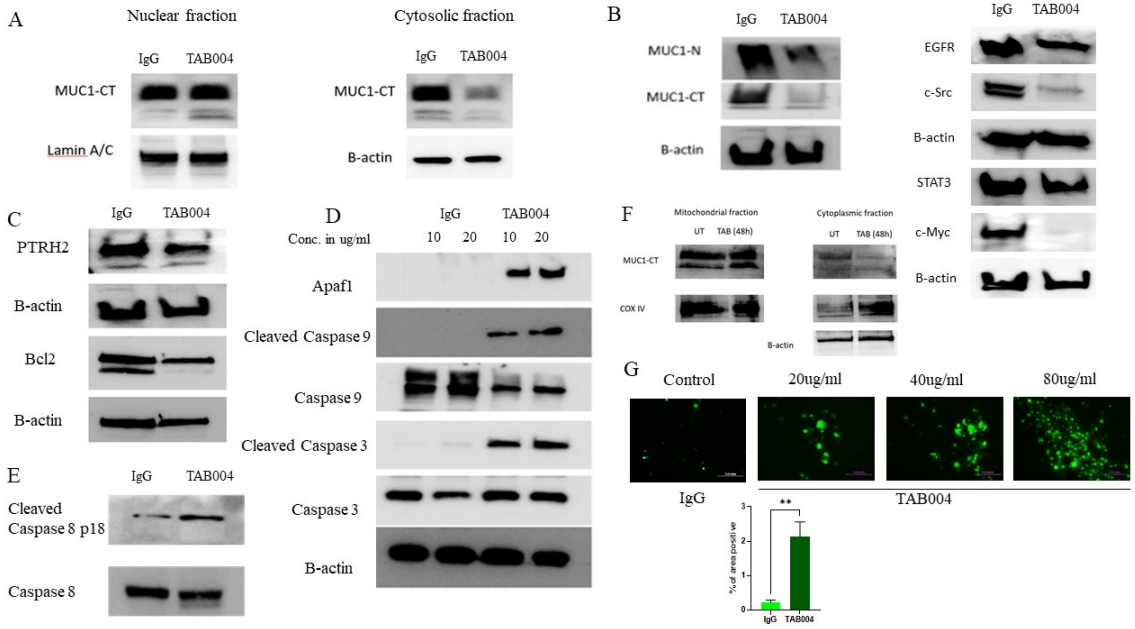


Figure 5.5: TAB004 degrades tMUC1 and induces extrinsic and intrinsic apoptosis

In Figure 5.5, A. Western blot showing levels of MUC1 in nuclear and cytosolic fractions of CFPAC cells after treatment with 10$\mu$g/ml of IgG and TAB004 for 48 hrs. Lamin A/C and $\beta$-actin were used as nuclear and cytosolic endogenous controls, respectively. B. (Right) Western blot showing levels of MUC1-N and MUC1-CT from whole cell lysates of CFPAC cells treated with 10$\mu$g/ml of IgG and TAB004 for 48 hrs. (Left) Western blot showing levels of EGFR, STAT3, c-SRC and c-MYC from the same CFPAC lysates. C. Western blot showing levels of PTRH2 and BCL2 in the same CFPAC lysates. D. Western blot showing levels of Apaf1, cleaved Caspase 9, Caspase 9, cleaved Caspase 3, and Caspase 3 in CFPAC cells treated with 10$\mu$g/ml and 20$\mu$g/ml of IgG and TAB004 for 48hrs. $\beta$-actin was used as endogenous loading control for all western blots. E. Western blot showing levels of MUC1 and Cytochrome C subunit IV (COX IV) in mitochondrial and cytosolic fractions of CFPAC cells after treatment with 10$\mu$g/ml IgG and TAB004 for 48 hrs. COXIV and $\beta$-actin were

used as endogenous loading controls for the mitochondrial and cytosolic fractions, respectively. F. Fluorescent microscopic images of MiaPaca2 cells treated with IgG and 20, 40 and 80 $\mu$g/ml of TAB004 for 48 hrs followed by staining with JC-1 dye for 30 minutes. Number of apoptotic cells in IgG and 20$\mu$g/ml of TAB004 were plotted as a graph. All experiments were performed in three independent replicates and one representative image is shown.

### 5.2.6 Differential response of MUC1 cytoplasmic tail mutants to treatment with TAB004

Various non-receptor and receptor tyrosine kinases phosphorylate MUC1-CT at specific tyrosine residues which enables MUC1-CT to function as a co-transcription factor to regulate gene expression (schematic shown in Figure 5.6Ai). Therefore, to assess if binding of TAB004 to tMUC1 blocks signaling through the tyrosines in MUC1 CT and confers TAB004s anti-colony forming effects (Figure 5.2), we generated point mutations to replace the tyrosines (Y) with phenylalanine (F) (Figure 5.6Aii) and further transfected MiaPaca2 cells with the mutant constructs. We observed differential sensitivity to TAB004 mediated inhibition of colony forming potential in the mutants. We report that Y0, Y6F and Y7F were the least sensitive to TAB004 with the highest $IC_{50}$ dose (Figure 5.6B). Representative Images of the colony forming results are shown in Figure 5.6C. At 10$\mu$g/ml, TAB004 treatment did not significantly reduce the colony forming potential of Y0, Y6F and Y7F (Figure 5.6D). JC-1 staining of TAB004 treated cells showed highest mitochondrial membrane damage in MiaPaca2.Neo cells (cells that have been transfected with an empty vector and deemed as the true control for the other mutant), followed by MiaPaca2.MUC1 and almost no mitochondrial damage in MiaPaca2.Y0 cells after 48 hrs (Figure 5.6E). Therefore, MUC1-CT signaling via its tyrosine plays a significant role in the TAB004 mediated inhibition of colony formation and mitochondrial damage.

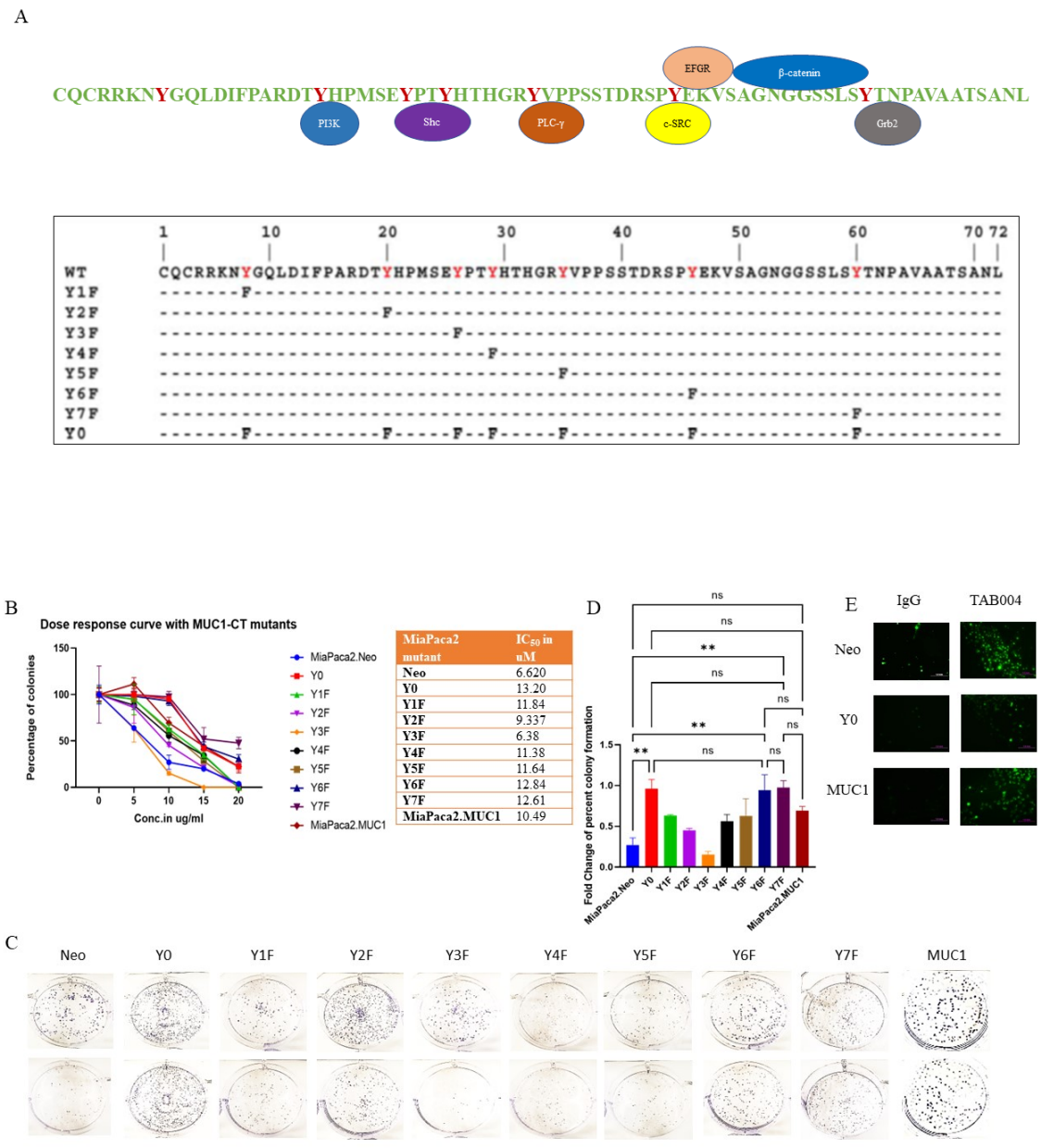


Figure 5.6: MUC1-CT tyrosine mutants show differential sensitivity to TAB004.

In Figure 5.6, [Ai]: A schematic of the MUC1-CT with the seven tyrosine residues in red and the kinases that are known to phosphorylate them. [Aii]: A schematic of the WT and the point mutation of tyrosine to phenyl alanine substitution. Authenticity of the various mutated fragments carrying individual Y-F mutations was verified by sequencing. B. Graph showing the percentage of colonies formed by the ten MiaPaca2

MUC1-CT mutant cell lines after treatment with increasing concentrations of TAB004 (5, 10, 15 and 20$\mu$g/ml). $IC_{50}$ value of TAB004 in $\mu$g/ml for each of the mutants listed in a chart. C. Images of colonies formed by the MiaPaca2 MUC1-CT mutant cells after treatment with 10$\mu$g/ml IgG and TAB004 after 7 days. D. Graph showing the percentage of colonies formed by the MiaPaca2 MUC1-CT mutant cells after treatment with 10$\mu$g/ml IgG and TAB004 after 7 days. E. Fluorescent microscopic images of MiaPaca2.Neo, MiaPaca2.Y0 and MiaPaca2.MUC1 cells after treatment with 80$\mu$g/ml of IgG and TAB004 for 48 hrs followed by JC-1 staining for 30 minutes.

### 5.2.7 Treatment with TAB004 significantly reduces tumor growth in vivo, induces apoptosis, and shows reduction in MUC1 expression

To verify if TAB004 has any significant therapeutic efficacy alone, we treated CFPAC xenograft bearing nude mice with either IgG control or TAB004 once a week for 6 weeks. TAB004 slowed down tumor growth significantly compared to IgG (Figure 5.7A). At endpoint, the tumor burden in TAB004 treated samples were significantly less than the IgG treated samples (Figure 5.7B), and it did not have any adverse effect on the body weight of the animals (Figure 5.7C). TAB004 treated tumor tissues showed an increased level of cleaved Caspase 3 compared to the IgG treated tissues (Figure 5.7D). This data confirmed the intracellular activation of apoptotic signaling induced by TAB004 treatment in vivo. In addition, MUC1-N and MUC1-CT were both significantly reduced in TAB004 treated tissues (Figure 5.7E). To assess if TAB004 enhances the anti-tumor efficacy of 5-FU in vivo, we treated CFPAC xenograft bearing nude mice with PBS control, TAB004, 5-FU, and TAB004 + 5-FU. TAB004 + 5-FU was the most effective treatment showing significant reduction in tumor growth rate, tumor volume, and enhanced survival without any adverse effects on the animalsâ body weight (Figure 5.7E-H).

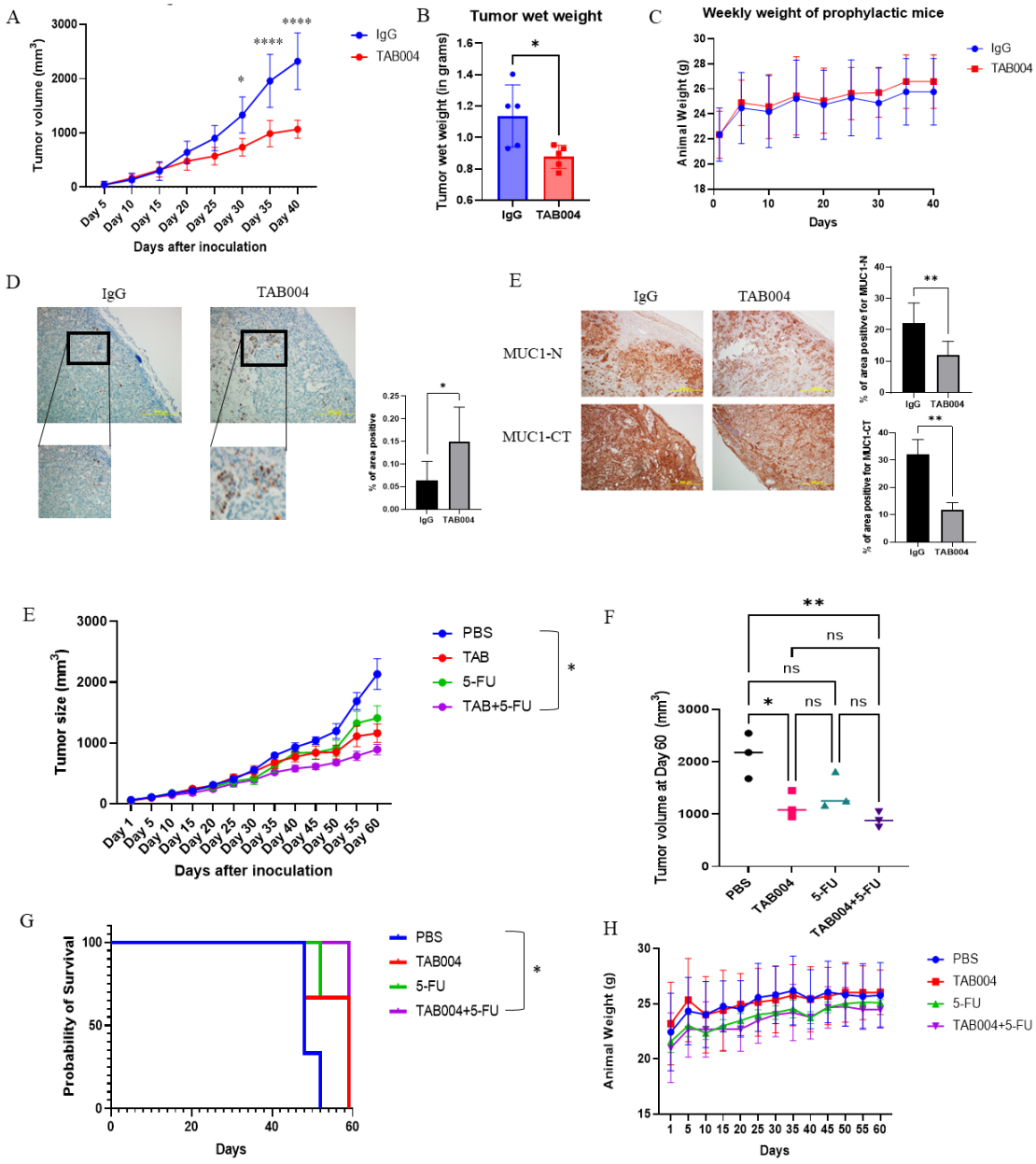


Figure 5.7: TAB004 attenuates PDA and enhances efficacy of 5-FU.

in Figure 5.7, A. Tumor growth in 10 nude mice with CFPAC xenografts treated with IgG (500$\mu$g/ml) (n=5) or TAB004 (500$\mu$g/ml) (n=5). B. Tumor wet weight at endpoint in IgG and TAB004 treated groups. C. Body weight of ten mice over the period of 40 days. D. Immunohistochemistry showing levels of cleaved Caspase 3 in IgG and TAB004 treated tumor tissues. E. Immunohistochemistry showing levels of

MUC1-N and MUC1-CT in IgG and TAB004 treated tumor tissues. The percentage of area positive was plotted by densitometric analysis of staining from five of the IgG and TAB004 treated tissue sections. F. Tumor growth in 12 nude mice with CFPAC xenografts treated with either PBS (n=3), TAB004 (500$\mu$g/ml) (n=3), 5-FU (20mg/kg) (n=3) or TAB004 (500$\mu$g/ml) + 5FU (20mg/kg) (n=3). F. Tumor volume on day 60 compared in all the four treatment groups. G. Kaplan-Meier survival plot for the four treatment groups. G. Body weight of 12 mice over the period of 60 days.

### 5.2.8 TAB004 compromises the desmosomal assembly and disrupts colony forming factors by degrading their association with MUC1

To prove that apoptosis was induced by disruption of cell-cell adhesion, we performed mass spectrometry analysis of cells treated with TAB004 for 20 minutes and found decreased binding of cell adhesion molecules Desmoplakin, Junction Plakoglobin ($\gamma$-catenin), Desmoglein, Keratin, Desmocollin and Galectin-7 with MUC1 (Figure 5.8A), indicating that TAB004 triggers detachment of cells from other cells and the matrix. It is well-known that $\gamma$-catenin can bind to MUC1 and translocate into the nucleus to drive oncogenic transcription, sometime it can substitute for $\beta$-catenin. TAB004 also inhibited phosphorylation and activation of Desmoplakin at Serine 2209, inhibited N-Acetylation of Junction Plakoglobin and induced methylation loss and N-acetylation gain of Keratins 14 and 16 (Figure 5.8B). It also significantly reduced the association of MUC1 with its well-known oncogenic binding partners Elongation factor 2, 14-3-3 Stratifin, Arginase1 and $\beta$-catenin further confirming the disruption of the co-transcriptional activity of MUC1 (Figure 5.8A). Microscopic images of single cells treated with TAB004 showed how it significantly reduces the capacity of cancer cells to remain attached to a matrix thus destroying their colony forming potential (Figure 5.8B). Albeit, not statistically significant, there appeared to be an increased association of MUC1 with the ER stress response and the proteasomal machineries, for instance, BIP, GRP-75, ER Resident Protein, Proteasomal subunit and Proteasomal

Ubiquitin receptor (Figure 5.8C). This indicates that TAB004 induced degradation of tMUC1 in a autophagy-lysosomal manner, as shown in Figure 5.4. To check whether TAB004 induces ubiquitination of MUC1, we performed co-immunoprecipitation of MUC1-CT after treatment with IgG or TAB004 and blotted for Ubiquitin. MUC1 was clearly found to have more binding to Ubiquitin in the TAB004 treated sample (Figure 5.8D). Therefore, TAB004 induced tyrosine phosphorylation led to ubiquitination followed by lysosomal degradation of MUC1, thus leading to increased anoikis in the PDA cells.

The mechanism of action of TAB004 in blocking tMUC1 oncogenic signaling and blocking anoikis-resistance is shown as a schematic diagram (Figure 5.8D). On binding of TAB004 to tMUC1, there is phosphorylation of MUC1-CT which tags it for lysosomal degradation, thus decreasing its binding with desmosomal proteins as well as transcriptional binding partners, in turn, blocking the oncogenic signaling. This blockage prevents activation of PI3K-PTRH2-BCL2 mediated anti-apoptotic gene functions, and reduces overall expression of STAT3, c-SRC and c-MYC (Figure 5.8). Furthermore, TAB004 binding to tMUC1 reduces the binding of EGF to EGFR, enhancing the inhibition of downstream signaling. Therefore, TAB004 abrogates the anoikis-resistance of PDA cells in both a ligand-dependent and independent manner.

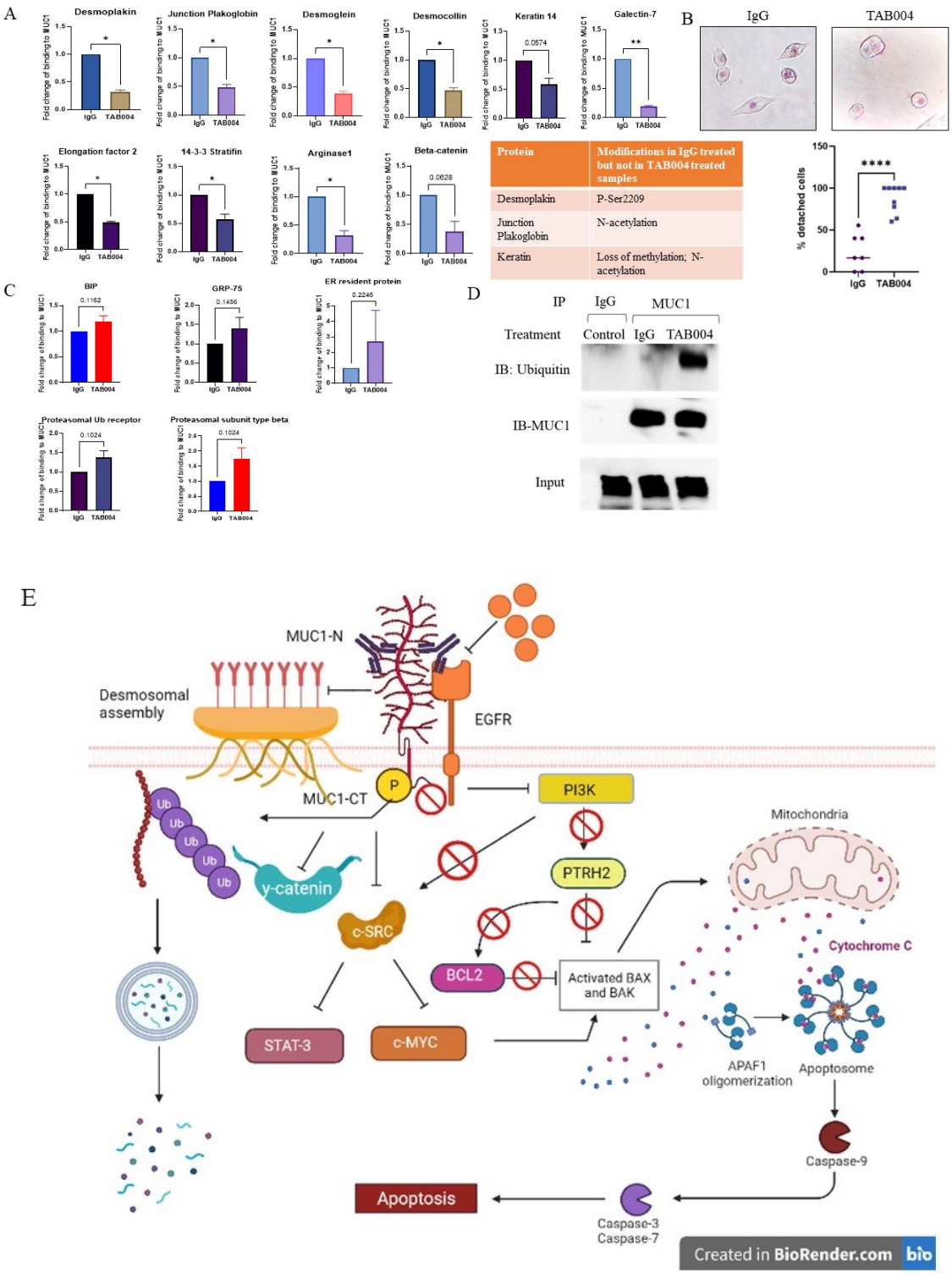


Figure 5.8: TAB004 disrupts the desmosomal assembly, triggers MUC1 degradation and reduces its binding with other tumorigenic factors.

In Figure 5.8, A. Mass spectrometry data plotted as fold change of relative abundance (PSM value) of cytoskeletal proteins and known tumorigenic factors found in Co-IP samples from CFPAC lysates treated with 10$\mu$g/ml IgG or TAB004 for 20 minutes. The mass spectrometry was performed on two independent biological replicates of CFPAC treated cells. B. Microscopic images of CFPAC cells treated with 20$\mu$g/ml IgG or TAB004 after 48 hrs showing detachment from the surface. Quantification was performed by counting the number of detached cells in IgG and TAB004 treated wells and plotted as a percentage of total number of cells. C. Mass spectrometry data plotted as fold change of relative abundance (PSM value) of proteins associated with ER stress and proteasomal degradation found in Co-IP samples from CFPAC lysates treated with 10$\mu$g/ml IgG or TAB004 for 20 minutes. D. Co-IP on CFPAC cell lysates after 20 minutes of treatment with 10 $\mu$g/ml of IgG or TAB004. Lysates were pulled down with isotype IgG control or MUC1-CT2 antibody and WB was performed for Ubiquitin and MUC1. Total MUC1 was used to show input. E. A schematic diagram showing the mechanism of action of TAB004 in blocking MUC1-oncogenic signaling.

## 5.3 Discussion

The data demonstrates the effect of a tMUC1 antibody, TAB004, in reversing anoikis resistance and colony forming potential of PDA cells (Figure 5.2) and identifying the underlying mechanism/s associated with the anti-tumor effects of the antibody. The DEGs in normal vs PDA from the TCGA database included nine anoikis-resistance genes Figure 5.1C), with seven of these genes correlating with MUC1 expression (Figure 5.1D) including EGF, EGFR, PI3KR1, PI3KCB, PI3KCD, c-MYC and BCL2.The genes that positively correlated with MUC1 also correlated with poor overall prognosis (Figure 5.1E). Further bioinformatic analysis illustrated that these genes were significantly associated with enhanced stemness, drug resistance, and autophagy, decreased apoptosis, and in rearrangement of the cytoskeleton (Figure 5.1F). MUC1 is known to enhance the expression and function of the ABC transporters to

confer chemoresistance via upregulation of EGFR [320, 45]. Thus, it was interesting to observe that TAB004 treatment significantly increased the sensitivity of PDA cells to chemotherapeutic drugs like Gemcitabine and 5-FU (Supplementary Figure 5.9A). Because tMUC1 and EGFR-PI3K associated signaling collaborate extensively to enhance many of the oncogenic pathways listed above [22, 319, 320, 45, 23] including anoikis resistance and drug resistance, we hypothesized that TAB004 may block activation of EGF-PI3K pathway via blocking signaling through its CT.

Indeed, pre-treatment of CFAC with TAB004, failed to significantly phosphorylate EGFR and PI3K even after 10 minutes of EGF exposure (Figure 5.3A-B). TAB004 binding to MUC1-N prevented the binding of EGF to EGFR, thus inhibiting phosphorylation and activation of the EGFR-PI3K signaling. Although we hypothesize that binding of TAB004 to tMUC1 increases steric hindrance that blocks the binding of EGFR to its ligand, thorough biochemical studies should be undertaken in the future to elucidate the exact mechanism. TAB004 binds to MUC1-N and phosphorylates its CT at tyrosine 1229 (Y6) at 10 minutes and the phosphorylation increases at 20 minutes and declines at 30 minutes (Supplementary Figure 5.10A). c-SRC is known to phosphorylate MUC1-CT at Tyr1229 [318] therefore, we hypothesized that the kinase responsible for MUC1 phosphorylation may be c-SRC, especially since c-SRC phosphorylation was also observed at 10 minutes post TAB004 treatment and declines by 20 minutes (Supplementary Figure 5.10A). We inhibited c-SRC activation for 30, 45 and 60 minutes with a pan-SRC inhibitor PP2 and then treated CFPAC cells with TAB004 for 20 minutes. With increasing time of PP2 treatment, there was decreasing phosphorylation of both MUC1 at Tyr1229 and c-SRC at Ser416 (Supplementary Figure 5.10B). This is the first time that MUC1 antibody (TAB004) is shown to function as a direct ligand to tMUC1, inducing phosphorylation of its CT and blocking EGF-induced oncogenic signaling. Further confirmation that the effects of TAB004 binding to tMUC1 triggers signaling through MUC1 CT, we determined that inhibition of

colony formation induced by TAB004 treatment was clearly reversed in MiaPaca-2-Y0, Y6 and Y7 (MUC1 CT tyrosine replaced with phenylalanine) (Figure 5.6A-E). One possible explanation of this differential sensitivity of the tyrosine mutants could be that MUC1 turnover rate is maintained by ubiquitination at lysine 1231 by the Ubiquitin E3 ligase WWP1 [321], we hypothesize that both tyrosines 1229 (Y6) and 1243 (Y7) aid in binding of WWP1 to K1231, and therefore, when these two sites are mutated to phenylalanine, there is less binding of WWP1, leading to reduced degradation of MUC1-CT by the proteasomal machinery. In addition to that, members of the Cbl, Hakai, and SOCS-Cul5-RING E3 Ubiquitin ligase families, induce ubiquitination of phosphotyrosine-containing proteins, for example, receptor and nonreceptor tyrosine kinases and their phosphorylated substrates [322, 323]. Ubiquitin-dependent lysosomal degradation has been reported in regulation of numerous membrane proteins, especially receptor proteins [323, 324, 325]. Ubiquitination of these membrane proteins triggers their internalization and targets them for degradation by the lysosomal pathway [326]. Therefore, mutation of some of the tyrosines, block phosphorylation and hamper the binding of these proteins, thus decreasing MUC1 degradation thus resisting TAB004 induced apoptosis. Further transcriptomics analysis revealed that treatment withTAB004 induced nutrient deprivation, ER stress and autophagy in PDA cells (Figure 5.4A-C). All these intracellular stress signals converge at the mitochondria eventually and decide the fate of a cell [327]. Most interestingly, TAB004 treatment enhances the degradation of tMUC1 itself (Figure 5.5A) and significantly reduces total protein expression of EGFR, STAT3, c-SRC and c-MYC (Figure 5.5B), almost obliterating the expression of c-MYC (Figure 5.5B). This reduction in the key proteins of oncogenesis is not exactly surprising as MUC1 drives activation of c-MYC in multiple cancers [317, 213]; and MUC1 is known to regulate EGFR expression [23], and physically interact with it to drive tumor progression [125].

To confirm that treatment with TAB004 reduces the anti-apoptotic signaling thereby

enhancing apoptosis, we show that treatment with TAB004 reduced levels of PTRH2 (Peptidyl-tRNA Hydrolase) and BIT-1 (Bcl-2 Inhibitor of Transcription) (Figure 5.5C). The mitochondrial / intrinsic apoptotic pathway is known to be activated during ER stress, nutrient deprivation and anoikis [327, 328]. PI3K regulates the expression of a protein called PTRH-2 or Bit-1, which in turn regulates the anti-apoptotic BCL-2 [319]. PTRH2 regulates adhesion-mediated pro-survival signaling by upregulation of BCL2 transcription. Loss of adhesion promotes PTRH2-mediated anoikis [329]. Thus, treatment with TAB004 significantly reduced expression of the anti-apoptotic BCL2 (Figure 5.5C), while inducing expression of Apaf1 and cleaved Caspases 9 and 3; a clear indication of induction of the intrinsic / mitochondrial apoptotic pathway (Figure 5.5D). BCL-2 is the master anti-apoptotic member of the BCL-family of proteins which avoids mitochondrial dysfunction and prevents apoptosis by various mechanisms [319]. The BCL-2 modifying factor (Bmf) can register cytoskeleton damage and convey death signals. Upon detachment of cells, Bmf accumulates in the mitochondria, neutralizing Bcl-2, leading to cytochrome c release and anoikis execution [330, 331]. TAB004 treatment released cytochrome C into the mitochondria (Figure 5.5E) and significantly damaged the mitochondrial membrane as is evident by the presence of green fluorescence in cells after staining with the JC-1 dye (Figure 5.5F). JC-1 is a cationic green dye that remains as a monomer in damaged mitochondria, emitting green fluorescence [332].

TAB004 was most potent in reducing the colony forming potential of the PDA cells and induced detachment and rounding of the cells by cytoskeletal rearrangement, therefore, a phenomenon consistent with anoikis. In normal cells, loss of attachment to the ECM induces anoikis. Resistance to anoikis in cancer cells promotes their ability to survive in circulation, with subsequent colonization to distant anatomic sites, leading to tumor metastasis [333, 334].

TAB004 treatment reversed anoikis-resistance in these cells in both a ligand de-

pendent and independent manner. 1) Ligand-dependent: It blocked the binding of EGF to EGFR and reduced activation of PI3K, thus inhibiting growth signal that help cells survive nutrient deprivation and stress (Figure 5.3). In addition to that, TAB004 forced the detached cells to commit to apoptosis by inducing mitochondrial membrane damage, after a battle between the stress response and activation of apoptotic factors (Figure 5.4). Therefore, the detached cells reached a point of no return, thus losing the potential to colonize (Figure 5.2). 2) Ligand-independent: TAB004 degraded MUC1-N and MUC1-CT (most probably by tyrosine-dependent ubiquitination and degradation by either proteasomal or lysosomal machinery or both), as indicated by increased expression of Ub-E3 ligase and autophagy genes from the microarray data (Figure 5.4). Mass spectrometry showed increased binding of ER chaperone BIP, GRP75, ER resident protein, Proteasomal Ubiquitin receptor and proteasomal subunit $\beta$ to MUC1 in the TAB004 treated samples, indicating degradation of MUC1 (Figure 5.8C). Mass spectrometry data also showed significantly decreased binding of Desmoplakin, Myosin 9 (MYH9), Junction Plakoglobin, Desmoglein, Keratin, Galectin-7 post TAB004 treatment indicative of disruption of the colonizing potential of the cells (Figure 5.8A). Additional modifications observed were loss of phosphorylation at Ser 2209 of Desmoplakin, loss of acetylation of Junction Plakoglobin and loss of methylation and gain of N-acetylation of Keratins after TAB004 treatment (Figure 5.8A). The role of these post-translational modifications of the desmosomal proteins have been well documented to keep cell membrane integrity and potential for adhesion [335]. There was decreased association of MUC1 with other pro-tumorigenic factors including $\beta$-catenin, thus blocking majority of the co-transcriptional activity of MUC1 (Figure 5.8A).

Taken together the data suggests that degradation of MUC1 destroyed the docking site of crucial pro-survival factors like EGFR, PI3K, c-SRC, STAT3 and c-MYC (Figure 5.5), thus blocking the whole oncogenic cascade. Transcription factors like $\beta$-

catenin and NF-$\kappa$B, STAT3 and c-MYC, out of many, use MUC1-CT as an adaptor protein or co-transcription factor to regulate expression of oncogenes. Therefore, TAB004 destroys the hub of this oncogenic nexus and renders tumor cells unable to revive and colonize to different locations after dissemination (Figure 5.5). Figure 5.8D is an attempt to summarize the mechanism of action of TAB004 antibody and its anti-tumor effects.

Finally, to confirm anti-tumoral effects of TAB004 in vivo in an animal model, we treated CFPAC xenograft bearing nude mice with TAB004 or IgG isotype (Figure 5.6A). Initially, the TAB004-treated group did not show any difference in tumor growth rate compared to the IgG group. However, starting approximately 20 days post treatment, growth rate of the TAB004 treated group was significantly reduced compared to that of the IgG treated group (Figure 5.6B). At the end of the experiment, the total tumor burden in the TAB004 treated group was significantly lower than that of the IgG (Figure 5.6C). We report significant increase in cleaved Caspase 3 (hallmark of apoptosis activation) in the TAB004 treated group (Figure 5.8D). The overall levels of both MUC1-N and MUC1-CT were significantly reduced in the TAB004 treated tissue samples (Figure 5.8E) which mimic the in vitro data (Figure 5.5). Mice treated with TAB004 in combination with 5FU showed the slowest tumor growth rate and significantly enhanced survival (Figure 5.7E-G), without any mal-effects on their body weight (Figure 5.7H). Therefore, TAB004 may confer drug sensitivity in CFPAC PDA tumor. Therefore, TAB004 can be an excellent combination agent to curb tumor cell survival in both primary tumor and residual cells that have disseminated from the primary tumor site and would try to gain anoikis-resistance. TAB004 will be helpful clinically to destroy the residual cells because it takes away the essential machinery using which these cells develop the ability to survive in detachment (anoikis-resistance), thus, pushing them to undergo apoptosis and rendering them unable to colonize any tissue.

Although, the data presented thus far is in PDA cells, we found that other epithelial tumor cell lines responded to TAB004 as effectively as PDA. TAB004 treatment significantly reduced the colony forming potential of several other human epithelial cancer cell types, including, hepatocellular carcinoma cell lines (SNU-449 and SNU-475), ovarian cancer cell lines (SKOV-2 and CAOV-3) and triple-negative breast cancer cell lines (HCC-1937 and HCC-70) (Supplementary Figure 5.9B).

Thus, TAB004 must be further explored for future combination therapies to reverse drug and small molecule inhibitor resistance and explore its impact on minimal residual disease to diminish recurrence and metastasis in epithelial cancers.

## 5.4 Materials and Methods

### 5.4.1 Data analysis from TCGA

1. *RNA sequencing data*

   RNA-seq data was downloaded from the GDC (Genomics Data Commons Portal) for all available cancer types, with a majority from TCGA (The Cancer Genome Atlas) program. A total of 15,112 samples were included for the analysis, 13,509 tumor and 1,603 normal samples. Tumor types chosen include primary and metastatic solid tumor tissue samples (n=13,509) and normal samples available in GDC, (n=1,603) were also downloaded for the analysis. Data was downloaded using the gdc-client tool. Samples are considered to have low MUC1 expression if the expression value is less than 100, otherwise, the sample is considered to have high MUC1 expression.

   Plot for MUC1 expression in normal and tumor samples was generated from the DGCA (1.0.2) package in R (3.6.3).

2. *Gene Correlation Analysis*

   Gene correlation analysis of all genes were run using the R package: DGCA (Differential Gene Correlation Analysis). DGCA calculates gene-gene correla-

tions between different groups and the correlation significance values. Genes with the lowest expression levels were filtered out by the dispersion measure, with the filter dispersion percentile at 0.3. This dataset was the input to run differential correlation analysis across tumor and normal samples, identifying gene correlations with the MUC1 gene. P-value adjustment was done with the Benjamini  Hochberg correction method.

3. *Survival Analysis*

   Survival analyses for select genes and overall survival were computed using the Kaplan-Meier estimate and plots were made using ggplot2 (3.3.5) package in R (3.6.3). Tumor (12,042) samples from 48 cancer projects were included for this analysis. Overall survival time was used for this analysis. The survival (3.2-13) package in R (3.6.3) calculated the survival curve estimated, which was plotted using ggplot2 (3.3.5) package in R.

4. *KEGG Pathway Analysis*

   Pathway analysis was performed for the following genes: BCL2, EGF, EGFR, MYC, PIK3CB, PIK3CD, PIK3R1, PTRH2, and SRC. These genes were input to the Database for Annotation, Visualization, and Integrated Discovery (DAVID 2021) to identify associated pathways. DAVID contains a large knowledge base of functional annotations including GO terms, KEGG pathways, etc. Functional annotation results were filtered to only include those with a Benjamini and Hochberg adjusted p-value of $<0.05$. KEGG pathways were selected for further analysis and visualization. The bar plot figure of KEGG pathways was plotted using ggplot2 (3.3.6) in R (4.1.0).

### 5.4.2 Cell culture

Human PDA, HCC, and breast cancer cell lines HPDE, Capan2, CFPAC, HPAFII, MiaPaca2, SNU449, SNU479, Hep-G2, HCC70, BT20, SKOV-2, CAOV-3 and Hela

cells were obtained from ATCC (Manassas, VA) and cultured accordingly. Cell lines were maintained in Dulbeccoâs Modified Eagle Medium (DMEM; Gibco) supplemented with 10% heat-inactivated fetal bovine serum (HI-FBS; Gibco or Hyclone), 3.4 mM l-glutamine, 90 units (U) per ml penicillin, 90 $\mu$g/ml streptomycin, and 1% non-essential amino acids (Cellgro) and cultured at 37°C and 5% $CO_2$.

### 5.4.3 Flow cytometry to check MUC1 expression

PDA cells were harvested and washed with PBS, followed by incubation with IgG-conjugated to FITC or TAB004-conjugated to FITC in flow buffer (5% FBS in PBS) for 30 minutes in dark on ice. Then the cells were washed and suspended in flow buffer and analyzed by FACS Diva. The data was analyzed using Flow Jo software.

### 5.4.4 MUC1 mutant generation and transfection

MUC1 Y0, Y1F through Y7F were created using the Quick-Change mutagenesis kit (Stratagene, La Jolla, CA) [336]. Briefly, primers based on the MUC1 sequence were designed containing single-base alterations resulting in mutation of the tyrosine residues (Y) in MUC1 CT to phenylalanine (F) as shown schematically (Figure 5.7A). Successful mutations were confirmed with DNA sequencing. MUC1-CT mutants and MUC1 WT were cloned into the pLNCX.1 vector consisting of the neomycin resistance gene for retroviral infection. Cells were transfected with Lipofectamine 3000 (Thermo Fisher) according to the manufacturerâs protocol and maintained in complete DMEM containing Geneticin (G418; Invitrogen, Carlsbad, CA, USA). Note: Cells designated as MiaPaca2.Neo were transfected with only the empty vector with neomycin resistance gene. Cells designated as MiaPaca2.MUC1 represent cells expressing full length MUC1 that consists of the extracellular domain, the transmembrane domain and wild type cytoplasmic tail domain. Cells designated as MiaPaca2.Y0 represents cells expressing full length MUC1 that consists of the extracellular domain, the transmembrane domain and mutant cytoplasmic tail domain in which all the seven tyrosines

are replaced by phenylalanine. Similarly, cells designated as MiaPaca2.Y1F through Y7F represent cells expressing full length MUC1 with the tyrosine at that position replaced by phenyl alanine, respectively. very passage of MiaPaca2 transfected cells were maintained in a final concentration of 150 $\mu$g/ml of the antibiotic G418 (50 mg/ml) (Thermo Fisher) to ensure positive selection.

### 5.4.5 Cell survival assay by MTT

Cells were plated at a seeding density of 1x 103 cells per well in a 96-well plate and grown overnight. Cells were left untreated or treated with Gemcitabine, Paclitaxel, 5-FU, TAB004 alone or IgG isotype control antibody for 24, 48 and 72 hrs. Next, MTT (Biotium, Hayward, Calif) solution was added (20 $\mu$L/well) to cells incubated for an additional 3 to 4 hrs. In the final step, media was removed, formazan was dissolved in dimethyl sulfoxide (200 $\mu$L/well), and the absorbance read at 560nm using a colorimetric plate reader. The O.D. value of treated group were calculated as a percentage of the PO.D. values of the IgG treated group and plotted as kill curve or bar graph in GraphPad Prism. A p value of $<0.05$ was considered significant.

### 5.4.6 Colony Forming Assay

500-1000 cancer cells were plated in a 6-well tissue culture plate and allowed to adhere overnight. Next day, the cells were treated with increasing concentrations of TAB004 (5, 10, 15 and 20 $\mu$g/ml) for 7-14 days (depending on the doubling time of each cell line). The highest concentration of 20 $\mu$g/ml of IgG was used as the isotype control. After 7-14 days, the media was removed, colonies were washed with PBS and fixed with 3:1 solution of Methanol: Acetic acid for 5 minutes, followed by staining with 0.5% (w/v) of Crystal Violet in Methanol for 15 minutes. Then the colonies were washes under running tap water, images were taken, and colonies were counted manually. Colonies consisting of $>25$ cells were considered. The number of colonies in treated were calculated as a percentage of colonies in the IgG treated

group and plotted as kill curve or bar graph in GraphPad Prism. A p value of $<0.05$ was considered significant.

### 5.4.7 Invasion Assay

Cells were serum starved for 18 hrs before plating for the invasion assay. 50,000 CFPAC cells were plated over transwell inserts (Sarstedt) precoated with diluted Matrigel (1:1) in serum free media, with 10 and 20 $\mu$g/ml of IgG and TAB004. The cells were allowed to invade through the Matrigel coating for 48 hrs towards the serum-containing medium in the bottom chamber. After 48 hrs, only the control wells were swabbed with a cotton swab, followed by staining of all inserts with 5% crystal violet. The excess stain was washed off and the inserts were allowed to dry. The membrane was cut and dipped in 10% acetic acid for 10 minutes to elute the dye, which was read by a Spectrophotometer at 560 nm. Percent invasion was calculated as (O.D. of TAB004 treated sample (x $\mu$g/ml) / O.D. of IgG treated sample (x $\mu$g/ml)) X 100.

### 5.4.8 Microarray analysis

CFPAC and MiaPaca2 cells were grown overnight in complete DMEM with heat-inactivated FBS. Next day, the cells were treated with 10$\mu$g/ml of IgG or TAB004 for 24 hrs and then RNA was extracted from the cells using the Qiagen RNA Mini kit according to the manufacturer protocol. The Clariom S transcriptomics was performed by Thermo Fisher Scientific.

1. *Differential Gene Expression Analysis*

   Differential gene expression analysis was performed on the MiaPaca2 and CFPAC1 cell line microarray data using the limma (3.42.2) package in R (3.6.3). Three separate differential expression analyses were performed: MiaPaca2 data, CFPAC1 data, and then combined analysis of both MiaPaca2 and CFPAC1 data. Normalization was done using RMA. Limma identified differentially expressed genes between the IgG control and TAB004 antibody groups. Genes

with an adjusted p-value of less than 0.05 were to be considered statistically significant. The top 30 DEGs between the two groups in both CFPAC and MiaPaca2 cells were presented using a heatmap.

2. *Pathway Analysis*

   The top 30 genes (by unadjusted p-value $<0.05$ between IgG and TAB004 treatment) were input into Ingenuity Pathway Analysis (IPA) to identify top associated pathways in both MiaPaca2 and CFPAC1 datasets.

### 5.4.9 JC1 staining for mitochondrial membrane potential damage

Around 1000-2000 cells were plated in a 24 well plate overnight, next day they were treated with IgG or TAB004 for 48 hrs. After 48 hrs, cells were incubated for 30 minutes with JC-1 dye (Cayman Chemicals) according to the manufacturers protocol. Images were taken using a fluorescence microscope after applying a filter for FITC. Number of cells with green fluorescence from five randomly selected fields in 80$\mu$g/ml TAB004-treated wells were calculated as a percentage of the same in the IgG treated group and plotted as a bar graph in GraphPad Prism. A p value of $<0.05$ was considered as significant.

### 5.4.10 Western Blot

CFPAC cells were serum-starved for 48-72 hrs and treated with 10$\mu$g/ml of IgG or TAB004 for 10, 20 and 30 minutes for analysis of phosphorylation. For detection of other proteins, CFPAC cells were treated with 10$\mu$g/ml and 20$\mu$g/ml of IgG or TAB004 for 48 hrs. Cell lysates were prepared using complete lysis buffer (RIPA buffer and Halt Protease and Phosphatase Inhibitor), and 25 to 60$\mu$g of protein was subjected to denaturing sodium dodecyl sulfate-polyacrylamide gel electrophoresis (SDS-PAGE) and Western blot. The polyvinylidene fluoride membrane was blocked for 30 minutes with commercial blocking buffer (Thermo Fisher Scientific) and probed with anti-MUC1 antibody CT2, TAB004 antibody for MUC1-N, Phospho-EGFR (Cell

Signaling Technology), EGFR, Lamin A/C (Santa Cruz), phospho-PI3K, PI3K, c-SRC, STAT-3, c-MYC, Apaf1, anti-Cleaved Caspase 3, anti-full-length Caspase 3, anti-cleaved Caspase 9, anti-full-length Caspase 9, COX-IV, and anti-$\beta$-actin (Cell Signaling Technology) antibodies. Appropriate secondary antibodies conjugated to horseradish peroxidase were used, and protein detected using the chemiluminescence kit (Thermo Dura). All antibodies were used according to manufacturerâs recommendations.

### 5.4.11 Densitometric Analyses

The bands on Western blot were quantified using image analysis software Image J from the National Institutes of Health (Bethesda, Md).

### 5.4.12 Co-Immunoprecipitation and Mass Spectrometry

CFPAC cells were serum-starved for 24 hrs and treated with 10$\mu$g/ml of IgG or TAB004 for 20 minutes. After that, the media was removed, cells were washed with PBS and lysate was collected with complete lysis buffer (RIPA buffer with 1x Halt Protease and Phosphatase inhibitor), with the help of a cell scraper. The lysate was vortexed briefly and then sonicated and kept on ice for 10 minutes, followed by centrifugation at 14,000 RPM for 15 minutes at 4°C. The supernatant was collected in a fresh tube, BCA was performed to estimate protein concentration and 2000 mg of protein was used to pull down MUC1. Pierce Co-IP kit was used to pull down MUC1 with 100$\mu$g of TAB004 antibody using the manufacturerâs protocol. From the eluate, protein concentration and purity were measured using a Nanodrop (Thermo Fisher Scientific), and at least 0.5$\mu$g of protein was used for mass spectrometric analysis. Mass spectrometry was performed by Poochon Scientific LLC. At first, double digestion of the MUC1 protein was performed with both Trypsin and Chymotrypsin, followed by mass spectrometry of the digested peptide fragments. A summary of the proteins identified were analyzed in the IgG treated vs the TAB004 treated samples,

and the relative abundance of binding to MUC1 (PSM) was analyzed. A ratio of the PSM in the TAB treated and IgG treated samples was generated for each binding partner and the ones with a fold change of >2 with a p value of <0.05 were plotted as a bar graph in GraphPad Prism.

### 5.4.13 Xenograft Studies

Ten 6-8 weeks old athymic nude, Foxn1nu mice (strain number 002019; 5 female and 5 male) were purchased from The Jackson Laboratories and housed at UNC Charlotteâs vivarium. These mice were injected subcutaneously (n = 10) with 1x 106 CFPAC cells (50$\mu$l) with Matrigel (50$\mu$l) (total = 100$\mu$l) in a 1:1 ratio, mixed with 500$\mu$g/ml solution of IgG or TAB004 prepared in sterile PBS into the left flank. Once the tumors reached a palpable size (∼3 x 3mm, ∼5 days post tumor inoculation), tumor measurements were taken twice a week. 500 $\mu$g/ml of IgG or TAB004 in sterile PBS (50$\mu$l) was injected once a week intratumorally once a week. Mice were monitored thrice a week for general health and tumor volumes were measured. Caliper measurements were taken twice a week over 40 days until endpoint and once euthanized, tumor wet weight was taken (Figure 5.6). This study and all procedures were performed after approval from the Institutional Animal Care and Use Committee of UNC Charlotte under IACUC protocol number 21-008. For the combination treatment, 12 6-8 weeks old athymic nude mice (6 males and 6 females) were injected with 5x105 CFPAC cells subcutaneously (50$\mu$l) with Matrigel (50$\mu$l) (total = 100$\mu$l) in a 1:1 ratio, into the left flank. Mice were randomized into four groups and the treatments were 1) PBS control, 2) TAB004 (500$\mu$g/ml), 3) 5-FU (20 mg/kg) and 4) TAB004 (500$\mu$g/ml) + 5-FU (20mg/kg). For groups 2 and 4, on the day of injection, CFPAC cells were mixed with 500$\mu$g/ml solution of TAB004 prepared in sterile PBS and then injected into the mice. 5-FU injection was started only after the tumors reached a palpable size. Treatments were injected once every week for 60 days. Measurements were taken with Vernier Calipers and the survival of the mice

were monitored.

### 5.4.14 Immunohistochemistry

Paraffin-embedded sections were incubated at 65°C for 30 minutes in a humidity chamber. Then slides were washed in three changes of Xylene for 3 minutes each, followed by hydration in 100%, 90% and 70% ethanol for 2 minutes each. For nonenzymatic antigen retrieval, sections were heated to 85°C in Dako antigen retrieval solution for 90 min and cooled for 20 min; all subsequent steps occurred at room temperature. To quench endogenous peroxidase, slides were rinsed and incubated 2% $H_2O_2$ in methanol for 10 minutes. Sections were then washed, blocked in 50% fetal bovine serum (FBS) in PBS for 45 min, and incubated overnight with primary antibodies. Sections were incubated for 1 hr with secondary antibody, developed with a diaminobenzidine (DAB) substrate (Vector Inc., Burlingame, CA, USA), counterstained with hematoxylin, washed, dehydrated in 70%, 90% and 100% ethanol for 2 minutes each, followed by 3 changes of Xylene for 3 minutes each and mounted with Permount. Primary antibodies used were Armenian hamster anti-MUC1-CT CT2 antibody (1:50), TAB004 antibody (1:100) and anti-cleaved Caspase 3 antibody (1:150). Secondary antibodies used were mouse anti-Armenian hamster HRP conjugated antibody (1:100, Jackson Labs) and anti-mouse HRP conjugated antibody (Cell Signaling Technology) (1:100). Mouse IgG was used as negative control. Immunopositivity was assessed using light microscopy and images taken at 100x magnification. Images were quantified using Image J software.

### 5.4.15 Statistical Analysis

Statistical analysis was performed with GraphPad software 9.0 (La Jolla, Calif). Statistical significance was determined using Student T-test to compare between treatment and control groups, one-way analysis of variance (ANOVA) and 2-way ANOVA were used to compare between three or more groups.

## 5.5 Supplementary Materials

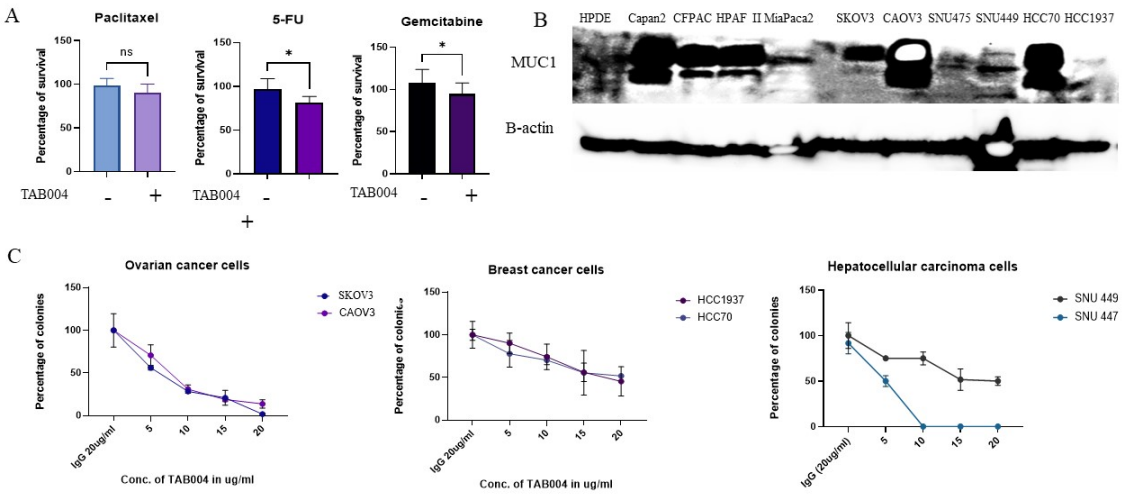


Figure 5.9: TAB004 increases the efficacy of chemotherapeutic drugs and reduces colony forming potential of multiple epithelial cancer cells.

In Figure 5.9, A. MTT cell survival assay on CFPAC cells with 10$\mu$M of Gemcitabine, Paclitaxel and 5-FU alone or in combination with 20$\mu$g/ml TAB004 for 48 hrs. Percentage of survival was calculated as a fold change of combination over drug alone. B. MUC1-CT expression by western blotting with MUC1-CT2 antibody on pancreatic epithelial cell line HPDE, PDA cell lines, ovarian (SKOV3 and CAOV3), hepatocellular (SNU449 and SNU475) and triple negative breast cancer cells (HCC70 and HCC1937). C. Colony forming assay on two hepatocellular carcinoma cell lines (SNU449 and SNU475), two ovarian cancer cells (SKOV2 and CAOV3) and two TNBC cell lines (HCC1937 and HCC70) with increasing concentrations of TAB004 (5, 10,15 and 20 $\mu$g/ml).

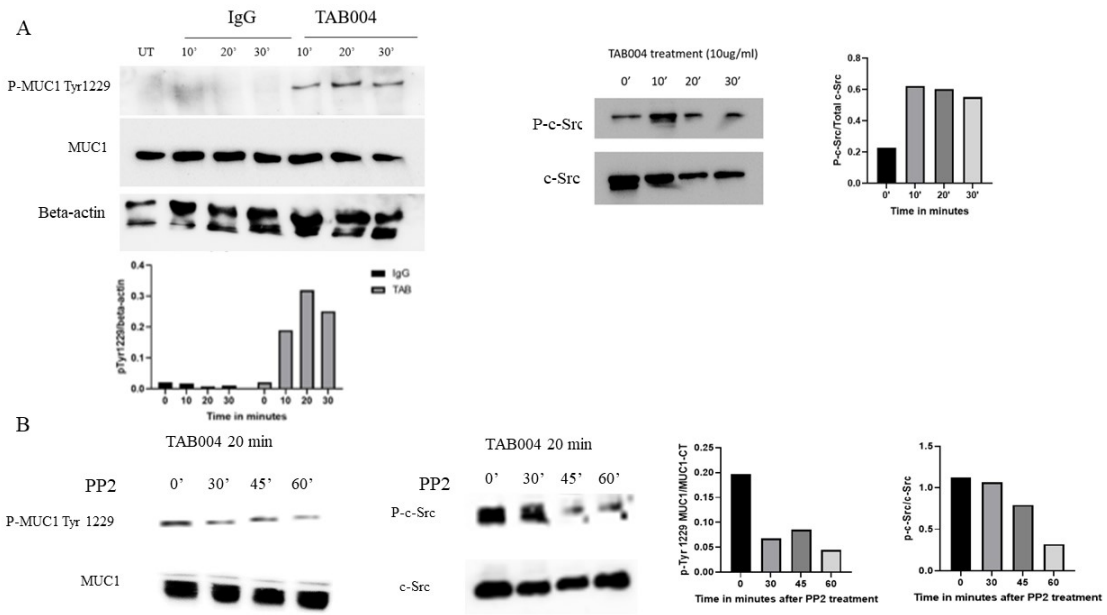


Figure 5.10: TAB004 induces phosphorylation of MUC1-CT through c-Src.

In Figure 5.10, A. Western blot showing increased phosphorylation of MUC1-CT at Tyr 1229 at 10, 20 and 30 minutes after treatment with 10$\mu$g/ml of TAB004. CFPAC cells were serum-starved for 72 hrs and then treated with 10$\mu$g/ml of IgG and TAB0004. Total MUC1 levels are shown and $\beta$-actin was used as the endogenous loading control (top). Densitometric analysis showing increased phosphorylation of MUC1-CT at Tyr 1229 at 10minutes that goes up at 20 minutes and then comes down at 30minutes (bottom). B. Western blot showing increased phosphorylation of c-Src at 10 minutes which goes down after 20 and 30 minutes. Total c-Src was used as the endogenous control. Densitometric analysis showing increased phosphorylation of c-Src after TAB004 treatment. C. Western blot showing phosphorylation of MUC1-CT at Tyr 1229 (left) and c-Src (right) after CFPAC cells were serum-starved for 24 hours and treated with Src inhibitor PP2 for 30, 45 and 60 minutes followed by treatment with 10 $\mu$g/ml of TAB004 for 20 minutes. Total MUC1 and c-Src were used as controls. Densitometric analysis showing that pre-treatment with PP2 led to decreased phosphorylation of MUC1 at Tyr1229 and p-c-Src after TAB004 treatment.

Table 5.1: Cancer Types

| **Project** | **Primary Site** | **Count** |
|---|---|---|
| TCGA-BRCA | Breast | 1109 |
| CPTAC-3 | Brain, Bronchus and lung, Kidney, Other and ill-defined sites, Pancreas, Uterus, NOS | 872 |
| TCGA-UCEC | Corpus uteri, Uterus, NOS | 552 |
| TCGA-KIRC | Kidney | 538 |
| TCGA-LUAD | Bronchus and lung | 535 |
| TCGA-LGG | Brain | 529 |
| TCGA-THCA | Thyroid gland | 510 |
| TCGA-HNSC | Base of tongue, Bones, joints and articular cartilage of other and unspecified sites, Floor of mouth, Gum, Hypopharynx, Larynx, Lip, Oropharynx, Other and ill-defined sites in lip, oral cavity and pharynx, Other and unspecified parts of mouth, Other and unspecified parts of tongue, Palate, Tonsil | 502 |
| TCGA-LUSC | Bronchus and lung | 502 |
| TCGA-PRAD | Prostate gland | 499 |
| NCICCR-DLBCL | Lymph nodes | 481 |
| TCGA-COAD | Colon, Rectosigmoid junction | 480 |
| TCGA-SKCM | Skin | 470 |
| REBC-THYR | Thyroid gland | 428 |
| TCGA-BLCA | Bladder | 414 |
| TCGA-OV | Ovary | 379 |
| TCGA-STAD | Stomach | 375 |
| TCGA-LIHC | Liver and intrahepatic bile ducts | 374 |
| CPTAC-2 | Breast, Colon, Other and unspecified female genital organs, Ovary, Rectum, Retroperitoneum and peritoneum | 340 |
| TARGET-OS | Bones, joints and articular cartilage of limbs, Bones, joints and articular cartilage of other and unspecified sites, Not Reported | 88 |
| TCGA-MESO | Bronchus and lung, Heart, mediastinum, and pleura | 86 |

Cancer Types (contd.)

| | | |
|---|---|---|
| TCGA-CESC | Cervix uteri | 306 |
| TCGA-KIRP | Kidney | 288 |
| TCGA-SARC | Bones, joints and articular cartilage of limbs, Colon, Connective, subcutaneous and other soft tissues, Corpus uteri, Kidney, Meninges, Other and unspecified male genital organs, Other and unspecified parts of tongue, Ovary, Peripheral nerves and autonomic nervous system, Retroperitoneum and peritoneum, Stomach, Uterus, NOS | 263 |
| CMI-MBC | Breast | 203 |
| CGCI-HTMCP-CC | Cervix uteri | 196 |
| TCGA-PCPG | Adrenal gland, Connective, subcutaneous and other soft tissues, Heart, mediastinum, and pleura, Other and ill-defined sites, Other endocrine glands and related structures, Retroperitoneum and peritoneum, Spinal cord, cranial nerves, and other parts of central nervous system | 180 |
| TCGA-PAAD | Pancreas | 178 |
| TCGA-GBM | Brain | 169 |
| TCGA-READ | Colon, Connective, subcutaneous and other soft tissues, Rectosigmoid junction, Rectum, Unknown | 167 |
| TCGA-ESCA | Esophagus, Stomach | 162 |
| TARGET-NBL | Adrenal gland, Bones, joints and articular cartilage of limbs, Bones, joints and articular cartilage of other and unspecified sites, Connective, subcutaneous and other soft tissues, Heart, mediastinum, and pleura, Hematopoietic and reticuloendothelial systems, Kidney, Liver and intrahepatic bile ducts, Lymph nodes, Meninges, Other and ill-defined sites, Other endocrine glands and related structures, Peripheral nerves and autonomic nervous system, Renal pelvis, Retroperitoneum and peritoneum, Skin, Spinal cord, cranial nerves, and other parts of central nervous system, Stomach, Unknown, Uterus, NOS | 160 |
| TCGA-TGCT | Testis | 150 |
| TARGET-WT | Kidney | 130 |
| TCGA-THYM | Heart, mediastinum, and pleura, Thymus | 119 |

Cancer Types (contd.)

| | | |
|---|---|---|
| CGCI-BLGSP | Hematopoietic and reticuloendothelial systems | 111 |
| WCDT-MCRPC | Prostate gland | 99 |
| TARGET-OS | Bones, joints and articular cartilage of limbs, Bones, joints and articular cartilage of other and unspecified sites, Not Reported | 88 |
| TCGA-ACC | Adrenal gland | 79 |
| HCMI-CMDC | Bones, joints and articular cartilage of other and unspecified sites, Brain, Breast, Bronchus and lung, Colon, Connective, subcutaneous and other soft tissues, Esophagus, Kidney, Liver and intrahepatic bile ducts, Other and unspecified parts of biliary tract, Pancreas, Rectosigmoid junction, Rectum, Skin, Small intestine, Stomach | 75 |
| TCGA-KICH | Kidney | 65 |
| TARGET-RT | Kidney, Lip, Liver and intrahepatic bile ducts | 64 |
| TCGA-UCS | Uterus, NOS | 56 |
| TCGA-DLBC | Bones, joints and articular cartilage of other and unspecified sites, Brain, Breast, Colon, Connective, subcutaneous and other soft tissues, Heart, mediastinum, and pleura, Hematopoietic and reticuloendothelial systems, Lymph nodes, Other and unspecified major salivary glands, Retroperitoneum and peritoneum, Small intestine, Stomach, Testis, Thyroid gland | 48 |
| CTSP-DLBCL1 | Lymph nodes, Unknown | 41 |
| TCGA-CHOL | Gallbladder, Liver and intrahepatic bile ducts, Other and unspecified parts of biliary tract | 36 |
| TARGET-CCSK | Kidney | 13 |
| CMI-ASC | Bladder, Breast, Bronchus and lung, Heart, mediastinum, and pleura, Lymph nodes, Other and ill-defined digestive organs, Other and ill-defined sites, Other and ill-defined sites within respiratory system and intrathoracic organs, Skin | 8 |

Table 5.2: Patient Dataset

| | | **Total** | |
|---|---|---|---|
| | | **N** | **%** |
| **Sex** | | | |
| Male | | 5777 | 49% |
| Female | | 5915 | 51% |
| **Age** | | | |
| <65 | | 6239 | 62% |
| >65 | | 3875 | 38% |

*Some patients' characteristics information was missing in the GDC clinical datasets.

# CHAPTER 6: CONCLUSION

MUC1 remains a top target for epithelial cancers as is evidenced by our analysis of pan-epithelial cancer data from TCGA (Chapter 5). MUC1 was found to be overexpressed in 12,042 out of 13,509 tumor samples when compared to 1603 normal samples, thus showing the clinical relevance of MUC1. Overexpression of MUC1 also significantly correlated with poor overall survival in these tumors. In addition, if GI tumors overexpress both, MUC1 and STAT3, the survival becomes worse. Therefore, we need to find better ways to target these proteins. Learning from the reasons of failure of current MUC1 and STAT3-targeted therapies, and from the oncogenesis data generated in this thesis, we hope to be closer to determining a combination therapy that will be clinically successful in the future. MUC1 is known to regulate oncogenesis in a variety of ways. In this thesis, we first show that MUC1 overexpression in PDA regulates the function of TGF-$\beta$. TCGA data analysis based solely on MUC1 levels suggests that genes in the TGF-$\beta$, MAPK and BMP pathways are significantly altered. Overexpression of MUC1 induces the non-canonical TGF-$\beta$ pathway by directly activating JNK and c-MYC, thus switching TGF-$\beta$ from a tumor suppressor to a tumor-promoter in the later stages. We have shown the differential outcomes of TGF-$\beta$ targeted therapy in endogenously low vs high MUC1 tumors in vivo. Targeting TGF-$\beta$ in a high-MUC1 setting can be beneficial as a tumor-promoter is being targeted. However, in a low-MUC1 setting, targeting TGF-$\beta$ may be detrimental as it is inhibiting a tumor suppressor. Hence, MUC1 can be used as a surrogate biomarker to predict outcomes of TGF-$\beta$ targeted therapies. Indeed, combination of MUC1 and TGF-$\beta$ inhibitors may turn out to be beneficial in high-MUC1 expressing tumors.

Another crucial transcription factor that aids in oncogenesis is STAT3. It is known

to be overexpressed in CSCs and regulate their plasticity. STAT3 is known to induce EMT and MET in CSCs that help them to change phenotypes during metastasis. Recently, it was shown that BM-MSCs elicit EMT in epithelial-type cells through the IL-6/pY705-STAT3 pathway and induce MET in mesenchymal-type cells through LIFR/pS727-STAT3 signaling. These results support the theory that stem or stem-like cells may use differential STAT3 phosphorylation as a way to control their fate. In this thesis, we have shown that a STAT3 inhibitor Napabucasin significantly reduces viability, colony and spheroid forming potentials of PDA cells. STAT3 is involved in regulation of MUC1 expression in an auto-inductive loop. We overexpressed MUC1 in an endogenously low MUC1 expressing PDA cell line MiaPaca2 and knocked down MUC1 in an endogenously high MUC1 expressing PDA cell line HPAF II. Interestingly, we found that overexpression of MUC1 increased pY705 and decreased pS727 of STAT3, and knocking MUC1 down had an exactly reverse effect. We also showed that in high MUC1 cells, MUC1-STAT3 pathway is constitutively activated and thus functions as the main survival pathway for PDA cells. Thus, Napabucasin was more potent against high-MUC1 cells and blocking MUC1 signaling with a homodimerization inhibitor peptide GO-203 reversed the sensitivity of high-MUC1 cells. Napabucasin reduced pY705 in high MUC1 cells CFPAC and HPAFII but not in low MUC1 MiaPaca2. Small doses of Napabucasin also reduced STAT3 and MUC1 levels in CFPAC cells, but had no effect on MiaPaca2 and HPAFII. Since HPAFII cells are relatively resistant to all treatment including Napabucasin, albiet being high MUC1 expressors, we hypothesized that adding an anti-MUC1 antibody will be helpful to enhance the outcome of Napabucasin. Napabucasin also significantly disrupted the binding of MUC1 with STAT3, which is a novel mechanism of action of the drug. Thus, as with TGF-$\beta$ targeted therapies, MUC1 expression might serve as a biomarker to predict outcome of STAT3-inhibitor therapies as well. Overall, we hope that the data from these studies will lead to the development of clinically relevant combination regimens.

The main reason of cancer related mortality is not the primary tumor, but metastasis and recurrence. A phenomenon widely associated with metastasis in EMT. EMT is a cellular process defined as a loss of the epithelial features of tight cell-cell adhesion and apico-basal polarization and a gain of mesenchymal features of motility and invasion [337]. The hypothesis that EMT and mesenchymal-to-epithelial transition (MET) drive the invasion-metastasis cascade [338] has been pursued enthusiastically for over a decade [339, 340, 341, 342, 343, 344, 345], but recent studies have questioned the indispensability of these transitions in establishing metastasis [346, 347, 348, 202]. These results have triggered provocative discussions on what steps are necessary and sufficient to establish macrometastases in vivo [5]. An assumption on the role of EMT and MET during the metastasis-invasion cascade was that, epithelial and mesenchymal carcinoma cells can attain either a fully epithelial or a fully mesenchymal state [338]. This assumption was supported by labeling co-expressing canonical epithelial and mesenchymal markers as 'metastable', that strongly suggested that these observations were only a snapshot of the full EMT/MET and thus could not reflect a real-time state or an end point of a transition in itself [349]. However, recently the concept of a hybrid epithelial/mesenchymal (E/M) state in cancer has been discussed [350, 351, 352, 353, 354, 355, 356, 357, 358, 310],and this state has been shown to be stable over multiple passages in vitro [5]. This revised understanding of cancer cell plasticity has been partially driven by computational analysis of EMT/MET regulatory networks [359, 360, 361, 362] and have lead to investigations of single-cell phenotypes in terms of their EMT status [363, 352].

EMT progression is not a uni-dimensional linear process. Recent progress in considering EMT as more of a spectrum of phenotypes instead of a binary process has driven an emerging notion that unlike during development, in which terminally differentiated epithelial and mesenchymal states exist, carcinoma cells might undergo more partial transitions to an incomplete mesenchymal phenotype [364, 365]. This notion

is supported by observations that induction of a fully mesenchymal state through overexpression of an EMT-TF may lead to a loss of tumor-initiating potential and thus the ability to colonize [366, 367, 368, 344]. Earlier studies based on similar overexpression of EMT-TFs proposed an increase in tumor-initiating potential [369]. Reconciling these contradictions, recent studies that categorized cells into E (epithelial), M (mesenchymal), and hybrid E/M, instead of just E and M, have proposed that tumor-initiating potential might be maximum when cells are in a hybrid E/M state [352, 370, 371, 368]. Such hybrid E/M cells co-expressing various epithelial and mesenchymal markers have been observed in breast, ovarian, lung, and renal cell carcinoma cell lines [363, 352, 353, 357, 358], in mouse models of prostate cancer and PDAC [372, 368], primary breast and ovarian cancer tissue [310, 373], in the bloodstream of breast, lung, and prostate cancer patients [374, 354, 373], and in metastatic brain tumors [375]. More importantly, triple-negative breast cancer patients had a significantly higher number of such hybrid E/M cells as compared to other subtypes, suggesting a correlation between a hybrid E/M phenotype and tumor aggressiveness [373]. The quasi-mesenchymal cells that disseminate from the primary tumor have the capability to evade cell death, migrate to distant anatomic sites and eventually colonize there forming a secondary tumor. The ability of the detached cells to evade apoptosis is called anoikis-resistance, which is an emerging hallmark of cancer metastasis [5].

In this thesis, we have shown that MUC1 contributes to the different hallmarks of cancer including increased proliferation through TGF-$\beta$ and increased plasticity through regulation of STAT3 activity. There have only been a few studies thusfar that suggested that high MUC1 in cancer cells can lead to anoikis-resistance [298, 187, 313]. In this thesis, We have analysed TCGA data across 48 cancer projects to show the clinical relevance of MUC1 as a target in epithelial cancers, and its correlation with anoikis-resistance genes. We have shown how targeting tMUC1 using

a specific antibody can overcome anoikis resistance in PDA cells. The anti-MUC1 antibody called TAB004 has been previously shown to be effective against epithelial tumors in syngeneic mouse models and elicited a significant immune response [231]. However, the intracellular molecular mechanism of this antibody has been elucidated in this thesis. We have shown for the first time that TAB004 can bind MUC1-N and induce phosphorylation of MUC1-CT at Tyr1229 by c-Src. This phosphorylation leads to ubiquitination and autophagy-lysosomal degradation of tMUC1. Treatment of PDA cells with TAB004 antibody also decreases binding of tMUC1 to cell-adhesion molecules Desmoplakin, Junction plakoglobin ($\gamma$-catenin, Desmocollin, Keratin, Galectin-7 etc., thus compromising the desmosomal assembly, in turn reducing the ability of the cells to form colonies.

We also demonstrate that treatment with TAB004 not only disrupts the cell-cell and cell-matrix adhesion but also blocks major oncogenic signaling pathways. This is exemplified by TAB004 treatment blocking the binding of EGF to EGFR, thus inhibiting activation of the EGFR-PI3K pathway. TAB004 mediated degradation of tMUC1 also leads to significant reduction in overall intracellular levels of tMUC1 binding partners EGFR, c-Src, and transcriptional targets STAT3 and c-Myc. This in turn leads to the activation of both the extrinsic and intrinsic apoptotic pathways, thus inducing anoikis in the detached cells. Now that the detached cells undergo apoptosis, these will not be able to form colonies at a secondary site.

In vitro studies were confirmed with in vivo mouse studies. We found that treatment with TAB004 significantly slowed down the growth of PDA tumor xenografts in vivo and enhanced the efficacy of 5-FU.

Therefore, we propose to utilize TAB004 as a combination agent with other drugs to reverse chemoresistance and as a prophylactic vaccine with or without chemotherapeutic drugs to curb minimal residual disease to reduce recurrence and metastasis. We also found that the mechanism of action of TAB004 could be extended to other

epithelial cancer cells such as ovarian, breast and hepatocellular carcinomas.

# REFERENCES


[1] Y. Du, B. Zhao, Z. Liu, X. Ren, W. Zhao, Z. Li, L. You, and Y. Zhao, "Molecular subtyping of pancreatic cancer: translating genomics and transcriptomics into the clinic," *Journal of Cancer*, vol. 8, no. 4, p. 513, 2017.

[2] E. A. Collisson, P. Bailey, D. K. Chang, and A. V. Biankin, "Molecular subtypes of pancreatic cancer," *Nature reviews Gastroenterology & hepatology*, vol. 16, no. 4, pp. 207–220, 2019.

[3] A. Maitra and R. H. Hruban, "Pancreatic cancer," *Annual review of pathology*, vol. 3, p. 157, 2008.

[4] C.-W. Lee, B. Rickman, A. B. Rogers, Z. Ge, T. C. Wang, and J. G. Fox, "Helicobacter pylori eradication prevents progression of gastric cancer in hypergastrinemic ins-gas mice," *Cancer research*, vol. 68, no. 9, pp. 3540–3548, 2008.

[5] M. K. Jolly, K. E. Ware, S. Gilja, J. A. Somarelli, and H. Levine, "Emt and met: necessary or permissive for metastasis?," *Molecular oncology*, vol. 11, no. 7, pp. 755–769, 2017.

[6] S. Nath and P. Mukherjee, "Muc1: a multifaceted oncoprotein with a key role in cancer progression," *Trends in molecular medicine*, vol. 20, no. 6, pp. 332–342, 2014.

[7] C. L. Hattrup and S. J. Gendler, "Structure and function of the cell surface (tethered) mucins," *Annu. Rev. Physiol.*, vol. 70, pp. 431–457, 2008.

[8] S. Gendler, J. Burchell, T. Duhig, D. Lamport, R. White, M. Parker, and J. Taylor-Papadimitriou, "Cloning of partial cdna encoding differentiation and tumor-associated mucin glycoproteins expressed by human mammary epithelium," *Proceedings of the National Academy of Sciences*, vol. 84, no. 17, pp. 6060–6064, 1987.

[9] M. Bose, A. Vora, T. Colleton, and P. Mukherjee, "Muc1 confers sensitivity to stat-3 inhibitor napabucasin in pancreatic ductal adenocarcinoma cells," *Cancer Research*, vol. 80, no. 16_Supplement, pp. 1837–1837, 2020.

[10] C. L. Hattrup and S. J. Gendler, "Structure and function of the cell surface (tethered) mucins," *Annu. Rev. Physiol.*, vol. 70, pp. 431–457, 2008.

[11] F. Levitin, O. Stern, M. Weiss, C. Gil-Henn, R. Ziv, Z. Prokocimer, N. I. Smorodinsky, D. B. Rubinstein, and D. H. Wreschner, "The muc1 sea module is a self-cleaving domain," *Journal of Biological Chemistry*, vol. 280, no. 39, pp. 33374–33386, 2005.

[12] M. Brayman, A. Thathiah, and D. D. Carson, "Muc1: a multifunctional cell surface component of reproductive tissue epithelia," *Reproductive Biology and Endocrinology*, vol. 2, no. 1, p. 4, 2004.

[13] A. Thathiah, C. P. Blobel, and D. D. Carson, "Tumor necrosis factor-$\alpha$ converting enzyme/adam 17 mediates muc1 shedding," *Journal of Biological Chemistry*, vol. 278, no. 5, pp. 3386–3394, 2003.

[14] A. Thathiah and D. D. Carson, "Mt1-mmp mediates muc1 shedding independent of tace/adam17," *Biochemical Journal*, vol. 382, no. 1, pp. 363–373, 2004.

[15] D. D. Carson, "The cytoplasmic tail of muc1: a very busy place," *Science signaling*, vol. 1, no. 27, pp. pe35–pe35, 2008.

[16] S. Mahanta, S. P. Fessler, J. Park, and C. Bamdad, "A minimal fragment of muc1 mediates growth of cancer cells," *PloS one*, vol. 3, no. 4, p. e2054, 2008.

[17] B. J. Smagghe, A. K. Stewart, M. G. Carter, L. M. Shelton, K. J. Bernier, E. J. Hartman, A. K. Calhoun, V. M. Hatziioannou, G. Lillacci, and B. A. Kirk, "Muc1* ligand, nm23-h1, is a novel growth factor that maintains human stem cells in a more naive state," *PloS one*, vol. 8, no. 3, p. e58601, 2013.

[18] J. Julian, N. Dharmaraj, and D. D. Carson, "Muc1 is a substrate for $\gamma$-secretase," *Journal of cellular biochemistry*, vol. 108, no. 4, pp. 802–815, 2009.

[19] S. Aubert, V. Fauquette, B. Hémon, R. Lepoivre, N. Briez, D. Bernard, I. Van Seuningen, X. Leroy, and M. Perrais, "Muc1, a new hypoxia inducible factor target gene, is an actor in clear renal cell carcinoma tumor progression," *Cancer research*, vol. 69, no. 14, pp. 5707–5715, 2009.

[20] H. Huang, H. Wu, P. Chu, I. Lai, P. Huang, S. Kulp, S. Pan, C. Teng, and C. Chen, "Role of integrin-linked kinase in regulating the protein stability of the muc1-c oncoprotein in pancreatic cancer cells," *Oncogenesis*, vol. 6, no. 7, pp. e359–e359, 2017.

[21] G. Berclaz, H. J. Altermatt, V. Rohrbach, A. Siragusa, E. Dreher, and P. D. Smith, "Egfr dependent expression of stat3 (but not stat1) in breast cancer," *International journal of oncology*, vol. 19, no. 6, pp. 1155–1160, 2001.

[22] N. Dharmaraj, B. J. Engel, and D. D. Carson, "Activated egfr stimulates muc1 expression in human uterine and pancreatic cancer cell lines," *Journal of cellular biochemistry*, vol. 114, no. 10, pp. 2314–2322, 2013.

[23] B. J. Engel, J. L. Bowser, R. R. Broaddus, and D. D. Carson, "Muc1 stimulates egfr expression and function in endometrial cancer," *Oncotarget*, vol. 7, no. 22, p. 32796, 2016.

[24] B. G. Bitler, A. Goverdhan, and J. A. Schroeder, "Muc1 regulates nuclear localization and function of the epidermal growth factor receptor," *Journal of cell science*, vol. 123, no. 10, pp. 1716–1723, 2010.

[25] T. M. Horm and J. A. Schroeder, "Muc1 and metastatic cancer: expression, function and therapeutic targeting," *Cell adhesion  migration*, vol. 7, no. 2, pp. 187–198, 2013.

[26] Y. Li, D. Liu, D. Chen, S. Kharbanda, and D. Kufe, "Human df3/muc1 carcinoma-associated protein functions as an oncogene," *Oncogene*, vol. 22, no. 38, pp. 6107–6110, 2003.

[27] W. Chen, Z. Zhang, S. Zhang, P. Zhu, J. K.-S. Ko, and K. K.-L. Yung, "Muc1: structure, function, and clinic application in epithelial cancers," *International Journal of Molecular Sciences*, vol. 22, no. 12, p. 6567, 2021.

[28] S. Ramasamy, S. Duraisamy, S. Barbashov, T. Kawano, S. Kharbanda, and D. Kufe, "The muc1 and galectin-3 oncoproteins function in a microrna-dependent regulatory loop," *Molecular cell*, vol. 27, no. 6, pp. 992–1004, 2007.

[29] Y. Leng, C. Cao, J. Ren, L. Huang, D. Chen, M. Ito, and D. Kufe, "Nuclear import of the muc1-c oncoprotein is mediated by nucleoporin nup62," *Journal of Biological Chemistry*, vol. 282, no. 27, pp. 19321–19330, 2007.

[30] D. W. Kufe, "Mucins in cancer: function, prognosis and therapy," *Nature Reviews Cancer*, vol. 9, no. 12, pp. 874–885, 2009.

[31] R. Ahmad, D. Raina, V. Trivedi, J. Ren, H. Rajabi, S. Kharbanda, and D. Kufe, "Muc1 oncoprotein activates the ib kinase $\beta$ complex and constitutive nf-$\kappa$b signalling," *Nature cell biology*, vol. 9, no. 12, p. 1419, 2007.

[32] R. Ahmad, D. Raina, M. D. Joshi, T. Kawano, J. Ren, S. Kharbanda, and D. Kufe, "Muc1-c oncoprotein functions as a direct activator of the nuclear factor-$\kappa$b p65 transcription factor," *Cancer research*, vol. 69, no. 17, pp. 7013–7021, 2009.

[33] D. M. Besmer, J. M. Curry, L. D. Roy, T. L. Tinder, M. Sahraei, J. Schettini, S.-I. Hwang, Y. Y. Lee, S. J. Gendler, and P. Mukherjee, "Pancreatic ductal adenocarcinoma mice lacking mucin 1 have a profound defect in tumor growth and metastasis," *Cancer research*, vol. 71, no. 13, pp. 4432–4442, 2011.

[34] D. Raina, S. Kharbanda, and D. Kufe, "The muc1 oncoprotein activates the anti-apoptotic phosphoinositide 3-kinase/akt and bcl-xl pathways in rat 3y1 fibroblasts," *Journal of Biological Chemistry*, vol. 279, no. 20, pp. 20607–20612, 2004.

[35] C. L. Hattrup and S. J. Gendler, "Muc1 alters oncogenic events and transcription in human breast cancer cells," *Breast Cancer Research*, vol. 8, no. 4, pp. 1–10, 2006.

[36] M. E. Behrens, P. M. Grandgenett, J. M. Bailey, P. K. Singh, C.-H. Yi, F. Yu, and M. A. Hollingsworth, "The reactive tumor microenvironment: Muc1 signaling directly reprograms transcription of ctgf," *Oncogene*, vol. 29, no. 42, pp. 5667–5677, 2010.

[37] T. Hayashi, T. Takahashi, S. Motoya, T. Ishida, F. Itoh, M. Adachi, Y. Hinoda, and K. Imai, "Muc1 mucin core protein binds to the domain 1 of icam-1," *Digestion*, vol. 63, no. Suppl. 1, pp. 87–92, 2001.

[38] S. D. Rodgers, R. T. Camphausen, and D. A. Hammer, "Sialyl lewisx-mediated, psgl-1-independent rollingadhesion on p-selectin," *Biophysical journal*, vol. 79, no. 2, pp. 694–706, 2000.

[39] B. Mann, E. Klussmann, V. Vandamme-Feldhaus, M. Iwersen, M.-L. Hanski, E.-O. Riecken, H. J. Buhr, R. Schauer, Y. S. Kim, and C. Hanski, "Low o-acetylation of sialyl-lex contributes to its overexpression in colon carcinoma metastases," *International journal of cancer*, vol. 72, no. 2, pp. 258–264, 1997.

[40] J. Wesseling, S. W. Van Der Valk, H. L. Vos, A. Sonnenberg, and J. Hilkens, "Episialin (muc1) overexpression inhibits integrin-mediated cell adhesion to extracellular matrix components.," *The Journal of cell biology*, vol. 129, no. 1, pp. 255–265, 1995.

[41] S. Cascio, A. M. Farkas, R. P. Hughey, and O. J. Finn, "Altered glycosylation of muc1 influences its association with cin85: the role of this novel complex in cancer cell invasion and migration," *Oncotarget*, vol. 4, no. 10, p. 1686, 2013.

[42] L. Yin, Y. Li, J. Ren, H. Kuwahara, and D. Kufe, "Human muc1 carcinoma antigen regulates intracellular oxidant levels and the apoptotic response to oxidative stress," *Journal of Biological Chemistry*, vol. 278, no. 37, pp. 35458–35464, 2003.

[43] L. Yin, S. Kharbanda, and D. Kufe, "Mucin 1 oncoprotein blocks hypoxia-inducible factor $1\alpha$ activation in a survival response to hypoxia," *Journal of Biological Chemistry*, vol. 282, no. 1, pp. 257–266, 2007.

[44] M. Dean, T. Fojo, and S. Bates, "Tumour stem cells and drug resistance," *Nature Reviews Cancer*, vol. 5, no. 4, pp. 275–284, 2005.

[45] S. Nath, K. Daneshvar, L. D. Roy, P. Grover, A. Kidiyoor, L. Mosley, M. Sahraei, and P. Mukherjee, "Muc1 induces drug resistance in pancreatic cancer cells via upregulation of multidrug resistance genes," *Oncogenesis*, vol. 2, no. 6, pp. e51–e51, 2013.

[46] L. D. Roy, M. Sahraei, D. B. Subramani, D. Besmer, S. Nath, T. L. Tinder, E. Bajaj, K. Shanmugam, Y. Y. Lee, and S. I. Hwang, "Muc1 enhances invasiveness of pancreatic cancer cells by inducing epithelial to mesenchymal transition," *Oncogene*, vol. 30, no. 12, pp. 1449–1459, 2011.

[47] P. K. Singh, Y. Wen, B. J. Swanson, K. Shanmugam, A. Kazlauskas, R. L. Cerny, S. J. Gendler, and M. A. Hollingsworth, "Platelet-derived growth factor receptor $\beta$–mediated phosphorylation of muc1 enhances invasiveness in pancreatic adenocarcinoma cells," *Cancer research*, vol. 67, no. 11, pp. 5201–5210, 2007.

[48] J. Lüttges, B. Feyerabend, T. Buchelt, M. Pacena, and G. Klöppel, "The mucin profile of noninvasive and invasive mucinous cystic neoplasms of the pancreas," *The American journal of surgical pathology*, vol. 26, no. 4, pp. 466–471, 2002.

[49] S. Nakamori, D. M. Ota, K. R. Cleary, K. Shirotani, and T. Irimura, "Muc1 mucin expression as a marker of progression and metastasis of human colorectal carcinoma," *Gastroenterology*, vol. 106, no. 2, pp. 353–361, 1994.

[50] H. Kashiwagi, H. Kijima, S. Dowaki, Y. Ohtani, K. Tobita, M. Tsukui, Y. Tanaka, H. Matsubayasi, T. Tsuchida, H. Yamazaki, *et al.*, "Df3 expression in human gallbladder carcinoma: significance for lymphatic invasion.," *International journal of oncology*, vol. 16, no. 3, pp. 455–464, 2000.

[51] E. Delva, D. K. Tucker, and A. P. Kowalczyk, "The desmosome," *Cold Spring Harbor perspectives in biology*, vol. 1, no. 2, p. a002543, 2009.

[52] K. J. Green and C. A. Gaudry, "Are desmosomes more than tethers for intermediate filaments?," *Nature reviews Molecular cell biology*, vol. 1, no. 3, pp. 208–216, 2000.

[53] H.-J. Choi, J. C. Gross, S. Pokutta, and W. I. Weis, "Interactions of plakoglobin and $\beta$-catenin with desmosomal cadherins," *Journal of Biological Chemistry*, vol. 284, no. 46, pp. 31776–31788, 2009.

[54] M. Hatzfeld, "Plakophilins: Multifunctional proteins or just regulators of desmosomal adhesion?," *Biochimica et Biophysica Acta (BBA)-Molecular Cell Research*, vol. 1773, no. 1, pp. 69–77, 2007.

[55] T. Yin, S. Getsios, R. Caldelari, L. M. Godsel, A. P. Kowalczyk, E. J. MuÌller, and K. J. Green, "Mechanisms of plakoglobin-dependent adhesion: desmosome-specific functions in assembly and regulation by epidermal growth factor receptor," *Journal of Biological Chemistry*, vol. 280, no. 48, pp. 40355–40363, 2005.

[56] A. De Bruin, R. Caldelari, L. Williamson, M. M. Suter, T. Hunziker, M. Wyder, and E. J. Müller, "Plakoglobin-dependent disruption of the desmosomal plaque in pemphigus vulgaris," *Experimental dermatology*, vol. 16, no. 6, pp. 468–475, 2007.

[57] T. Yin, S. Getsios, R. Caldelari, A. P. Kowalczyk, E. J. Müller, J. C. Jones, and K. J. Green, "Plakoglobin suppresses keratinocyte motility through both cell–cell adhesion-dependent and-independent mechanisms," *Proceedings of the National Academy of Sciences*, vol. 102, no. 15, pp. 5420–5425, 2005.

[58] V. Todorović, B. V. Desai, M. J. S. Patterson, E. V. Amargo, A. D. Dubash, T. Yin, J. C. Jones, and K. J. Green, "Plakoglobin regulates cell motility through rho-and fibronectin-dependent src signaling," *Journal of cell science*, vol. 123, no. 20, pp. 3576–3586, 2010.

[59] Y. Li, W.-h. Yu, J. Ren, W. Chen, L. Huang, S. Kharbanda, M. Loda, and D. Kufe, "Heregulin targets $\gamma$-catenin to the nucleolus by a mechanism dependent on the df3/muc1 oncoprotein," *Molecular Cancer Research*, vol. 1, no. 10, pp. 765–775, 2003.

[60] Z. Aktary, K. Chapman, L. Lam, A. Lo, C. Ji, K. Graham, L. Cook, L. Li, J. Mackey, and M. Pasdar, "Plakoglobin interacts with and increases the protein levels of metastasis suppressor nm23-h2 and regulates the expression of nm23-h1," *Oncogene*, vol. 29, no. 14, pp. 2118–2129, 2010.

[61] F. Safi, I. Kohler, H.-G. Beger, and E. Röttinger, "The value of the tumor marker ca 15-3 in diagnosing and monitoring breast cancer. a comparative study with carcinoembryonic antigen," *Cancer*, vol. 68, no. 3, pp. 574–582, 1991.

[62] W. Steinberg, "The clinical utility of the ca 19-9 tumor-associated antigen.," *American Journal of Gastroenterology (Springer Nature)*, vol. 85, no. 4, 1990.

[63] J. M. Winter, L. H. Tang, D. S. Klimstra, M. F. Brennan, J. R. Brody, F. G. Rocha, X. Jia, L.-X. Qin, M. I. DâAngelica, R. P. DeMatteo, *et al.*, "A novel survival-based tissue microarray of pancreatic cancer validates muc1 and mesothelin as biomarkers," *PloS one*, vol. 7, no. 7, p. e40157, 2012.

[64] J. M. Curry, K. J. Thompson, S. G. Rao, D. M. Besmer, A. M. Murphy, V. Z. Grdzelishvili, W. A. Ahrens, I. H. McKillop, D. Sindram, and D. A. Iannitti, "The use of a novel muc1 antibody to identify cancer stem cells and circulating muc1 in mice and patients with pancreatic cancer," *Journal of surgical oncology*, vol. 107, no. 7, pp. 713–722, 2013.

[65] L. Yin and D. Kufe, "Muc1-c oncoprotein blocks terminal differentiation of chronic myelogenous leukemia cells by a ros-mediated mechanism," *Genes & cancer*, vol. 2, no. 1, pp. 56–64, 2011.

[66] A. McGuigan, P. Kelly, R. C. Turkington, C. Jones, H. G. Coleman, and R. S. McCain, "Pancreatic cancer: A review of clinical diagnosis, epidemiology, treatment and outcomes," *World journal of gastroenterology*, vol. 24, no. 43, p. 4846, 2018.

[67] A.-M. Noone, K. A. Cronin, S. F. Altekruse, N. Howlader, D. R. Lewis, V. I. Petkov, and L. Penberthy, "Cancer incidence and survival trends by subtype using data from the surveillance epidemiology and end results program, 1992–2013cancer incidence and survival trends by subtype, 1992–2013," *Cancer Epidemiology, Biomarkers & Prevention*, vol. 26, no. 4, pp. 632–641, 2017.

[68] M. Namwanje and C. W. Brown, "Activins and inhibins: roles in development, physiology, and disease," *Cold Spring Harbor perspectives in biology*, vol. 8, no. 7, p. a021881, 2016.

[69] J. Carcamo, F. Weis, F. Ventura, R. Wieser, J. L. Wrana, L. Attisano, and J. Massague, "Type i receptors specify growth-inhibitory and transcriptional responses to transforming growth factor beta and activin," *Molecular and cellular biology*, vol. 14, no. 6, pp. 3810–3821, 1994.

[70] Y. Shi, "Structural insights on smad function in tgf$\beta$ signaling," *Bioessays*, vol. 23, no. 3, pp. 223–232, 2001.

[71] I. Fabregat, J. Fernando, J. Mainez, and P. Sancho, "Tgf-beta signaling in cancer treatment," *Current pharmaceutical design*, vol. 20, no. 17, pp. 2934–2947, 2014.

[72] S. Colak and P. Ten Dijke, "Targeting tgf-$\beta$ signaling in cancer," *Trends in cancer*, vol. 3, no. 1, pp. 56–71, 2017.

[73] J. Massague, "Tgf-$\beta$ signal transduction," *Annual review of biochemistry*, vol. 67, no. 1, pp. 753–791, 1998.

[74] V. Mittal, "Epithelial mesenchymal transition in tumor metastasis," *Annu Rev Pathol*, vol. 13, no. 1, pp. 395–412, 2018.

[75] J. Massagué and Y.-G. Chen, "Controlling tgf-$\beta$ signaling," *Genes & development*, vol. 14, no. 6, pp. 627–644, 2000.

[76] J. L. Wrana, L. Attisano, R. Wieser, F. Ventura, and J. Massagué, "Mechanism of activation of the tgf-$\beta$ receptor," *Nature*, vol. 370, no. 6488, pp. 341–347, 1994.

[77] T. Tsukazaki, T. A. Chiang, A. F. Davison, L. Attisano, and J. L. Wrana, "Sara, a fyve domain protein that recruits smad2 to the tgf$\beta$ receptor," *Cell*, vol. 95, no. 6, pp. 779–791, 1998.

[78] K. Eppert, S. W. Scherer, H. Ozcelik, R. Pirone, P. Hoodless, H. Kim, L.-C. Tsui, B. Bapat, S. Gallinger, I. L. Andrulis, *et al.*, "Madr2 maps to 18q21 and encodes a tgf$\beta$–regulated mad–related protein that is functionally mutated in colorectal carcinoma," *Cell*, vol. 86, no. 4, pp. 543–552, 1996.

[79] L. Attisano and J. L. Wrana, "Signal transduction by the tgf-$\beta$ superfamily," *Science*, vol. 296, no. 5573, pp. 1646–1647, 2002.

[80] J. Massagué and D. Wotton, "Transcriptional control by the tgfâ$\beta$/smad signaling system," *The EMBO journal*, vol. 19, no. 8, pp. 1745–1754, 2000.

[81] Y. E. Zhang, "Non-smad pathways in tgf-$\beta$ signaling," *Cell research*, vol. 19, no. 1, pp. 128–139, 2009.

[82] M. K. Lee, C. Pardoux, M. C. Hall, P. S. Lee, D. Warburton, J. Qing, S. M. Smith, and R. Derynck, "Tgf-$\beta$ activates erk map kinase signalling through direct phosphorylation of shca," *The EMBO journal*, vol. 26, no. 17, pp. 3957–3967, 2007.

[83] T. L. Tinder, D. B. Subramani, G. D. Basu, J. M. Bradley, J. Schettini, A. Million, T. Skaar, and P. Mukherjee, "Muc1 enhances tumor progression and contributes toward immunosuppression in a mouse model of spontaneous pancreatic adenocarcinoma," *The Journal of Immunology*, vol. 181, no. 5, pp. 3116–3125, 2008.

[84] R. Zhou, J. M. Curry, L. D. Roy, P. Grover, J. Haider, L. J. Moore, S. Wu, A. Kamesh, M. Yazdanifar, and W. A. Ahrens, "A novel association of neuropilin-1 and muc1 in pancreatic ductal adenocarcinoma: role in induction of vegf signaling and angiogenesis," *Oncogene*, vol. 35, no. 43, pp. 5608–5618, 2016.

[85] K. Kato, E. P. Lillehoj, W. Lu, and K. C. Kim, "Muc1: the first respiratory mucin with an anti-inflammatory function," *Journal of clinical medicine*, vol. 6, no. 12, p. 110, 2017.

[86] E. J. Thompson, K. Shanmugam, K. L. Kotlarczyk, C. L. Hattrup, A. Gutierrez, J. M. Bradley, P. Mukherjee, and S. J. Gendler, "Tyrosines in the muc1 cytoplasmic tail modulate oncogenic signaling pathways," *Cancer Research*, vol. 65, no. 9_Supplement, pp. 222–222, 2005.

[87] P. K. Singh and M. A. Hollingsworth, "Cell surface-associated mucins in signal transduction," *Trends in cell biology*, vol. 16, no. 9, pp. 467–476, 2006.

[88] P. Grover, S. Nath, M. D. Nye, R. Zhou, M. Ahmad, and P. Mukherjee, "Smad4-independent activation of tgf-$\beta$ signaling by muc1 in a human pancreatic cancer cell line," *Oncotarget*, vol. 9, no. 6, p. 6897, 2018.

[89] J. Zhang, X. Zhang, S. Yang, Y. Bao, D. Xu, and L. Liu, "Foxh1 promotes lung cancer progression by activating the wnt/$\beta$-catenin signaling pathway," *Cancer cell international*, vol. 21, no. 1, pp. 1–13, 2021.

[90] M. Zhang, L. Zeng, Y. Peng, B. Fan, P. Chen, and J. Liu, "Immune-related genes lama2 and il1r1 correlate with tumor sites and predict poor survival in pancreatic adenocarcinoma," *Future Oncology*, no. 0, 2021.

[91] S. Hamada, K. Satoh, M. Hirota, K. Kimura, A. Kanno, A. Masamune, and T. Shimosegawa, "Bone morphogenetic protein 4 induces epithelialâmesenchymal transition through msx2 induction on pancreatic cancer cell line," *Journal of cellular physiology*, vol. 213, no. 3, pp. 768–774, 2007.

[92] J. M. Davis, B. Cheng, M. M. Drake, Q. Yu, B. Yang, J. Li, C. Liu, M. Younes, X. Zhao, and J. M. Bailey, "Pancreatic stromal gremlin 1 expression during pancreatic tumorigenesis," *Genes  Diseases*, 2020.

[93] D. Cao, S. R. Hustinx, G. Sui, P. Bala, N. Sato, S. Martin, A. Maitra, K. M. Murphy, J. L. Cameron, and C. J. Yeo, "Identification of novel highly expressed genes in pancreatic ductal adenocarcinomas through a bioinformatics analysis of expressed sequence tags," *Cancer biology  therapy*, vol. 3, no. 11, pp. 1081–1089, 2004.

[94] M. Sahraei, L. D. Roy, J. M. Curry, T. L. Teresa, S. Nath, D. Besmer, A. Kidiyoor, R. Dalia, S. J. Gendler, and P. Mukherjee, "Muc1 regulates pdgfa expression during pancreatic cancer progression," *Oncogene*, vol. 31, no. 47, pp. 4935–4945, 2012.

[95] X. Wang, M. Cunningham, X. Zhang, S. Tokarz, B. Laraway, M. Troxell, and R. C. Sears, "Phosphorylation regulates c-myc's oncogenic activity in the mammary gland," *Cancer research*, vol. 71, no. 3, pp. 925–936, 2011.

[96] Q. Li, G. Liu, D. Shao, J. Wang, H. Yuan, T. Chen, R. Zhai, W. Ni, and G. Tai, "Mucin1 mediates autocrine transforming growth factor beta signaling through activating the c-jun n-terminal kinase/activator protein 1 pathway in human hepatocellular carcinoma cells," *The international journal of biochemistry  cell biology*, vol. 59, pp. 116–125, 2015.

[97] S. Y. Tam and H. K.-W. Law, "Jnk in tumor microenvironment: Present findings and challenges in clinical translation," *Cancers*, vol. 13, no. 9, p. 2196, 2021.

[98] M. Bose and P. Mukherjee, "Microbe-muc1 crosstalk in cancer-associated infections," *Trends in molecular medicine*, vol. 26, no. 3, pp. 324–336, 2020.

[99] M. Sahraei, M. Bose, J. A. Sanders, C. De, L. DasRoy, S. Nath, C. R. Brouwer, and P. Mukherjee, "Repression of muc1 promotes expansion and suppressive function of myeloid-derived suppressor cells in pancreatic and breast cancer murine models," *International journal of molecular sciences*, vol. 22, no. 11, p. 5587, 2021.

[100] M. A. Cheever, J. P. Allison, A. S. Ferris, O. J. Finn, B. M. Hastings, T. T. Hecht, I. Mellman, S. A. Prindiville, J. L. Viner, and L. M. Weiner, "The prioritization of cancer antigens: a national cancer institute pilot project for the acceleration of translational research," *Clinical cancer research*, vol. 15, no. 17, pp. 5323–5337, 2009.

[101] J. Massagué, "Tgf$\beta$ in cancer," *Cell*, vol. 134, no. 2, pp. 215–230, 2008.

[102] J. Zhang, X. Zhang, S. Yang, Y. Bao, D. Xu, and L. Liu, "Foxh1 promotes lung cancer progression by activating the wnt/$\beta$-catenin signaling pathway," *Cancer cell international*, vol. 21, no. 1, pp. 1–13, 2021.

[103] K. J. Gordon, K. C. Kirkbride, T. How, and G. C. Blobe, "Bone morphogenetic proteins induce pancreatic cancer cell invasiveness through a smad1-dependent

mechanism that involves matrix metalloproteinase-2," *Carcinogenesis*, vol. 30, no. 2, pp. 238–248, 2009.

[104] A. Arlt, J. Vorndamm, S. Müerköster, H. Yu, W. E. Schmidt, U. R. Fölsch, and H. Schäfer, "Autocrine production of interleukin 1$\beta$ confers constitutive nuclear factor $\kappa$b activity and chemoresistance in pancreatic carcinoma cell lines," *Cancer research*, vol. 62, no. 3, pp. 910–916, 2002.

[105] Y. Matsuo, H. Sawai, H. Funahashi, H. Takahashi, M. Sakamoto, M. Yamamoto, Y. Okada, T. Hayakawa, and T. Manabe, "Enhanced angiogenesis due to inflammatory cytokines from pancreatic cancer cell lines and relation to metastatic potential," *Pancreas*, vol. 28, no. 3, pp. 344–352, 2004.

[106] F. Rückert, G. Dawelbait, C. Winter, A. Hartmann, A. Denz, O. Ammerpohl, M. Schroeder, H. K. Schackert, B. Sipos, and G. Klöppel, "Examination of apoptosis signaling in pancreatic cancer by computational signal transduction analysis," *PloS one*, vol. 5, no. 8, p. e12243, 2010.

[107] M. A. Mouti and S. Pauklin, "Tgfb1/inhba homodimer/nodal-smad2/3 signalling network: A pivotal molecular target in pdac treatment," *Molecular Therapy*, 2021.

[108] M. S. Razzaque and A. Atfi, "Tgif1-twist1 axis in pancreatic ductal adenocarcinoma," *Computational and Structural Biotechnology Journal*, 2020.

[109] K.-W. Kang, M.-J. Lee, J. Song, J.-Y. Jeong, Y.-K. Kim, C. Lee, T.-H. Kim, K.-B. Kwak, O.-J. Kim, and H. J. An, "Overexpression of goosecoid homeobox is associated with chemoresistance and poor prognosis in ovarian carcinoma," *Oncology reports*, vol. 32, no. 1, pp. 189–198, 2014.

[110] T.-C. Xue, N.-L. Ge, L. Zhang, J.-F. Cui, R.-X. Chen, Y. You, S.-L. Ye, and Z.-G. Ren, "Goosecoid promotes the metastasis of hepatocellular carcinoma by modulating the epithelial-mesenchymal transition," *PloS one*, vol. 9, no. 10, p. e109695, 2014.

[111] W. Xu, Z. Liu, Q. Bao, and Z. Qian, "Viruses, other pathogenic microorganisms and esophageal cancer," *Gastrointestinal tumors*, vol. 2, no. 1, pp. 2–13, 2015.

[112] Q. Jiang, M. Xie, M. He, F. Yan, M. Chen, S. Xu, X. Zhang, and P. Shen, "Pitx2 methylation: a novel and effective biomarker for monitoring biochemical recurrence risk of prostate cancer," *Medicine*, vol. 98, no. 1, 2019.

[113] M. Aubele, M. Schmitt, R. Napieralski, S. Paepke, J. Ettl, M. Absmaier, V. Magdolen, J. Martens, J. A. Foekens, and O. G. Wilhelm, "The predictive value of pitx2 dna methylation for high-risk breast cancer therapy: current guidelines, medical needs, and challenges," *Disease markers*, vol. 2017, 2017.

[114] G. Vaidyanathan, M. J. Cismowski, G. Wang, T. S. Vincent, K. D. Brown, and S. M. Lanier, "The ras-related protein ags1/rasd1 suppresses cell growth," *Oncogene*, vol. 23, no. 34, pp. 5858–5863, 2004.

[115] R. Zhao, L. Chen, B. Zhou, Z.-H. Guo, and S. Wang, "Recognizing novel tumor suppressor genes using a network machine learning strategy," *IEEE Access*, vol. 7, pp. 155002–155013, 2019.

[116] H. Valderrama-Carvajal, E. Cocolakis, A. Lacerte, E.-H. Lee, G. Krystal, S. Ali, and J.-J. Lebrun, "Activin/tgf-$\beta$ induce apoptosis through smad-dependent expression of the lipid phosphatase ship," *Nature cell biology*, vol. 4, no. 12, pp. 963–969, 2002.

[117] S. Ross and C. S. Hill, "How the smads regulate transcription," *The international journal of biochemistry  cell biology*, vol. 40, no. 3, pp. 383–408, 2008.

[118] S. Bunda, P. Heir, T. Srikumar, J. D. Cook, K. Burrell, Y. Kano, J. E. Lee, G. Zadeh, B. Raught, and M. Ohh, "Src promotes gtpase activity of ras via tyrosine 32 phosphorylation," *Proceedings of the National Academy of Sciences*, vol. 111, no. 36, pp. E3785–E3794, 2014.

[119] D. Fey, D. Matallanas, J. Rauch, O. S. Rukhlenko, and B. N. Kholodenko, "The complexities and versatility of the ras-to-erk signalling system in normal and cancer cells," in *Seminars in cell  developmental biology*, vol. 58, pp. 96–107, Elsevier.

[120] R. L. Grossman, A. P. Heath, V. Ferretti, H. E. Varmus, D. R. Lowy, W. A. Kibbe, and L. M. Staudt, "Toward a shared vision for cancer genomic data," *New England Journal of Medicine*, vol. 375, no. 12, pp. 1109–1112, 2016.

[121] M. Love, S. Anders, and W. Huber, "Deseq2 vignette," *Genome Biol. doi*, vol. 110, 2016.

[122] M. V. Kuleshov, M. R. Jones, A. D. Rouillard, N. F. Fernandez, Q. Duan, Z. Wang, S. Koplev, S. L. Jenkins, K. M. Jagodnik, and A. Lachmann, "Enrichr: a comprehensive gene set enrichment analysis web server 2016 update," *Nucleic acids research*, vol. 44, no. W1, pp. W90–W97, 2016.

[123] D. Szklarczyk, A. L. Gable, K. C. Nastou, D. Lyon, R. Kirsch, S. Pyysalo, N. T. Doncheva, M. Legeay, T. Fang, and P. Bork, "The string database in 2021: customizable proteinâprotein networks, and functional characterization of user-uploaded gene/measurement sets," *Nucleic acids research*, vol. 49, no. D1, pp. D605–D612, 2021.

[124] P. Shannon, A. Markiel, O. Ozier, N. S. Baliga, J. T. Wang, D. Ramage, N. Amin, B. Schwikowski, and T. Ideker, "Cytoscape: a software environment for integrated models of biomolecular interaction networks," *Genome research*, vol. 13, no. 11, pp. 2498–2504, 2003.

[125] J. A. Schroeder, M. C. Thompson, M. M. Gardner, and S. J. Gendler, "Transgenic muc1 interacts with egfr and correlates with map kinase activation in the mouse mammary gland," *Journal of Biological Chemistry*, 2001.

[126] A. M. Murphy, D. M. Besmer, M. Moerdyk-Schauwecker, N. Moestl, D. A. Ornelles, P. Mukherjee, and V. Z. Grdzelishvili, "Vesicular stomatitis virus as an oncolytic agent against pancreatic ductal adenocarcinoma," *Journal of virology*, vol. 86, no. 6, pp. 3073–3087, 2012.

[127] N. K. Sharma, S. Shankar, and R. K. Srivastava, "Stat3 as an emerging molecular target in pancreatic cancer," *Gastrointestinal Cancer: Targets and Therapy*, vol. 4, p. 115, 2014.

[128] A. K. Mankan and F. R. Greten, "Inhibiting signal transducer and activator of transcription 3: rationality and rationale design of inhibitors," *Expert opinion on investigational drugs*, vol. 20, no. 9, pp. 1263–1275, 2011.

[129] A. Scholz, S. Heinze, K. M. Detjen, M. Peters, M. Welzel, P. Hauff, M. Schirner, B. Wiedenmann, and S. Rosewicz, "Activated signal transducer and activator of transcription 3 (stat3) supports the malignant phenotype of human pancreatic cancer," *Gastroenterology*, vol. 125, no. 3, pp. 891–905, 2003.

[130] T. Miyatsuka, H. Kaneto, T. Shiraiwa, T.-a. Matsuoka, K. Yamamoto, K. Kato, Y. Nakamura, S. Akira, K. Takeda, Y. Kajimoto, *et al.*, "Persistent expression of pdx-1 in the pancreas causes acinar-to-ductal metaplasia through stat3 activation," *Genes & development*, vol. 20, no. 11, pp. 1435–1440, 2006.

[131] T. Toyonaga, K. Nakano, M. Nagano, G. Zhao, K. Yamaguchi, S. Kuroki, T. Eguchi, K. Chijiiwa, M. Tsuneyoshi, and M. Tanaka, "Blockade of constitutively activated janus kinase/signal transducer and activator of transcription-3 pathway inhibits growth of human pancreatic cancer," *Cancer letters*, vol. 201, no. 1, pp. 107–116, 2003.

[132] D. Wei, X. Le, L. Zheng, L. Wang, J. A. Frey, A. C. Gao, Z. Peng, S. Huang, H. Q. Xiong, J. L. Abbruzzese, *et al.*, "Stat3 activation regulates the expression of vascular endothelial growth factor and human pancreatic cancer angiogenesis and metastasis," *Oncogene*, vol. 22, no. 3, pp. 319–329, 2003.

[133] J.-Y. Lee and L. Hennighausen, "The transcription factor stat3 is dispensable for pancreatic $\beta$-cell development and function," *Biochemical and biophysical research communications*, vol. 334, no. 3, pp. 764–768, 2005.

[134] T. Decker and P. Kovarik, "Serine phosphorylation of stats," *Oncogene*, vol. 19, no. 21, pp. 2628–2637, 2000.

[135] H. R. Qin, H.-J. Kim, J.-Y. Kim, E. M. Hurt, G. J. Klarmann, B. T. Kawasaki, M. A. Duhagon Serrat, and W. L. Farrar, "Activation of signal transducer and activator of transcription 3 through a phosphomimetic serine 727 promotes

prostate tumorigenesis independent of tyrosine 705 phosphorylation," *Cancer research*, vol. 68, no. 19, pp. 7736–7741, 2008.

[136] I. Hazan-Halevy, D. Harris, Z. Liu, J. Liu, P. Li, X. Chen, S. Shanker, A. Ferrajoli, M. J. Keating, and Z. Estrov, "Stat3 is constitutively phosphorylated on serine 727 residues, binds dna, and activates transcription in cll cells," *Blood, The Journal of the American Society of Hematology*, vol. 115, no. 14, pp. 2852–2863, 2010.

[137] B. B. Aggarwal, A. B. Kunnumakkara, K. B. Harikumar, S. R. Gupta, S. T. Tharakan, C. Koca, S. Dey, and B. Sung, "Signal transducer and activator of transcription-3, inflammation, and cancer: how intimate is the relationship?," *Annals of the New York Academy of Sciences*, vol. 1171, no. 1, pp. 59–76, 2009.

[138] X. Shi, H. Zhang, H. Paddon, G. Lee, X. Cao, and S. Pelech, "Phosphorylation of stat3 serine-727 by cyclin-dependent kinase 1 is critical for nocodazole-induced mitotic arrest," *Biochemistry*, vol. 45, no. 18, pp. 5857–5867, 2006.

[139] T. Burdon, A. Smith, and P. Savatier, "Signalling, cell cycle and pluripotency in embryonic stem cells," *Trends in cell biology*, vol. 12, no. 9, pp. 432–438, 2002.

[140] D. A. Frank, "Stat3 as a central mediator of neoplastic cellular transformation," *Cancer letters*, vol. 251, no. 2, pp. 199–210, 2007.

[141] N. De La Iglesia, G. Konopka, S. V. Puram, J. A. Chan, R. M. Bachoo, M. J. You, D. E. Levy, R. A. DePinho, and A. Bonni, "Identification of a pten-regulated stat3 brain tumor suppressor pathway," *Genes & development*, vol. 22, no. 4, pp. 449–462, 2008.

[142] R. S. Chapman, P. Lourenco, E. Tonner, D. Flint, S. Selbert, K. Takeda, S. Akira, A. R. Clarke, and C. J. Watson, "The role of stat3 in apoptosis and mammary gland involution," *Biology of the Mammary Gland*, pp. 129–138, 2002.

[143] R. S. Chapman, P. C. Lourenco, E. Tonner, D. J. Flint, S. Selbert, K. Takeda, S. Akira, A. R. Clarke, and C. J. Watson, "Suppression of epithelial apoptosis and delayed mammary gland involution in mice with a conditional knockout of stat3," *Genes & development*, vol. 13, no. 19, pp. 2604–2616, 1999.

[144] A.-M. O'Farrell, Y. Liu, K. W. Moore, and A. L.-F. Mui, "Il-10 inhibits macrophage activation and proliferation by distinct signaling mechanisms: evidence for stat3-dependent and-independent pathways," *The EMBO journal*, vol. 17, no. 4, pp. 1006–1018, 1998.

[145] A. P. Hutchins, D. Diez, Y. Takahashi, S. Ahmad, R. Jauch, M. L. Tremblay, and D. Miranda-Saavedra, "Distinct transcriptional regulatory modules underlie stat3âs cell type-independent and cell type-specific functions," *Nucleic acids research*, vol. 41, no. 4, pp. 2155–2170, 2013.

[146] G. Huang, H. Yan, S. Ye, C. Tong, and Q.-L. Ying, "Stat3 phosphorylation at tyrosine 705 and serine 727 differentially regulates mouse esc fates," *Stem cells*, vol. 32, no. 5, pp. 1149–1160, 2014.

[147] J. Gao, M. J. McConnell, B. Yu, J. Li, J. M. Balko, E. P. Black, J. O. Johnson, M. C. Lloyd, S. Altiok, and E. B. Haura, "Muc1 is a downstream target of stat3 and regulates lung cancer cell survival and invasion," *International journal of oncology*, vol. 35, no. 2, pp. 337–345, 2009.

[148] I. C. Gaemers, H. L. Vos, H. H. Volders, S. W. van der Valk, and J. Hilkens, "A stat-responsive element in the promoter of the episialin/muc1 gene is involved in its overexpression in carcinoma cells," *Journal of Biological Chemistry*, vol. 276, no. 9, pp. 6191–6199, 2001.

[149] Z.-l. Yuan, Y.-j. Guan, L. Wang, W. Wei, A. B. Kane, and Y. E. Chin, "Central role of the threonine residue within the p+ 1 loop of receptor tyrosine kinase in stat3 constitutive phosphorylation in metastatic cancer cells," *Molecular and cellular biology*, vol. 24, no. 21, pp. 9390–9400, 2004.

[150] A. Al Masri and S. J. Gendler, "Muc1 affects c-src signaling in pyv mt-induced mammary tumorigenesis," *Oncogene*, vol. 24, no. 38, pp. 5799–5808, 2005.

[151] J. A. Schroeder, A. A. Masri, M. C. Adriance, J. C. Tessier, K. L. Kotlarczyk, M. C. Thompson, and S. J. Gendler, "Muc1 overexpression results in mammary gland tumorigenesis and prolonged alveolar differentiation," *Oncogene*, vol. 23, no. 34, pp. 5739–5747, 2004.

[152] A. Spicer, T. Duhig, B. Chilton, and S. Gendler, "Analysis of mammalian muc1 genes reveals potential functionally important domains," *Mammalian Genome*, vol. 6, no. 12, pp. 885–888, 1995.

[153] suwat, *Increased invasiveness of MUC1 cDNA-transfected human gastric cancer MKN74 cells*. PhD thesis, suwat, 1998.

[154] R. Ahmad, H. Rajabi, M. Kosugi, M. D. Joshi, M. Alam, B. Vasir, T. Kawano, S. Kharbanda, and D. Kufe, "Muc1-c oncoprotein promotes stat3 activation in an autoinductive regulatory loop," *Science Signaling*, vol. 4, no. 160, pp. ra9–ra9, 2011.

[155] M. B. Sonbol, D. H. Ahn, D. Goldstein, T. Okusaka, J. Tabernero, T. Macarulla, M. Reni, C.-P. Li, B. O'Neil, E. Van Cutsem, *et al.*, "Canstem111p trial: a phase iii study of napabucasin plus nab-paclitaxel with gemcitabine," *Future Oncology*, vol. 15, no. 12, pp. 1295–1302, 2019.

[156] R. Wakahara, H. Kunimoto, K. Tanino, H. Kojima, A. Inoue, H. Shintaku, and K. Nakajima, "Phospho-ser727 of stat3 regulates stat3 activity by enhancing dephosphorylation of phospho-tyr705 largely through tc45," *Genes to Cells*, vol. 17, no. 2, pp. 132–145, 2012.

[157] J. Yang, H. Kunimoto, B. Katayama, H. Zhao, T. Shiromizu, L. Wang, T. Ozawa, T. Tomonaga, D. Tsuruta, and K. Nakajima, "Phospho-ser727 triggers a multistep inactivation of stat3 by rapid dissociation of py705–sh2 through c-terminal tail modulation," *International immunology*, vol. 32, no. 2, pp. 73–88, 2020.

[158] M. L. Adams, D. L. Katz, and J. Grandpre, "Updated estimates of chronic conditions affecting risk for complications from coronavirus disease, united states," *Emerging infectious diseases*, vol. 26, no. 9, p. 2172, 2020.

[159] Y. Li, Q. Han, H. Zhao, Q. Guo, and J. Zhang, "Napabucasin reduces cancer stem cell characteristics in hepatocellular carcinoma," *Frontiers in pharmacology*, vol. 11, p. 597520, 2020.

[160] A. Bradshaw, A. Wickremsekera, S. T. Tan, L. Peng, P. F. Davis, and T. Itinteang, "Cancer stem cell hierarchy in glioblastoma multiforme," *Frontiers in surgery*, vol. 3, p. 21, 2016.

[161] J. Zhang, A. Zhang, Y. Wang, N. Liu, Y. You, C. Kang, and P. Pu, "New insights into the roles of ncrna in the stat3 pathway," *Future Oncology*, vol. 8, no. 6, pp. 723–730, 2012.

[162] M. S. Wake and C. J. Watson, "Stat 3 the oncogene–still eluding therapy?," *The FEBS journal*, vol. 282, no. 14, pp. 2600–2611, 2015.

[163] Y. Li, H. A. Rogoff, S. Keates, Y. Gao, S. Murikipudi, K. Mikule, D. Leggett, W. Li, A. B. Pardee, and C. J. Li, "Suppression of cancer relapse and metastasis by inhibiting cancer stemness," *Proceedings of the National Academy of Sciences*, vol. 112, no. 6, pp. 1839–1844, 2015.

[164] J. M. Hubbard and A. Grothey, "Napabucasin: an update on the first-in-class cancer stemness inhibitor," *Drugs*, vol. 77, no. 10, pp. 1091–1103, 2017.

[165] D. J. Jonker, L. Nott, T. Yoshino, S. Gill, J. Shapiro, A. Ohtsu, J. Zalcberg, M. M. Vickers, A. C. Wei, Y. Gao, *et al.*, "Napabucasin versus placebo in refractory advanced colorectal cancer: a randomised phase 3 trial," *The lancet Gastroenterology & hepatology*, vol. 3, no. 4, pp. 263–270, 2018.

[166] D. Zuo, K. L. Shogren, J. Zang, D. E. Jewison, B. E. Waletzki, A. L. Miller, S. H. Okuno, Z. Cai, M. J. Yaszemski, and A. Maran, "Inhibition of stat3 blocks protein synthesis and tumor metastasis in osteosarcoma cells," *Journal of Experimental & Clinical Cancer Research*, vol. 37, no. 1, pp. 1–11, 2018.

[167] F. Bray, J. Ferlay, I. Soerjomataram, R. L. Siegel, L. A. Torre, and A. Jemal, "Global cancer statistics 2018: Globocan estimates of incidence and mortality worldwide for 36 cancers in 185 countries," *CA: a cancer journal for clinicians*, vol. 68, no. 6, pp. 394–424, 2018.

[168] S. Yang, S. Wu, Y. Huang, Y. Shao, X. Y. Chen, L. Xian, J. Zheng, Y. Wen, X. Chen, and H. Li, "Screening for oesophageal cancer," *Cochrane Database of Systematic Reviews*, no. 12, 2012.

[169] G. Bjelakovic, D. Nikolova, R. G. Simonetti, and C. Gluud, "Antioxidant supplements for preventing gastrointestinal cancers," *Cochrane Database of Systematic Reviews*, no. 3, 2008.

[170] S. Linden, P. Sutton, N. Karlsson, V. Korolik, and M. McGuckin, "Mucins in the mucosal barrier to infection," *Mucosal immunology*, vol. 1, no. 3, pp. 183–197, 2008.

[171] L. S. Ostedgaard, T. O. Moninger, J. D. McMenimen, N. M. Sawin, C. P. Parker, I. M. Thornell, L. S. Powers, N. D. Gansemer, D. C. Bouzek, and D. P. Cook, "Gel-forming mucins form distinct morphologic structures in airways," *Proceedings of the National Academy of Sciences*, vol. 114, no. 26, pp. 6842–6847, 2017.

[172] S. Rachagani, M. P. Torres, N. Moniaux, and S. K. Batra, "Current status of mucins in the diagnosis and therapy of cancer," *Biofactors*, vol. 35, no. 6, pp. 509–527, 2009.

[173] M. S. Lan, S. K. Batra, W.-N. Qi, R. S. Metzgar, and M. Hollingsworth, "Cloning and sequencing of a human pancreatic tumor mucin cdna," *Journal of Biological Chemistry*, vol. 265, no. 25, pp. 15294–15299, 1990.

[174] M. Ligtenberg, H. Vos, A. Gennissen, and J. Hilkens, "Episialin, a carcinoma-associated mucin, is generated by a polymorphic gene encoding splice variants with alternative amino termini," *Journal of Biological Chemistry*, vol. 265, no. 10, pp. 5573–5578, 1990.

[175] J. Siddiqui, M. Abe, D. Hayes, E. Shani, E. Yunis, and D. Kufe, "Isolation and sequencing of a cdna coding for the human df3 breast carcinoma-associated antigen," *Proceedings of the National Academy of Sciences*, vol. 85, no. 7, pp. 2320–2323, 1988.

[176] S. J. Gendler and A. Spicer, "Epithelial mucin genes," *Annual review of physiology*, vol. 57, no. 1, pp. 607–634, 1995.

[177] S. J. Gendler, "Muc1, the renaissance molecule," *Journal of mammary gland biology and neoplasia*, vol. 6, no. 3, pp. 339–353, 2001.

[178] J.-F. Chang, H.-L. Zhao, J. Phillips, and G. Greenburg, "The epithelial mucin, muc1, is expressed on resting t lymphocytes and can function as a negative regulator of t cell activation," *Cellular immunology*, vol. 201, no. 2, pp. 83–88, 2000.

[179] R. H. Yolken, J. A. Peterson, S. L. Vonderfecht, E. T. Fouts, K. Midthun, and D. S. Newburg, "Human milk mucin inhibits rotavirus replication and prevents experimental gastroenteritis," *The Journal of clinical investigation*, vol. 90, no. 5, pp. 1984–1991, 1992.

[180] H. Schroten, F. Hanisch, R. Plogmann, J. Hacker, G. Uhlenbruck, R. Nobis-Bosch, and V. Wahn, "Inhibition of adhesion of s-fimbriated escherichia coli to buccal epithelial cells by human milk fat globule membrane components: a novel aspect of the protective function of mucins in the nonimmunoglobulin fraction," *Infection and immunity*, vol. 60, no. 7, pp. 2893–2899, 1992.

[181] A. Baruch, M.-l. Hartmann, M. Yoeli, Y. Adereth, S. Greenstein, Y. Stadler, Y. Skornik, J. Zaretsky, N. I. Smorodinsky, and I. Keydar, "The breast cancer-associated muc1 gene generates both a receptor and its cognate binding protein," *Cancer research*, vol. 59, no. 7, pp. 1552–1561, 1999.

[182] T. Stasyk and L. A. Huber, "Spatio-temporal parameters of endosomal signaling in cancer: Implications for new treatment options," *Journal of cellular biochemistry*, vol. 117, no. 4, pp. 836–843, 2016.

[183] S. Parry, H. S. Silverman, K. McDermott, A. Willis, M. A. Hollingsworth, and A. Harris, "Identification of muc1 proteolytic cleavage sites in vivo," *Biochemical and biophysical research communications*, vol. 283, no. 3, pp. 715–720, 2001.

[184] D. W. Kufe, "Muc1-c oncoprotein as a target in breast cancer: activation of signaling pathways and therapeutic approaches," *Oncogene*, vol. 32, no. 9, pp. 1073–1081, 2013.

[185] E. P. Bennett, U. Mandel, H. Clausen, T. A. Gerken, T. A. Fritz, and L. A. Tabak, "Control of mucin-type o-glycosylation: a classification of the polypeptide galnac-transferase gene family," *Glycobiology*, vol. 22, no. 6, pp. 736–756, 2012.

[186] M. Movahedin, T. M. Brooks, N. T. Supekar, N. Gokanapudi, G.-J. Boons, and C. L. Brooks, "Glycosylation of muc1 influences the binding of a therapeutic antibody by altering the conformational equilibrium of the antigen," *Glycobiology*, vol. 27, no. 7, pp. 677–687, 2017.

[187] T. Piyush, J. M. Rhodes, and L.-G. Yu, "Muc1 o-glycosylation contributes to anoikis resistance in epithelial cancer cells," *Cell Death Discovery*, vol. 3, no. 1, pp. 1–9, 2017.

[188] S. Parry, F. G. Hanisch, S.-H. Leir, M. Sutton-Smith, H. R. Morris, A. Dell, and A. Harris, "N-glycosylation of the muc1 mucin in epithelial cells and secretions," *Glycobiology*, vol. 16, no. 7, pp. 623–634, 2006.

[189] E. Tian and K. G. Ten Hagen, "Recent insights into the biological roles of mucin-type o-glycosylation," *Glycoconjugate journal*, vol. 26, no. 3, pp. 325–334, 2009.

[190] T. Ju, Y. Wang, R. P. Aryal, S. D. Lehoux, X. Ding, M. R. Kudelka, C. Cutler, J. Zeng, J. Wang, and X. Sun, "T n and sialyl-tn antigens, aberrant o-glycomics as human disease markers," *PROTEOMICS-Clinical Applications*, vol. 7, no. 9-10, pp. 618–631, 2013.

[191] H. Clausen and E. P. Bennett, "A family of udp-galnac: polypeptide n-acetylgalactosaminyl-transferases control the initiation of mucin-type o-linked glycosylation," *Glycobiology*, vol. 6, no. 6, pp. 635–646, 1996.

[192] I. Breloy and F.-G. Hanisch, "Functional roles of o-glycosylation," *Molecules*, vol. 23, no. 12, 2018.

[193] I. Brockhausen, "Mucin-type o-glycans in human colon and breast cancer: glycodynamics and functions," *EMBO reports*, vol. 7, no. 6, pp. 599–604, 2006.

[194] R. L. Hanson and M. A. Hollingsworth, "Functional consequences of differential o-glycosylation of muc1, muc4, and muc16 (downstream effects on signaling)," *Biomolecules*, vol. 6, no. 3, p. 34, 2016.

[195] E. Chandrasekaran, J. Xue, J. Xia, R. D. Locke, S. A. Patil, S. Neelamegham, and K. L. Matta, "Characterization of cancer associated mucin type o-glycans using the exchange sialylation properties of mammalian sialyltransferase st3gal-ii," *Journal of proteome research*, vol. 11, no. 4, pp. 2609–2618, 2012.

[196] E. Saeland, A. I. Belo, S. Mongera, I. van Die, G. A. Meijer, and Y. van Kooyk, "Differential glycosylation of muc1 and ceacam5 between normal mucosa and tumour tissue of colon cancer patients," *International journal of cancer*, vol. 131, no. 1, pp. 117–128, 2012.

[197] S. K. Ghosh, P. Pantazopoulos, Z. Medarova, and A. Moore, "Expression of underglycosylated muc1 antigen in cancerous and adjacent normal breast tissues," *Clinical breast cancer*, vol. 13, no. 2, pp. 109–118, 2013.

[198] J. Taylor-Papadimitriou, J. M. Burchell, R. Graham, and R. Beatson, "Latest developments in muc1 immunotherapy," *Biochemical Society Transactions*, vol. 46, no. 3, pp. 659–668, 2018.

[199] A. D. Posey Jr, R. D. Schwab, A. C. Boesteanu, C. Steentoft, U. Mandel, B. Engels, J. D. Stone, T. D. Madsen, K. Schreiber, and K. M. Haines, "Engineered car t cells targeting the cancer-associated tn-glycoform of the membrane mucin muc1 control adenocarcinoma," *Immunity*, vol. 44, no. 6, pp. 1444–1454, 2016.

[200] M. Pourjafar, P. Samadi, H. M. Khoshinani, and M. Saidijam, "Are mimotope vaccines a good alternative to monoclonal antibodies?," *Immunotherapy*, vol. 11, no. 9, pp. 795–800, 2019.

[201] S. K. Lau, L. M. Weiss, and P. G. Chu, "Differential expression of muc1, muc2, and muc5ac in carcinomas of various sites: an immunohistochemical study," *American journal of clinical pathology*, vol. 122, no. 1, pp. 61–69, 2004.

[202] Y. Zeng, Q. Zhang, Y. Zhang, M. Lu, Y. Liu, T. Zheng, S. Feng, M. Hao, and H. Shi, "Muc1 predicts colorectal cancer metastasis: a systematic review and meta-analysis of case controlled studies," *PloS one*, vol. 10, no. 9, p. e0138049, 2015.

[203] N. Agata, R. Ahmad, T. Kawano, D. Raina, S. Kharbanda, and D. Kufe, "Muc1 oncoprotein blocks death receptorâmediated apoptosis by inhibiting recruitment of caspase-8," *Cancer research*, vol. 68, no. 15, pp. 6136–6144, 2008.

[204] L. Yin, M. Kosugi, and D. Kufe, "Inhibition of the muc1-c oncoprotein induces multiple myeloma cell death by down-regulating tigar expression and depleting nadph," *Blood, The Journal of the American Society of Hematology*, vol. 119, no. 3, pp. 810–816, 2012.

[205] M. Pochampalli, R. El Bejjani, and J. Schroeder, "Muc1 is a novel regulator of erbb1 receptor trafficking," *Oncogene*, vol. 26, no. 12, pp. 1693–1701, 2007.

[206] X. Liu, T. Caffrey, M. Steele, A. Mohr, P. Singh, P. Radhakrishnan, D. L. Kelly, Y. Wen, and M. A. Hollingsworth, "Muc1 regulates cyclin d1 gene expression through p120 catenin and $\beta$-catenin," *Oncogenesis*, vol. 3, no. 6, pp. e107–e107, 2014.

[207] X. Wei, H. Xu, and D. Kufe, "Human mucin 1 oncoprotein represses transcription of the p53 tumor suppressor gene," *Cancer research*, vol. 67, no. 4, pp. 1853–1858, 2007.

[208] L. Yin, L. Huang, and D. Kufe, "Muc1 oncoprotein activates the foxo3a transcription factor in a survival response to oxidative stress," *Journal of Biological Chemistry*, vol. 279, no. 44, pp. 45721–45727, 2004.

[209] J. Ren, A. Bharti, D. Raina, W. Chen, R. Ahmad, and D. Kufe, "Muc1 oncoprotein is targeted to mitochondria by heregulin-induced activation of c-src and the molecular chaperone hsp90," *Oncogene*, vol. 25, no. 1, pp. 20–31, 2006.

[210] S. Satoh, Y. Hinoda, T. Hayashi, M. D. Burdick, K. Imai, and M. A. Hollingsworth, "Enhancement of metastatic properties of pancreatic cancer cells by muc1 gene encoding an antiâadhesion molecule," *International journal of cancer*, vol. 88, no. 4, pp. 507–518, 2000.

[211] L. H. Regimbald, L. M. Pilarski, B. M. Longenecker, M. A. Reddish, G. Zimmermann, and J. C. Hugh, "The breast mucin muc1 as a novel adhesion ligand for endothelial intercellular adhesion molecule 1 in breast cancer," *Cancer research*, vol. 56, no. 18, pp. 4244–4249, 1996.

[212] P. K. Singh, Y. Wen, B. J. Swanson, K. Shanmugam, A. Kazlauskas, R. L. Cerny, S. J. Gendler, and M. A. Hollingsworth, "Platelet-derived growth factor receptor $\beta$-mediated phosphorylation of muc1 enhances invasiveness in pancreatic adenocarcinoma cells," *Cancer research*, vol. 67, no. 11, pp. 5201–5210, 2007.

[213] M. Bose, P. Grover, A. J. Sanders, R. Zhou, M. Ahmad, S. Shwartz, P. Lala, S. Nath, M. Yazdanifar, and C. Brouwer, "Overexpression of muc1 induces non-canonical tgf-$\beta$ signaling in pancreatic ductal adenocarcinoma," *Frontiers in cell and developmental biology*, p. 39, 2022.

[214] Q. Wang, J. Li, W. Wu, R. Shen, H. Jiang, Y. Qian, Y. Tang, T. Bai, S. Wu, and L. Wei, "Smad4-dependent suppressor pituitary homeobox 2 promotes ppp2r2a-mediated inhibition of akt pathway in pancreatic cancer," *Oncotarget*, vol. 7, no. 10, p. 11208, 2016.

[215] A. M. Scott, J. P. Allison, and J. D. Wolchok, "Monoclonal antibodies in cancer therapy," *Cancer Immunity Archive*, vol. 12, no. 1, 2012.

[216] L. M. Weiner, J. C. Murray, and C. W. Shuptrine, "Antibody-based immunotherapy of cancer," *Cell*, vol. 148, no. 6, pp. 1081–1084, 2012.

[217] J. Redman, E. Hill, D. AlDeghaither, and L. Weiner, "Mechanisms of action of therapeutic antibodies for cancer," *Molecular immunology*, vol. 67, no. 2, pp. 28–45, 2015.

[218] C. W. Shuptrine, R. Surana, and L. M. Weiner, "Monoclonal antibodies for the treatment of cancer," in *Seminars in cancer biology*, vol. 22, pp. 3–13, Elsevier.

[219] P. Samadi, S. Saki, F. K. Dermani, M. Pourjafar, and M. Saidijam, "Emerging ways to treat breast cancer: will promises be met?," *Cellular Oncology*, vol. 41, no. 6, pp. 605–621, 2018.

[220] M. Doi, A. Yokoyama, K. Kondo, H. Ohnishi, N. Ishikawa, N. Hattori, and N. Kohno, "Anti-tumor effect of the anti-klâ6/muc1 monoclonal antibody through exposure of surface molecules by muc1 capping," *Cancer science*, vol. 97, no. 5, pp. 420–429, 2006.

[221] N. Ohyabu, H. Hinou, T. Matsushita, R. Izumi, H. Shimizu, K. Kawamoto, Y. Numata, H. Togame, H. Takemoto, and H. Kondo, "An essential epitope of anti-muc1 monoclonal antibody kl-6 revealed by focused glycopeptide library," *Journal of the American Chemical Society*, vol. 131, no. 47, pp. 17102–17109, 2009.

[222] M. Namba, N. Hattori, H. Hamada, K. Yamaguchi, Y. Okamoto, T. Nakashima, T. Masuda, S. Sakamoto, Y. Horimasu, and S. Miyamoto, "Anti-kl-6/muc1 monoclonal antibody reverses resistance to trastuzumab-mediated antibody-dependent cell-mediated cytotoxicity by capping muc1," *Cancer letters*, vol. 442, pp. 31–39, 2019.

[223] M. Yamamoto, V. Bhavanandan, S. Nakamori, and T. Irimura, "A novel monoclonal antibody specific for sialylated muc1 mucin," *Japanese journal of cancer research*, vol. 87, no. 5, pp. 488–496, 1996.

[224] H. Suzuki, J. Shoda, T. Kawamoto, E. Shinozaki, N. Miyahara, S. Hotta, Y. Iizuka, A. Nakahara, N. Tanaka, and A. Yanaka, "Expression of muc1 recognized by monoclonal antibody my. 1e12 is a useful biomarker for tumor aggressiveness of advanced colon carcinoma," *Clinical experimental metastasis*, vol. 21, no. 4, pp. 321–329, 2004.

[225] Y. Yoshimura, K. Denda-Nagai, Y. Takahashi, I. Nagashima, H. Shimizu, T. Kishimoto, M. Noji, S. Shichino, Y. Chiba, and T. Irimura, "Products of chemoenzymatic synthesis representing muc1 tandem repeat unit with t-, st- or stn-antigen revealed distinct specificities of anti-muc1 antibodies," *Scientific reports*, vol. 9, no. 1, pp. 1–12, 2019.

[226] N. Muguruma and S. Ito, "Labeled anti-mucin antibody detectable by infrared-fluorescence endoscopy," *Cancer Biomarkers*, vol. 4, no. 6, pp. 321–328, 2008.

[227] M. A. Tarp, A. L. SÃžrensen, U. Mandel, H. Paulsen, J. Burchell, J. Taylor-Papadimitriou, and H. Clausen, "Identification of a novel cancer-specific immunodominant glycopeptide epitope in the muc1 tandem repeat," *Glycobiology*, vol. 17, no. 2, pp. 197–209, 2007.

[228] G. Wu, S. Maharjan, D. Kim, J. N. Kim, B. K. Park, H. Koh, K. Moon, Y. Lee, and H.-J. Kwon, "A novel monoclonal antibody targets mucin1 and attenuates growth in pancreatic cancer model," *International journal of molecular sciences*, vol. 19, no. 7, p. 2004, 2018.

[229] G. Wu, D. Kim, J. N. Kim, S. Park, S. Maharjan, H. Koh, K. Moon, Y. Lee, and H.-J. Kwon, "A mucin1 c-terminal subunit-directed monoclonal antibody targets overexpressed mucin1 in breast cancer," *Theranostics*, vol. 8, no. 1, p. 78, 2018.

[230] P. Mukherjee, C. S. Madsen, A. R. Ginardi, T. L. Tinder, F. Jacobs, J. Parker, B. Agrawal, B. M. Longenecker, and S. J. Gendler, "Mucin 1-specific immunotherapy in a mouse model of spontaneous breast cancer," *Journal of immunotherapy*, vol. 26, no. 1, pp. 47–62, 2003.

[231] D. Drèau, L. J. Moore, M. Wu, L. D. Roy, L. Dillion, T. Porter, R. Puri, N. Momin, K. D. Wittrup, and P. Mukherjee, "Combining the specific anti-muc1 antibody tab004 and lip-msa-il-2 limits pancreatic cancer progression in immune competent murine models of pancreatic ductal adenocarcinoma," *Frontiers in oncology*, p. 330, 2019.

[232] L. J. Moore, L. D. Roy, R. Zhou, P. Grover, S.-t. Wu, J. M. Curry, L. M. Dillon, P. M. Puri, M. Yazdanifar, and R. Puri, "Antibody-guided in vivo imaging for early detection of mammary gland tumors," *Translational Oncology*, vol. 9, no. 4, pp. 295–305, 2016.

[233] M. Bose and P. Mukherjee, "Role of microbiome in modulating immune responses in cancer," *Mediators of Inflammation*, vol. 2019, 2019.

[234] M. Yazdanifar, R. Zhou, P. Grover, C. Williams, M. Bose, L. J. Moore, S.-t. Wu, J. Maher, D. Drèau, and P. Mukherjee, "Overcoming immunological resistance enhances the efficacy of a novel anti-tmuc1-car t cell treatment against pancreatic ductal adenocarcinoma," *Cells*, vol. 8, no. 9, p. 1070, 2019.

[235] M. Bose and P. Mukherjee, "A novel antibody blocks anti-apoptotic activity of muc1 in pancreatic cancer cell lines," *Cancer Research*, vol. 79, no. 13_Supplement, pp. 2052–2052, 2019.

[236] J. A. Calvete, D. R. Newell, A. F. Wright, and M. S. Rose, "In vitro and in vivo antitumor activity of zeneca zd0490, a recombinant ricin a-chain immunotoxin for the treatment of colorectal cancer," *Cancer research*, vol. 54, no. 17, pp. 4684–4690, 1994.

[237] D. Baeckström, G. C. Hansson, O. Nilsson, C. Johansson, S. J. Gendler, and L. Lindholm, "Purification and characterization of a membrane-bound and a secreted mucin-type glycoprotein carrying the carcinoma-associated sialyl-lea epitope on distinct core proteins," *Journal of Biological Chemistry*, vol. 266, no. 32, pp. 21537–21547, 1991.

[238] A. W. Tolcher, L. Ochoa, L. A. Hammond, A. Patnaik, T. Edwards, C. Takimoto, L. Smith, J. de Bono, G. Schwartz, and T. Mays, "Cantuzumab mertansine, a maytansinoid immunoconjugate directed to the canag antigen: a phase i, pharmacokinetic, and biologic correlative study," *Journal of clinical oncology*, vol. 21, no. 2, pp. 211–222, 2003.

[239] N. K. Ibrahim, K. O. Yariz, I. Bondarenko, A. Manikhas, V. Semiglazov, A. Alyasova, V. Komisarenko, Y. Shparyk, J. L. Murray, and D. Jones, "Randomized phase ii trial of letrozole plus anti-muc1 antibody as1402 in hormone receptorâpositive locally advanced or metastatic breast cancer," *Clinical Cancer Research*, vol. 17, no. 21, pp. 6822–6830, 2011.

[240] I. Corraliza-Gorjòn, B. Somovilla-Crespo, S. Santamaria, J. A. Garcia-Sanz, and L. Kremer, "New strategies using antibody combinations to increase cancer treatment effectiveness," *Frontiers in Immunology*, vol. 8, p. 1804, 2017.

[241] N. K. Venepalli, C. C. Gandhi, H. Ozer, D. Ho, Y. Lu, H. Xie, S. A. Berg, R. A. Chowdhery, M. A. Gargano, A. H. Braun, *et al.*, "Phase ib study of pgg beta glucan in combination with anti-muc1 antibody (bth1704) and gemcitabine for the treatment of advanced pancreatic cancer.," 2015.

[242] D. V. Gold, Z. Karanjawala, D. E. Modrak, D. M. Goldenberg, and R. H. Hruban, "Pam4-reactive muc1 is a biomarker for early pancreatic adenocarcinoma," *Clinical cancer research*, vol. 13, no. 24, pp. 7380–7387, 2007.

[243] T. M. Cardillo, Z. Ying, and D. V. Gold, "Therapeutic advantage of 90yttrium-versus 131iodine-labeled pam4 antibody in experimental pancreatic cancer," *Clinical cancer research*, vol. 7, no. 10, pp. 3186–3192, 2001.

[244] D. V. Gold, G. Newsome, D. Liu, and D. M. Goldenberg, "Mapping pam4 (clivatuzumab), a monoclonal antibody in clinical trials for early detection and therapy of pancreatic ductal adenocarcinoma, to muc5ac mucin," *Molecular cancer*, vol. 12, no. 1, p. 143, 2013.

[245] D. V. Gold, T. Cardillo, Y. Vardi, and R. Blumenthal, "Radioimmunotherapy of experimental pancreatic cancer with 131iâlabeled monoclonal antibody pam4," *International journal of cancer*, vol. 71, no. 4, pp. 660–667, 1997.

[246] D. V. Gold, T. Cardillo, D. M. Goldenberg, and R. M. Sharkey, "Localization of pancreatic cancer with radiolabeled monoclonal antibody pam4," *Critical reviews in oncology/hematology*, vol. 39, no. 1-2, pp. 147–154, 2001.

[247] S. Gulec, K. Pennington, D. Bruetman, S. Garl, H. Horne, D. Gold, W. Wegener, and D. Goldenberg, "A phase-i study of 90y-hpam4 (humanized anti-muc1 monoclonal antibody) in patients with unresectable and metastatic pancreatic cancer," *Journal of Nuclear Medicine*, vol. 48, no. supplement 2, pp. 393P–393P, 2007.

[248] V. J. Picozzi, R. K. Ramanathan, M. A. Lowery, A. J. Ocean, E. P. Mitchel, B. H. ONeil, M. J. Guarino, P. R. Conkling, S. J. Cohen, and N. Bahary, "90y-clivatuzumab tetraxetan with or without low-dose gemcitabine: A phase ib study in patients with metastatic pancreatic cancer after two or more prior therapies," *European Journal of Cancer*, vol. 51, no. 14, pp. 1857–1864, 2015.

[249] A. Hisatsune, H. Nakayama, M. Kawasaki, I. Horie, T. Miyata, Y. Isohama, K. C. Kim, and H. Katsuki, "Anti-muc1 antibody inhibits egf receptor signaling in cancer cells," *Biochemical and biophysical research communications*, vol. 405, no. 3, pp. 377–381, 2011.

[250] M. A. Hollingsworth and B. J. Swanson, "Mucins in cancer: protection and control of the cell surface," *Nature Reviews Cancer*, vol. 4, no. 1, pp. 45–60, 2004.

[251] J. L. Vivero-Escoto, L. M. Jeffords, D. Dréau, M. Alvarez-Berrios, and P. Mukherjee, "Mucin1 antibody-conjugated dye-doped mesoporous silica nanoparticles for breast cancer detection in vivo," in *Colloidal Nanoparticles for Biomedical Applications XII*, vol. 10078, p. 100780B, International Society for Optics and Photonics.

[252] V. J. Kelly, S.-T. Wu, V. Gottumukkala, R. Coelho, K. Palmer, S. Nair, T. Erick, R. Puri, O. Ilovich, and P. Mukherjee, "Preclinical evaluation of an 111in/225ac theranostic targeting transformed muc1 for triple negative breast cancer," *Theranostics*, vol. 10, no. 15, p. 6946, 2020.

[253] S. Yonezawa, S. Kitajima, M. Higashi, M. Osako, M. Horinouchi, S. Yokoyama, S. Kitamoto, N. Yamada, Y. Tamura, and T. Shimizu, "A novel anti-muc1 antibody against the muc1 cytoplasmic tail domain: use in sensitive identification of

poorly differentiated cells in adenocarcinoma of the stomach," *Gastric Cancer*, vol. 15, no. 4, pp. 370–381, 2012.

[254] D. Dian, W. Janni, C. Kuhn, D. Mayr, U. Karsten, I. Mylonas, K. Friese, and U. Jeschke, "Evaluation of a novel anti-mucin 1 (muc1) antibody (pankomab) as a potential diagnostic tool in human ductal breast cancer; comparison with two established antibodies," *Oncology Research and Treatment*, vol. 32, no. 5, pp. 238–244, 2009.

[255] A. Danielczyk, R. Stahn, D. Faulstich, A. Löffler, A. Märten, U. Karsten, and S. Goletz, "Pankomab: a potent new generation anti-tumour muc1 antibody," *Cancer Immunology, Immunotherapy*, vol. 55, no. 11, pp. 1337–1347, 2006.

[256] W. Fiedler, S. DeDosso, S. Cresta, J. Weidmann, A. Tessari, M. Salzberg, B. Dietrich, H. Baumeister, S. Goletz, and L. Gianni, "A phase i study of pankomab-gex, a humanised glyco-optimised monoclonal antibody to a novel tumour-specific muc1 glycopeptide epitope in patients with advanced carcinomas," *European Journal of Cancer*, vol. 63, pp. 55–63, 2016.

[257] J. Ledermann, J. Sehouli, B. Zurawski, F. Raspagliesi, U. De Giorgi, S. Banerjee, J. Arranz Arija, M. Romeo Marin, A. Lisyanskaya, and R. Póka, "Lba41a double-blind, placebo-controlled, randomized, phase 2 study to evaluate the efficacy and safety of switch maintenance therapy with the anti-ta-muc1 antibody pankomab-gex after chemotherapy in patients with recurrent epithelial ovarian carcinoma," *Annals of Oncology*, vol. 28, no. suppl 5, 2017.

[258] W. Qi, B. C. Schultes, D. Liu, M. Kuzma, W. Decker, and R. Madiyalakan, "Characterization of an anti-muc1 monoclonal antibody with potential as a cancer vaccine," *Hybridoma and hybridomics*, vol. 20, no. 5-6, pp. 313–324, 2001.

[259] J. De Bono, S. Y. Rha, J. Stephenson, B. Schultes, P. Monroe, G. Eckhardt, L. Hammond, T. Whiteside, C. Nicodemus, and J. Cermak, "Phase i trial of a murine antibody to muc1 in patients with metastatic cancer: evidence for the activation of humoral and cellular antitumor immunity," *Annals of Oncology*, vol. 15, no. 12, pp. 1825–1833, 2004.

[260] K. Mehla, J. Tremayne, J. A. Grunkemeyer, K. A. O Connell, M. M. Steele, T. C. Caffrey, X. Zhu, F. Yu, P. K. Singh, and B. C. Schultes, "Combination of mab-ar20. 5, anti-pd-l1 and polyiclc inhibits tumor progression and prolongs survival of muc1. tg mice challenged with pancreatic tumors," *Cancer Immunology, Immunotherapy*, vol. 67, no. 3, pp. 445–457, 2018.

[261] K. P. Kearse, N. L. Smith, D. A. Semer, L. Eagles, J. L. Finley, S. Kazmierczak, C. J. Kovacs, A. A. Rodriguez, and A. E. Kellogg-Wennerberg, "Monoclonal antibody ds6 detects a tumor-associated sialoglycotope expressed on human serous ovarian carcinomas," *International journal of cancer*, vol. 88, no. 6, pp. 866–872, 2000.

[262] M. Trombe, A. Caron, A. Tellier, C. Carrez, S. Guérif, S. Clavier, N. Karst, J. Saarinen, T. Satomaa, V. Pitkänen, *et al.*, "Preclinical activity of an antibody drug conjugate targeting tumor specificmuc1 structural peptide-glycotope," *Cancer Research*, vol. 79, no. 13_Supplement, pp. 235–235, 2019.

[263] C. A. Gomez-Roca, V. Boni, V. Moreno, J. C. Morris, J.-P. Delord, E. Calvo, K. P. Papadopoulos, O. Rixe, P. Cohen, A. Tellier, S. Ziti-Ljajic, and A. W. Tolcher, "A phase i study of sar566658, an anti ca6-antibody drug conjugate (adc), in patients (pts) with ca6-positive advanced solid tumors (sts)(nct01156870).," *Journal of Clinical Oncology*, vol. 34, no. 15_suppl, pp. 2511–2511, 2016.

[264] J. Rodon, M. Garrison, L. A. Hammond, J. De Bono, L. Smith, L. Forero, D. Hao, C. Takimoto, J. M. Lambert, and L. Pandite, "Cantuzumab mertansine in a three-times a week schedule: a phase i and pharmacokinetic study," *Cancer chemotherapy and pharmacology*, vol. 62, no. 5, pp. 911–919, 2008.

[265] M. Mita, A. Ricart, A. Mita, A. Patnaik, J. Sarantopoulos, K. Sankhala, R. Fram, A. Qin, J. Watermill, and A. Tolcher, "A phase i study of a canag-targeted immunoconjugate, huc242-dm4, in patients with can ag-expressing solid tumors," *Journal of clinical oncology*, vol. 25, no. 18 suppl, pp. 3062–3062, 2007.

[266] L. Goff, K. Papadopoulos, J. Posey, A. Phan, A. Patnaik, J. Miller, S. Zildjian, J. O'Leary, A. Qin, and A. Tolcher, "A phase ii study of imgn242 (huc242-dm4) in patients with canag-positive gastric or gastroesophageal (ge) junction cancer," *Journal of Clinical Oncology*, vol. 27, no. 15 suppl, pp. e15625–e15625, 2009.

[267] B. St. Croix, C. Sheehan, J. W. Rak, V. A. Flørenes, J. M. Slingerland, and R. S. Kerbel, "E-cadherinâdependent growth suppression is mediated by the cyclin-dependent kinase inhibitor p27kip1," *The Journal of cell biology*, vol. 142, no. 2, pp. 557–571, 1998.

[268] K. Matsumura, I. Niki, H. Tian, M. Takuma, N. Hongo, S. Matsumoto, and H. Mori, "Radioimmunoscintigraphy of pancreatic cancer in tumor-bearing athymic nude mice using 99m technetium-labeled anti-kl-6/muc1 antibody," *Radiation medicine*, vol. 26, no. 3, pp. 133–139, 2008.

[269] Y. Li, C. Zhou, J. Li, J. Liu, L. Lin, L. Li, D. Cao, Q. Li, and Z. Wang, "Single domain based bispecific antibody, muc1-bi-1, and its humanized form, muc1-bi-2, induce potent cancer cell killing in muc1 positive tumor cells," *PloS one*, vol. 13, no. 1, p. e0191024, 2018.

[270] H. Kodama, M. Suzuki, Y. Katayose, M. Shinoda, N. Sakurai, S.-i. Takemura, H. Yoshida, H. Saeki, R. Asano, and M. Ichiyama, "Specific and effective targeting cancer immunotherapy with a combination of three bispecific antibodies," *Immunology letters*, vol. 81, no. 2, pp. 99–106, 2002.

[271] Y. Hinoda, N. Nakagawa, Y. Ohe, H. Kakiuchi, M. Tsujisaki, K. Imai, and A. Yachi, "Recognition of the polypeptide core of mucin by monoclonal antibody muse11 against an adenocarcinomaâassociated antigen," *Japanese journal of cancer research*, vol. 81, no. 12, pp. 1206–1209, 1990.

[272] Y. Katayose, T. Kudo, M. Suzuki, M. Shinoda, S. Saijyo, N. Sakurai, H. Saeki, K. Fukuhara, K. Imai, and S. Matsuno, "Muc1-specific targeting immunotherapy with bispecific antibodies: inhibition of xenografted human bile duct carcinoma growth," *Cancer research*, vol. 56, no. 18, pp. 4205–4212, 1996.

[273] S.-i. Takemura, R. Asano, K. Tsumoto, S. Ebara, N. Sakurai, Y. Katayose, H. Kodama, H. Yoshida, M. Suzuki, and K. Imai, "Construction of a diabody (small recombinant bispecific antibody) using a refolding system," *Protein Engineering*, vol. 13, no. 8, pp. 583–588, 2000.

[274] S.-i. Takemura, T. Kudo, R. Asano, M. Suzuki, K. Tsumoto, N. Sakurai, Y. Katayose, H. Kodama, H. Yoshida, and S. Ebara, "A mutated superantigen sea d227a fusion diabody specific to muc1 and cd3 in targeted cancer immunotherapy for bile duct carcinoma," *Cancer Immunology, Immunotherapy*, vol. 51, no. 1, pp. 33–44, 2002.

[275] J. Schuhmacher, G. Klivényi, S. Kaul, M. Henze, R. Matys, H. Hauser, and J. Clorius, "Pretargeting of human mammary carcinoma xenografts with bispecific anti-muc1/anti-ga chelate antibodies and immunoscintigraphy with pet," *Nuclear medicine and biology*, vol. 28, no. 7, pp. 821–828, 2001.

[276] K. Runcie, D. R. Budman, V. John, and N. Seetharamu, "Bi-specific and tri-specific antibodies-the next big thing in solid tumor therapeutics," *Molecular Medicine*, vol. 24, no. 1, p. 50, 2018.

[277] T. King and A. Posey, "Co-expression of an engineered cell-surface sialidase by cart cells improves anti-cancer activity of nk cells in solid tumors," *Cytotherapy*, vol. 21, no. 5, p. S27, 2019.

[278] C. L. Brooks, A. Schietinger, S. N. Borisova, P. Kufer, M. Okon, T. Hirama, C. R. MacKenzie, L.-X. Wang, H. Schreiber, and S. V. Evans, "Antibody recognition of a unique tumor-specific glycopeptide antigen," *Proceedings of the National Academy of Sciences*, vol. 107, no. 22, pp. 10056–10061, 2010.

[279] A. Borgert, J. Heimburg-Molinaro, X. Song, Y. Lasanajak, T. Ju, M. Liu, P. Thompson, G. Ragupathi, G. Barany, and D. F. Smith, "Deciphering structural elements of mucin glycoprotein recognition," *ACS chemical biology*, vol. 7, no. 6, pp. 1031–1039, 2012.

[280] G. F. Springer, "Immunoreactive t and tn epitopes in cancer diagnosis, prognosis, and immunotherapy," *Journal of molecular medicine*, vol. 75, no. 8, pp. 594–602, 1997.

[281] M. R. Kudelka, T. Ju, J. Heimburg-Molinaro, and R. D. Cummings, *Simple sugars to complex diseaseâmucin-type O-glycans in cancer*, vol. 126, pp. 53–135. Elsevier, 2015.

[282] U. Karsten, N. Serttas, H. Paulsen, A. Danielczyk, and S. Goletz, "Binding patterns of dtr-specific antibodies reveal a glycosylation-conditioned tumor-specific epitope of the epithelial mucin (muc1)," *Glycobiology*, vol. 14, no. 8, pp. 681–692, 2004.

[283] T. Matsushita, W. Takada, K. Igarashi, K. Naruchi, R. Miyoshi, F. Garcia-Martin, M. Amano, H. Hinou, and S.-I. Nishimura, "A straightforward protocol for the preparation of high performance microarray displaying synthetic muc1 glycopeptides," *Biochimica et Biophysica Acta (BBA)-General Subjects*, vol. 1840, no. 3, pp. 1105–1116, 2014.

[284] S. Rangappa, G. Artigas, R. Miyoshi, Y. Yokoi, S. Hayakawa, F. Garcia-Martin, H. Hinou, and S.-I. Nishimura, "Effects of the multiple o-glycosylation states on antibody recognition of the immunodominant motif in muc1 extracellular tandem repeats," *MedChemComm*, vol. 7, no. 6, pp. 1102–1122, 2016.

[285] N. Martínez-Sáez, J. Castro-López, J. Valero-González, D. Madariaga, I. Compañón, V. J. Somovilla, M. Salvadó, J. L. Asensio, J. Jiménez-Barbero, A. Avenoza, *et al.*, "Deciphering the non-equivalence of serine and threonine o-glycosylation points: implications for molecular recognition of the tn antigen by an anti-muc1 antibody," *Angewandte Chemie International Edition*, vol. 54, no. 34, pp. 9830–9834, 2015.

[286] H. Wakui, Y. Tanaka, T. Ose, I. Matsumoto, K. Kato, Y. Min, T. Tachibana, M. Sato, K. Naruchi, and F. G. Martin, "A straightforward approach to antibodies recognising cancer specific glycopeptidic neoepitopes," *Chemical Science*, vol. 11, no. 19, pp. 4999–5006, 2020.

[287] H. Thie, L. Toleikis, J. Li, R. von Wasielewski, G. Bastert, T. Schirrmann, I. T. Esteves, C. K. Behrens, B. Fournes, and N. Fournier, "Rise and fall of an anti-muc1 specific antibody," *PLoS One*, vol. 6, no. 1, p. e15921, 2011.

[288] M. Moreno, H. J. Bontkes, R. J. Scheper, P. Kenemans, R. H. Verheijen, and S. von Mensdorff-Pouilly, "High level of muc1 in serum of ovarian and breast cancer patients inhibits huhmfg-1 dependent cell-mediated cytotoxicity (adcc)," *Cancer letters*, vol. 257, no. 1, pp. 47–55, 2007.

[289] Y. Tang, X. Cui, H. Xiao, S. Qi, X. Hu, Q. Yu, G. Shi, X. Zhang, J. Gu, and Y. Yu, "Binding of circulating anti-muc1 antibody and serum muc1 antigen in stage iv breast cancer," *Molecular Medicine Reports*, vol. 15, no. 5, pp. 2659–2664, 2017.

[290] S. P. Treon, P. Maimonis, D. Bua, G. Young, N. Raje, J. Mollick, D. Chauhan, Y.-T. Tai, T. Hideshima, and Y. Shima, "Elevated soluble muc1 levels and

decreased anti-muc1 antibody levels in patients with multiple myeloma," *Blood, The Journal of the American Society of Hematology*, vol. 96, no. 9, pp. 3147–3153, 2000.

[291] S. J. Storr, L. Royle, C. J. Chapman, U. M. A. Hamid, J. F. Robertson, A. Murray, R. A. Dwek, and P. M. Rudd, "The o-linked glycosylation of secretory/shed muc1 from an advanced breast cancer patient's serum," *Glycobiology*, vol. 18, no. 6, pp. 456–462, 2008.

[292] M. Pegram, V. Borges, J. Fuloria, N. Ibrahim, C. Shapiro, E. Perez, K. Wang, F. Schaedeli Stark, C. Yeon, and N. Courtenay-Luck, "Phase i pharmacokinetics (pk) of humanized anti-muc-1 antibody r1550," *Journal of Clinical Oncology*, vol. 24, no. 18 suppl, pp. 2533–2533, 2006.

[293] D. Zhou, L. Xu, W. Huang, and T. Tonn, "Epitopes of muc1 tandem repeats in cancer as revealed by antibody crystallography: toward glycopeptide signature-guided therapy," *Molecules*, vol. 23, no. 6, p. 1326, 2018.

[294] A. L. Sørensen, C. A. Reis, M. A. Tarp, U. Mandel, K. Ramachandran, V. Sankaranarayanan, T. Schwientek, R. Graham, J. Taylor-Papadimitriou, and M. A. Hollingsworth, "Chemoenzymatically synthesized multimeric tn/stn muc1 glycopeptides elicit cancer-specific anti-muc1 antibody responses and override tolerance," *Glycobiology*, vol. 16, no. 2, pp. 96–107, 2006.

[295] G. Rivalland, B. Loveland, and P. Mitchell, "Update on mucin-1 immunotherapy in cancer: a clinical perspective," *Expert Opinion on Biological Therapy*, vol. 15, no. 12, pp. 1773–1787, 2015.

[296] M. A. McGuckin, T. G. Hurst, and B. G. Ward, "Heterogeneity in production, secretion and glycosylation of muc1 epithelial mucin by primary cultures of ovarian carcinoma," *International journal of cancer*, vol. 63, no. 3, pp. 412–418, 1995.

[297] M. D. Walsh, S. M. Luckie, M. C. Cummings, T. M. Antalis, and M. A. McGuckin, "Heterogeneity of muc1 expression by human breast carcinoma cell lines in vivo and in vitro," *Breast cancer research and treatment*, vol. 58, no. 3, pp. 253–264, 1999.

[298] Q. Zhao, T. Piyush, C. Chen, M. A. Hollingsworth, J. Hilkens, J. M. Rhodes, and L.-G. Yu, "Muc1 extracellular domain confers resistance of epithelial cancer cells to anoikis," *Cell death  disease*, vol. 5, no. 10, pp. e1438–e1438, 2014.

[299] E. Pichinuk, I. Benhar, O. Jacobi, M. Chalik, L. Weiss, R. Ziv, C. Sympson, A. Karwa, N. I. Smorodinsky, and D. B. Rubinstein, "Antibody targeting of cell-bound muc1 sea domain kills tumor cells," *Cancer research*, vol. 72, no. 13, pp. 3324–3336, 2012.

[300] C. B. Madsen, H. H. Wandall, and A. E. Pedersen, "Potential for novel muc1 glycopeptide-specific antibody in passive cancer immunotherapy," *Immunopharmacology and immunotoxicology*, vol. 35, no. 6, pp. 649–652, 2013.

[301] R. M. Reilly, J. Sandhu, T. M. Alvarez-Diez, S. Gallinger, J. Kirsh, and H. Stern, "Problems of delivery of monoclonal antibodies," *Clinical pharmacokinetics*, vol. 28, no. 2, pp. 126–142, 1995.

[302] M. B. Sonbol, D. H. Ahn, D. Goldstein, T. Okusaka, J. Tabernero, T. Macarulla, M. Reni, C.-P. Li, B. O'Neil, and E. Van Cutsem, "Canstem111p trial: a phase iii study of napabucasin plus nab-paclitaxel with gemcitabine," *Future Oncology*, vol. 15, no. 12, pp. 1295–1302, 2019.

[303] M. Bose, A. Vora, T. Colleton, and P. Mukherjee, "Abstract 1837: MUC1 confers sensitivity to STAT-3 inhibitor napabucasin in pancreatic ductal adenocarcinoma cells," *Cancer Research*, vol. 80, pp. 1837–1837, 08 2020.

[304] X. Guan, "Cancer metastases: challenges and opportunities," *Acta pharmaceutica sinica B*, vol. 5, no. 5, pp. 402–418, 2015.

[305] F. O. Adeshakin, A. O. Adeshakin, L. O. Afolabi, D. Yan, G. Zhang, and X. Wan, "Mechanisms modulating anoikis resistance in cancer and the relevance of metabolic reprogramming," *Frontiers in Oncology*, vol. 11, p. 528, 2021.

[306] M. C. Guadamillas, A. Cerezo, and M. A. Del Pozo, "Overcoming anoikisâpathways to anchorage-independent growth in cancer," *Journal of cell science*, vol. 124, no. 19, pp. 3189–3197, 2011.

[307] M. Taddei, E. Giannoni, T. Fiaschi, and P. Chiarugi, "Anoikis: an emerging hallmark in health and diseases," *The Journal of pathology*, vol. 226, no. 2, pp. 380–393, 2012.

[308] C. D. Simpson, K. Anyiwe, and A. D. Schimmer, "Anoikis resistance and tumor metastasis," *Cancer letters*, vol. 272, no. 2, pp. 177–185, 2008.

[309] T. Uekita, M. Tanaka, M. Takigahira, Y. Miyazawa, Y. Nakanishi, Y. Kanai, K. Yanagihara, and R. Sakai, "Cub-domain-containing protein 1 regulates peritoneal dissemination of gastric scirrhous carcinoma," *The American journal of pathology*, vol. 172, no. 6, pp. 1729–1739, 2008.

[310] S. J. Strauss, T. Ng, A. Mendoza-Naranjo, J. Whelan, and P. H. Sorensen, "Understanding micrometastatic disease and anoikis resistance in ewing family of tumors and osteosarcoma," *The oncologist*, vol. 15, no. 6, pp. 627–635, 2010.

[311] M. Bose and P. Mukherjee, "Potential of anti-muc1 antibodies as a targeted therapy for gastrointestinal cancers," *Vaccines*, vol. 8, no. 4, p. 659, 2020.

[312] D. D. Carson, "The cytoplasmic tail of muc1: a very busy place," *Science signaling*, vol. 1, no. 27, pp. pe35–pe35, 2008.

[313] L.-G. Yu, "Cancer cell resistance to anoikis: Muc1 glycosylation comes to play," *Cell death  disease*, vol. 8, no. 7, p. e2962, 2017.

[314] R. Zhou, M. Yazdanifar, L. D. Roy, L. M. Whilding, A. Gavrill, J. Maher, and P. Mukherjee, "Corrigendum: Car t cells targeting the tumor muc1 glycoprotein reduce triple-negative breast cancer growth," *Frontiers in Immunology*, vol. 11, p. 3260, 2020.

[315] I. M. Wortel, L. T. van der Meer, M. S. Kilberg, and F. N. van Leeuwen, "Surviving stress: modulation of atf4-mediated stress responses in normal and malignant cells," *Trends in Endocrinology  Metabolism*, vol. 28, no. 11, pp. 794–806, 2017.

[316] F. Siu, P. J. Bain, R. LeBlanc-Chaffin, H. Chen, and M. S. Kilberg, "Atf4 is a mediator of the nutrient-sensing response pathway that activates the human asparagine synthetase gene," *Journal of Biological Chemistry*, vol. 277, no. 27, pp. 24120–24127, 2002.

[317] A. Tagde, H. Rajabi, A. Bouillez, M. Alam, R. Gali, S. Bailey, Y.-T. Tai, T. Hideshima, K. Anderson, and D. Avigan, "Muc1-c drives myc in multiple myeloma," *Blood, The Journal of the American Society of Hematology*, vol. 127, no. 21, pp. 2587–2597, 2016.

[318] Y. Li, H. Kuwahara, J. Ren, G. Wen, and D. Kufe, "The c-src tyrosine kinase regulates signaling of the human df3/muc1 carcinoma-associated antigen with gsk3$\beta$ and $\beta$-catenin," *Journal of Biological Chemistry*, vol. 276, no. 9, pp. 6061–6064, 2001.

[319] P. Paoli, E. Giannoni, and P. Chiarugi, "Anoikis molecular pathways and its role in cancer progression," *Biochimica et Biophysica Acta (BBA)-Molecular Cell Research*, vol. 1833, no. 12, pp. 3481–3498, 2013.

[320] W. Jin, X. Liao, Y. Lv, Z. Pang, Y. Wang, Q. Li, Y. Liao, Q. Ye, G. Chen, and K. Zhao, "Muc1 induces acquired chemoresistance by upregulating abcb1 in egfr-dependent manner," *Cell death  disease*, vol. 8, no. 8, pp. e2980–e2980, 2017.

[321] C. Liao, L. Yu, Z. Pang, H. Deng, X. Liao, S. Li, J. Cheng, M. Qi, G. Chen, and L. Huang, "Wwp1 targeting muc1 for ubiquitin-mediated lysosomal degradation to suppress carcinogenesis," *Signal transduction and targeted therapy*, vol. 6, no. 1, pp. 1–4, 2021.

[322] J. A. Cooper, T. Kaneko, and S. S. Li, "Cell regulation by phosphotyrosine-targeted ubiquitin ligases," *Molecular and cellular biology*, vol. 35, no. 11, pp. 1886–1897, 2015.

[323] A. A. de Melker, G. van der Horst, J. Calafat, H. Jansen, and J. Borst, "c-cbl ubiquitinates the egf receptor at the plasma membrane and remains receptor

associated throughout the endocytic route," *Journal of cell science*, vol. 114, no. 11, pp. 2167–2178, 2001.

[324] L. Hicke, "Gettin'down with ubiquitin: turning off cell-surface receptors, transporters and channels," *Trends in cell biology*, vol. 9, no. 3, pp. 107–112, 1999.

[325] A. K. deHart, J. D. Schnell, D. A. Allen, and L. Hicke, "The conserved pkh-ypk kinase cascade is required for endocytosis in yeast," *The Journal of cell biology*, vol. 156, no. 2, pp. 241–248, 2002.

[326] C. Marques, P. Pereira, A. Taylor, J. N. Liang, V. N. Reddy, L. I. Szweda, and F. Shang, "Ubiquitin-dependent lysosomal degradation of the hne-modified proteins in lens epithelial cells," *The FASEB Journal*, vol. 18, no. 12, pp. 1424–1426, 2004.

[327] J. Z. Roberts, N. Crawford, and D. B. Longley, "The role of ubiquitination in apoptosis and necroptosis," *Cell Death  Differentiation*, pp. 1–13, 2021.

[328] K. C. Kim, "Role of epithelial mucins during airway infection," *Pulmonary pharmacology  therapeutics*, vol. 25, no. 6, pp. 415–419, 2012.

[329] A. D. Corpuz, J. W. Ramos, and M. L. Matter, "Ptrh2: an adhesion regulated molecular switch at the nexus of life, death, and differentiation," *Cell Death Discovery*, vol. 6, no. 1, pp. 1–11, 2020.

[330] H. Puthalakath, A. Villunger, L. A. O'Reilly, J. G. Beaumont, L. Coultas, R. E. Cheney, D. C. Huang, and A. Strasser, "Bmf: a proapoptotic bh3-only protein regulated by interaction with the myosin v actin motor complex, activated by anoikis," *Science*, vol. 293, no. 5536, pp. 1829–1832, 2001.

[331] T. Shibue, K. Takeda, E. Oda, H. Tanaka, H. Murasawa, A. Takaoka, Y. Morishita, S. Akira, T. Taniguchi, and N. Tanaka, "Integral role of noxa in p53-mediated apoptotic response," *Genes  development*, vol. 17, no. 18, pp. 2233–2238, 2003.

[332] F. Sivandzade, A. Bhalerao, and L. Cucullo, "Analysis of the mitochondrial membrane potential using the cationic jc-1 dyeas a sensitive fluorescent probe," *Bio-protocol*, vol. 9, no. 1, 2019.

[333] D. Hanahan and R. A. Weinberg, "Hallmarks of cancer: the next generation," *cell*, vol. 144, no. 5, pp. 646–674, 2011.

[334] S. Das and S. K Batra, "Pancreatic cancer metastasis: are we being pre-emted?," *Current pharmaceutical design*, vol. 21, no. 10, pp. 1249–1255, 2015.

[335] L. Müller, M. Hatzfeld, and R. Keil, "Desmosomes as signaling hubs in the regulation of cell behavior," *Frontiers in cell and developmental biology*, p. 2636, 2021.

[336] E. J. Thompson, K. Shanmugam, C. L. Hattrup, K. L. Kotlarczyk, A. Gutierrez, J. M. Bradley, P. Mukherjee, and S. J. Gendler, "Tyrosines in the muc1 cytoplasmic tail modulate transcription via the extracellular signal-regulated kinase 1/2 and nuclear factor-$\kappa$b pathways," *Molecular Cancer Research*, vol. 4, no. 7, pp. 489–497, 2006.

[337] P. Savagner, "Epithelial–mesenchymal transitions: from cell plasticity to concept elasticity," *Current topics in developmental biology*, vol. 112, pp. 273–300, 2015.

[338] J. P. Thiery, "Epithelial–mesenchymal transitions in tumour progression," *Nature reviews cancer*, vol. 2, no. 6, pp. 442–454, 2002.

[339] K. A. Hartwell, B. Muir, F. Reinhardt, A. E. Carpenter, D. C. Sgroi, and R. A. Weinberg, "The spemann organizer gene, goosecoid, promotes tumor metastasis," *Proceedings of the National Academy of Sciences*, vol. 103, no. 50, pp. 18969–18974, 2006.

[340] H. Jung, K. Lee, S. Park, J. Park, Y. Jang, S. Choi, J. Jung, K. Jo, D. Park, J. Yoon, *et al.*, "Tmprss4 promotes invasion, migration and metastasis of human tumor cells by facilitating an epithelial–mesenchymal transition," *Oncogene*, vol. 27, no. 18, pp. 2635–2647, 2008.

[341] T. T. Onder, P. B. Gupta, S. A. Mani, J. Yang, E. S. Lander, and R. A. Weinberg, "Loss of e-cadherin promotes metastasis via multiple downstream transcriptional pathways," *Cancer research*, vol. 68, no. 10, pp. 3645–3654, 2008.

[342] S. Spaderna, O. Schmalhofer, M. Wahlbuhl, A. Dimmler, K. Bauer, A. Sultan, F. Hlubek, A. Jung, D. Strand, A. Eger, *et al.*, "The transcriptional repressor zeb1 promotes metastasis and loss of cell polarity in cancer," *Cancer research*, vol. 68, no. 2, pp. 537–544, 2008.

[343] M. Stankic, S. Pavlovic, Y. Chin, E. Brogi, D. Padua, L. Norton, J. Massagué, and R. Benezra, "Tgf-$\beta$-id1 signaling opposes twist1 and promotes metastatic colonization via a mesenchymal-to-epithelial transition," *Cell reports*, vol. 5, no. 5, pp. 1228–1242, 2013.

[344] J. H. Tsai, J. L. Donaher, D. A. Murphy, S. Chau, and J. Yang, "Spatiotemporal regulation of epithelial-mesenchymal transition is essential for squamous cell carcinoma metastasis," *Cancer cell*, vol. 22, no. 6, pp. 725–736, 2012.

[345] J. Yang, S. A. Mani, J. L. Donaher, S. Ramaswamy, R. A. Itzykson, C. Come, P. Savagner, I. Gitelman, A. Richardson, and R. A. Weinberg, "Twist, a master regulator of morphogenesis, plays an essential role in tumor metastasis," *cell*, vol. 117, no. 7, pp. 927–939, 2004.

[346] K. R. Fischer, A. Durrans, S. Lee, J. Sheng, F. Li, S. T. Wong, H. Choi, T. El Rayes, S. Ryu, J. Troeger, *et al.*, "Epithelial-to-mesenchymal transition is

not required for lung metastasis but contributes to chemoresistance," *Nature*, vol. 527, no. 7579, pp. 472–476, 2015.

[347] E. R. Shamir, E. Pappalardo, D. M. Jorgens, K. Coutinho, W.-T. Tsai, K. Aziz, M. Auer, P. T. Tran, J. S. Bader, and A. J. Ewald, "Twist1-induced dissemination preserves epithelial identity and requires e-cadherin," *Journal of Cell Biology*, vol. 204, no. 5, pp. 839–856, 2014.

[348] J. A. Somarelli, D. Schaeffer, M. S. Marengo, T. Bepler, D. Rouse, K. E. Ware, A. J. Hish, Y. Zhao, A. F. Buckley, J. I. Epstein, *et al.*, "Distinct routes to metastasis: plasticity-dependent and plasticity-independent pathways," *Oncogene*, vol. 35, no. 33, pp. 4302–4311, 2016.

[349] J. M. Lee, S. Dedhar, R. Kalluri, and E. W. Thompson, "The epithelial-mesenchymal transition: new insights in signaling, development, and disease," *The Journal of cell biology*, vol. 172, no. 7, pp. 973–981, 2006.

[350] P. Bronsert, K. Enderle-Ammour, M. Bader, S. Timme, M. Kuehs, A. Csanadi, G. Kayser, I. Kohler, D. Bausch, J. Hoeppner, *et al.*, "Cancer cell invasion and emt marker expression: a three-dimensional study of the human cancer–host interface," *The Journal of pathology*, vol. 234, no. 3, pp. 410–422, 2014.

[351] Y. Chao, Q. Wu, M. Acquafondata, R. Dhir, and A. Wells, "Partial mesenchymal to epithelial reverting transition in breast and prostate cancer metastases," *Cancer Microenvironment*, vol. 5, no. 1, pp. 19–28, 2012.

[352] A. Grosse-Wilde, A. Fouquier d'Hérouël, E. McIntosh, G. Ertaylan, A. Skupin, R. E. Kuestner, A. del Sol, K.-A. Walters, and S. Huang, "Stemness of the hybrid epithelial/mesenchymal state in breast cancer and its association with poor survival," *PloS one*, vol. 10, no. 5, p. e0126522, 2015.

[353] R. Y. Huang, M. Wong, T. Tan, K. Kuay, A. Ng, V. Chung, Y. Chu, N. Matsumura, H. Lai, Y. Lee, *et al.*, "An emt spectrum defines an anoikis-resistant and spheroidogenic intermediate mesenchymal state that is sensitive to e-cadherin restoration by a src-kinase inhibitor, saracatinib (azd0530)," *Cell death & disease*, vol. 4, no. 11, pp. e915–e915, 2013.

[354] A. Lecharpentier, P. Vielh, P. Perez-Moreno, D. Planchard, J. Soria, and F. Farace, "Detection of circulating tumour cells with a hybrid (epithelial/mesenchymal) phenotype in patients with metastatic non-small cell lung cancer," *British journal of cancer*, vol. 105, no. 9, pp. 1338–1341, 2011.

[355] A. E. McCart Reed, J. R. Kutasovic, A. C. Vargas, J. Jayanthan, A. Al-Murrani, L. E. Reid, R. Chambers, L. Da Silva, L. Melville, E. Evans, *et al.*, "An epithelial to mesenchymal transition programme does not usually drive the phenotype of invasive lobular carcinomas," *The Journal of Pathology*, vol. 238, no. 4, pp. 489–494, 2016.

[356] H. P. Naber, Y. Drabsch, B. E. Snaar-Jagalska, P. ten Dijke, and T. van Laar, "Snail and slug, key regulators of tgf-$\beta$-induced emt, are sufficient for the induction of single-cell invasion," *Biochemical and biophysical research communications*, vol. 435, no. 1, pp. 58–63, 2013.

[357] V. B. Sampson, J. M. David, I. Puig, P. U. Patil, A. G. De Herreros, G. V. Thomas, and A. K. Rajasekaran, "Wilms' tumor protein induces an epithelial-mesenchymal hybrid differentiation state in clear cell renal cell carcinoma," *PloS one*, vol. 9, no. 7, p. e102041, 2014.

[358] M. J. Schliekelman, A. Taguchi, J. Zhu, X. Dai, J. Rodriguez, M. Celiktas, Q. Zhang, A. Chin, C.-H. Wong, H. Wang, *et al.*, "Molecular portraits of epithelial, mesenchymal, and hybrid states in lung adenocarcinoma and their relevance to survivalmolecular signatures of emt status in lung adenocarcinoma," *Cancer research*, vol. 75, no. 9, pp. 1789–1800, 2015.

[359] D. Jia, M. K. Jolly, M. Boareto, P. Parsana, S. M. Mooney, K. J. Pienta, H. Levine, and E. Ben-Jacob, "Ovol guides the epithelial-hybrid-mesenchymal transition," *Oncotarget*, vol. 6, no. 17, p. 15436, 2015.

[360] C. Li, T. Hong, and Q. Nie, "Quantifying the landscape and kinetic paths for epithelial–mesenchymal transition from a core circuit," *Physical Chemistry Chemical Physics*, vol. 18, no. 27, pp. 17949–17956, 2016.

[361] M. Lu, M. K. Jolly, H. Levine, J. N. Onuchic, and E. Ben-Jacob, "Microrna-based regulation of epithelial–hybrid–mesenchymal fate determination," *Proceedings of the National Academy of Sciences*, vol. 110, no. 45, pp. 18144–18149, 2013.

[362] S. Zadran, R. Arumugam, H. Herschman, M. E. Phelps, and R. Levine, "Surprisal analysis characterizes the free energy time course of cancer cells undergoing epithelial-to-mesenchymal transition," *Proceedings of the National Academy of Sciences*, vol. 111, no. 36, pp. 13235–13240, 2014.

[363] F. Andriani, G. Bertolini, F. Facchinetti, E. Baldoli, M. Moro, P. Casalini, R. Caserini, M. Milione, G. Leone, G. Pelosi, *et al.*, "Conversion to stem-cell state in response to microenvironmental cues is regulated by balance between epithelial and mesenchymal features in lung cancer cells," *Molecular oncology*, vol. 10, no. 2, pp. 253–271, 2016.

[364] A. W. Lambert, D. R. Pattabiraman, and R. A. Weinberg, "Emerging biological principles of metastasis," *Cell*, vol. 168, no. 4, pp. 670–691, 2017.

[365] M. A. Nieto, R. Y.-J. Huang, R. A. Jackson, and J. P. Thiery, "Emt: 2016," *Cell*, vol. 166, no. 1, pp. 21–45, 2016.

[366] T. Celià-Terrassa, O. Meca-Cortés, and F. Mateo, "Martínez de paz a, rubio n, arnal-estapé a, et al. epithelial-mesenchymal transition can suppress major

attributes of human epithelial tumor-initiating cells," *The Journal of Clinical Investigation*, vol. 122, no. 5, pp. 1849–1868, 2012.

[367] O. H. Ocaña, R. Córcoles, Á. Fabra, G. Moreno-Bueno, H. Acloque, S. Vega, A. Barrallo-Gimeno, A. Cano, and M. A. Nieto, "Metastatic colonization requires the repression of the epithelial-mesenchymal transition inducer prrx1," *Cancer cell*, vol. 22, no. 6, pp. 709–724, 2012.

[368] M. Ruscetti, B. Quach, E. L. Dadashian, D. J. Mulholland, and H. Wu, "Tracking and functional characterization of epithelial–mesenchymal transition and mesenchymal tumor cells during prostate cancer metastasis," *Cancer research*, vol. 75, no. 13, pp. 2749–2759, 2015.

[369] S. A. Mani, W. Guo, M.-J. Liao, E. N. Eaton, A. Ayyanan, A. Y. Zhou, M. Brooks, F. Reinhard, C. C. Zhang, M. Shipitsin, *et al.*, "The epithelial-mesenchymal transition generates cells with properties of stem cells," *Cell*, vol. 133, no. 4, pp. 704–715, 2008.

[370] M. K. Jolly, B. Huang, M. Lu, S. A. Mani, H. Levine, and E. Ben-Jacob, "Towards elucidating the connection between epithelial–mesenchymal transitions and stemness," *Journal of The Royal Society Interface*, vol. 11, no. 101, p. 20140962, 2014.

[371] L. Ombrato and I. Malanchi, "The emt universe: space between cancer cell dissemination and metastasis initiation," *Critical Reviewsâ¢ in Oncogenesis*, vol. 19, no. 5, 2014.

[372] A. D. Rhim, E. T. Mirek, N. M. Aiello, A. Maitra, J. M. Bailey, F. McAllister, M. Reichert, G. L. Beatty, A. K. Rustgi, R. H. Vonderheide, *et al.*, "Emt and dissemination precede pancreatic tumor formation," *Cell*, vol. 148, no. 1-2, pp. 349–361, 2012.

[373] M. Yu, A. Bardia, B. S. Wittner, S. L. Stott, M. E. Smas, D. T. Ting, S. J. Isakoff, J. C. Ciciliano, M. N. Wells, A. M. Shah, *et al.*, "Circulating breast tumor cells exhibit dynamic changes in epithelial and mesenchymal composition," *science*, vol. 339, no. 6119, pp. 580–584, 2013.

[374] A. J. Armstrong, M. S. Marengo, S. Oltean, G. Kemeny, R. L. Bitting, J. D. Turnbull, C. I. Herold, P. K. Marcom, D. J. George, and M. A. Garcia-Blanco, "Circulating tumor cells from patients with advanced prostate and breast cancer display both epithelial and mesenchymal markersepithelial/mesenchymal markers on circulating tumor cells," *Molecular cancer research*, vol. 9, no. 8, pp. 997–1007, 2011.

[375] D. S. Jeevan, J. B. Cooper, A. Braun, R. Murali, and M. Jhanwar-Uniyal, "Molecular pathways mediating metastases to the brain via epithelial-to-mesenchymal transition: genes, proteins, and functional analysis," *Anticancer research*, vol. 36, no. 2, pp. 523–532, 2016.

# VITAE

Mukulika Bose was born in Kolkata, India, in 1990. She received her Bachelor of Science in Microbiology from the University of Calcutta, West Bengal, India, with First Class marks in 2012. In 2014, she received her Masters in Biotechnology from Presidency University, and was awarded Gold medal for securing the first rank from the Department of Biotechnology. She was awarded the Department of Biotechnology Junior Research Fellowship (DBT-JRF) funded by Ministry of Science and Technology, Govt. of India to pursue her doctoral studies. She began her Ph.D. in National Institute of Biomedical Genomics (NIBMG) in 2015. She transferred and continued her research at University of North Carolina at Charlotte, NC, USA in 2017, where she earned her second Masters in Biology with a concentration in Molecular, Cell and Developmental Biology in 2020. Her main research interests include elucidating the molecular mechanism of tumor progression in solid tumors, designing targeted therapies and finding resistance mechanisms to new therapies to improve survival.